The Development of a Comprehensive Metric Which Characterises the Thermal Performance of Complete Buildings

Aiman M. K. Albatayneh

B.Sc. (Mech Eng), M.Sc. (Mech Eng), B.Sc. (RE Eng) (Hons)

A thesis submitted to the University of Newcastle in fulfilment of the requirements for the degree of Doctor of Philosophy in Engineering

School of Engineering
Faculty of Engineering and Built Environment
The University of Newcastle
March 2016

Statement of Originality

The thesis contains no material which has been accepted for the award of any other degree or diploma in any university or other tertiary institution and, to the best of my knowledge and belief, contains no material previously published or written by another person, except where due reference has been made in the text. I give consent to the final version of my thesis being made available worldwide when deposited in the University's Digital Repository, subject to the provisions of the Copyright Act 1968.

Signature ………… Date:…../…../…..

I hereby certify that the work embodied in this thesis contains published papers work of which I am a joint author. I have included as part of the thesis, a written statement, endorsed by my supervisor, attesting to my contribution to the joint publications work.

Aiman Albatayneh ………………………..

Dr. Dariusz Alterman……………………..

Acknowledgements

I am greatly thankful to my beloved family. This journey would not have been possible without the support of my father, mother, wife and my kids, whose love and emotional sacrifice to support me in finishing this work have always been with me, no matter how far apart we are.

I would like to thank my principal supervisor, Prof. Behdad Moghtaderi, who inspired me with his respectful knowledge and understanding. I would also like to thank my co-supervisor, Dr. Dariusz Alterman, for his right-to-the-point advice, collaboration, careful supervision, and constructive criticism throughout my PhD research, in addition to assisting in the direction in my research which helped me to finish this work. I would also like to thank Prof. Adrian Page for his invaluable advice and support, especially in writing skills, which benefited me in writing this thesis. Without their supervision, the completion of this research and the writing of this thesis would not have been possible.

Aiman Albatayneh

22-10-2015

ABSTRACT

The growing demand for energy, energy supply security, climate change and ways to reduce greenhouse gases (GHG) have all played a significant role in the designing of new sustainable buildings. To design efficient sustainable buildings, the accuracy of a building's thermal simulation will have direct implications on the prediction of the thermal performance of the building and the operational energy costs for the life of the building. Therefore, the output of any simulation should reflect the actual performance in order to save more building operating energy and reduce GHG emissions.

The main purpose of this research is to verify the validity of a universal metric, proposed for the first time in this study, to characterise the thermal performance of complete buildings called the Adaptive Thermal Metric (ATM). This metric facilitates the assessment of the thermal performance of whole building envelopes which leads to more thermally efficient housing designs. Using the building's internal air temperature the new method takes into consideration the various building materials, orientation, shading, occupant behaviour, weather at the site and the environment surrounding the building. The ATM uses temperature to assess the building's thermal performance, thus differing from other widely accepted methods that are based on energy consumption.

This research consists of three stages. In the first stage, the variations of the internal air temperature of four existing housing test modules (Cavity Brick (CB), Insulated Cavity Brick (InsCB), Insulated Brick Veneer (InsBV) and Insulated Reverse Brick Veneer (InsRBV)) are compared with CFD simulation results to determine the accuracy of the CFD simulation. Long period CFD simulations have typically faced some issues, such as long computing times and internal air temperature increases over time.

After addressing these issues, the simulations were carried out for one year, using larger time steps (minimizing the computing time by more than 99% when compared to a 1 minute time step simulation) and with results with an average accuracy of 93% compared with the real data at any given time during the studied

year. This is the first attempt to use CFD alone, without the assistance of any additional software to find the internal air temperatures of buildings over long periods.

In the second stage of the research, two universal metrics using an adaptive thermal comfort range with 90% and 80% acceptability limits are developed (designated ATM90 and ATM80 respectively). There ATM's account for the percentage of time over which the internal temperature of a building remains within the define comfort limits. The results of the characterisation of the thermal performances for both limits indicated that the best performing module was the InsCB, followed by the InsRBV, InsBV and CB modules, respectively.

These results are consistent with the previous findings from University of Newcastle research on walling systems and the AccuRate building assessment tool used in Australia, and thus justify the possibility of using this metric as a new assessment tool to characterise the thermal performance of complete building.

In the final stage of the research, appropriate ways to improve building energy design in order to reduce the amount of energy required to sustain thermal comfort are considered. This includes a feasibility study to find the best energy efficient design with the least cost. As a case study CFD simulations were carried out and the ATM determined for a complete house in a different climate zone. CFD simulations resulted in an average accuracy of 92% which is consistent with the previous CFD simulations for the housing test modules at the University of Newcastle. The ATM was able to reproduce the thermal performance of different housing types in different locations. This illustrates the possibility of using the ATM as a new universal metric which could be applied anywhere around the world.

The results found in this research are promising and may facilitate the use of this metric as a new building assessment method to accurately predict the thermal performance of any building envelope. Since the occupants are able to use various strategies to control their perception of the internal conditions, the method also has the potential to reduce the amount of heating and cooling energy necessary to sustain thermal comfort.

Table of Contents

Chapter Eight: Conclusions and Recommendations for Future Research

List of Figures

List of Tables

List of Abbreviations

CB-CFD (one ext. boundary):	CFD simulation using one external boundary to measure internal air temperature for a cavity brick module (ºC).
CB-CFD (two ext. boundaries):	CFD simulation using two external boundaries to measure internal air temperature for a cavity brick module (ºC).
CB-CFD x min:	CFD simulation using x minutes time steps to measure internal air temperature for a cavity brick module (ºC).
CB:	Cavity Brick module.
CB-Real inside:	Real internal air temperature for a cavity brick module (ºC).
DBT:	Dry-Bulb Temperature
InsBV-CFD (one ext. boundary):	CFD simulation using one external boundary to measure internal air temperature for an insulated brick veneer module (ºC).
InsBV-CFD (two ext. boundaries):	CFD simulation using two external boundaries to measure internal air temperature for an insulated brick veneer module (ºC).
InsBV-CFD x min:	CFD simulation using x minutes time steps to measure internal air temperature for an insulated brick veneer module (ºC).
InsBV:	Insulated Brick Veneer module.
InsBV-Real inside:	Real internal air temperature for an insulated brick veneer module (ºC).
InsCB (two ext. boundaries):	CFD simulation using two external boundaries to measure internal air temperature for an insulated cavity brick module (ºC).
InsCB-CFD (one ext. boundary):	CFD simulation using one external boundary to measure internal air temperature for an insulated cavity brick module (ºC).
InsCB-CFD x min:	CFD simulation using x minutes time steps to measure internal air temperature for an insulated cavity brick module (ºC).
InsCB:	Insulated Cavity Brick module
InsCB-Real inside:	Real internal air temperature for an insulated cavity brick module (ºC).
InsRBV-CFD (one ext. boundary):	CFD simulation using one external boundary to measure internal air temperature for an insulated reverse brick veneer module (ºC).

InsRBV-CFD x min:	CFD simulation using x minutes time steps to measure internal air temperature for an insulated reverse brick veneer module (ºC).
InsRBV-CFD (two ext. boundaries):	CFD simulation using two external boundaries to measure internal air temperature for an insulated reverse brick veneer module (ºC).
InsRBV:	Insulated Reverse Brick Veneer module.
InsRBV-Real inside:	Real internal air temperature for an insulated reverse brick veneer module (ºC).
LW:	Leeward (remainder of incidence angles)
Outside Temp.:	Outside air temperature (ºC).
PMV:	Predicted Mean Vote
PPD:	Predicted Percentage Dissatisfied
PWF:	Present Worth Factor
WBT:	Wet-Bulb Temperature
WW:	Windward incidence angles from -90 to 90

Nomenclature

T_{air}:	Ambient air temperature (K)
S:	Annual cost or value into the future (cost –ve, saving +ve)
$u(z_r)$:	Available wind speed at z height
Clo	Clothing insulation (1Clo = $0.155m^2 \cdot K/W$)
T_c:	Comfort temperature (^oC)
h_c:	Convective heat transfer coefficient ($W/m^2.K$)
h_{forced} :	Forced convective heat transfer coefficients for exterior building surface
C:	Heat capacity of air constant pressure
q:	Heat energy (W)
f:	Inflation
i:	Interest rate
Q_i:	Internal Heat Gains
G:	Irradiance (W/m^2)
L:	Length (m) or Thermal load
$\mathring{m}$:	Mass flow rate of air (kg/s).
$h_{natural}$:	Natural convection heat transfer coefficient with no wind = 3.5 $W/m^2.K$
N:	Number of air changes per hour
T_{total} :	Outside air temperature with wind speed = V_{actual}
$T_{natural}$:	Outside air temperature with wind speed equal zero (no wind effect)
U:	Overall heat transfer co-efficient
Met:	Rate of metabolic generation per unit surface area (1Met= $58.2W/m^2$)
C_p:	Specific heat capacity of the air equal 1 kJ/kg ^oC
v:	Specific volume (m^3/kg)
A_s:	Surface area (m^2)
z_o:	Surface roughness
T_s:	Surface temperature (K)

A:	Swept area of the rotor blade (m^2) for wind turbines
T:	Temperature (^oC)
dT:	Temperature difference
ΔT:	Temperature difference between inside and outside.
m_{ev}:	The evaporation rate (kg/hour)
T_o:	The monthly mean of the outdoor air temperature (^oC)
h_{total} :	Total heat transfer coefficient (h_{forced} + $h_{natural}$)
t:	Transmissivity
V:	Volume of the zone (m^3)
$\mathring{V}$:	Volumetric flow rate of air (m^3/s)
v:	Wind speed (m/s) for wind turbines
u(z):	Wind speed at 10m height
U_{10} :	Wind speed at a height of 10m above the ground
	Greek Symbols
α:	Absorptivity
ρ:	Density (kg/m^3)
ρ:	Reflectivity

List of Publications

Albatayneh A., Alterman A., Page A., Moghtaderi B., The Significance of Time Step Size in Simulating the Thermal Performance of Buildings, Advances in Research; (2015), Vol. 5, Issue: 6. ISSN: 2348-0394.

- Incorporated as Section 4.3

Albatayneh A., Alterman A., Page A., Moghtaderi B., Warming issues associated with the prolonged simulation of housing using CFD analysis, Accepted to be published in Journal of Green Building; (2016), V11 N2, spring issue.

- Incorporated as Section 4.2

Albatayneh A., Alterman A., Page A., Moghtaderi B., Assessment of the Thermal Performance of Complete Buildings Using Adaptive Thermal Comfort, Urban Planning and Architecture Design for Sustainable Development Conference in Italy 2015, Accepted to be published in Sciencedirect.com - Social and Behavioral Sciences (2016).

- Incorporated as Chapter 5

Albatayneh A., Alterman A., Page A., Moghtaderi B., A Universal Metric to Characterise the Thermal Performance of Complete Buildings, Submitted to Energy and Buildings.

- Incorporated as Chapter 5

Albatayneh A., Alterman A., Page A., Moghtaderi B., An Alternative Approach to the Simulation of Wind Effects on the Thermal Performance of Buildings, To be Submitted to Energy and Buildings.

- Incorporated as Section 4.5

Albatayneh A., Alterman A., Page A., Moghtaderi B., Discrepancies in Peak Temperature Time for Long Duration Building CFD Simulation, To be Submitted to Journal of Green Building.

- Incorporated as Section 4.4

Chapter One: Introduction

Responding to climate change and finding ways to reduce greenhouse gas (GHG) emissions play a major part in designing new sustainable buildings. To tackle climate change in Australia there is a need to reduce greenhouse gas emissions and this can achieved by reducing energy consumption by designing economic and energy efficient buildings that respond to the climatic conditions found at the site.

1.1 Climate Change

Since the mid-1700s, from the beginning of the industrial revolution, the concentrations of methane (CH_4), carbon dioxide (CO_2) and nitrous oxide (N_2O) in the atmosphere have increased significantly and have contributed to an increase in global average temperature (USGCRP, 2009). Now, atmospheric concentrations of these three gases are higher than at any time in human history and are increasing at alarming rates, as shown in Figure 1.1. These emissions have been increasing since the eighteenth century and are mainly attributed to human activities in the industrial era (Larsen et al. 2011).

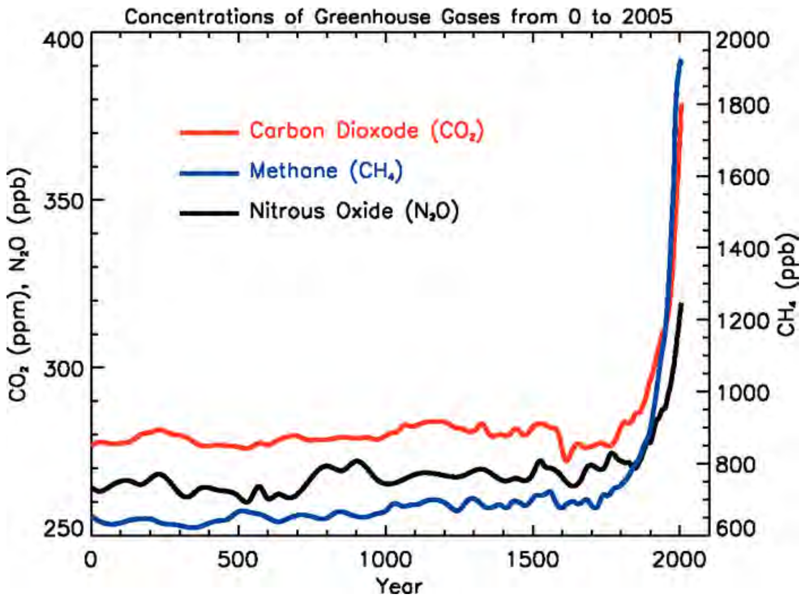

Figure 1.1 Atmospheric concentrations of the main greenhouse gases over the last 2,000 years (IPCC 2007).

Concentration units are parts per million (ppm) or parts per billion (ppb), indicating the number of molecules of the greenhouse gas per million or billion in air molecules, respectively, in an atmospheric sample (IPCC 2007).

World climate change experts, such as the U.S. Global Change Research Program (USGCRP), the Intergovernmental Panel on Climate Change (IPCC) and the U.S. Environmental Protection Agency (EPA), have indicated that the world will almost definitely face, to some extent, the consequences of climate change, no matter how rapidly greenhouse gas emissions are reduced (Larsen et al. 2011). Climate change will cause a rise in the earth's temperature, changes to hydrological cycles, ocean acidification, rises in sea levels and higher frequencies of extreme weather events (like storm surges, heavy precipitation and heat waves) (US GCRP 2013).

1.2 The Impact of Climate Change in Australia

Australia has a number of unique challenges and some of the future implications from climate change will be (Preston 2006):

- Temperatures expected to increase 0.4 - 2.0ºC above 1990 levels by 2030 and 1.0 - 6.0°C by 2070.
- Rainfall in the south west and south east of the content to decline and the north west of the continent may experience increased rainfall.

- Coastline erosion/immersion and an 8 - 88cm sea-level rise.
- More extreme weather and sudden changes in the climate.

It is predicted that Australia's climate will become hotter in the coming decades and many locations will experience heatwaves with higher temperatures for longer periods. For example, a lengthy heat wave hit across Australia from early December 2012 to late January 2013, the highest recorded maximum in the Sydney metropolitan area was 47.8°C on 18 January 2013 (Sydney weather 2014). Recent extreme heat events in Australia have demonstrated a wide range of difficulties related to heatwaves, from infrastructure failure, bushfires and economic loss through to increased illness, injuries and mortality. It is estimated that these problems will get worse in the future and that the number of deaths due to heat could double in the next 40 years (Soebarto and Bennetts 2014).

Because of these reasons, it is vital for future sustainable building designers to understand how climate change will affect future building design. A study in Australia indicates that with global warming the temperature may increase by 5^{o}C, which may increase the energy consumption in buildings by up to 56% by 2050. There is a need to incorporate suitable adaptation plans into our practices so that the buildings we design and build today will be appropriate for a range of uncertain futures (Wang et al. 2010).

1.3 Energy Demand in Australia

Australia's main energy demand is expected to increase at a lower annual rate compared to previous years, but still increase by 2.1% each year until 2020, as shown in Figure 1.2, and stationary energy emissions are also predicted to increase incrementally, with different scenarios, as shown in Figure 1.3.

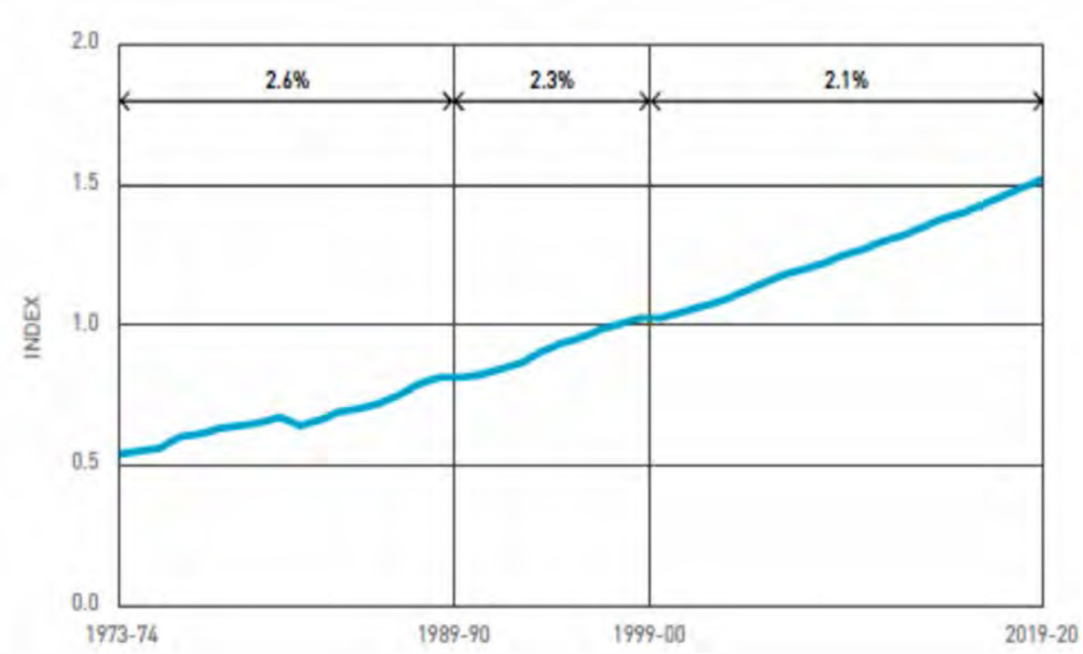

Figure 1.2 Australian principal energy consumption in the past and future projected (PMC 2004).

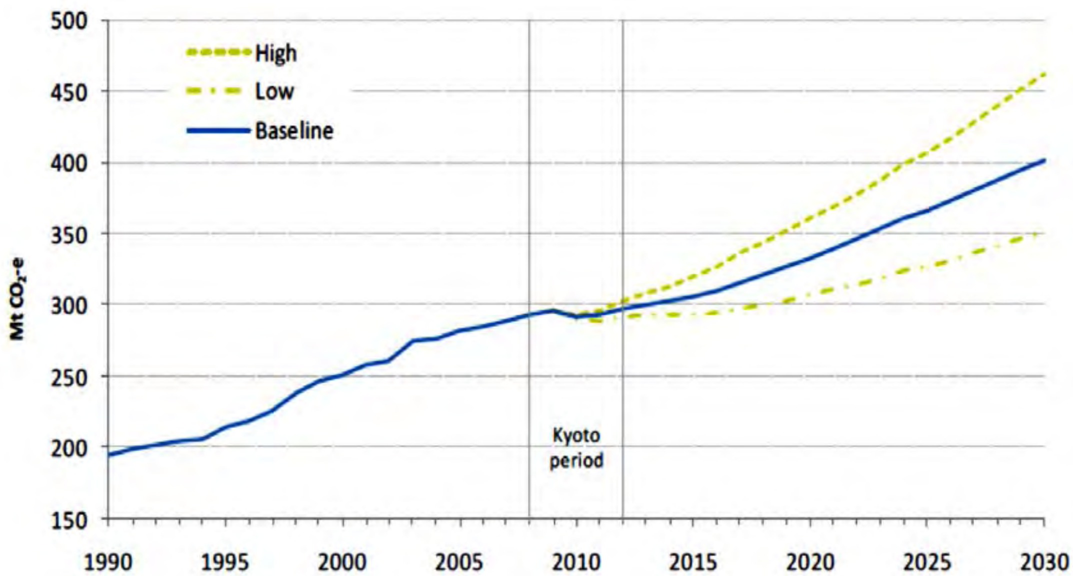

Figure 1.3 Stationary energy emissions projection (DCCEE 2010). Note: Mt CO_2-e Million metric tons of carbon dioxide equivalent. The Kyoto period is the first commitment period (2008 – 2012) to reach emission reduction targets.

The top twenty-five emitting economies responsible for more than 80 percent of total emissions are shown in Figure 1.4 (a), where Australia is the highest emitting economy per capita. Most of these emissions result from domestic use (not for industrial purposes) and that is why the emissions per unit of GDP is lower, as shown in Figure 1.4 (b) (UNIDO 2011).

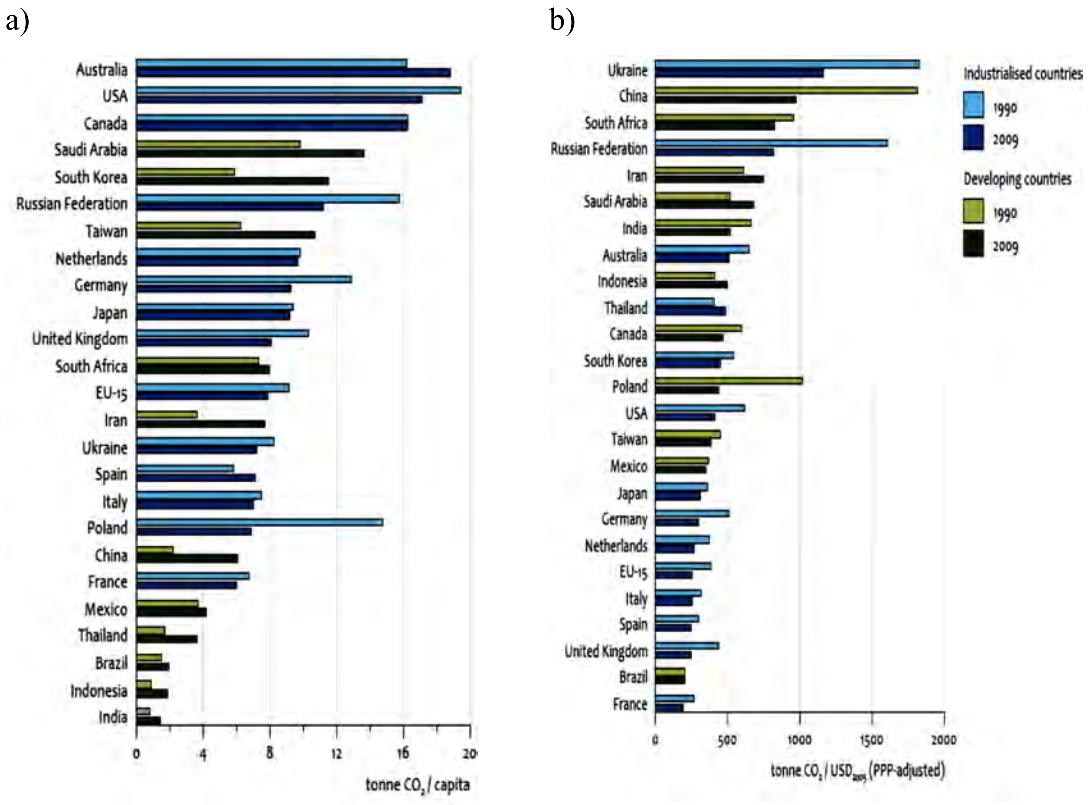

Figure 1.4 Carbon dioxide emissions in the top 25 emitting economies in 1990 and 2009 ((a) CO_2 emissions per capita, (b) CO_2 emissions per unit of GDP) (NEAA 2010). Note: GDP per capita based on purchasing power parity (PPP).

To prepare for climate change there is a need to integrate appropriate adaptation approaches into our practices so that the buildings we design and build today will be appropriate for a range of uncertain futures. However, our codes, standards, and practices assume that the future will be similar to the past, but this is not the case. Climate change will require new updates to these codes, standards, and practices and that we start planning to adapt to the effects of climate change in new buildings (Larsen et al. 2011).

1.4 Buildings and Energy Consumption in Australia

Buildings are responsible for about one-third of the emissions of heat-trapping carbon dioxide from burning fossil fuel and 40% of acid rain. 40% of the world's total energy usage is dedicated to the construction and operation of buildings, as shown in Figure 1.5. Heating and cooling energy in the residential sector account for more than 16% of the total energy usage (U.S. Dept. of Energy 2008).

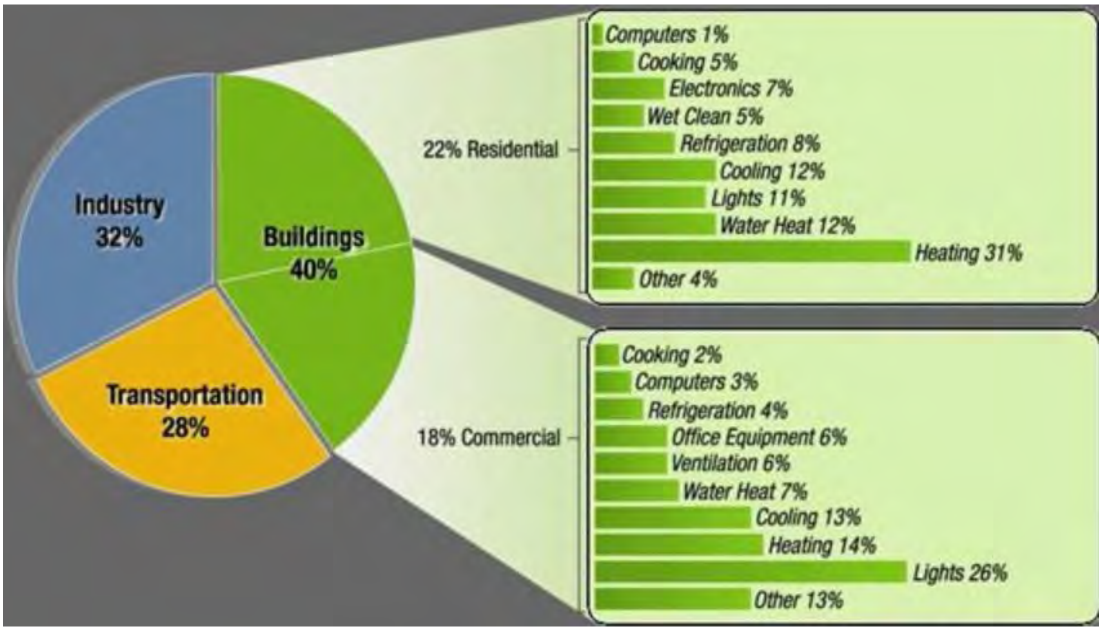

Figure 1.5. The building sector responsible for the largest percentage of generated energy consumption (U.S. Dept. of Energy 2008)

The impacts of global warming and climate change can be stopped or reduced simply by reducing energy consumption, which leads to a reduction in greenhouse gas emissions. In Australia, the stationary energy sector is the largest emissions segment and in 2009 it represented 51% of Australia's total greenhouse gas emissions. The stationary energy sector includes emissions from electricity generation and the direct combustion of fuels (fuels consumed directly in the manufacturing, mining, construction and commercial sectors and other sources such as domestic heating and cooking) (DCCEE 2010).

Space heating and cooling, from different types of fuel; consume enormous amounts of energy in Australia, as shown in Figures. 1.6 for 2007, and are predicted to increase in 2020 (see Figure 1.7). Massive amounts of this energy can be saved, for example, by heating and cooling loads using appropriate climate passive design.

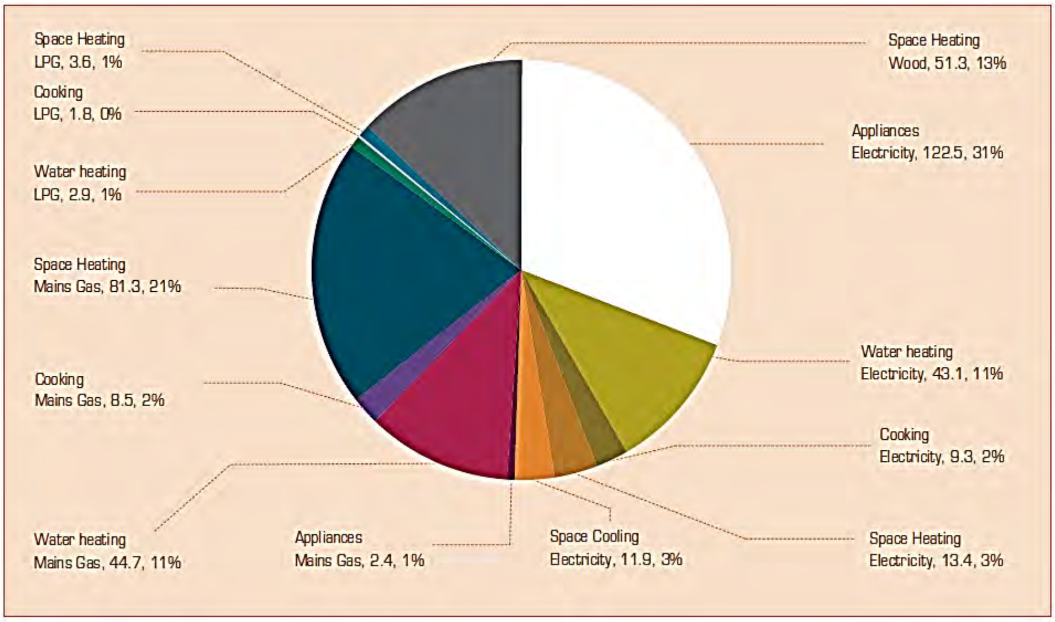

Figure 1.6 Breakdown of energy for major end uses – 2007 Australia (DEWHA 2008). Note: Energy consumption shown in PJ followed by % share of total energy.

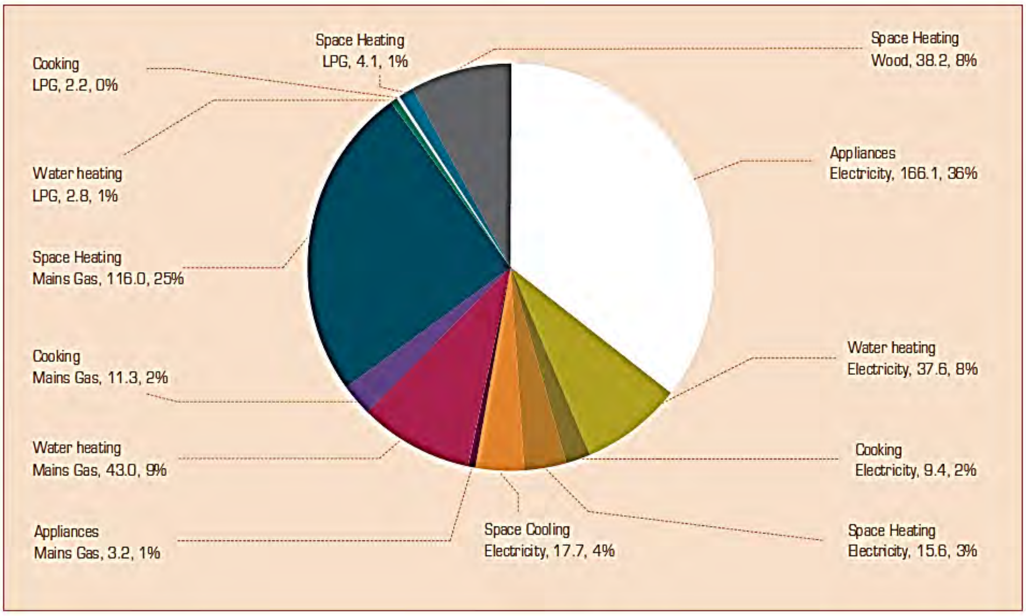

Figure 1.7 Breakdown of energy for major end uses – 2020 Australia (DEWHA 2008).

To tackle climate change in Australia we need to reduce greenhouse gas emissions and the energy consumed in buildings by designing economic and energy efficient buildings that respond to the climatic conditions found at the site. Designing energy efficient buildings requires studying and analysing the current building components and design practices in Australia to reduce energy consumption and prepare for climate changes.

There is a need to design buildings to minimize their negative environmental impact by enhancing their efficiency and moderation in the use of energy and materials to ensure that our actions and decisions today will help the future generations to meet their own material and energy needs **(**Brundtland 1987).

1.5 Aims and Objectives

The principal aim of this research is to derive a new metric for characterising whole building thermal performances called the Adaptive Thermal Metric (ATM) and using this metric, to compare the thermal performance of complete buildings, taking into consideration the various building materials, orientation, shading, occupant behaviour , weather at the site and the environment surrounding the building. The main characteristics of the metric are:

- Encourages sustainability and energy saving.
- Applicable anywhere in the world.
- Fast computing time.
- Ability to compare the thermal performance of various buildings.
- Requires minimum weather data (only the outside air temperature and average wind speed and direction).

The main objectives of this research are:

- To use CFD simulation alone to accurately predict a building’s thermal performance for a long period analysis by solving these issues:
    - To avoid the air temperature inside the simulated modules warming with time.
    - To speed up the simulation time and give a higher temperature fluctuation range, with the least lag, compared with the real data.
    - To apply the wind effect in the CFD simulation by finding new air temperature $T_{natural}$ which enables the direct inclusion of the wind effect and a decrease in the computing time.

- To design a simulation module that is capable of predicting the thermal performance of a building envelope for any given set of climatic data.
- To account for the occupants' behaviour when computing a building's thermal performance.
- To improve the energy efficiency of a building design, this will enhance the economic and environmental performance of the building.

1.6 Hypotheses and Research Questions

This research is based on these two hypotheses;

- The thermal performance of a complete building envelope can be assessed by a universal metric which accounts for the percentage of time over which the internal temperature of a building remains within the comfort range.

- The internal air temperature inside the building can be calculated accurately over long periods by using CFD analysis alone, without the assistance of any other software.

This research will attempt to answer these questions;

- Is it possible to use CFD simulation only to accurately predict internal air temperatures inside the buildings?
- Is there ways to speed up the simulation with the least computing time?
- Can we combine the wind effect with the external air temperature of the building to significantly decrease the computing time?
- Can we develop a universal metric to accurately characterise the thermal performance of complete buildings?
- Can we design a thermally comfortable building without using any form of energy from fossil fuels with the least cost?

1.7 Structure of the Thesis

This thesis consists of eight chapters. The thesis begins in Chapter 1 with an introduction to climate change and its effect on Australia, as well as a discussion of building energy consumption in Australia. This was followed by the aims and objectives of the research.

Chapter 2 provides theoretical background information on the research field, such as: factors affecting the energy consumption of buildings, including a building's components and design for the climate, shading, orientation, occupant behaviour; the types of thermal comfort module; a building's thermal properties; Computational Fluid Dynamics (CFD); and renewable energy systems used to reach 100% energy sustainable modules. A critical literature review of house energy rating methods is presented and the knowledge gap with current rating softwares is identified.

Chapter 3 defines the key tools used in this research such as: full-scale housing test modules; a Western Australia house used in the case study; Computational Fluid Dynamics (CFD); AccuRate software; Autodesk Ecotect and adaptive thermal comfort which is used to define the ATM.

Chapters 4 uses CFD analysis to find a building's internal air temperature and focus on the issues associated with prolonged simulation and the best ways to solve it. This facilitates the use of an adaptive thermal comfort range to calculate the ATM and find ways to improve the module's thermal performance.

Chapter 5 develops the ATM (ATM90, ATM80) then examines the results of the ATM and compares them with the previous research at the University of Newcastle and with the results of the AccuRate rating assessment tool which is used in Australia.

Chapter 6 presents a case study in a different climate zone using an actual Western Australia house in order to examine the accuracy of the CFD simulation and the use of the ATM by comparing it with the AccuRate results.

Chapter 7 demonstrates strategies to improve the thermal performance of the modules are developed and used to investigate their impact on the design compared with the original performance using the ATM approach. In addition to, investigate cost-effective ways to improve the module's design to reach an almost 100% energy efficient building. This is done by employing a feasibility study to compare the building's components or the renewable energy systems (e.g. photovoltaics, wind turbines and solar heating systems) which provide the greatest energy savings with the least cost.

Chapter 8 summarises the main conclusions of this research and makes recommendations for future research.

Chapter Two: Background Information and Literature Review

This chapter presents background information relevant to the thermal performance of buildings, such as: factors affecting the energy consumption of buildings; building design for climate; a building's thermal properties and renewable energy systems which can be used to improve its thermal performance. A critical review of the assessment tools used to analyse building thermal performance is also presented.

2.1 Factors Affecting the Energy Consumption of Buildings

Studying and analysing the current building components and design practices in Australia will potentially improve the thermal performance of a building by considering both the building design and the choice of the appropriate building materials.

There are limitations to the material properties and the models available to assist with building design. These need to be identified and addressed to find the proper solution to improve building design and the thermal energy assessment for current and future buildings (Azhar et al. 2012).

2.1.1 Building Characterisations and Thermal properties

2.1.1.1 Building Components

There are different types of building components with different thermal characteristics which can be used to enhance the thermal performance of a building and reduce energy consumption. As shown in Figure 2.1, the main heat losses/ gains are through ceilings, windows, walls, floors and air leakage. To achieve thermal comfort with the least amount of energy requires the study and analysis of building components to combine the appropriate material with the correct thermal characteristics.

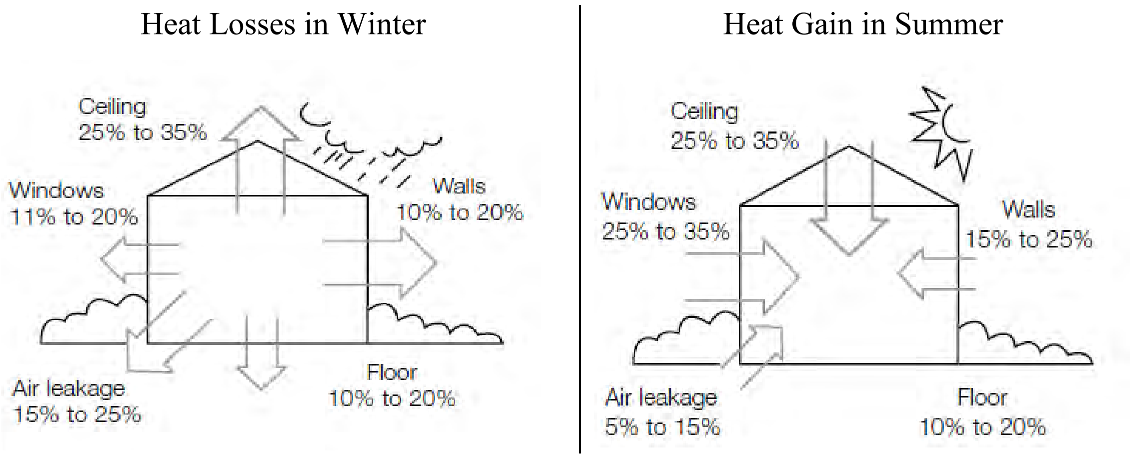

Figure 2.1. Typical heat gains and losses in a temperate climate (Department of Climate Change and Energy Efficiency (DCCEE 2011).

This section covers the common types of building components and their thermal properties to identify ways to improve a building's thermal performance.

Walls: The main components of any building are the walls, which are constructed from different materials such, as (DCCEE, 2011):

- **Cavity Brick (CB)**: Which have a high thermal mass but may need insulation otherwise they are usually cold in winter and hot in summer, especially in long heat wave conditions.
- **Insulated Cavity Brick (InsCB):** If the cavity brick wall is insulated, the internal thermal mass (internal brick layer) is sheltered from external

temperature changes, and this becomes highly efficient in regulating temperatures within the home because it has a higher thermal mass.

- **Brick Veneer (BV):** Walls that have a brick skin on the outside of a timber or stud frame, which is not the ideal location for the thermal mass. The bricks heat up in summer and radiate heat later into the building, while in winter they stay cold and absorb heat from the building.
- **Insulated Brick Veneer (InsBV):** The brick veneer wall is insulated by an insulation layer either between the inner and outer skins or between each stud. Insulation is essential in shielding the interior of the building from the external temperature environment which is aggravated by the contribution of the external brick skin.
- **Timber Framed Lightweight:** A low mass construction consisting of a stud frame externally with cement sheets and internally by plasterboard. It relies on insulation to maintain thermal comfort. Effective for hot-humid climates where the night temperatures are only slightly below the daytime ones, so the low thermal mass allows the buildings to cool quickly.

Floor: Constructed mainly from concrete slabs covered by carpet or timber for better insulation in cold climates. Suspended timber floors are an environmentally friendly alternative choice for sloping sites and flood prone areas. These types of floors also provide extra space for pipes and ease of inspection under the building, especially for termites.

Roof and Ceiling: The roof is fabricated from concrete, clay or metal material so the insulation is important to reduce heat loss in winter and heat gain in summer as 25 - 35% of losses/gain occur through the plaster board ceiling, as shown in Figure 2.1.

Insulation: Insulation minimises heat loss and heat gain through the walls, roof and floors. Insulation acts as a blockade to heat flow, measured by R-value (resistance to heat flow) in (m^2.K/W) where a higher R-value means better insulation. There are several types of insulation (DCCEE 2011):

- **Bulk Insulation:** Contains pockets of caught air within its structure to resist convection and conduction heat transfer. It should be dry and not be compressed. The main two types of bulk insulation are batt insulation and blanket insulation.
- **Reflective Foil Insulation:** Contains a highly reflective surface and very low emissivity to resist radiant heat transfer. However, it needs an air gap of at least 20 - 25mm and any dust accumulated on the foil surface will reduce its performance.

Glazing: Glazing provides a view, natural light, connection to the outdoors and adjustable ventilation. There is a wide variety of glass products currently available and these are of two important types:

- **Double Glazed:** Losses from glazing (single glazed - low insulation) are often greater than solar gains and daylights energy savings combined. Often in winter a high transmission of solar radiation is desirable, but with minimum losses by conduction.

  Double glazing with the air between the glazing replaced with Argon will reduce convective heat losses and the overall heat losses further. Double glazed windows allow radiation to penetrate so they can be used in north-facing windows to allow winter sun in and be used for other windows which need proper shading from the sun (DCCEE 2011).
- **Low Emittance Glass:** Allows visible transmission but Low-Emittance Glass reduces solar heat gain in winter. Low-Emittance (Low-E) coatings are microscopically thin, virtually invisible, and are primarily used to reduce the U-value by reflecting long-wave radiation (heat) (DCCEE 2011). Low-Emittance glass can be used to minimize solar radiation entering the building which means it cannot be used for north-facing windows but can be used for other windows.

Window Frame Materials: Aluminium is a good conductor and causes more rapid heat loss/gain, while timber is a better insulator. Polymers frames can also be used as a window frame, which has better moisture and decay resistance.

Airtight Construction Design: Using weather strips for doors and window will reduce air leakage and save more energy, especially in colder zones.

Ventilation: Is important in a building because an air speed of 0.5 m/s equates to a 3 degree drop in temperature at a relative humidity of 50% (DCCEE 2011). A typical Australian home with wall vents in each room and ceiling increases the overall heating energy costs but allows acceptable ventilation.

Ventilation highly depends on the building openings and the wind speed, which is nearly impossible to calculate because the openings depend on the occupant's behaviour, which is hard to predict, and the wind speed which is highly variable and unpredictable (with changing speed and direction).

Fast moving air causes a physiological cooling effect by convecting heat away from the body, and evaporating perspiration, which cools the skin. Ventilation can be increase:

- Building higher than the ground for increased exposure to cooling breezes.
- Windows need to be at opposite ends of the room for better inlet and outlet. Bigger inlets and outlets are better, as shown in Figure 2.2.
- Inlet at 45° to predominant wind direction during most overheated periods, which moves air around the space.

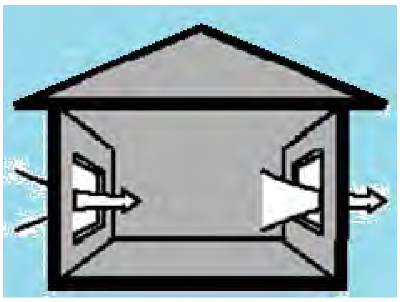

Figure 2.2. Inlet and outlet for ventilation.

Window Types: Window shapes and sizes affect the natural ventilation. There are different types of window shapes to serve different purposes, such as:

- Louvres, as shown in Figure 2.3, which offer high ventilation and prevent sun radiation.

Figure 2.3. Louvre window (IndiaMART)

- Casement windows (side hung, as shown in Figure 2.4) can be used to catch breezes blowing parallel to the window, so are a good choice when the summer wind direction is variable.

Figure 2.4. Casement window (Window Sash)

- Double-hung (sash) windows, as shown in Figure 2.5, offer a choice between high and low level ventilation.

Figure 2.5. Double-hung (Window Sash)

- Awning (hopper) windows (hinged at the bottom and opening inwards, as shown in Figure 2.6) can be left open in wet weather but their ventilation potential is poor.

Figure 2.6. Awning (hopper) windows (Window Sash)

Studying and analysing the current building components in Australia showed that the thermal performance of buildings can be improved by taking into account building thermal properties. The two main thermal properties of building materials are the thermal mass and the thermal resistance (R-value). The main difference between them is that the R-value is the thermal resistance to the heat flow, where a higher R-value means more resistance to the heat flow (better insulator), while the thermal mass is the ability to absorb, store and release energy, which results in a delayed heat transfer and reduced temperature fluctuation inside the building. Using thermal mass in buildings depends on the climate, building components/types and configurations, which can significantly reduce annual energy demand.

2.1.1.2 Thermal Mass

The main purpose of thermal mass is to absorb and store the heat from the sun during the day and later release the thermal energy, which will enhance thermal comfort and reduce energy costs by averaging the day/night (diurnal) extremes. A lot of heat energy is required to change the temperature of high density materials like concrete, bricks and tiles since they have high thermal mass. Lightweight materials, such as timber have a low thermal mass. The appropriate use of thermal mass can make a big difference to thermal comfort and heating and cooling bills, and are particularly beneficial where there is more than 10^{o}C difference between the day and night outdoor temperatures (Green Building Advisor 2015).

Internal materials have a direct implication on the thermal mass of a building. For example, covering a high mass material with a light weight material diminishes its effectiveness as a thermal mass (e.g., carpet or timber flooring over a concrete slab). On the other hand, high energy emittance to thermal mass is achieved by covering a high mass material with a denser material, such as ceramic tiles over a concrete slab.

Thermal mass can be achieved by using heavy soil or masonry materials in floors, walls, and ceilings. To work most effectively, the mass in floors, walls, and ceilings must be exposed, with no carpets or floor coverings, or bare walls and bare ceilings.

Thermal mass is useful in environments with a high diurnal range, such as hot-dry climates, by allowing ventilation at night where comfortable night average temperatures cool the building's interior mass with night breezes, or by closing it up during the heat of the day to keep heat out. Thermal mass can also be used in winter in temperate climates to store winter heat during the daytime through north-facing windows. The north-facing windows should be double glazed to minimize heat losses especially at night.

2.1.1.3 Thermal Resistance (R-value)

Reliance solely on thermal resistance leads to significant energy demand inaccuracies, since the thermal inertia of building components has a profound impact on heating and cooling loads in buildings (Zhu L et al. 2009).

Several techniques have been developed for determining overall heat transfer coefficients (U-values). One commonly used method is the steady-state measurement of thermal properties with a ‘hot box’. The other commonly used method is the dynamic simulation of a ‘test cell’, where the test cell is fabricated in a way that enables the calculation of the thermal properties of a building’s components from simple temperature measurements, without the need for the measurement of input and output power (Leftheriotis and Yianoulis 2000). But the test cell does not consider the high thermal mass which results in imprecise estimation to the thermal properties under real weather conditions. However the accurate results must be compared by applying dynamic conditions. (Leftheriotis and Yianoulis 2000).

A calibrated hot-box unit is adjusted for the static and dynamic thermal characterisation of different types of identical walls, using 2m X 2m samples. A numerical analysis is carried out to obtain the thermal performance of a wall in static and dynamic structures. The correct evaluation of heat losses through the walls of buildings requires the inclusion of thermal inertia. For this reason, it is vital to have a wall’s dynamic thermal characteristics (Sala et al. 2008).

Whilst the R-value (one of the thermal properties of a building material) is a significant thermal property of a building material, because of its static nature, it is unable to effectively characterise the dynamic thermal response of a wall (or building interior) to the external thermal fluctuations. It is also unable to capture the effects of large diurnal temperature swings and the influence of thermal mass on the wall’s performance. Therefore, the R-value alone does not encapsulate all the characteristics involved in heat exchange (Alterman et al. 2012).

Comprehensive research at the University of Newcastle on the performance of the various walling systems used in Australian housing has confirmed that building thermal performance predictions cannot use R-values alone without considering thermal mass (Page et al. 2011).

Contrary to the common perception, the overall thermal performance under all weather conditions could not be defined solely by the thermal resistance (R-value) of walls because that parameter is not the sole predictor of the thermal performance of a building (Page et al. 2011). For example, from the DCCEE- 2011 manual, on page 101, states: "*The higher the R-value the better the thermal performance*" this is not highly accurate where in some cases the higher R-value results in better building insulation, but not better thermal performance for the buildings.

2.1.1.4 Other Physical Thermal properties

There are some physical properties which affect the thermal performance of buildings such as; emissivity, absorptivity, reflectivity and transmissivity. These mainly depend on the surface colour, material properties and the thickness of the component.

- Emissivity is the fraction of energy emitted by surface compared to that emitted by a black body and is a measure of the effectiveness of a surface to emit thermal energy. A black body is a perfect emitter of thermal energy (emissivity = 1).
- Absorptivity (α), reflectivity (ρ) and transmissivity (t)

  The total amount of radiation energy falling on a surface can be divided into three parts; absorbed, reflected and transmitted. Absorptivity is the fraction of radiation energy absorbed by a surface compared to total energy radiation energy. Reflectivity is the fraction of reflecting radiation to the total energy. Transmissivity is the fraction of the transmitted energy to the total energy and is a measure of the capacity of a material to transmit radiation. The sum of absorptivity, reflectivity and transmissivity is equal to 1 ($\alpha + \rho + t = 1$).

In the following sections some building design techniques and the limitations associated with each technique are discussed, such as:

- Design for the climate.
- Orientation effects.
- Shading and surrounding environment effects.
- Ventilation and air leakage.
- Thermal comfort.

2.1.2 Building Design for the Climate

Designing economical and energy efficient buildings that react to the climatic conditions found at the site, and which suit Australia`s different climates zones, require studying and analysing the impact of the different climate zones in Australia, as shown in Figure 2.7.

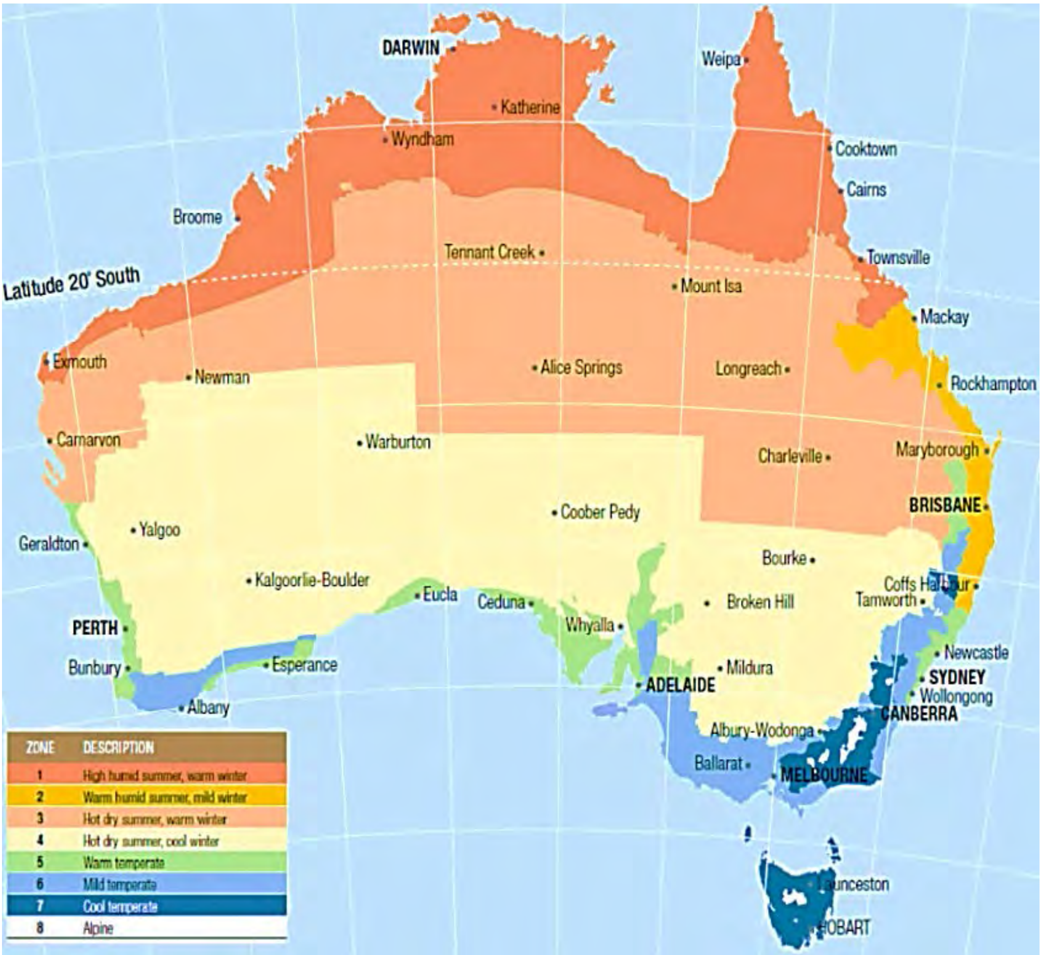

Figure 2.7 Australia’s Climate Zones (DCCEE 2011).

Improving the energy efficiency of the module could be achieved by general measures to avoid heat loss in all climates, such as:

- For Walls and Roofs:
  – Airtight construction (can save up to 25% of heating costs)
  – Bulk insulation
  – Thermal mass for the walls and floor
  – Passive heating using solar radiation in the winter months
- Windows:
  – Appropriately sized, oriented and shaded windows
  – Double glazed for better insulation.

There are general measures to avoid heat gain for all climates:

- Windows:
  – Small windows with proper orientation.
  – Shading and low-E glass for lower radiations absorption.
- Walls and Roofs:
  – Lightweight construction for rapid cooling.
  – Reflective Insulation and bulk Insulation.
  – Light colours to reflect radiation.
  – Airtight construction, especially when air-conditioning in use
  – Shading for external walls, for example by trees.
  – High thermal mass (where diurnal temperature swings are high).
  –Ventilation to dissipate heat from the building.

Each climate zone requires different design techniques which need to be addressed accurately by understanding these climate variables (include: solar radiation, rainfall, wind speed and direction and humidity).

Building design is important for saving energy and reducing GHG emissions (by applying passive solar heating and cooling design principal, and using the right materials and appropriate design tools). This will make the home healthier and more comfortable. For these reasons, a technical manual has been developed by DCCEE, to show how to design and build more comfortable homes that have less impact on the environment, are more economical to run, are healthier to live in and are adaptable to the climate changing. This manual gives general rules which apply in the different climate zones in Australia, as shown below.

2.1.2.1 Warm Summer, Cool Winter (Temperate Zone)

Figure 2.8 shows the temperate zone (warm summer and cool winter) in Australia which is mild to warm summers and cool winters.

In this climate the need for winter heating is greater than the need for summer cooling.

Figure 2.8.Temperate zone (DCCEE 2011).

The main features of a temperate climate are high diurnal (day/night) temperature range and four distinct seasons:

- Autumn: ideal human comfort range
- Winter: mild winters with low humidity which exceed the human comfort range
- Spring: ideal human comfort range
- Summer: hot to very hot summers with moderate humidity which exceed the human comfort range. For the summer months the temperature at night is lower than 20ºC. Allowing the cool night air in summer to ventilate the building to cool the air and dissipate the thermal mass heat of the walls make the building cool during the day.

Design requirements in a temperate climate:

- Most glass facing north, with shading designed to admit the sun's heat in winter, but not in summer.
- Internal thermal mass to soak up the heat during the day and reradiate it inside the building during the night.
- Air tight construction to minimise heat losses in winter.
- Light coloured roof which will reflect much of the sun's radiation in summer. Because the winter sun is lower in the sky, it shines more on the walls and windows than on the roof, so the loss of winter solar heating via the roof is not as great.
- Cross ventilation can cool the house by opening windows at night, and keeping them closed during the hot days.
- Shade the east and west walls in summer (trees can be used).

- In Melbourne, where there is not a lot of winter sun, north-facing glazing should be from 25 to 40% of the floor area. Windows in Sydney should be from 20 to 30% of the floor area (DCCEE 2011).
- Evaporative cooling does not work well in Sydney and Newcastle because of the higher summer humidity but works better in Melbourne and Adelaide.
- Ceiling insulation is needed for Sydney and Newcastle but more insulation is required for Melbourne and Adelaide.
- Using refrigerated air conditioning necessitates thicker ceiling insulation and insulating the floor.

Based on the weather data collected by the Bureau of meteorology, Australia has data for different climate zones but these data cannot be available for each construction site. With the climate changing this creates more challenges for the thermal assessment models to analyse the data in order to accurately design energy efficient buildings.

The main issue for designing buildings for a temperate climate zone is to accurately predict the thermal performance of a building. This requires real data for the building components under temperate climate conditions, not simplifying assumptions (Kordjamshidi and King 2009).

2.1.2.2 Hot Humid Climate

A hot humid climate, as shown in Figure 2.9, is located in the northern part of Australia.

Figure 2.9. Hot humid climate zone (DCCEE 2011)

North of the tropic of Capricorn the sun is in the southern sky during some of the summer. The summer (wet season) is hot, humid and usually the rainy season. The winter (dry season) is warm, dry and sunny.

Design requirements for a hot humid climate:

- Because of the high humidity, air movement is crucial to help perspiration to evaporate.
- Windows opposite each other to allow cross ventilation.
- Long, narrow floor-plan to maximise ventilation in bedrooms.
- Open-plan living areas with high ceilings, to maximise air movement and minimise radiant heat to the inhabitants.
- Elevate house to catch the breezes if the area is not directly exposed to tropical cyclones.
- Because it is hot and humid, evaporation cooling does not work efficiently.
- Building heat gain can be minimised by orienting the long axis of the house east-west for cross ventilation.
- Minimum window size on the east and west walls to decrease heat gain throughout the year.
- Ventilating the roof space to reduce accumulated heat.

Construction materials for the hot humid climate:

- Because the night-to-day temperature swing is small and the average outdoor temperature is too high for comfort, materials with high thermal mass, such as bricks and concrete are of little benefit. A lighter house construction (timber, fibrous cement) will store less heat and cool quicker at night.
- Window styles with good airflow, such as louvres rather than awning/hopper windows.
- Shading the walls and windows with suitable shutters, verandas and eaves.
- Light colours for walls and roof, to reflect the heat of the sun.
- If there is no air-conditioning, reflective foil insulation performs better than bulk insulation because it prevents the house cooling down at night.
- If there is air-conditioning it requires bulk insulation and double-glazed windows.
- Using metal to cover the roof which will dissipate heat quickly at night.

2.1.2.3 Hot Dry Zone with Warm Winter

Figure 2.10 shows the hot dry zone with warm winter in Australia, and its main zone characteristics are: hot summers, winter days may be warm and cool winter nights. Dry air with high sun glare. Big temperature differences between day and night.

Figure 2.10. Hot dry with warm winter zone (DCCEE 2011).

Because of the intense solar radiation we have to apply:

- Light coloured external surfaces to reflect the sun.
- Reflective foil insulation in the walls and roof. If air-conditioned, the building requires bulk insulation.
- Small north-facing windows and well shaded. The hotter the summer, the smaller the windows, but smaller windows will reduce night ventilation.
- If the house site is north of the Tropic of Capricorn, shading for any south-facing windows.
- No windows or very small windows on the eastern or western side of the house.
- Earth sheltered and underground housing – a large thermal mass to maintain the building's thermal comfort.
- Perfect climate to generate energy from solar power.
- Because of the low humidity of the air, evaporative coolers work well in the dry air, and use less energy.

Because of the large day/night temperature swing:

- Considerable thermal mass in the living areas to keep daytime temperatures down but the bedrooms should be of lighter construction so they cool quickly at night.
- Cross ventilation on summer nights is essential.
- Roof mounted exhaust fans for night cooling.

2.1.2.4 Hot Dry with Cold Winter

Figure 2.11 shows the hot dry with cold winter zone in Australia, which has: hot summers with high sun glare; winter can be cold, dry air; big temperature differences between day and night.

Figure 2.11. Hot dry with cold winter zone (DCCEE 2011).

Similar in some features to a hot dry climate, but with mild winters because of the large difference between summer and winter temperatures, shading is important to keep out the summer sun and to allow the winter sun to enter (trees may be used for shading around the house) and because the winter is cold:

- To allow solar passive heating in winter, windows (north-facing) should be larger than in a hot dry climate with a warm winter.
- Bulk insulation is required to reduce heat loss through the walls and ceilings. Moderate insulation for bedrooms with lighter construction to cool fast at night, with air tight construction to reduce heat loss.

2.1.2.5 Mild to Warm Summer, Cold Winter (Cool Temperate Zone)

Figure 2.12 shows the cool temperate zone in Australia, which is: mild to warm summers and cold winters and in the higher parts of the Snowy Mountains, snow can fall at any time of the year. In Tasmania, summer snow has been known to fall at elevations as low as 300 m.

Figure 2.12. Cool temperate zone (DCCEE 2011).

In a cool temperate climate, we need strategies as per the temperate zone, and more:

- North-facing windows with double glazing.
- East-facing windows with double glazing (with external shading to restrict the summer sun) to provide morning sunlight during the cooler months.
- Airtight construction with heavier bulk insulation.

2.1.3 Orientation Effects

A low cost option to improve comfort and decrease energy bills is to orient buildings correctly. Accurate orientation, correct location on a site, and landscaping changes may decrease the energy consumption of a typical building by 20% (Spanos et al. 2005).

There are two ways to ensure optimal orientation:

- Analyse various parameters and certify optimal design and orientation for each building but this approach consume more designing time and cost.
- Develop 'adaptable' designs which perform well across a range of orientations, which is used in the volume build industry (Morrissey and Moore 2011), but this approach does not give the optimal building orientation.

2.1.4 Shading Effects

The requirements for shading vary according to the house's orientation and the climate (to eliminate the summer sun and allow the full winter sun to enter the building). Shading in summer in a hot climate improves comfort and decreases energy bills, and on top of that appropriate shading reduces the chance of exposure to harmful UV rays in Australia.

There are two types of shading:

- Internal shading, such as blinds, rollers and curtains.
- External shading caused by overhangs or nearby trees or buildings.

For the current building thermal assessment model used in Australia, such as AccuRate, the internal shading is considered but not the external shading because it keeps changing with time (growing trees and new buildings constructed).

2.1.5 Influence of the Occupant's Behaviour

Occupant can save energy by:

- Closing doors to air-conditioned areas.
- Closing curtains to prevent heating in rooms from the summer sun.
- Adjusting shading and ventilation if necessary.
- Use energy efficient air-conditioning/fans with appropriate thermostat settings and switch off when not in use.
- Change clothes to adapt to the surrounding environment (heavier clothes in winter and lighter in summer).

A method of weighting the physiological, psychological and behavioural weightings of the adaptation thermal comfort process specifies that physiological adaptation is the leading aspect contributing to the establishment of an acceptable thermal environment, while the other two adaptations, the behavioural and psychological, and share similar weightings (Jing et al. 2012).

Occupant behaviour has a significant role in building energy consumption but it is impossible for software modelling to predict occupant behaviour for an accurate energy assessment. Occupants should take part in a building simulation and adapt to a wider range of weather conditions instead of relying on mechanical heating and cooling (more details in the adaptive thermal section).

2.2 Thermal Comfort

2.2.1 Overview

Thermal comfort is a single valuation of the state of mind that states the satisfaction with the thermal environment. Comfort temperature is not a fixed value for everybody as there are many influences which vary the comfort zone, such as air temperature, air speed and direction, metabolic rate, clothing levels, mean radiant temperature and the humidity. Inhabitant thermal comfort is calculated by finding the comfortable zone for a specified percentage of the occupants (ASHRAE 55).

To define the comfort necessities in buildings, the American Society of Heating, Refrigerating, and Air-Conditioning Engineers (ASHRAE) has developed an industry standard, which is known as the Thermal Environmental Conditions for Human Occupancy / ASHRAE Standard 55-2010. The main goal of this standard is to categorize the combinations of indoor thermal environmental and personal factors which create the thermal environmental conditions acceptable to a majority of the occupants (ASHRAE 55).

Finding the precise thermal comfort prediction in mechanically heated and cooled buildings can save large amounts of energy. These savings are probably above 50% (Ferreira et al. 2012).

Thermal comfort is defined by six variables (see Table 2.1): air temperature; wind velocity; mean radiant temperature and air humidity are obtained through sensors. On the other hand, clothing insulation and metabolic rate are determined by the user situation which is hard to accurately determine the exact value of (Castilla et al. 2011).

Table 2.1. Variables which define thermal comfort (Castilla et al. 2011)

Parameter	Range	Unit
Metabolic rate	0.8–4	Met (W/m^2)
Clothing insulation	0–2	Clo (m^2 ºC/W)
Mean radiant temperature	10–40	ºC
Air temperature	10–30	ºC
Air velocity	0–1	m/s
Air humidity	30–70	%

Where;

- Metabolic rate: the ASHRAE 55-2010 Standard defines metabolic rate as "*the level of transformation of chemical energy into heat and mechanical work by metabolic activities within an organism, usually expressed in terms of the unit area of the total body surface*". Metabolic rate is stated in Met units (1Met= 58.2W/m^2 (18.4 Btu/h·ft^2)), which is equal to the energy created per unit surface area of an average seated person (no activity) where the surface area of an average person is 1.8 m^2 (19 ft^2) (ASHRAE 55).

- Clothing insulation: measured by Clo, where 1Clo = 0.155m^2·K/W (0.88 °F·ft^2·h/Btu). The amount of clothing worn by somebody has a significant influence on thermal comfort because it impacts on the heat loss and, therefore, the thermal balance (ASHRAE 55).

- The mean radiant temperature (MRT): when the "*radiant heat transfer from the human body is equal to the radiant heat transfer in the actual non-uniform enclosure*" (ISO7726, 1998). The uniform temperature of an imaginary enclosure where the average temperature of the surfaces that surround a particular point which would result in the same heat loss by radiation from the person as the actual enclosure (ASHRAE 55).

2.2.2 Psychrometric Chart

The Psychrometric Chart helps to develop a suitable climate inside the building. It presents the relationship between the air temperature and the humidity in graphical form.

The main expressions needing to be understood before reading the Psychrometric charts are:

- Wet-Bulb Temperature (WBT) (ºC) is measured by a Sling Psycho-motor or a Hygrometer and is shown as inclined lines (see Figure 2.13).
- Dry-Bulb Temperature (DBT) (ºC) is the temperature of air measured by a thermometer wide-open to the air but sheltered from the sun’s radiation.
- Moisture Content of air at a given temperature can carry a specific quantity of vapour, given in grams or kg of vapour per kg of air. It is also known as saturation humidity, absolute humidity or humidity ratio.
- Percentage Saturation or Relative Humidity (%) which is the moisture content (at the same temperature) as a percentage of the saturation humidity.
- Specific Volume (m^3/kg) is the number of cubic metres of air filled by one kilogram of a water vapour and is shown as a group of slightly inclined lines on the Psychrometric chart.
- Specific Enthalpy (H) is the heat content of a unit mass of the atmosphere, in kJ/kg. It is indicated on the Psychrometric chart by a third set of sloping lines, near to, but not quite the same as the web-bulb lines.

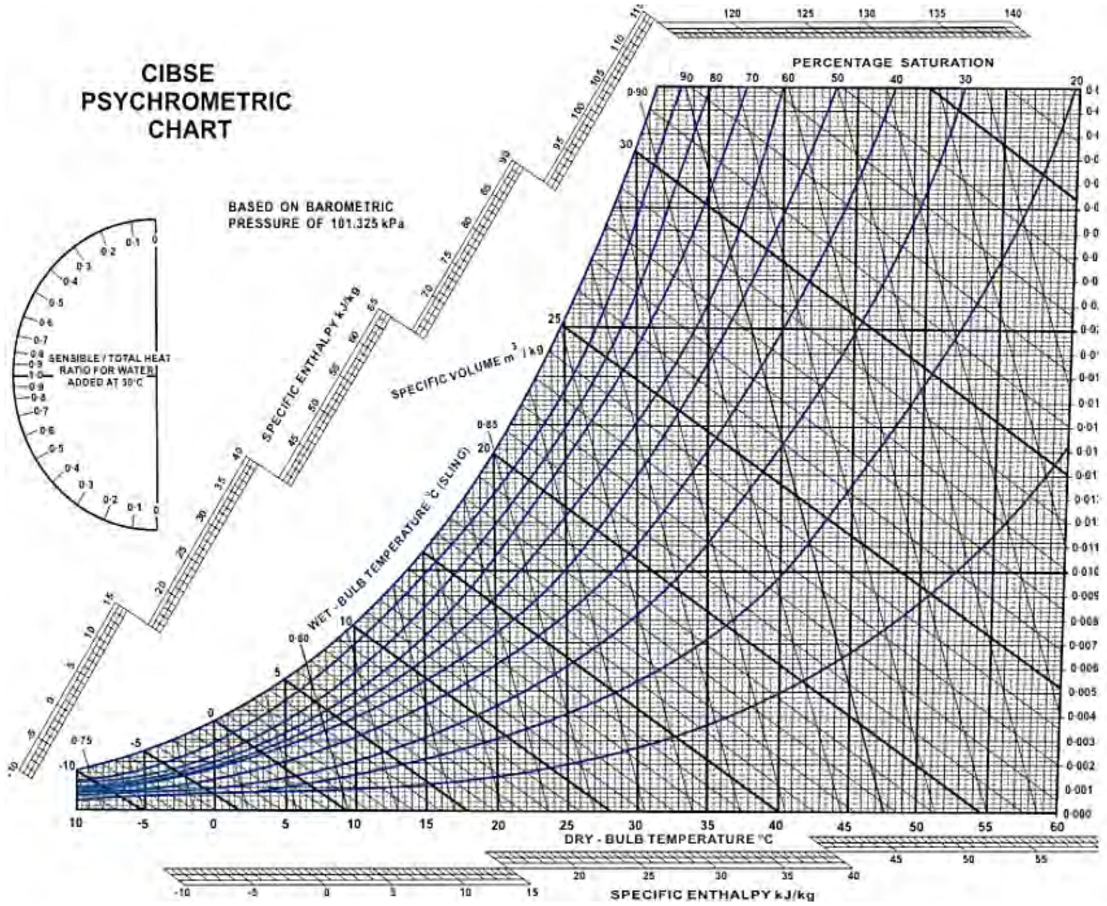

Figure 2.13. Psychrometric Chart (UHK 2010)

Note: In order to avoid confusion, there are no lines shown, but external scales are given on two sides (UHK 2010).

Different climates zones can be plotted in the Psychrometric chart as shown in Figure 2.14 and this will help to find the best technique to suite each climate zone, for example evaporative cooling is effective in regions or periods with high temperatures and low humidity (Bhattacharya 2010).

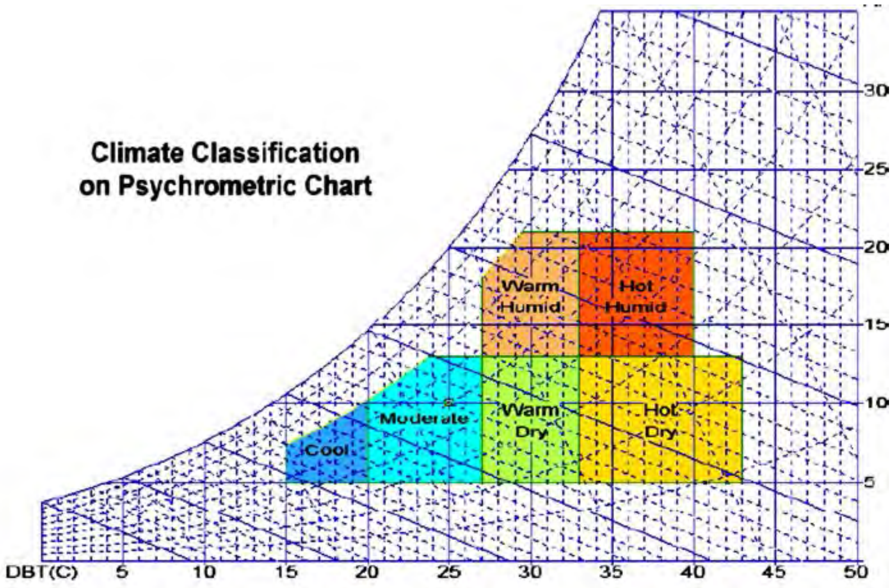

Figure 2.14.Psychrometric Chart for different climate conditions (HU 2006)

2.2.3 Main Thermal Comfort Models

There are two main thermal comfort modules used by ASHRAE Standard 55-2010:

1. The Predicted Mean Vote (PMV) and the Predicted Percentage Dissatisfied (PPD) Module.
2. Adaptive Thermal Comfort Module.

2.2.3.1 The Predicted Mean Vote (PMV) / the Predicted Percentage Dissatisfied (PPD) Module

Established using heat balance principles and data collected in a controlled climate chamber under steady state conditions. The PMV index calculates the mean response of the general public, according to the ASHRAE thermal sensation scale (Fanger, 1982):

+3 = hot

+2 = warm

+1 = slightly warm

0 = neutral

-1 = slightly cool

-2 = cool

-3 = cold

The acceptable thermal comfort range for PMV from the ASHRAE 55 2010 is between -0.5 and +0.5. Visual demonstrations are available at the Autodesk community website; http://sustainabilityworkshop.autodesk.com/buildings/human-thermal-comfort#sthash.sQcMOvnS.dpuf. The equations to calculate the factors for PMV have been implemented in a software tool that is available freely on: http://smap.cbe.berkeley.edu/comforttool (Tyler et al.2013).

By combining the function of the six variables with the thermal energy balance equations, the following relationship between the PMV and the thermal load is developed (CEAE 2005):

$$PMV = 3.155(0.303e^{-0.114M} + 0.028)L \qquad (2.1)$$

Where;

M: Rate of metabolic generation per unit surface area.
L: Thermal load.

PPD is the percentage of occupants that are dissatisfied with their thermal environments. The recommended acceptable PPD range for thermal comfort is less than 10% of occupants who are dissatisfied with their situation (ASHRAE 55 2010). PPD is a function of PMV (the average response of satisfaction among a large group of people), as shown in Figure 2.15 the empirical relationship between the PPD and the thermal environment as a function of the PMV (CEAE 2005).

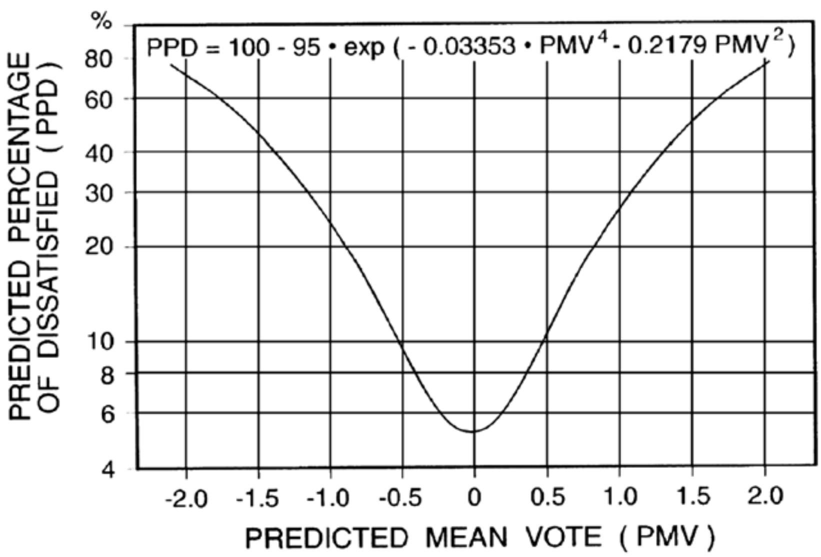

Figure 2.15. Relationship between PPD and PMV (CEAE 2005).

There are issues with the predicted mean vote (PMV/PPD), such as:

- PMV requires knowledge of clothing insulation and metabolic rate, which are difficult to estimate accurately.
- PMV to thermal comfort tries to find the response of occupants to the thermal environment, in terms of the physiology and physics of heat transfer, which is a complex procedure, without reflection to the psychological factor which plays a significant part in determining the suitable thermal comfort conditions (Nicol and Humphreys 2002).
- Many field studies propose that the PMV is challenging to use in the real world which leads to inaccuracies in the prediction of comfortable conditions (Nicol and Humphreys 2002).

A new method was established, called the adaptive thermal comfort, which helps building designers to calculate the comfortable internal air temperature in free-running buildings.

2.2.3.2 Adaptive Thermal Comfort Model

"*If a change occurs such as to produce discomfort, people react in ways which tend to restore their comfort*" (Nicol and Humphreys 2002).

The adaptive module was established, based on many field studies, with the idea that inhabitants dynamically interact with their environment by changing clothes, opening/closing windows, using low energy fans, drinking water and shades. One of the expectations of the adaptive hypothesis is that individuals in warm climates desire warmer indoor air temperatures than those who live in colder climates (De Dear and Brager 1998).

One of the main methods applied to create the adaptive thermal module is meta-analysis, which uses large databases of several thermal comfort field surveys, such as: Humphreys 1975–81 database (Humphreys 1981); the ASHRAERP-884 database (de Dear and Brager 1998; de Dearetal 1997), which was used to develop the ASHRAE adaptive standard (ASHRAE 2010). The steps used to find the meta-analysis method were (Toe et al. 2013):

1. Data classification by climate; classify each data file in the database to a specific climate zone according to the survey location.

2. Data consistency and refinement; checking the consistency of each variable to be analysed and refining the data where necessary. Variables analysed in the database included a thermal survey (subjective votes and personal variables), calculated indices (physical variables) and thermal indices (external weather conditions).

3. Analysis of the refined data base mainly by using linear or probit regression models.

Table 2.2 shows the adaptive module's thermal comfort temperature for different locations.

Table 2.2. Adaptive modules for different locations (Wang et al. 2010).

Adaptive module	Location	Reference
$T_c = 0.42T_o + 15.12$	Shanghai, China	X.J. Ye et al. 2006
$T_c = 0.31T_o + 17.6$	Singapore	Dear et al. 1991
$T_c = 0.31T_o + 17.8$	Australia	Dear and Brager 1998
$T_c = 0.534T_o + 11.9$	Australia	Humphreys and Nicol 1998
$T_c = 0.38T_o + 17.0$	Pakistan	Nicol et al. 1999
$T_c = 0.31T_o + 19.4$	Europe	K.J. Mc Cartney, 2002
$T_c = 0.16T_o + 18.3$	Hong Kong	K.W.H. Mui et al. 2003
$T_c = 0.52T_o + 10.35$	Tunisia	Bouden and Ghrab 2005
$T_c = 0.486T_o + 11.8$	Harbin, China	Wang Z et al. 2010

Figure 2.16 shows the way in which the results can be used to calculate the ideal comfort temperatures at different times of year. Comfort temperature (T_c) for Islamabad, Pakistan, is calculated from the outdoor temperature T_o using;

$$\mathbf{T_c = 12.9 + 0.534T_o} \qquad (2.2)$$

Note: T_o is calculated as the mean of the monthly mean maximum ($T_{o\ max}$) and minimum ($T_{o\ min}$) is the average max/min outside air temperature (Nicol and Humphreys 2002).

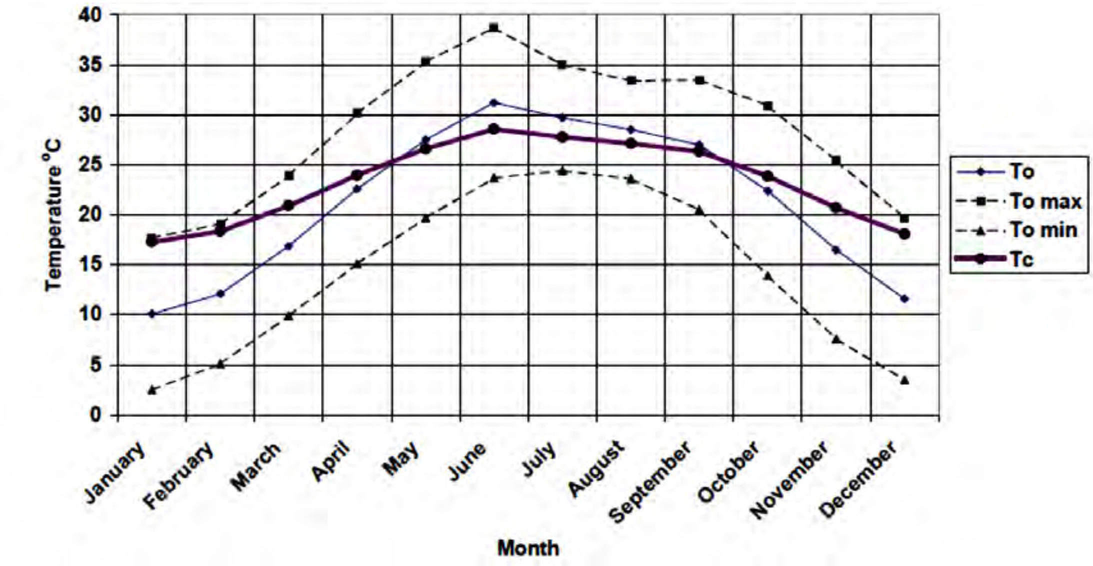

Figure 2.16. Comfort temperature and outside average, max and minimum air temperature for Islamabad, Pakistan (Nicol and Humphreys 2002).

A comfort zone of 2–3ºC either side of the ideal thermal comfort temperature can be considered as an acceptable limit. If fans are available, another 2ºC either side can be added to the comfort zone in hot dry climates and 1ºC in humid climates (Nicol and Humphreys 2002). This range of temperatures matching 90% and 80% ***acceptability limits***, could reach around 30°C according to the adaptive method in the ASHRAE 55-2010 Standard, as shown in Figure 2.17 (Tyler et al. 2013).

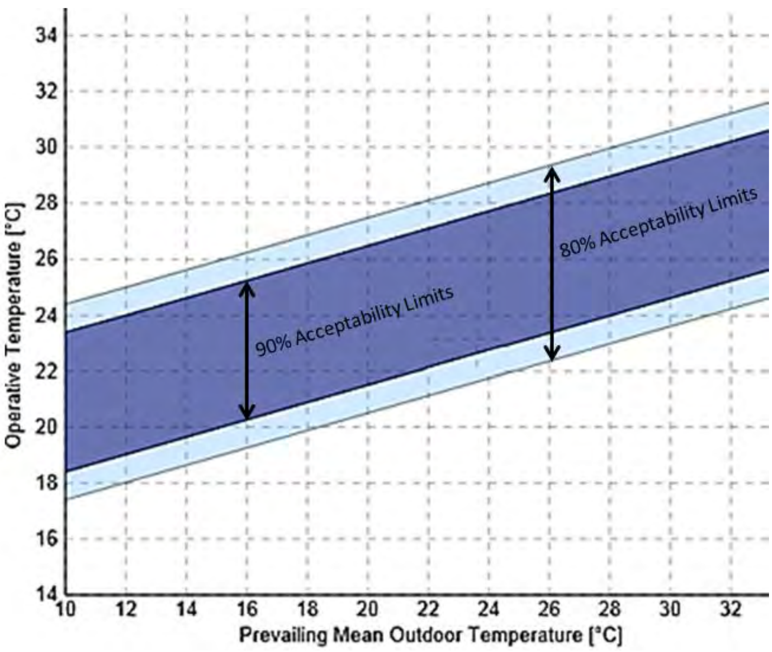

Figure 2.17. The 90% and 80% acceptability limits for indoor operative temperature based on the prevailing mean outdoor temperature (Tyler et al. 2013).

Field studies identified the comfortable temperature and acceptability limits at 80% for naturally ventilated buildings, for different locations, as summarized in Table 2.3.

Tables 2.3. Comfortable temperature and acceptability limits at 80% for different locations (Wang Z et al. 2010).

Location	Comfort temperature (◦C)	Acceptability limits at 80% (◦C)	Reference
Brisbane, Australia	25.5		De Dear and Auliciems 1985
San Francisco, USA	22.6	21–26	Schillerl 1988
Bangkok, Thailand	28.5		Busch, 1990
Brazil	Summer 21.7. Winter 24.1	20.7–25.2	Paula Xavier et al. 2000
Singapore	28.5		De Dear et al. 1991
Hawaii, USA	27.4		Kwok 1998
Iran	28.4	25.1–32.8 at 75% 27.1–30.9 at 90%	Heidari and Sharples 2002
Indonesia	29.2/26	23–30.5	Feriadi et al. 2004
Singapore	29.3/25.1		Wong et al. 2002
Singapore	28.8	27.1–29.3	Wong et al. 2003
Karlsruhe, Germany	23.5		Wagner et al. 2007
Hyderabad, India	29.23	26–32.45	M. Indraganti 2010
Beijing, China	26.7		Y.Z. Xia et al. 1999
Changsha/ Guangzhou/ Shenzhen, China	28.6/22.8		J. Han et al. 2007
Shanghai, China	27.0 (July) 28.1 (August)	14.7–29.8	X.J. Ye et al. 2006
Harbin, China	24.0–28.0	21.5–31.0	Wang Z et al.2010

One of the main advantages of the adaptive thermal comfort module is that air speed and humidity are not required to be calculated. However, to understand the impact of air speed and humidity on the inhabitants' thermal comfort, the data from the occupants about whether the windows and doors were opened or fans running, while they were responding to the thermal comfort questionnaires, was considered in the analysis (Soebarto and Bennetts 2014).

Field experiments carried out in 10 naturally ventilated and 26 air-conditioned classrooms using survey and physical measurements indicated that humidity has a very low statistical impact on the thermal comfort (Hwang et al. 2006).

2.2.3.3 Relationship between PMV and Adaptive Thermal Comfort

Operative indoor temperature limits (comfortable temperature) are given as a function of the running mean outdoor temperature (T_{ref}) for two similar building types in Netherland Alpha and Beta. T_{ref} is calculated from the averages of the maximum and minimum outdoor (air) temperature of the day under study and the three earlier days (van der Linden et al. 2006):

$$\mathbf{T_{ref} = (1T_{today} + 0.8T_{yesterday} + 0.4T_{day\ before\ yesterday} + 0.2T_{day\ before\ day\ before\ yesterday}) / 2.4} \qquad (2.3)$$

Limits are specified for 90%, 80% and 65% ***acceptability limits*** where the 90% acceptability limit is equivalent to the +0.5 Fanger PMV limit and 10% PPD which means that 90% of the occupants are satisfied during at least 90% of the time (van der Linden et al. 2006).

Designing new energy efficient buildings requires thermal simulation software to find the accurate temperature inside the buildings, which is then used to find the building's energy consumption (heating and cooling loads) to sustain thermal comfort.

It is challenging to calculate the shading, ventilation and air leakage as it keeps changing with time so a new approach is needed for new and existing building energy assessment in order to capture the entire range of variables which is impossible for the current building energy assessment programs to capture.

2.3 Computational Fluid Dynamics (CFD)

There are two main methods to analysis the gradients, i.e. CFD and Finite Element Analysis (FEA). The FEA method is usually used in the stress concentration analysis whilst the CFD method simulates fluids performance including heat transfer, combustion and thermodynamic effects. The main reason of selecting CFD was the nature of the problem which involves the analysis of solar radiation, humidity, air temperature and movements. Although, FEM may be used for the analysis of the temperature gradient for solids (i.e. walls, slab and roof) but it would be difficult to accurately simulate the convection effects of the air. CFD is well recognized in range of applications in building design, from building site layout design to individual room planning. It has been used in various applications where fluid analysis was required such as active heating, ventilation and air-conditioning system design (Zhai, 2006).

2.3.1 CFD Techniques

Computational Fluid Dynamics (CFD) is a simulation technique that mathematically simulates fluid flow and heat transfer. Computational Fluid Dynamics (CFD) is a branch of fluid mechanics that uses numerical methods and algorithms to solve and analyse problems that involve fluid flows (BMT 2014).

Computers are used to perform the calculations required to simulate the interaction of liquids and gases with surfaces defined by boundary conditions. With high-speed supercomputers, superior results can be accomplished. Continuing research has produced software that improves the precision and speed of complex simulation scenarios, such as transonic or turbulent flows (Ajmire and Nilesh 2013).

CFD is a powerful tool that creates a virtual airflow and building thermal model to evaluate and optimise a design before construction begins. Changes to an existing building can also be assessed using CFD prior to any renovations. This method has the advantages of decreasing design risks and avoiding costly inaccuracies while allowing innovations and improvements (BMT 2014).

CFD has been playing an increasingly important role in building design by contributing to achieving a comfortable, healthy, and energy-efficient building design. CFD can be used in a wide range of applications in building design, from building site layout design to individual room planning. It can also be used for active heating, ventilating and air-conditioning (HVAC) system design through to passive ventilation studies, and from consistent indoor air quality valuation to serious fire smoke and toxin control (Zhai 2006).

Autodesk Simulation CFD software turns a 3D CAD workstation into a fully interactive flow workbench. 3D gatherings become zero-cost prototypes showing critical engineering information and data not obtainable from physical experiments. Immediate results are obtainable if any changes take place to the design (Autodesk 2014).

Computational Fluid Dynamics (CFD) has been playing an increasingly important role in building design, following its continuing expansion for decades. Some of these energy simulation programs BES coupled with computational fluid dynamics where CFD simulations use a small time-step and BES handles a long-term simulation (Zhai et al. 2001, 2002, 2005, 2006; Yi et al. 2013).

The results provided by CFD can be used to analyse whole buildings to find the internal air temperature at any point inside the building but using CFD for long-term simulations results in excessive computing time.

Autodesk Simulation CFD can be used throughout the design process by systematizing the procedures by applying settings directly in the CAD model and then connecting (export) CAD model designs in the Autodesk Simulation CFD to designs, studies and analysis. Throughout the design, development and marketing processes of any project CFD can be used (Autodesk 2014):

- In the concept stage, CFD can be used to try new ideas and designs, optimise various scenarios, understand the implications of the concept before starting the design process and determine how it will perform in the real world.

- In the development stage, CFD can be used to analyse the effects of design changes to reach a final design that brings the projected performance.
- For the marketing stage, CFD can be used to visualize the products/ideas by creating 2D and 3D images and videos that show the design assets and advantages.

2.3.2 CFD Applications

CFD can be used in a wide range of building design, such as:

- **Site Planning**

The first phase of building design is site planning. CFD can assist in optimising building sites by calculating humidity, temperature, air velocity, turbulence concentrations and pollutant concentrations surrounding the buildings. It can also improve energy efficiency by optimising passive HVAC by using natural ventilation for summer (Zhai 2006).

Applying CFD for building site design has become more convenient since CFD can import AutoCAD building site design into the CFD computational domain for analysis. The main obstacle is the lengthy computing time due to the great number of mesh grids and nodes essential to shield the design structure and the computing time becomes greater when dynamic wind conditions are applied (Zhai 2006).

- **Natural Ventilation Analysis**

Optimising natural ventilation is one of the most essential methods to decrease energy consumption in buildings (in summer, by allowing cool air to enter the building and, in winter, by preventing cold air from inflowing). CFD can simulate indoor and outdoor airflows to reach optimal natural ventilation.

- **HVAC System Design**

CFD was used to assess the thermal comfort and air quality generated from various HVAC models to reach efficient and operational system designs. It is more comprehensive than the conventional analysis methods which depend on the use of various companies' charts and equations (Zhai 2006).

- **Regulate Pollution and Dust**

CFD was able to simulate the movements of pollutants with a high degree of accuracy and low costs. Also it can be effortlessly applied to examine the effect of a specific flow factor (air temperature or wind speed) or the scattering of a specific pollutant in extremely hot conditions or contaminated situations (Zhai 2006).

The main issues with CFD analysis for prolonged simulation are: its lengthy computing time (Wang and Wong 2009; Tan and Glicksman 2005; Hong et al. 2000; Hulme et al. 2005); internal air temperature increases with longer simulation periods (warming up); smaller fluctuation range; discrepancies in peak temperature time; and applying wind to the external surface. This research will find new ways to solve these issues to accurately simulate the thermal performance of buildings for long periods (weeks and months).

The main purpose of this research is to verify the validity of the ATM, proposed for the first time in this study, to characterise the thermal performance of complete buildings using the internal air temperature obtained from CFD simulations. An additional aim of this research was, with appropriate adjustments, to achieve 100% thermal comfort inside the housing test modules for all weather conditions without using any energy from fossil fuels (with all the required energy coming from renewable energy systems).

2.4 Renewable Energy Systems to Improve Thermal Performance

Renewable systems will be used to provide the modules with the required energy to obtain thermal comfort instead of using energy from fossil fuels for appropriate heating and cooling. This section will discuss the main systems which can be used to improve the thermal performance.

2.4.1 Energy Required Inside the Building to Reach Thermal Comfort

Finding the amount of solar heat gain required to provide the occupants with sufficient amount of heat to reach thermal comfort and compensate any heat losses.

The steady state equation to calculate total heat required inside the building (Soteris et al. 2003):

$$\mathbf{Q_{total} = Q_i + Q_c + Q_s + Q_v + Q_e} \tag{2.4}$$

(The positive value for heat flow going into the building and negative values for heat flow out of the building), where;

Q_i: Internal Heat Gains

Heat generated inside the building by appliances, inhabitants and lighting which increase the temperature in the building.

Q_c: Conduction Heat Losses/Gains

Conduction heat losses between the outside environment and the interior temperature can be calculated through this equation;

$$\mathbf{Q_c = \Delta T \times \Sigma (A \times U)} \tag{2.5}$$

Where;

U: Overall heat transfer co-efficient.
A: Surface area (m^2).
ΔT: Temperature difference between inside and outside environment.

Q_s: Solar Heat Gain and Heat from the Solar Collector

Energy from solar radiation fallen on the collector can be calculated by;

$$\mathbf{Q_s = G \times A \times SHGC} \tag{2.6}$$

G: Irradiance (W/m^2)
A: Surface area (m^2)
SHGC: Solar heat gain coefficient for the collector (collector efficiency).

Q_v: Ventilation Losses

Ventilation is crucial to sustain a healthy indoor environment but it will cause some heat losses in winter which can be calculated through the following equation;

$$Q_v = \mathring{m} C \Delta T = \rho \mathring{V} C \Delta T = 0.33 N V \Delta T \tag{2.7}$$

$\mathring{m}$: Mass flow rate of air (kg/s).
ρ: Density of air (typically 1.2 kg/m^3)
C: Heat capacity of air constant pressure
N: Number of air changes per hour
V: Volume of the zone (m^3)
$\mathring{V}$: Volumetric flow rate of air (m^3/s)
ΔT: Temperature difference between inside and outside.

Q_e: Evaporative Losses:

When water changes phases from liquid to gas it requires this amount of energy;

$$Q_e = 667 \times m_{ev} \tag{2.8}$$

Where;

m_{ev}: The evaporation rate (kg/hour)
667: Latent heat of the evaporation of water (Wh/kg)

This number 667 is derived from the latent heat of the evaporation of water per hour (2400,000 J/kg /3600 seconds/hour = 667 Wh/kg).

2.4.2 Solar Heating Systems

Solar heating systems absorb solar energy through a solar collector then transform it to heat which can be used for space heating, as shown in Figure 2.18. Minimum energy requirements to run active solar air heating systems are mostly for the auxiliary equipment, such as the air pump/fan and the equipment's controls. Using the sun's energy to heat the space is called an active solar air heating system while passive solar air heating systems use backup heaters to heat the air. Most solar air heaters use air as the working fluid inside the system.

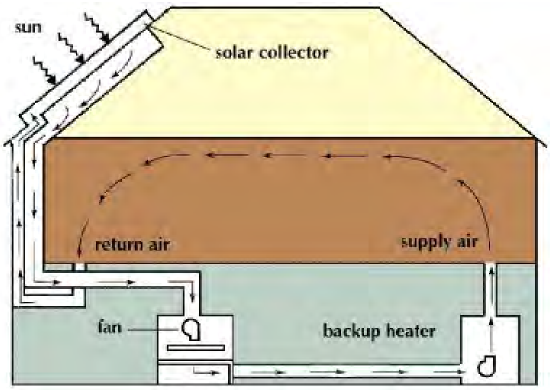

Figure 2.18. Active and passive solar air heating systems (Your solar energy home 2013).

Types of Active Solar Air Heating Systems

The main types of active solar air heating systems, based on the collector types, are glazed and unglazed solar collectors.

- **Glazed Solar Collector**

Solar air heating systems with flat glazed collector are the most common types of solar collectors, as shown in Figure 2.19.

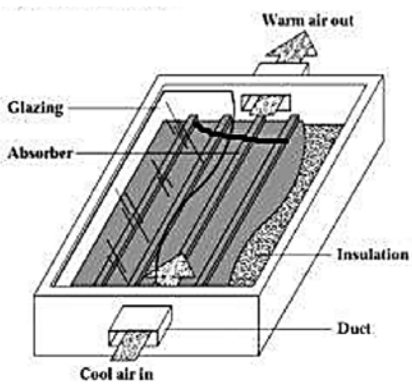

Figure 2.19. Glazed solar air collector (Solar retrofit 2015).

Glazed solar collectors absorb the solar radiation into a high absorptivity black duct inside the collector to heat the air used in building heating. The glazed cover of the collector is vital to shield the collector from the outside environment to achieve greater air temperatures. Glazed solar air collector efficiency can reach up to 75% of the solar energy absorbed and transferred to the air used for heating.

- **Unglazed Solar Air Heating Collector**

Flat plate solar air collectors without a glass cover cost less than the glazed collector but have lower efficiency because the heat losses to the environment are greater because of the wind. One of the main types of unglazed solar air heater collector is the transpired air heating collector, as shown in Figure 2.20.

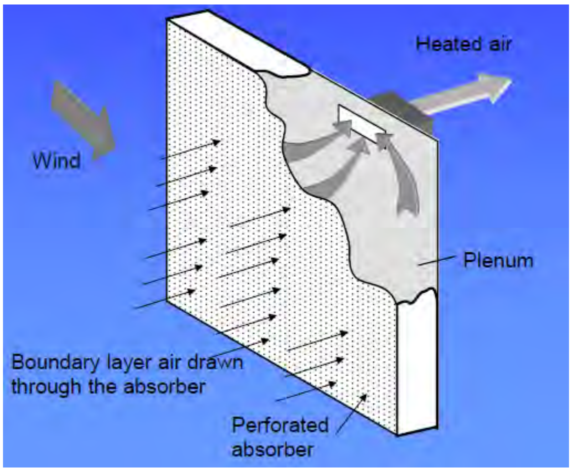

Figure 2.20. Unglazed transpired air heating collector (Enerconcept 2015).

When solar radiation reaches a transpired air heating collector some heat is absorbed by the perforated absorber and the hot air mounts up inside the collector. When hot air needed for heating the fan pull air from outside to go through the small holes in the absorber (plenum) to the collector and heated the air by mixing with the trapped hot air in the collector (Bodycote 2013).

In unglazed collectors, the efficiency rises with a higher flow rate because the heat losses become less since the collector rapidly transfers the heat from the collector to the building. When solar radiation increases, the temperature inside the collector increases, and decreases when the air flow rates increase, this takes the hot air away from the collector and replaces it with cooler air, as shown in Figure 2.21.

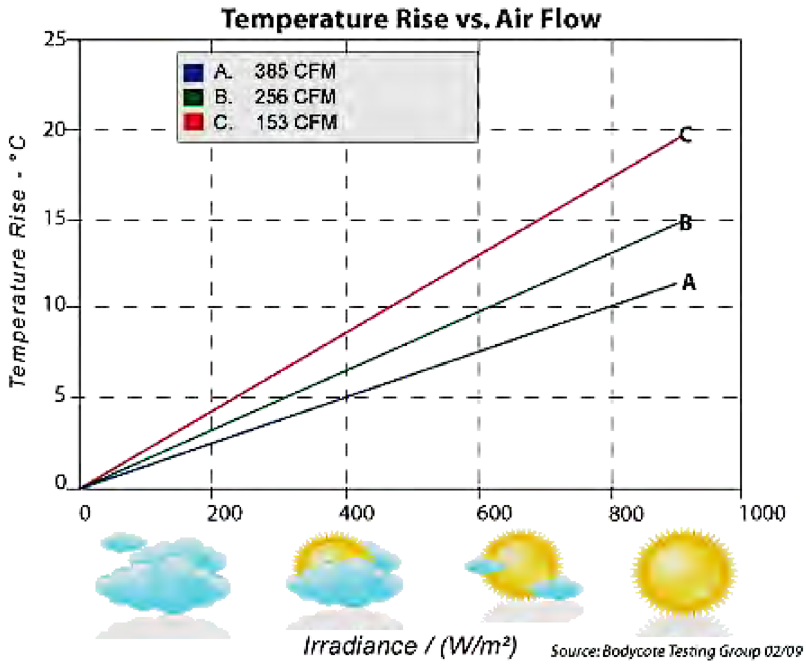

Figure 2.21. Temperature rise from solar radiation and air flow rate (CFM: Cubic Feet per Minute) (Bodycote 2013).

The size of a solar air heating system depends on a building's location (latitude), wind speed, solar radiation and the amount of energy required to obtain thermal comfort inside the building. The main elements affecting the size and solar collector type are;

- **Building location and type:** location is important to determine the shading and roof accessibility.
- **Wind speed and direction:** When solar panel facing the wind direction or located in higher wind speed area that is required using glazed collector to minimize heat losses.
- **Solar radiation:** the amount of solar radiation falls on the collector especially in colder months.
- **Energy required:** as discussed in Section 2.4.1.

2.4.3 Evaporative Cooling

In evaporative cooling systems, air is cooled by pulling the air through a wetted film or a spray of water. When water is evaporated, cooling proceeds by absorbing the energy needed to transform water from a liquid to a vapour from the building's interior air. Evaporative cooling is an energy efficient method for cooling which just requires energy to run the fan that circulates the air over the evaporator and a pump that moves the water, as shown in Figure 2.22. However, evaporative systems can use considerable quantities of water from10 to 30 litres per hour, depending on the size of the evaporative unit and the air humidity (Basix).

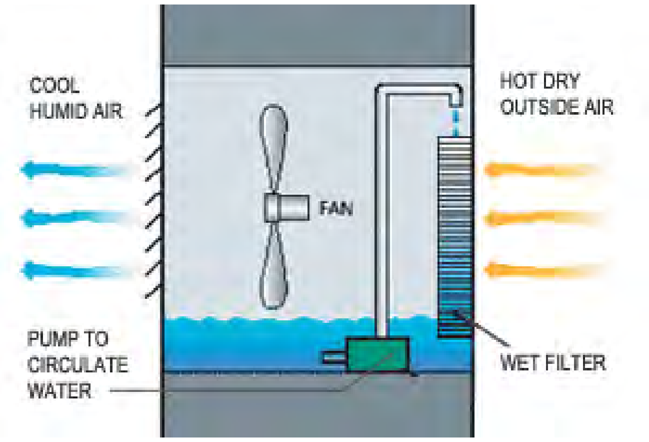

Figure 2.22. Evaporative cooling unit (Basix).

There are two types of evaporative cooling systems:

- **Direct Evaporative Cooling**: occurs by passing air directly over a wetted film or spray of water.
- **Indirect Evaporative Cooling**: this cools the main air via a heat exchanger. Therefore, the primary air is not moistened which uses less water but is less efficient.

In humid zones evaporative cooling will not operate effectively. If it is hot and humid, the gap between the dry and wet bulb temperatures is small and the cooler will not be able to lower the temperature of the air by much. Using a Psychrometric Chart will assist in finding human thermal comfort conditions. Applying different passive strategies (passive solar heating, thermal mass, natural ventilation, direct and indirect evaporative cooling) helps to expand that comfort zone.

2.4.4 Photovoltaics Systems (Building-Integrated Photovoltaics (BIPV))

Photovoltaics systems (PV) convert solar energy into electrical energy. The main components of Photovoltaics systems are: solar panels to absorb solar radiation and convert it into electricity; inverters to change the electrical current from DC to AC; fuses to protect the system from electrical overloading; and it may also include a solar tracking system to improve the system's overall performance. Some systems contain an integrated battery for storage, as shown in Figure 2.23.

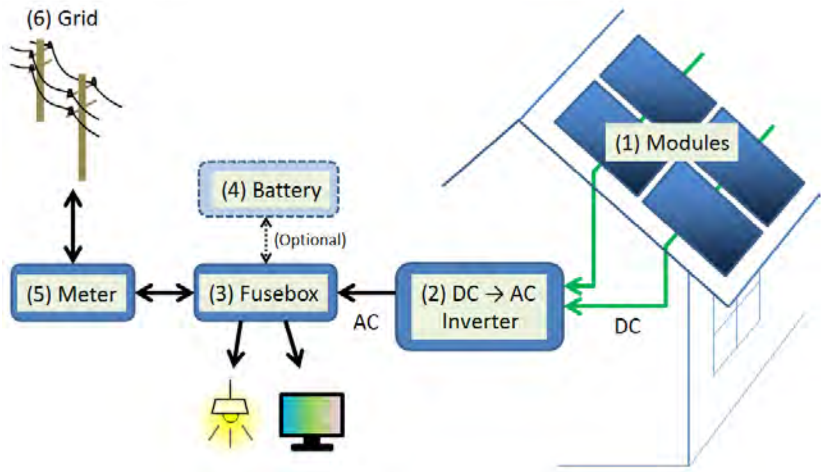

Figure 2.23. Simplified schematic diagram of a PV system (Solar Cells 2013).

Solar PV systems can supply much of a household's energy needs. The size of the system depends on the household's energy requirements; the amount of solar radiation falling on the panels; and the location and shading on the panels. The typical PV system conversion efficiency from 15-20% of the total falling solar energy on panels (Fraunhofer Institute 2015) which is vary throughout the year but are usually averaged as shown in Table 2.4.

Table 2.4. Monthly and annual average solar radiation for different cities (kWh/m^2) (Australian Solar Energy Society 2015).

Month	Melbourne	Sydney	Perth	Darwin	Brisbane	Adelaide	Hobart
January	6.9	6.7	8.2	5.4	6.5	7.8	6.3
February	6.4	5.8	7.2	5.2	6.2	7.3	5.6
March	5.2	5.7	6	5.6	5.7	6.3	4.1
April	3.8	4.4	4.3	5.9	4.8	5	2.8
May	2.8	3.6	3.1	5.6	4.2	3.8	1.8
June	2.4	3.4	2.5	5.3	4.1	3.5	1.4
July	2.7	3.3	2.7	5.5	4.2	3.4	1.7
August	3.3	4.4	3.5	6	5.2	4.4	2.4
September	4.3	5.2	4.7	6.3	6	5.3	3.5
October	5.3	5.8	6.1	6.5	5.9	6.5	4.8
November	6.1	6.3	7.2	6.4	6	7	5.7
December	6.6	6.9	8.1	5.9	6.3	7.46	6.2
Average	4.6	5.1	5.3	5.8	5.4	5.6	3.9
Total annual solar irradiation ($kWh/m^2/year$)	**1679**	**1862**	**1935**	**2117**	**1971**	**2060**	**1424**

One of the interesting photovoltaic system types is building-integrated photovoltaics (BIPV), which are photovoltaic materials that are used to replace conventional building materials, such as the roof, shading devices or facades, as shown in Figures 2.24 and 2.25. The main advantage of BIPV is that the initial cost can be compensating for by reducing the amount spent on the building materials replaced by BIPV.

Figure 2.24. BIPV Roof - BMW World, Munich (BMW Group)

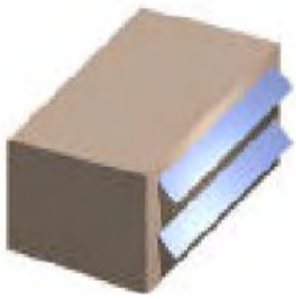

Figure 2.25. BIPV used for shading (Taiwan Solar Energy)

2.4.5 Wind Systems

Wind systems extract wind energy to produce electrical power. The main wind system components are the wind turbine, charger/controller, battery bank and invertor. The wind system layout is shown in Figure 2.26.

Figure 2.26. Domestic wind turbine (Green Remodelling 2014).

There are restraints control the power generated from wind turbine, the turbine blades need minimum wind speed to overcome friction and begin to rotate which called cut in wind speed, when the wind speed peaks the wind turbine generate maximum power till wind reach cut out wind speed at this moment the blades are brought to rest to avoid damage from high wind speed (Wind Power Program 2013).

Wind speed in a cubic relationship with output wind power and the wind turbine generate power only when wind speed between cut in wind speed and cut out wind speed as shown in Figure 2.27.

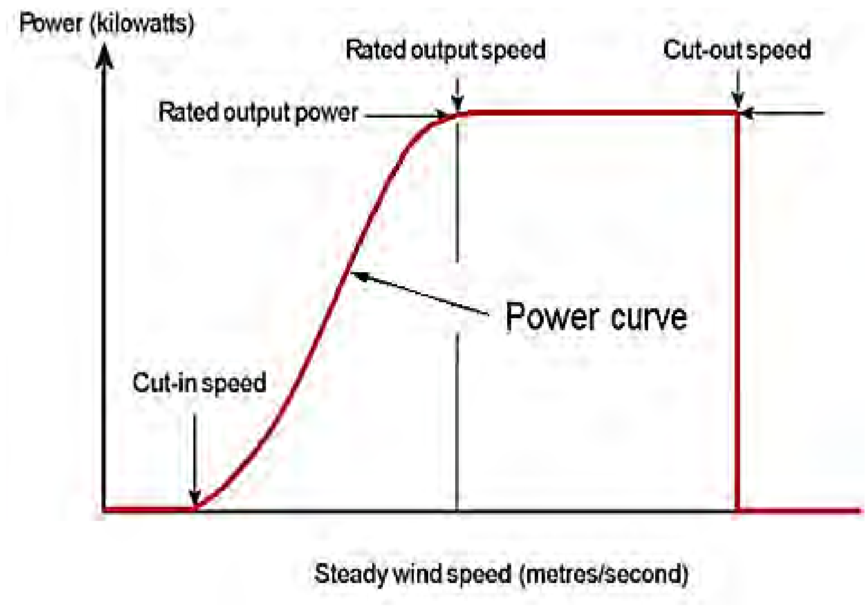

Figure 2.27. Typical wind turbine power output (Wind Power Program 2013).

It is impossible for wind turbines to capture all the wind energy, therefore the theoretical maximum power percentage a wind turbine can extract is less than 59% of the wind energy according to Betz law. Wind power in watts can be calculated through this equation:

$$\mathbf{(P) = 0.5 * \rho * A * v^3} \qquad (2.9)$$

Where;

ρ: Density of air (kg/m^3).
A: Swept area of the rotor blade (m^2).
v: Wind speed (m/s).

Wind turbines need smooth wind flows (no turbulence) and are not disturbed by obstacles, such as steep hills, cliffs, trees, buildings. Coastal locations and flat rural areas without substantial trees or buildings offer the best wind flow for wind turbines.

2.4.6 Hybrid Systems

Hybrid systems such as wind and photovoltaics systems combined as shown in Figure 2.28 can be used to take a full gain of seasonal and daily variations in wind and solar resources by using more than one technology combined to sustain the power supply.

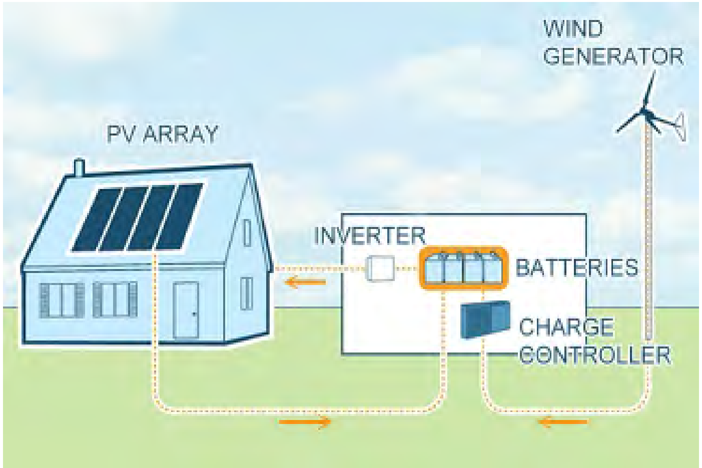

Figure 2.28. Wind-PV (Solar) hybrid power system (Nanjing 2015).

2.5 Housing Energy Rating Methods

2.5.1 Energy Rating Methods of a Complete System

Many factors influence the thermal performance of a complete building, some of these factors are self-governing, while others are inter-related, and not all factors affect the thermal performance of the building in the same way as some have a greater influence than others (Rabah 2005).

These many variables are changing all the time, which makes it challenging to precisely calculate the thermal performance of a complete building. To achieve an accurate thermal performance of a building, account must be taken of the building as a complete system (Alterman et al. 2012).

Buildings and their heating, cooling and ventilation systems have become significantly more varied and complex in recent years, which affects the accuracy of the existing thermal assessment packages. The enormous numbers of materials, glazing systems, wide range of passive techniques, different construction types and heating and cooling systems have become broader and more complex. In addition, the move towards highly insulated, more airtight, low energy buildings has modified the energy balances so the internal and solar energy gains have a much greater effect (Strachan 2011).

Heat transfer in buildings is in dynamic conditions with continuous change with time. There are different methods for solving dynamic heat transfer equations, such as the heat balance method, the admittance method, various finite difference methods, and even electrical circuit solving programs, but these modules have huge numbers of inputs, elements and variables, such as:

- The physical elements of the building (e.g., orientation, width, height, length)
- The thermal properties of all the elements (e.g., thermal conductivity, heat capacity, R-value)

- The climatic conditions (temperatures, solar radiation, wind speeds and direction, humidity)

To solve all these variables, a set of equations describing the heat flow through all the elements and the heat stored inside the elements. However, these large numbers of coupled differential equations are usually solved numerically.

The key to efficient design is the implementation of a factor which correctly encapsulates the influences of the thermal mass and insulation properties under a dynamic temperature environment. A more representative parameter than the R-value is essential to fully capture the dynamic thermal behaviour of a building's walling system (Alterman et al. 2012).

A new thermal performance factor has been developed at the University of Newcastle. It is called the dynamic temperature response (T-value), which encapsulates the impact of all of the physical parameters affecting the thermal performance of walls, which not only accounts for the wall thermal resistance (R-value), but also its thermal mass (Alterman et al. 2012).

There are three principal approaches to house energy rating based on the energy consumption of a building (Kordjamshidi 2010):

- **Prescriptive Approach:** Offer least standards for the materials, equipment and the methods and it are mandatory to meet the requirements for an energy efficiency evaluation such as Deemed-To-Satisfy Provision.
- **Calculation-based Approach:** Used computer based softwares to calculate building thermal performance then compare to that mandatory in each country/ state in order to be eligible for construction under the program such as AccuRate in NSW, Australia.
- **Performance-based Approach:** Applies real building energy consumption records to assess a building's energy efficiency then compares these with the compulsory standards required in the proposed construction area. This approach is applicable to existing buildings only.

The prescriptive and calculation approaches are more dominant, while the performance-based rating approach is uncommon because it is time-consuming to collect the data (Kordjamshidi 2010).

The precision of any thermal simulation has direct consequences on the estimation of the thermal performance of any building, so the results of any simulation should imitate the real performance of the building.

Current building assessment systems lean towards creating a number of simplifying assumptions and results in inconsistencies between the free-running mode and the conditioned mode. For example, an efficient design for a building in a conditioned running mode differs from exactly the same building in the free-running operation mode, which is a primary reason for the incapability of existing energy based rating schemes to effectively assess a building's performance in a temperate climate (Kordjamshidi and King 2009).

A comparison of Home Energy Rating Systems (HERS) ratings and real utility billing data for about 500 houses in four states in the United States found that HERS can, on average, forecast annual energy cost accurately. However, on an individual house basis, the match between the predicted energy cost and the actual energy cost was often poor, especially for older houses

There are a wide range of building assessment tools and the comparison between the tools and their results are very difficult because different tools were designed for evaluating different types of buildings, they are applied to different stages of the life cycle, and depend on different guidelines, databases and questionnaires (Haapio and Viitaniemi 2008).

2.5.2 Australia's Housing Energy Rating Methods

The main energy rating schemes in Australia are:

2.5.2.1 Nationwide House Energy Rating Scheme (NatHERS)

The Nationwide House Energy Rating Scheme (NatHERS) was introduced in 1998 using the CSIRO's simulation software named CHEETAH, then CHENATH.

The NatHERS simulation tool was criticised for allowing inadequate natural ventilation to maintain comfort, especially in subtropical and tropical regions of Australia. The ventilation segment in the NatHERS simulation did not account for opening sizes, wind direction and building location. To solve these issues, in 2002 the Australian Greenhouse Office decided to support and fund a major restoration of NatHERS and introduced the new simulation engine CHENATH (Delsante 2005). The Commonwealth Scientific and Industrial Research Organisation's (CSIRO) Manufacturing and Infrastructure Technology Division agreed to develop the second generation simulation program, known as AccuRate (Delsante 2005).

2.5.2.2 AccuRate Software

AccuRate Sustainability (V2.3.3.13 SP1) is a rating tool that gives a star rating to a residential building in Australia, based on its calculated annual heating and cooling energy requirements (not its energy consumption, because the efficiency of heating and cooling equipment is not considered). A building's assessment is quantified as a star rating between 0 and 10, with the more stars, the better the performance. Star ratings (bands) are set for each specific climate zone for an unbiased comparison of buildings through different climate zones (AccuRate Sustainability, V2.3.3.13 SP1).

Occupant behaviour is taken into account in AccuRate and this intensely affects the calculated heating and cooling energy. The following characteristics of occupant behaviour are considered (AccuRate Sustainability, V2.3.3.13 SP1):

- Number of hours for heating and cooling inside each zone.
- Thermostat settings in winter and summer.
- Windows and other openings to increase ventilation.

- Adjustable outside and inside window's shading/covering.

The large inconsistencies between the AccuRate results and the measured temperatures in various building zones necessitates an additional examination for the ongoing development and adjustment of the AccuRate software to avoid compromising the precision of the heating and cooling loads and, therefore, the accuracy of the star rating (Geard 2011).

The second generation AccuRate energy assessment tool improved the user-defined construction, sub-floor spaces, natural ventilation, horizontal reflective air gaps, modelling of roof spaces and the accessibility of a wider range of zones. A lack of confidence in the accuracy of AccuRate arose when it was shown to be incapable of modelling heavyweight building elements (Daniel et al. 2013).

2.5.3 International Rating Tools

Most developed countries have different building assessment programs, such as:

- Green Star (Australia).
- Leadership in Energy and Environmental Design, LEED (US).
- ASHRAE Building Energy Quotient. ASHRAE BEQ (US).
- Department of Energy, DOE energy asset rating (AR, US).
- EnergyPlus (US). https://energyplus.net/
- Cal-Arch A California Building Energy Tool for Owners and Operators (US).
- Building Research Establishment Environmental Assessment Methodology, BREEAM (UK).
- Energy Assessment and Reporting Methodology-Office Assessment Method, EARM-OAM (UK).
- House Energy Labelling Procedure, HELP (EU).
- ELO for large buildings (>1500 m^2) EM for small buildings (Denmark).
- EPA-W for existing dwellings, EPA-U for existing non-residential, EPC for new buildings (Netherlands).
- "*Energiebedarfsausweis*" for new buildings and renovated buildings (Germany).

- Energy Advice Procedure, Energy Charter, Passive House Platform (Belgium).
- Energy Performance Assessment for Existing Dwellings (EPA-ED), Energy Performance Assessment for Non-Residential Buildings (EPA-NR) (EU).
- A Method to Assess the Energy Performance of Existing Commercial Complexes (HK).
- Hong Kong Building Environmental Assessment Method, HK-BEAM (HK).
- Energy efficiency diagnosis for air conditioning systems (China).
- Energy Smart Office Label (Singapore).

The next sections will outline the leading energy simulation programs used in US, United Kingdom and in Europe.

2.5.3.1 Energyplus

EnergyPlus is an energy simulation program for a whole building which is able to compute energy consumption, lighting, HVAC, ventilation and water usage. EnergyPlus development was financed by the U.S. Department of Energy Building Technologies Office.

EnergyPlus has large databases of building materials and components. EnergyPlus includes many simulation abilities such as time steps of less than an hour, heat balance and air flow analysis for each area, photovoltaic systems, and thermal comfort (U.S. Department of Energy (DOE)). In EnergyPlus users are able to use smaller time steps for accurate interaction between thermal zones and the environment. However using larger time steps allows EnergyPlus to simulate faster but with less accurate results.

2.5.3.2 BREEAM

BREEAM (Building Research Establishment Environmental Assessment Methodology) is an assessment method and rating system for buildings where more than 250,000 buildings have been BREEAM certified and over a million are registered for certification. Many counties including the UK used BREEAM for building simulation as shown in Figure 2.29 (BREEAM).

Figure 2.29 Countries used BREEAM for building simulation (BREEAM).

A BREEAM assess a building's materials, layout and construction type. They include aspects related to energy consumption and water usage, contamination and waste management methods (BREEAM).

2.5.3.3 House Energy Labelling Procedure (HELP)

The main idea of the House Energy Labelling Procedure is to attain the building thermal behaviour from uninterrupted recording of internal air temperature inside the building in response to outdoor temperature, humidity, wind and solar radiation, and to the internal loads come from mechanical heating and cooling.

These recorded parameters are then used to calculate a Normalized Heating Annual Consumption (NHAC) for a standard environment and operation of the building which help to establish point temperature and air change rate (Richalet et a1, 2001).

2.6 Knowledge Gap with the Current Rating Modelling Software

The accuracy of any thermal simulation has substantial effects on the prediction of the thermal performance of a building. The outcomes of any simulation should replicate the actual performance of the building, but current rating modules have issues, such as:

- Current building assessment methods are entirely energy-based approaches. Energy estimation is highly variable and there are great differences between theoretical and real results, which prove the incapability of energy-based approaches to accurately predict the thermal performance of buildings.

- Existing assessment programs encourage energy consumption when they require using energy to obtain thermal comfort, which is not an energy sustainable approach.

- Existing thermal assessment tools making various assumptions lead to significant differences between buildings in free running and air conditioning mode. This is mainly due to the incapability of energy based rating systems to effectively assess the influence of passive design in a temperate climate (Kordjamshidi and King 2009).

- There are a wide range of variables affecting the thermal performance of buildings. Some of these variables are independent, while others are related to each other, and all variables have different impacts on the thermal performance of the building. This creates a greater challenge to accurately calculate the thermal performance of a complete building (Rabah 2005).

- The main issue for designing buildings for temperate climate zones is to correctly predict the thermal performance of a building, which needs real data for the building materials, under temperate climactic conditions, not assumptions used by the modelling software.

- Currently, climate data is based on historic climate data, assuming the climate will remain stable, but this is not the case as the climate is changing. For example, the current heating and cooling loads estimation were based on average historical weather data called typical meteorological year (TMY) without considering the future climate change. This will make building systems design exposed to climate change, and to the more extreme weather conditions, resulting in inaccuracy in thermal energy prediction leading to increased energy consumption and less thermal comfort.

- Most energy assessment programs choose from a limited range of materials and some input data cannot be changed by the user. For example, the typical meteorological year in AccuRate cannot be changed.

- In AccuRate, internal shading is considered, but it still cannot accurately predict the heat gain or loss because it is hard to predict occupant behaviour inside the building. External shading is also considered, but since the external shading is constantly changing (growing trees, more leaves in spring than in winter, construction of more building) this creates real challenges for assessment tools.

- Air leakage accounts for 5%-25% of the energy lost. There are many variables affecting air leakage, such as wind speed and direction, outside and inside temperature, humidity, and the leakage area, which make it difficult for the energy model software to capture all the variables and accurately predict the future energy consumption for the building.

- Ventilation depends on the building openings and the wind speed. These are nearly impossible to predict because the nature of the openings depended on the occupant's behaviour (which is hard to predict) and the wind speed which is highly variable and unpredictable. This leads to differences between projected theoretical energy loads (by the energy assessment modules) and the real world energy consumption.

- The success of the R-value as a sole predictor was only observed from light weight walling systems (low thermal mass) not for high thermal mass walls. This is despite the fact that the R-value of the walls is not the only properly needed to define the thermal performance of a building, the energy demand and the thermal comfort (Page et al. 2011).

- Heat transfer in buildings is not in a steady-state condition but constantly changes with time (a dynamic condition). There are different methods for solving dynamic heat transfer, but since these modules require large numbers of inputs and variables, and powerful software/tools are needed to fully capture the dynamic thermal behaviour of the building.

- The number of material types, glazing systems, passive options, construction methods, heating and cooling equipment has become broader and more complex so the simulation tools need constant updating (Strachan 2011).

- There is a need for a universal approach to the assessment of energy performance applicable anywhere around the world. Energy assessment programs differ from country to country, and there are no building energy assessment programs for most developing countries.

2.7 Summary

The design of energy efficient and sustainable buildings is critical for the future. A key aspect of any design is the realistic and accurate prediction of the performance of the building under a wide range of weather conditions. This in turn requires an effective tool (or tools) to predict the internal conditions and thermal comfort. A number of modelling and assessment tools exist, but for the reasons outlined, they are not entirely effective.

A new universal metric is therefore needed to characterise and compare the thermal performance of complete buildings. This metric needs to capture the impact of all of the physical parameters influencing the thermal performance of the building and thus needs to account for the building's thermal resistance (R-value), thermal mass, structure, orientation, shading, occupant behaviour and the weather at the site. The development of such a metric is described in the ensuing chapters of this thesis.

Chapter Three: Approach and Methodology

3.1 Overview

As described in this chapter, several tools have been used in this research to develop the Adaptive Thermal Metric (ATM). Previous research at the University of Newcastle in this area has resulted in the availability of an extensive data set of the thermal performance of individual walls, of four full scale housing test modules in Newcastle under a range of weather conditions and of an actual house in Seville Grove in Western Australia. This enabled the simulated CFD results for the internal air temperatures for each module to be compared with the actual data over a one year period to assess the accuracy of the CFD simulation.

The adaptive thermal comfort model is used to define the ATM and assess its accuracy by comparing it with AccuRate. The Autodesk Ecotect is then used to calculate the monthly heating and cooling loads to find ways to improve the building energy efficiency.

3.2 Full-Scale Housing Test Modules

An intensive research program has been in progress in the Priority Research Centre for Energy at the University of Newcastle, Australia for more than ten years. This research has included the construction and monitoring of four full-scale housing modules (see Figure 3.1) under a variety of weather conditions. Each module was selected to characterize typical forms of local construction in Australia and are located at the University of Newcastle (UON), Callaghan campus (151.7 longitude and -32.89 latitude) (Page et al. 2011). The four modules are:

- Cavity Brick (CB)
- Insulated Cavity Brick (InsCB)
- Insulated Brick Veneer (InsBV)
- Insulated Reverse Brick Veneer (InsRBV)

Figure 3.1a. The south/west side of housing modules.

Figure 3.1b. The northern face of one housing module.

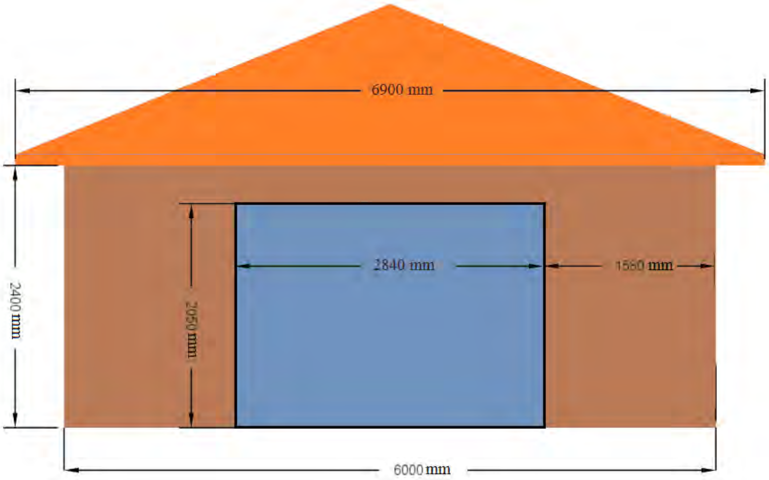

Figure 3.1c. North plan.

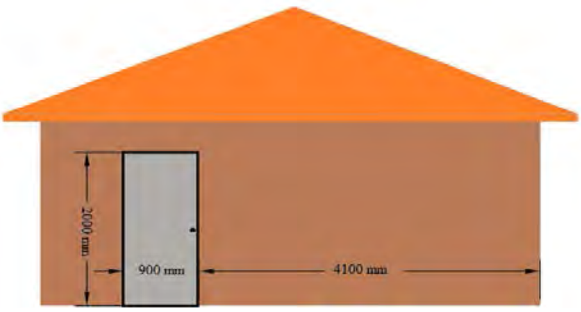

Figure 3.1d. South face

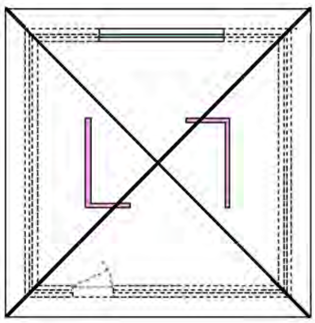

Figure 3.1e. Top view plan

All modules have a square floor plan of 6m x 6m and are spaced 7m away from each other to avoid shading and to minimise wind shielding. The details of the wall systems used are summarised in Table 3.1 (Page et al. 2011).

Table 3.1 Module elements and material configurations (Page et al. 2011).

Module Element		**Material Configurations**	**Modules Type**
External walls	Cavity Brick	Two 110mm brickwork skins with 50mm cavity between the walls and 10mm render covered the internal walls	CB
	Insulated Cavity Brick	Two 110mm brickwork skins with 50mm cavity with R1 polystyrene insulation and 10mm render covered the internal walls	InsCB
	Insulated Brick Veneer	Internal timber frame covered by low glare reflective foil and R1.5 glass wool batts covered by 10mm plasterboard. External walls constructed using 110 mm brickwork skin	InsBV
	Insulated Reverse Brick Veneer	Internal walls: 110mm brick skin covered by 10mm internal render. External walls: 2-3mm acrylic render on 7mm fibro-cement sheets fixed on timber stud frame insulated by R1.5 glass wool batts	InsRBV
Roof	Clay	Clay tiles over a layer of foil sarking	InsCB, CB
	Concrete	Concrete tiles over a layer of foil sarking	InsBV
	Metal	Coated corrugated sheets over a layer of foil sarking	InsRBV
Door		2040 x 820mm standard solid timber door insulated by 75mm thick layer of polystyrene foam	InsCB, CB, InsBV, InsRBV
Window		2050 x 2840mm clear glass set in a light coloured aluminium frame	InsCB, CB, InsBV, InsRBV
Ceiling		10mm plasterboard and R3.5 glass-wool batts between rafters	InsCB, CB, InsBV, InsRBV
Slab		Concrete slab	InsCB, CB, InsBV, InsRBV

A major opening (window) was installed in the northern wall of each module, representing approximately 20% of the floor area (a typical living room / floor area ratio) to more accurately imitate the influence of the different walling systems to solar passive behaviour. Each module includes two internal L-shape walls 2m x 1m in plan with a height of 2m and 110mm thick (see Figure 3.1c). The ceilings were heavily insulated with R3.5 glass wool batts to minimise/eliminate heat losses through the ceiling (Page et al. 2011).

105 sensors were fitted in each module to record internal and external conditions, full details for sensor locations in Appendix A. The data were recorded using Datataker DT600 data loggers every 5 minutes for 24hours/day over the testing period. Temperatures were recorded at different heights inside the module (600mm, 1200mm and 1800mm) with no ventilation (airtight building modules).The temperature inside each module was determined only by the influence of the external weather conditions (free-floating state) and no heating or cooling was applied (Page et al. 2011).

The external weather conditions (air temperature, wind speed and direction, relative humidity, ground temperature, incident solar radiation on each wall surface and roof) were recorded for each module. The internal environment conditions (temperature and heat flux profiles through the walls, slab and ceiling, internal air temperature and relative humidity) were also recorded (Page et al. 2011).

3.3 Real Building-Case Study

The Western Australian house used in the study is located near Perth, where the weather is warm and sunny most of the year. This climate zone is unique in Australia because it has more sunny days per year than any other Australian capital city. In the summer months (December - February) the weather is warm to hot, and the hottest months are usually January and February. Autumn (March - May) has warm sunny days and cooler nights. Winter (June - August) is the rainy season, with cool sunny days. In spring (September - November), the days are warm and sunny (Weather in Perth 2015). The monthly average maximum and minimum temperatures for Perth are shown in Table 3.2.

Table 3.2. Mean maximum/minimum temperature for Perth (Weather in Perth 2015)

Temperature	Jan	Feb	Mar	Apr	May	Jun	Jul	Aug	Sep	Oct	Nov	Dec
Mean maximum temperature (°C)	31.7	31.9	29.7	25.5	21.8	18.9	17.9	18.5	20.1	22.6	25.8	28.9
Mean minimum temperature (°C)	17	17.5	15.9	12.9	10.4	9	8	8	8.8	10.2	12.7	14.9

The house, as shown in Figure 3.2, is located in Verdant Circuit, Seville Grove, Western Australia, Australia 6112 (Latitude = -32.131166, Longitude =116.000648). The closest weather station recording air temperature every minute is Jandakot Aero (Station numbers: 009172). The house was designed and built by HIA GreenSmart Professionals Jade Projects in partnership with Think Brick Australia.

The internal air temperature was recorded at 5 minute intervals in each room for the testing period to assess the thermal performance of the house.

Figure 3.2 Western Australian house (GreenSmart Building)

The house has three bedrooms and one activity area, an office, kitchen and family room, as shown in Figure 3.3. A detailed floor layout is provided in Appendix B. The total area of the house is 168.4 m^2 (160.1m^2 air-conditioned and 8.3m^2 unconditioned), the house was built using insulated cavity brickwork for the external walls with bulk insulation R 1.5, and the internal walls were built using single skin brickwork. 18^o Hip and Gale were used for the roof with a volume of 198m^2, and plasterboard bulk insulation R2.5 was used for the ceiling. There is a concrete slab on the ground for the floor with no insulation. Full details of the construction materials used in this house are provided in Appendix C.

Sensors were installed in each room inside the house to record the temperature every 5 minutes over one year. The sensor locations are shown in Appendix D.

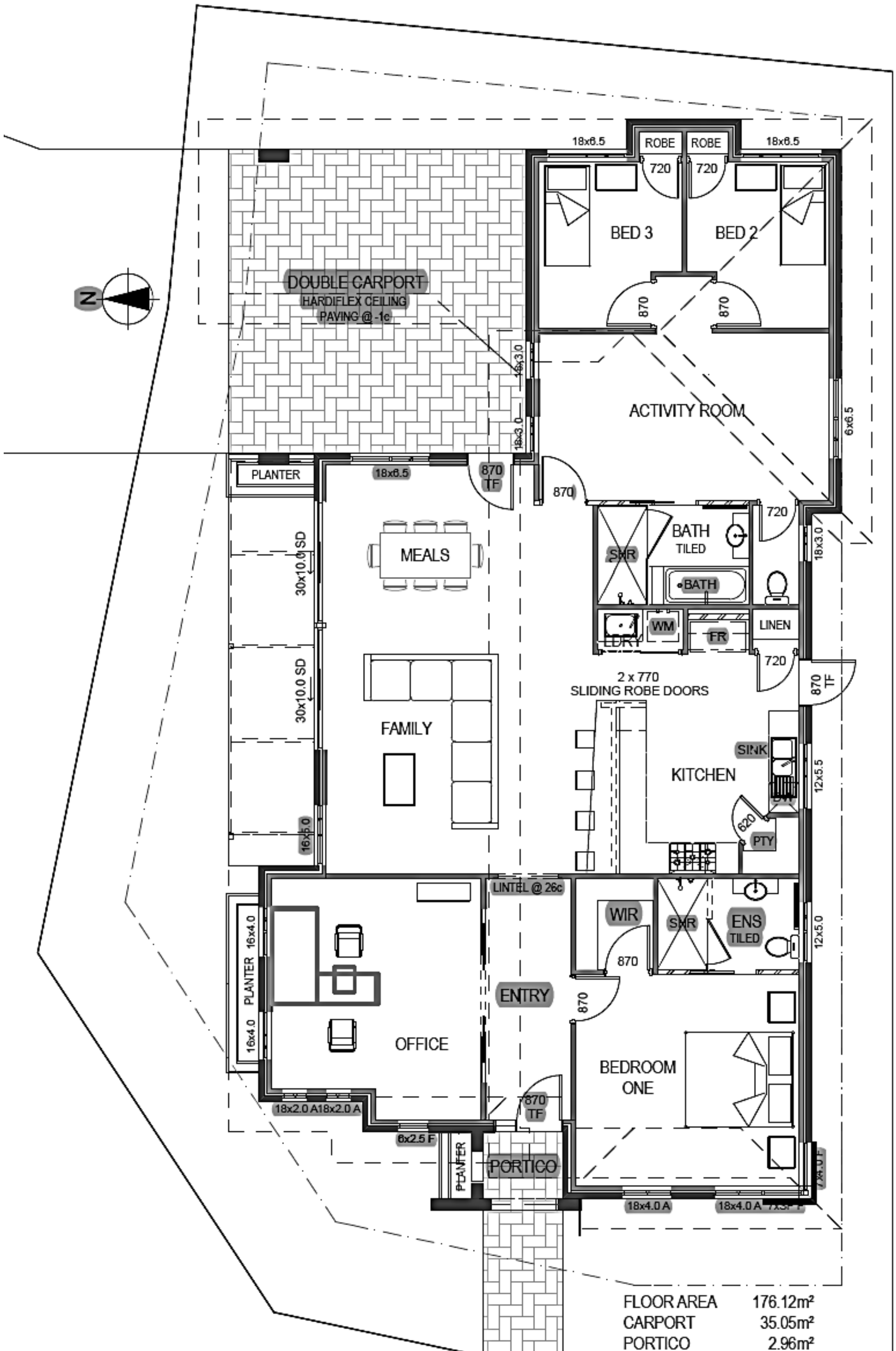

Figure 3.3. Floor plan for WA house (GreenSmart Building)

3.4 Computational Fluid Dynamics (CFD)

Computational Fluid Dynamics is an established simulation technique that mathematically simulates fluid flow and heat transfer. CFD analysis can be used to analyse whole buildings to find the internal air temperature at any point inside the building. CFD is not specifically designed to calculate a module's internal air temperature over long periods. It can be used for this purpose but lengthy computing times are required. Usually, CFD is used to evaluate a building's short term thermal performance and coupled with other programs to predict prolonged performance, such as Building Energy Simulation (ES), to avoid this excessive computing time (more details in Section 2.3) .

The first step in developing the ATM is determining the internal air temperature of a building under varying external conditions. The variations of internal air temperature of the four housing test modules with different walling systems can be compared to the simulated CFD results for the same modules, in order to determine the accuracy of the CFD simulations. The CFD modelling can then used to find the average volume temperature inside each module.

Each of the four modules were analysed using Autodesk Simulation CFD (2014). The CFD modules were modelled based on the actual physical characteristics and properties of each module to obtain results as close as possible to those recorded from the housing test modules. The simulations were based on the measured outside air temperature and the wind speed and direction recorded from the housing test modules. The simulation results were then compared with the actual air temperature recorded inside each module. The results from the CFD simulation are then used in the next stage.

General steps for an Autodesk CFD building simulation are (Autodesk 2014):

- Create CAD drawing for the real modules using Inventor Fusion 2013 R1 then launch/export it into the Autodesk Simulation CFD.
- Use geometry to perform these key functions: set the analysis length units, state the coordinate system for the 2D modules and access the geometry tools.

- Allocate materials to all parts in the module and assign boundary and initial conditions.
- Generate the mesh where the geometry is divided into small pieces called elements and the corner of each element is a node. These elements and nodes form the mesh.
- Start to solve the analysis using different time steps, where smaller time step sizes take a longer computing time.
- Results used visualization tools to help monitor, analyse, and present the results.

The geometrical characteristics of each module and their material properties were modelled using Inventor Fusion 2013 R1 then launched into the Autodesk Simulation CFD. A large external environment of a 100m x 100m x 100m external volume, in the shape of a cube to surround the building, was constructed in the CFD. Then the material properties for each module were assigned with the same thermal properties as the real modules.

A transient temperature boundary condition was applied to the surface of the external volume surrounding the modules and initial conditions applied, based on real data collected from the housing test modules.

An automatic mesh was generated for an analysis of the module (an automatic topological examination of the analysis geometry used to find the distribution on every element and the mesh size). In these analyses, 67,567 elements and 264,534 nodes as well as k-epsilon turbulence modelling for numerical/solver settings were used, then a grid independence test was conducted to ensure that the CFD simulation was correct.

A transient solution mode, heat transfer, flow and radiation were enabled and calculated in the CFD simulation software by entering the exact location and date of the real modules. The solar heating function was also enabled with the latitudinal and longitudinal position of the housing test modules reflecting their locations. An appropriate date, time and orientation were also entered to reflect the real conditions.

3.5 Autodesk Ecotect

The Autodesk Ecotect analysis program is sustainable building design software for building energy analysis which can perform thermal analysis to estimate a building's heating and cooling loads. This has the potential benefit of saving operating energy throughout the life time of the building. Psychrometric charts are the most commonly used tool for analysing this aspect of the climate in Autodesk Ecotect (Autodesk Ecotect 2011).

Ecotect can simulate and calculate the monthly heating and cooling loads for each module. The building geometry and material characteristics are input to Ecotect and the zone conditions setup which enables Ecotect to calculate the monthly heating and cooling loads

Also a Psychrometric chart tool is available within the Ecotect weather tool to incorporate human comfort areas into the climatic data on the chart (see Figure 3.4).

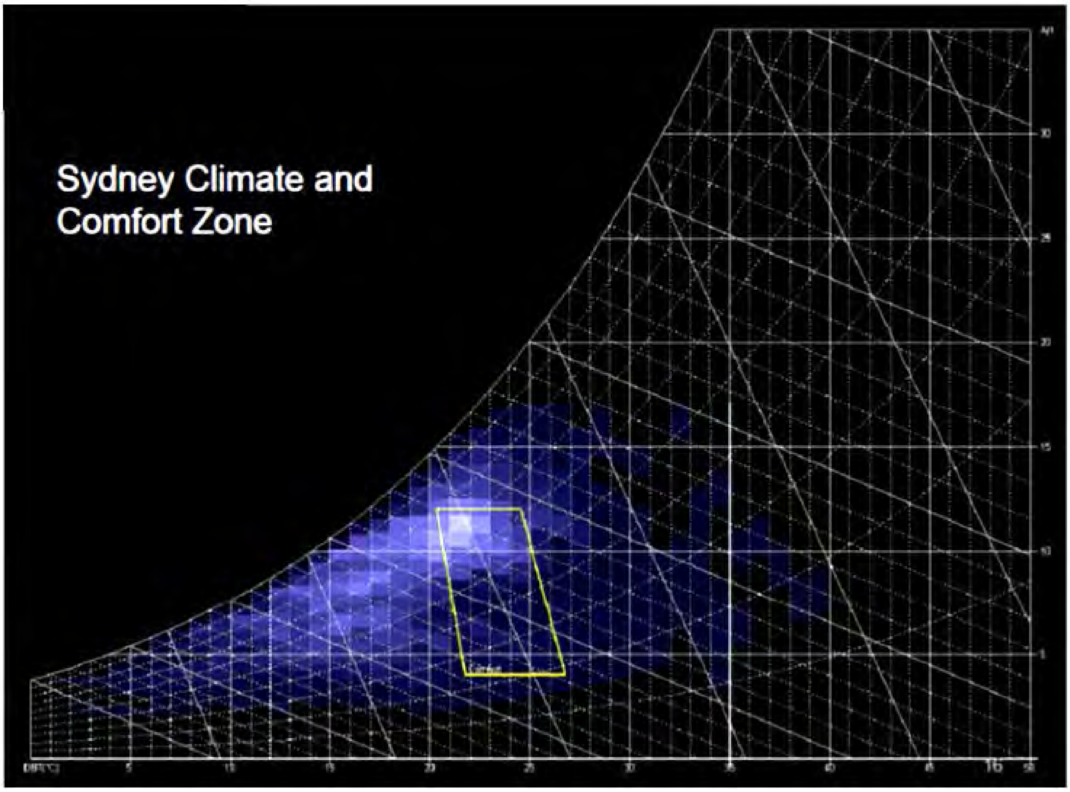

Figure 3.4 Sydney climate and comfort zone in yellow rectangle (Spoul 2012).

3.6 AccuRate

AccuRate Sustainability (V2.3.3.13 SP1) is a rating tool that assigns a star rating to residential buildings in Australia, based on its calculated annual heating and cooling energy requirements. The assessment of the building is stated as a star rating of between 0 and 10, the more stars, the better the performance (more details in Section 2.5.2.2).

Star ratings (bands) are set for each specific climate zone to allow fair comparison of the buildings across climates. Using one year of typical weather data appropriate for the location, the heating and cooling energy requirements are calculated hourly over a period of one year. Shown in Table 3.3 is an example for the Newcastle area (Zone 15), where the lower energy requirements, the higher the stars.

Table 3.3. Annual energy requirements (MJ/m^2. annum) for each star rating (bands) (AccuRate Sustainability V2.3.3.13 SP1).

Band 1	Band 2	Band 3	Band 4	Band 5	Band 6	Band 7	Band 8	Band 9	Band 10
349	232	159	114	86	67	50	34	19	6

3.7 Adaptive Thermal Comfort Model

In this study, the adaptive thermal comfort model is used to establish the ATM. The adaptive thermal comfort model has been outlined previously in Section 2.2.3.2.

Why Adaptive Thermal Comfort?

Many recent studies have favoured the adaptive thermal comfort model over the predicted mean vote (PMV) and predicted percentage dissatisfied (PPD) models for the following reasons:

- **Accuracy**

Studies of the indoor environments in tropical climates, based on Fanger's predicted mean vote (PMV/PPD), have found that this model does not effectively describe comfortable conditions because it fails to give correct information about an occupant's comfortable temperature. In addition, PMV/PPD studies do not provide the occupant's clothing details. This leads to specific clothing level assumptions which require a fixed internal air temperature, thereby encouraging the designers to use mechanical cooling to reach the thermal comfort level (Nicol and Humphreys 2002).

- **Saving of building operating energy**

Naturally ventilated buildings normally consume less than half the energy compared with air-conditioned buildings because the inhabitants adapt to a considerably broader range of temperatures that fall out of the comfort zone defined by the PMV model (Moujalled et al. 2008). The PMV model also predicts that inhabitants will feel hotter than they actually do, and therefore encourages the consumption of more air-conditioning than needed (Nicol and Humphreys 2002).

Heating and cooling can be reduced when occupants accept wider ranges of internal air temperature which results in lower energy usage and running costs, and therefore enhancing the economic and environmental performance of the building (Holopainen et al. 2014).

- **Occupants have more control of their environment**

Inhabitants with greater individual control over their environment have a tendency to accept wider ranges of indoor temperatures. On average, they accepted a 2.6^{o}C lower operative temperature and showed a lower motivation to modify their current environment (by using air-conditioning) compared with those without personal control. It is recommended that inhabitants have a chance to interact with their thermal environment through openable windows and doors, low energy fans and minimizing the usage of controllable heating/cooling systems (Maohui et al. 2014).

- **Encourage sustainability**

While the PMV/PPD models use energy to obtain comfortable conditions, the adaptive thermal approach uses low energy solutions, such as clothing, open windows/doors, fans, personal heaters/coolers, drinking water and sun shades. To encourage sustainability where reasonable low-energy solutions are accessible, they should be favoured.

This current research will use an adaptive thermal comfort temperature for free-running buildings (no mechanically cooled or heated buildings are included because the relationships for these buildings are more complex, and less stable). The relationship between the comfort temperature T_c and the outdoor temperature T_o for a temperate climate in Australia is as described by Brager (Brager and Dear 2001):

$$\mathbf{T_c = 17.8 + 0.31 \times T_o} \qquad (3.1)$$

Where;

T_o: The monthly mean of the outdoor air temperature (^{o}C).
T_c: Comfort temperature (^{o}C).

To find the adaptive thermal comfort ***acceptability limits*** inside the building, the following equations are used:

$$\textbf{\textit{90\% acceptability limits}} = \mathbf{T_c \pm 2.5\ ^{o}C} \quad \text{(ATM90)} \qquad (3.2)$$

$$\textbf{\textit{80\% acceptability limits}} = \mathbf{T_c \pm 3.5\ ^{o}C} \quad \text{(ATM80)} \qquad (3.3)$$

Equations 2.3 and 2.3 represent acceptability limits where at least 90% and 80% of the occupants are satisfied with these temperature ranges. These limits were used to calculate ATM90 and ATM80.

3.8 Summary

As described in this chapter, several tools are used in this research to develop the ATM. The tools used in this research are;

1. Observations from full-scale housing test modules and real building which are used in the case study to provide the internal air temperatures to be compared with the actual data to assess the accuracy of the CFD simulation.
2. Computational Fluid Dynamics (CFD) to find average volume internal air temperatures.
3. AccuRate software to assess the ATM accuracy.
4. Autodesk Ecotect to calculate the monthly heating and cooling loads.
5. Adaptive thermal comfort to define the ATM.

In the next Chapter, conventional CFD analysis is used in the first attempt to find the internal air temperatures of buildings over long periods. This approach is then modified and refined to develop a more representative approach which is used to develop the final metric.

Chapter Four:
Solutions to Issues Related to Prolonged CFD Simulations

4.1 Overview

By having external and internal data for all of the modules over one year, the observed internal air temperature for each module can be compared with the simulated CFD results. However, when compared with the observed data, CFD simulations for long periods face some potential issues which need to be addressed:

- Air temperature inside the building keeps warming with time
- Excessive computing time
- Smaller fluctuation range
- Discrepancies in peak temperature time
- Wind applied to the external surface

In this Chapter these issues are addressed, which then allows the use of long period simulations with a reasonable degree of accuracy.

4.2 Internal Air Temperature - Warming Issue

Using the Autodesk CFD simulation, it appears that the simulation results have an issue with simulating for long periods (weeks or months), since the air temperature inside the building keeps warming with time. A new method is presented which predicts internal building air temperature using the CFD simulation for long periods without the internal air temperature warming effects.

To properly simulate the effects of reflected and emitted radiative heat transfer between the object and its surroundings, cube environments extend 10 times the height of the module were created which fully enclosed the module and the ground as shown in Figure 4.1(Autodesk 2014).

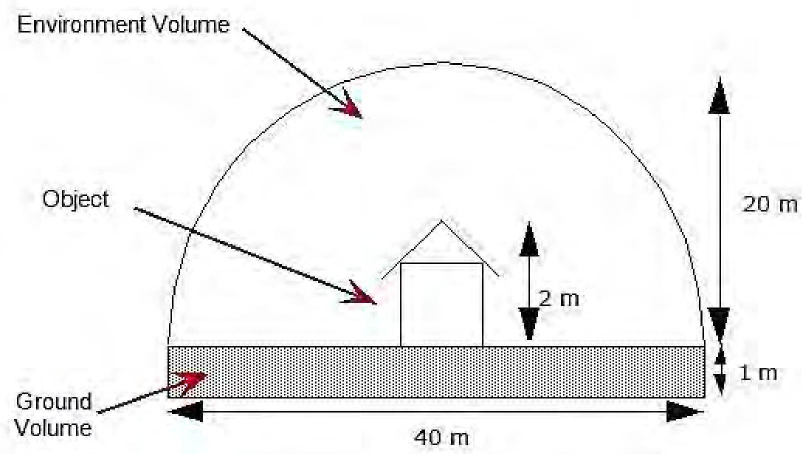

Figure 4.1 Geometry from Autodesk instruction webpage (Autodesk 2014).

When following the CFD instruction manual, with just one external boundary condition / sky boundary condition, for shorter periods the simulation gives reasonable results, but when applying it for longer periods (several days, weeks, and months) the internal air temperature inside the module keeps warming with time.

Figure 4.2 show the results for a simulation period of one week in summer (southern hemisphere) between 14/01/2010 to 22/01/2010 where the grass surfaces have an emissivity of about 0.3 and sky emissivity equals one. Using one external boundary condition the temperature keeps rising with time compared with the real data for all modules. This temperature difference was up to 14ºC.

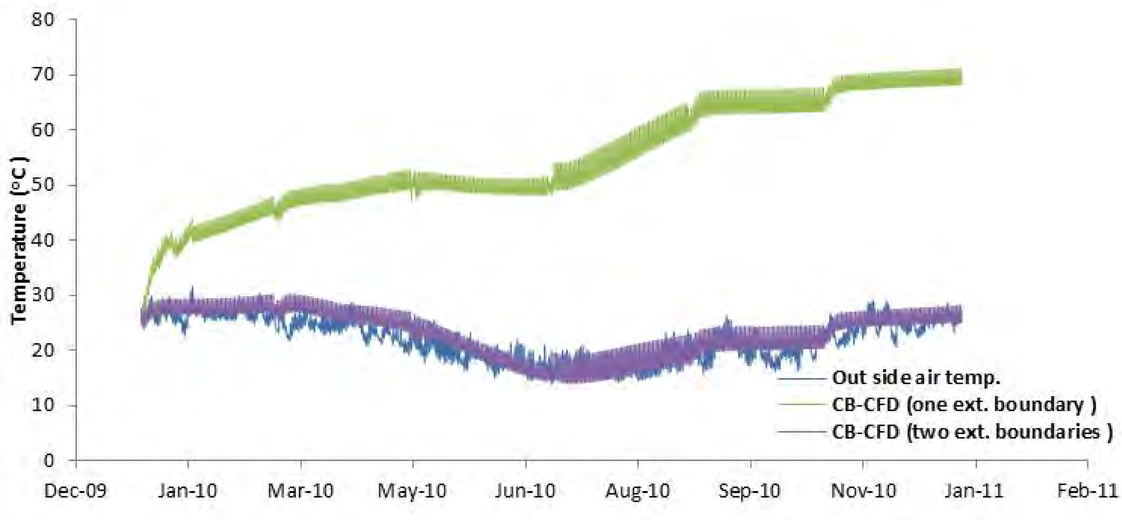

Figure 4.2. Temperature trends for one and two external boundaries for the CB module using CFD simulations. Note: the same trends were observed for the other modules (i.e. InsCB, InsBV and InsRBV).

Simulation following the Autodesk help guide indicated that there is an issue affecting the validation of the simulation results which make it inaccurate to simulate for long periods, and the reasons for that are:

- CFD simulation is not specialized in predicting internal temperatures for longer periods inside buildings. CFD simulation is designed for shorter simulation periods (milliseconds, seconds, minutes, hours and multiple days), not for weeks and months. The Autodesk help guide website states: "*To study the variation of solar loading over a longer period either within a single day or over multiple days and nights*" (Autodesk 2014). Therefore, multiple days are considered as a long period.

- Sky emits back some heat during the night "*but because of the low night-time sky temperature, it acts as an emitter that is cold, so little heat is emitted back to the object and ground if the sky emitted back some heat during the night*" (Autodesk 2014). That energy will keep increasing inside the CFD volume resulting in the continuous warming of the module.

Therefore, to avoid warming of the modules, a new method to measure the internal module air temperature for long period (weeks and months) using CFD simulation was developed using two external air boundary conditions, one for the external volume (the sky boundary condition which had previously been applied) and the other for the external air boundary condition surrounding the module, as shown in Figure 4.3.

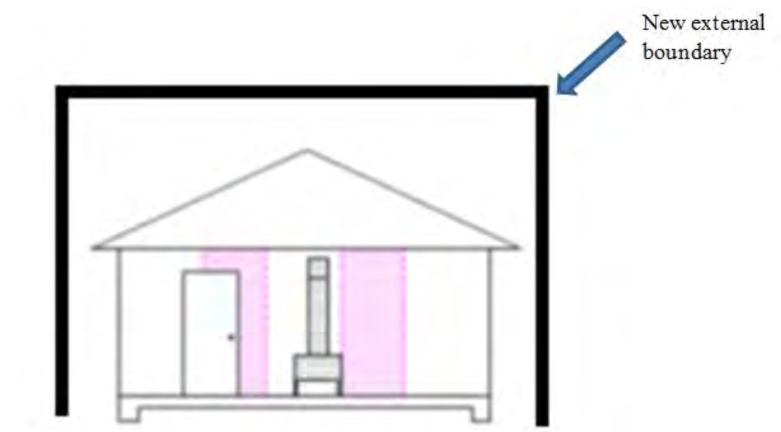

Figure 4.3. New boundary conditions applied to the module.

By adding a new volume (external air layer), this surrounds the module with the ambient external air temperature. By running the CFD simulation again and adding the external air temperature to the new boundary condition, the simulated modules were stable and the internal air temperature was prevented from warming, as shown in Figures 4.4 for all modules.

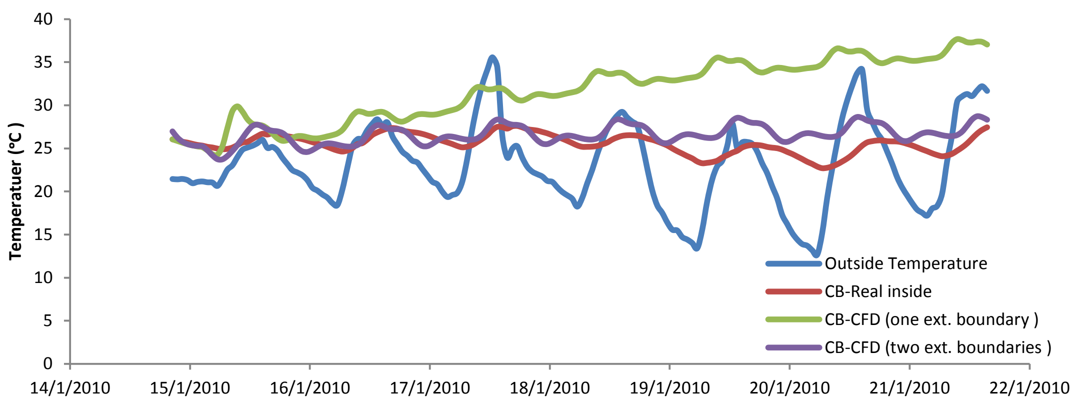

Figure 4.4a. Comparison between the real air temperatures and the CFD simulated results for the Cavity Brick Module.

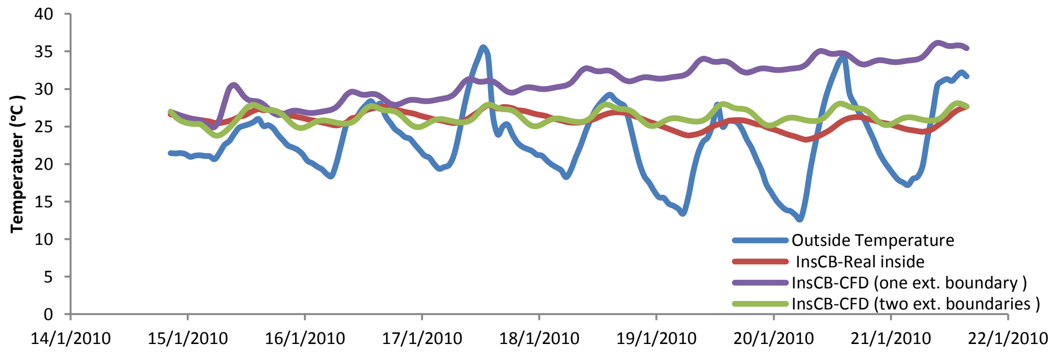

Figure 4.4b. Comparison between the real air temperatures and the CFD simulated results for the Insulated Cavity Brick Module.

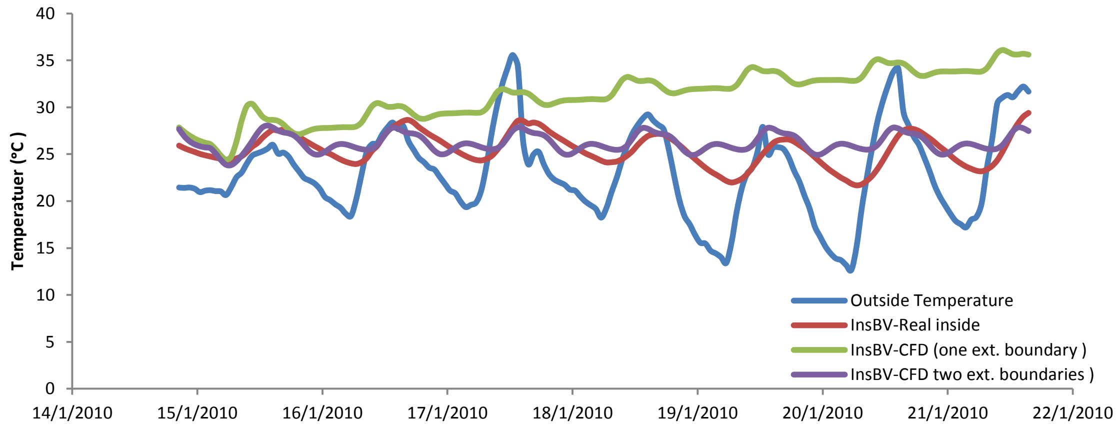

Figure 4.4c. Comparison between the real air temperatures and the CFD simulated results for the Insulated Brick Veneer Module.

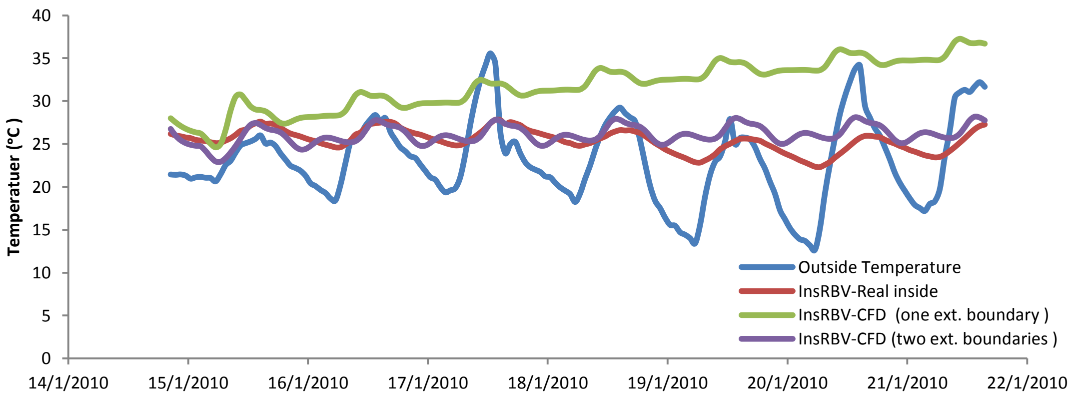

Figure 4.4d. Comparison between the real air temperatures and the CFD simulated results for the Insulated Reverse Brick Veneer Module.

Comparing the number of hours for each module falling within a certain range (called bin range in Microsoft Excel) of temperature difference between the CFD simulation and the real internal air temperature showed that all the modules with two external boundaries performed better. For example, after 16 hours of CFD simulation using one external boundary for the cavity brick module (CB- CFD (one ext. boundary)) the temperature fell within a range of 0 - 0.5ºC difference with the real inside air temperature, while in the CFD simulation using two external boundaries (CB- CFD (two ext. boundaries)) over 42 hours, the temperature fell within the same range of 0 - 0.5ºC difference, as shown in Figures 4.5.

a)

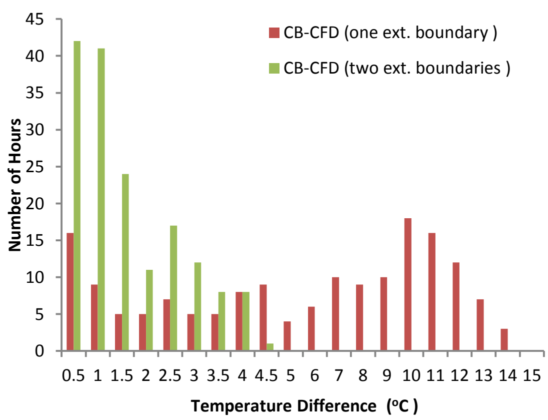

b)

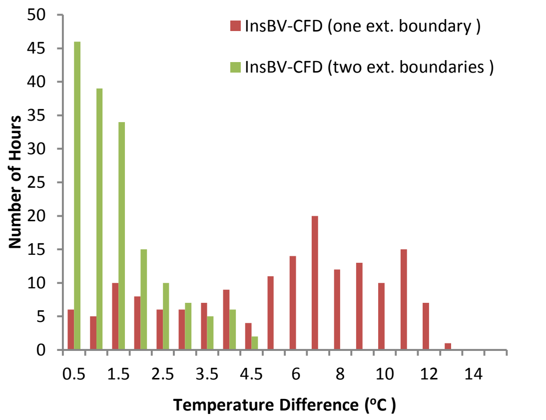

c)

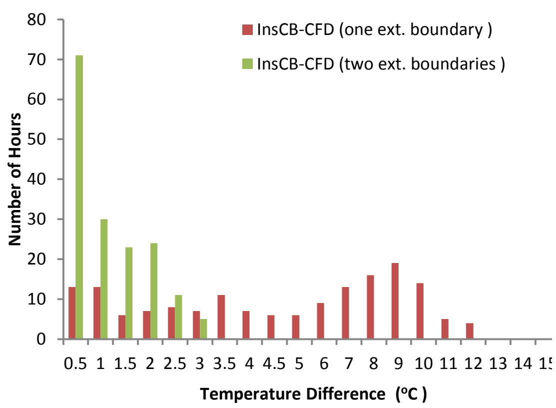

d)

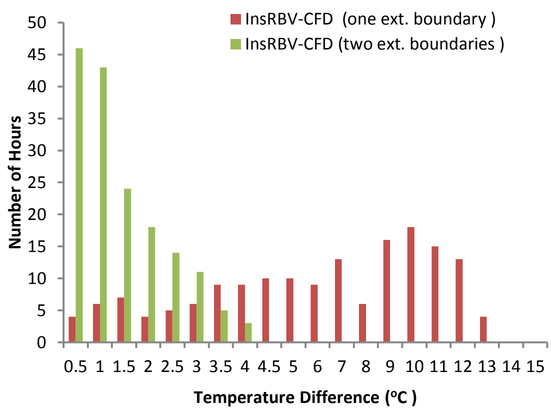

Figure 4.5. Number of hours for each temperature difference between real data and the CFD simulations with one and two boundaries for all modules ((a) Cavity Brick Module, (b) Insulated Cavity Brick Module, (c) Insulated Brick Veneer Module, (d) Insulated Reverse Brick Veneer Module). Note: 0.5, 1, 1.5, 2 temperature difference for the number of hours falls within 0-0.5, 0.5-1, 1-1.5, 1.5-2ºC range respectively.

A comparison was made of the percentages of the number of hours to the total number for the simulation period (164 hours) for each temperature difference (bins) between the real data and the CFD simulations (with one and two external boundary conditions) for each module. For all the CFD simulating modules with two external air boundary conditions the results fell within a 0 - 4.5ºC temperature difference with the real air temperature compared to a 0 - 14.5ºC range for one external boundary. In more than 89% of the CFD simulating modules with two external air boundary conditions the results fell within a 0 - 3ºC temperature difference, compared with the real air temperature, as shown in Figures 4.6.

a)

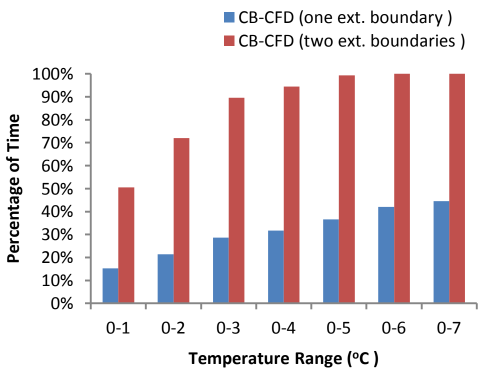

b)

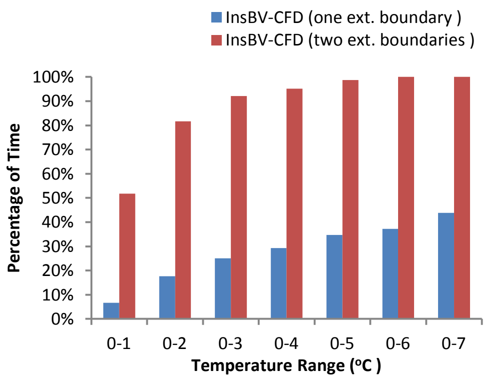

c)

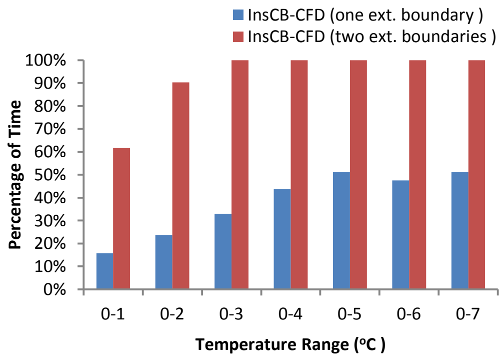

d)

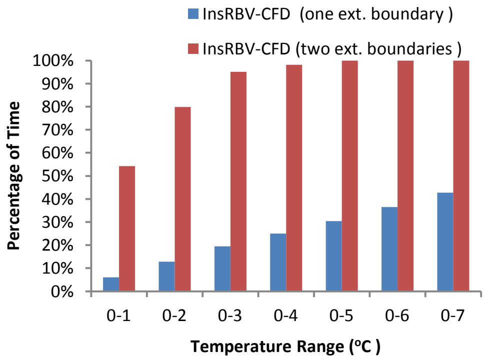

Figure 4.6. Comparison between the real data and the CFD simulations (with one and two external boundary conditions) for each module modules ((a) Cavity Brick Module, (b) Insulated Cavity Brick Module, (c) Insulated Brick Veneer Module, (d) Insulated Reverse Brick Veneer Module).

The results showed that the CFD simulation with two external air boundary conditions gave more accurate results, compared to the one external air boundary condition simulations, and a better representation of the real air temperature inside the module.

4.3 Longer Computing Time and Smaller Fluctuation Range

Using Autodesk CFD simulations for long periods (weeks or months) takes long computing times and the CFD simulation results for the smaller time steps have smaller daily temperature fluctuation ranges compared with the real data. In this section, new ways to solve these issues in a fast and accurate way are discussed.

Most weather stations record the temperature every minute or at 5 minute intervals. Simulated for long periods (weeks, months) using CFD, it takes a long computing time (for a normal PC it could takes weeks to simulate several months of temperatures) which is not practical. The main factors controlling the simulation time is the simulation period and the time step size. From the Autodesk CFD programme the time step size can be edited through the solver, as shown in Figure 4.7.

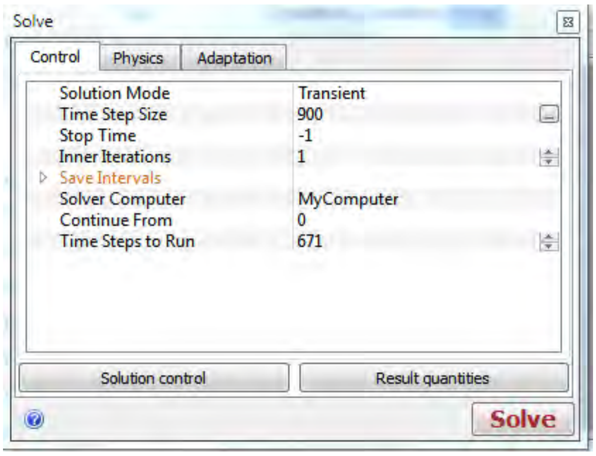

Figure 4.7. Solve window in the Autodesk CFD programme (Autodesk 2014)

Where;

- Solution Mode: steady or transient state. The transient state was used in this simulation.
- Time Step Size (seconds): depends on the time scale of the analysis and the type of the analysis.
- Stop Time (seconds): for transient analyses, the analysis can be stopped when a specific time has been reached, after a certain number of time steps,

or whichever comes first, or "-1" if it is not desired to stop the analysis at a certain time.

- Inner Iteration: number of iterations for every time step. We used one inner iteration in this analysis
- Save Intervals for how often the results and summary information are saved.
- Solver Computer: this enables an analysis to be built on one machine (the local computer is the default).
- Continue From: if continuing an analysis, select the iteration or time step to continue from.
- Iterations to Run**:** the number of iterations or time steps to run in the analysis.

The CFD help manual states: "*a time step for a typical solar heating analysis can be in the order of 100 seconds or more*" (Autodesk 2014). Following the CFD help manual and using small time step sizes (1 or 5 minutes) for typical housing modules will take a very long computing time, as shown in the Table 4.1.

Table 4.1. Computing times for different time steps.

Time step (minutes)	Computing time for one week simulation	Computing time for 30 days simulation	Computing time for a season (120 days)
1	1 Days 1 hour 5 minutes	4 Days 4 hours 13 minutes	17 Days 17 hours 39 minutes
5	5 hours 5 minutes	21 hours 30 minutes	3 Days 3 hours 47 minutes
15	1 hour 45 minutes	7 hours 13 minutes	1 Days 1 hour 39 minutes
20	1 hour 20 minutes	5 hours 26 minutes	21 hour 30 minutes
30	55 minutes	3 hours 39 minutes	14 hours 22 minutes
40	42 minutes	2 hours 45 minutes	10 hours 47 minutes
45	38 minutes	2 hours 27 minutes	9 hours 36 minutes
60	30 minutes	1 hour 52 minutes	7 hours 13 minutes
80	23 minutes	1 hour 25 minutes	5 hours 26 minutes
100	20 minutes	1 hour 9 minutes	4 hours 22 minutes
120	17 minutes	58 minutes	3 hours 39 minutes
150	15 minutes	47 minutes	2 hours 56 minutes
180	13 minutes	40 minutes	2 hours 27 minutes

Note: The simulation was carried out on a Dell latitude e5440 with an Intel ® Core ™ i5-4200 U CPU @ 2.3 GHz and an installed memory (RAM) of 8GB. Windows experience index 5.9 which assesses key system components on scale of 1- 7.9.

Smaller time steps will result in smaller daily temperature fluctuation ranges compared with the real data temperature fluctuation ranges. A temperature fluctuation range (peak to peak amplitude) for a 24 hour daily cycle is shown in Figure 4.8, where temperature fluctuation range difference is the difference between daily maximum temperature and daily minimum temperature.

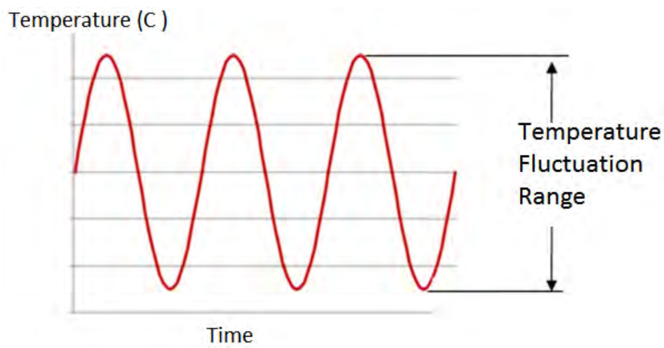

Figure 4.8. Temperature fluctuation range for a 24 hour daily cycle.

The CFD simulation results for smaller time steps have smaller daily temperature fluctuation ranges compared with the real data temperature fluctuation ranges, as shown in Figure 4.9. For the 15 minute time step, the fluctuation range was 2.53ºC for the CFD simulation compared to 4.58ºC for the real data.

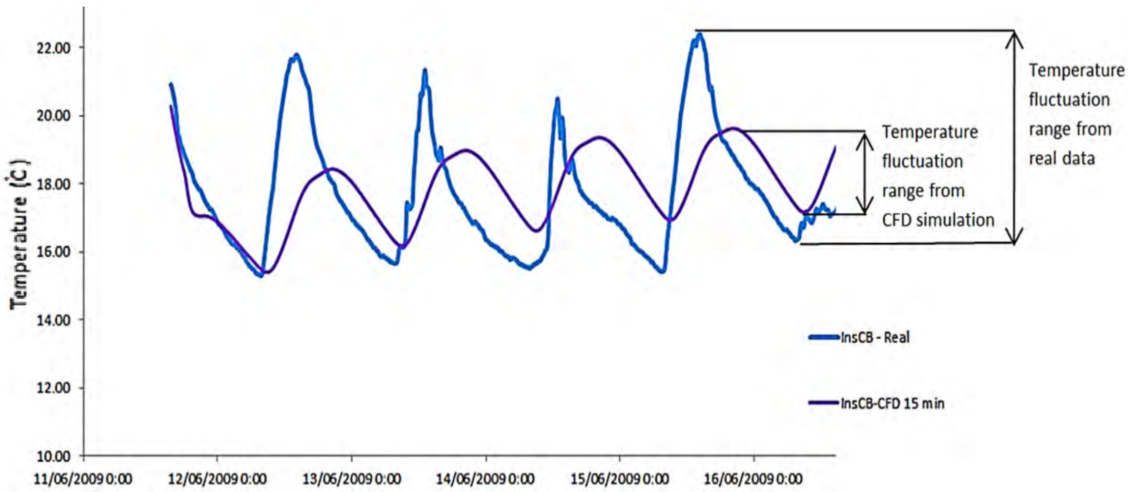

Figure 4.9 .Temperature fluctuation range difference between the real data and the CFD simulation for InsCB.

To solve these issues (the long computing times and smaller temperature fluctuation range), CFD analysis alone, without coupling with any software, was used to simulate the buildings, using large time steps and one inner iteration for economic and faster simulation. The larger time steps were employed to speed up the simulation time and to produce higher temperature fluctuation ranges.

CFD simulation analyses were run for each module using the different time steps of 15, 20, 30, 35, 40, 45, 60, 80, 100, 120, 150 and 180 minutes (the only difference in each simulation was the time step), and the simulation results compared with the real data. To run simulations for the different time steps, a representative external air temperature was needed to be calculated for each time step. This was obtained by averaging the external air temperature surrounding a module over the required time step.

The initial temperatures (T1, T2, ... etc.,) were taken at 5 minute intervals. For example, to find the 80 min time step on 17/02/2012 at 00:00 the new time steps= ∑(T1,T16)/16 and the new time interval is 40 minutes after T1. The new time steps and new intervals used in the CFD simulations are shown in Table 4.2.

Table 4.2. Calculating new outside air temperature for different time steps

Time steps	New time steps (minutes)	New interval (minutes)
15 minutes	$[\sum_{i=1}^{3}(\mathrm{Ti})]/3$	7.5
30 minutes	$[\sum_{i=1}^{6}(\mathrm{Ti})]/6$	15
60 minutes	$[\sum_{i=1}^{12}(\mathrm{Ti})]/12$	30
80 minutes	$[\sum_{i=1}^{16}(\mathrm{Ti})]/16$	40
100 minutes	$[\sum_{i=1}^{20}(\mathrm{Ti})]/20$	50
120 minutes	$[\sum_{i=1}^{24}(\mathrm{Ti})]/24$	60
150 minutes	$[\sum_{i=1}^{30}(\mathrm{Ti})]/30$	75
180 minutes	$[\sum_{i=1}^{36}(\mathrm{Ti})]/36$	90

As shown in Figures 4.10, the simulations of the average external air temperature for the different time intervals resulted in minimal difference between the 15, 30, 40, 45, 60, 120, 180 minute time intervals, with less than a 2% error between the maximum and minimum values for any time interval. The sharp changes of peak air temperatures for a day were also captured. However, this may be more predominant for the larger time intervals with small difference of about 0.5°C for only peak temperatures between the 5 and 180 minutes time intervals.

a)

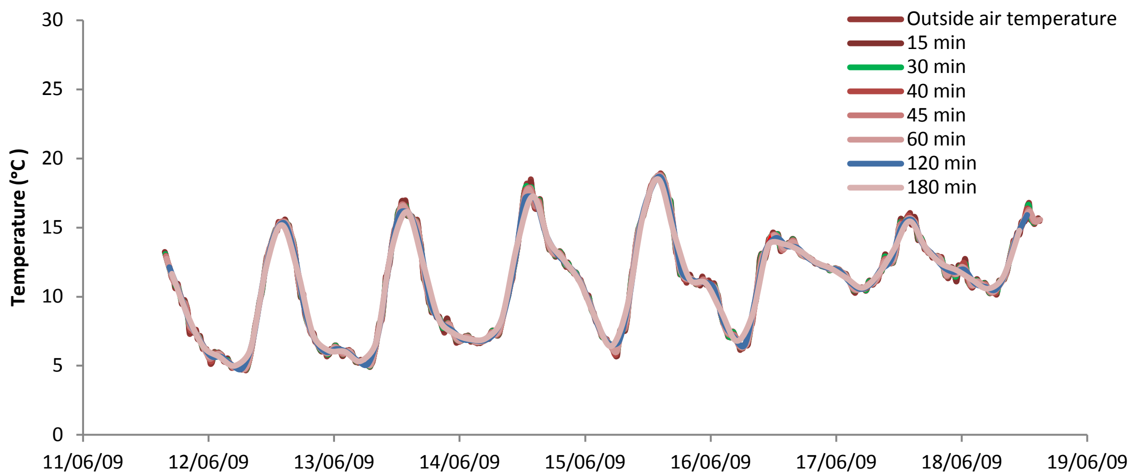

b)

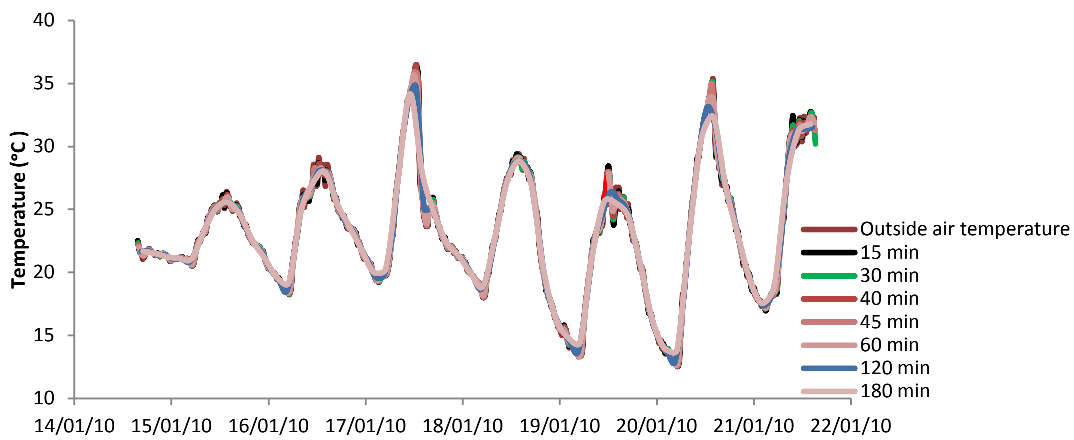

Figure 4.10. Outside air temperatures in a winter and summer week for the different time intervals ((a) winter week, (b) summer week)

Simulations were carried out for all the modules using the different time steps for one week in winter (southern hemisphere) between 11/06/2009 and 19/06/2009 and for one week in summer from 14/01/2010 to 22/01/2010. The objective was to find which time step size delivered the best temperature fluctuation range (i.e., the closest to the real results) and to also accelerate the simulation process with larger time steps. Simulations were run for all modules and the results for the InsCB are presented here in detail, as shown in Figures 4.11 for different time steps.

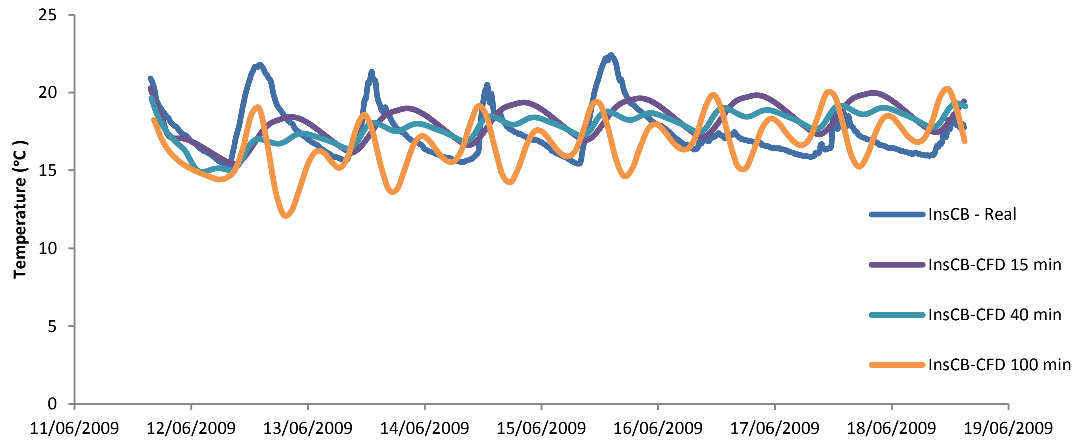

Figure 4.11a. Comparison between the real data and the CFD simulations for 15, 40 and 100 minutes time steps for the InsCB module in winter week.

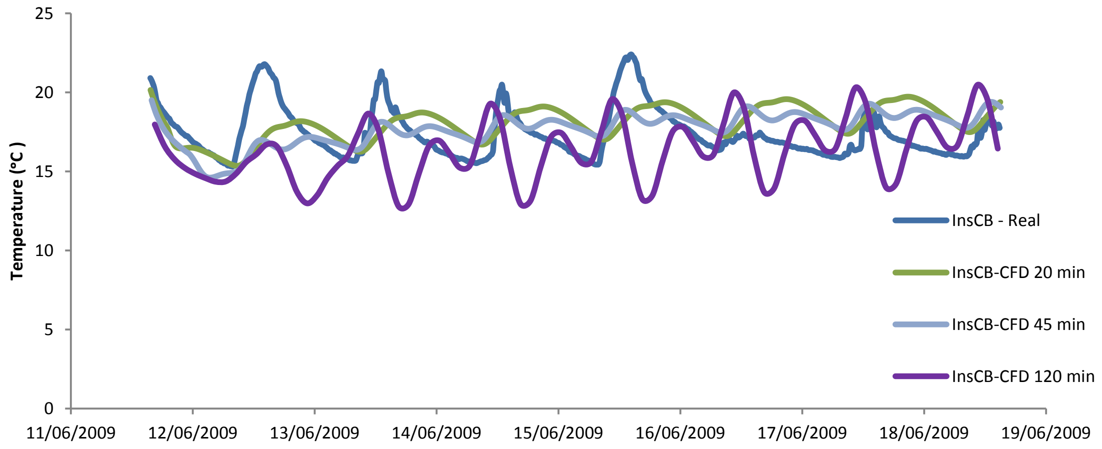

Figure 4.11b. Comparison between the real data and the CFD simulations for 20, 45 and 120 minutes time steps for the InsCB module in winter week.

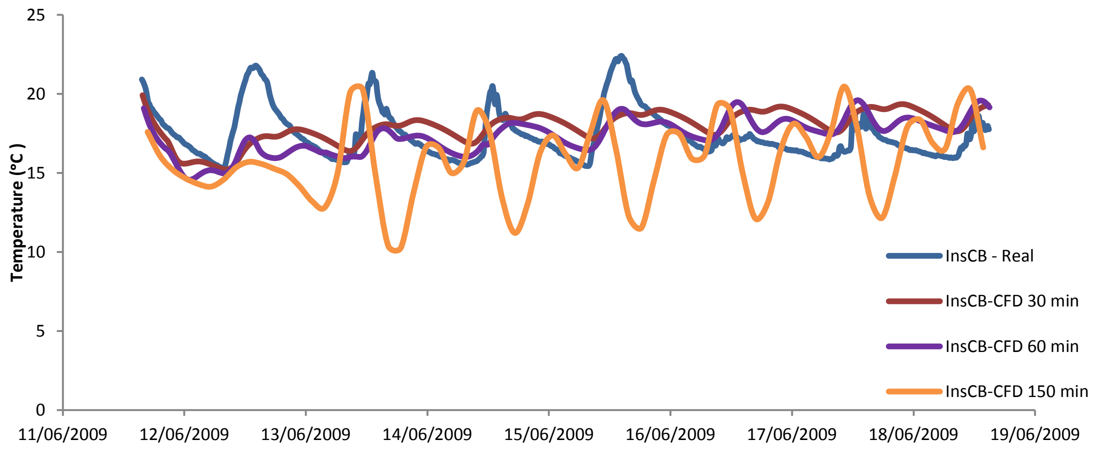

Figure 4.11c. Comparison between the real data and the CFD simulations for 30, 60 and 150 minutes time steps for the InsCB module in winter week.

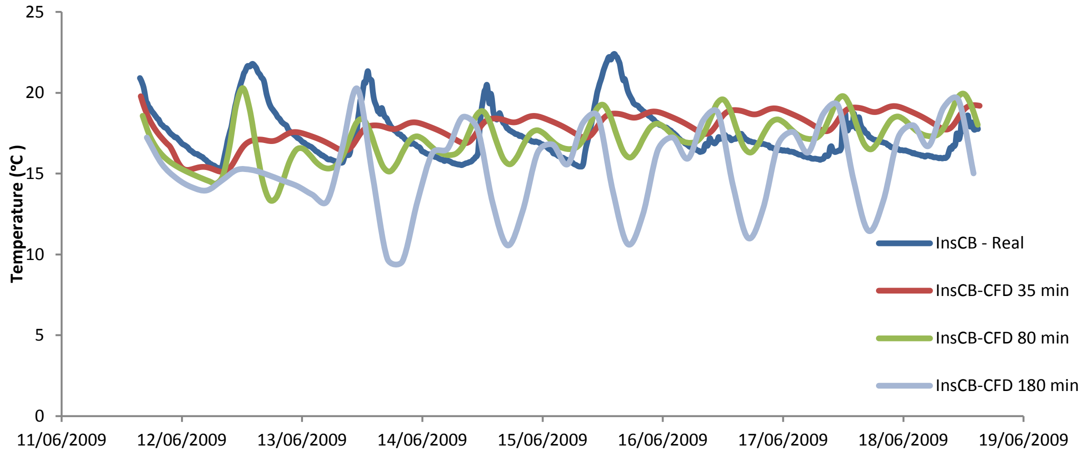

Figure 4.11d. Comparison between the real data and the CFD simulations for 35, 80 and 180 minutes time steps for the InsCB module in winter week.

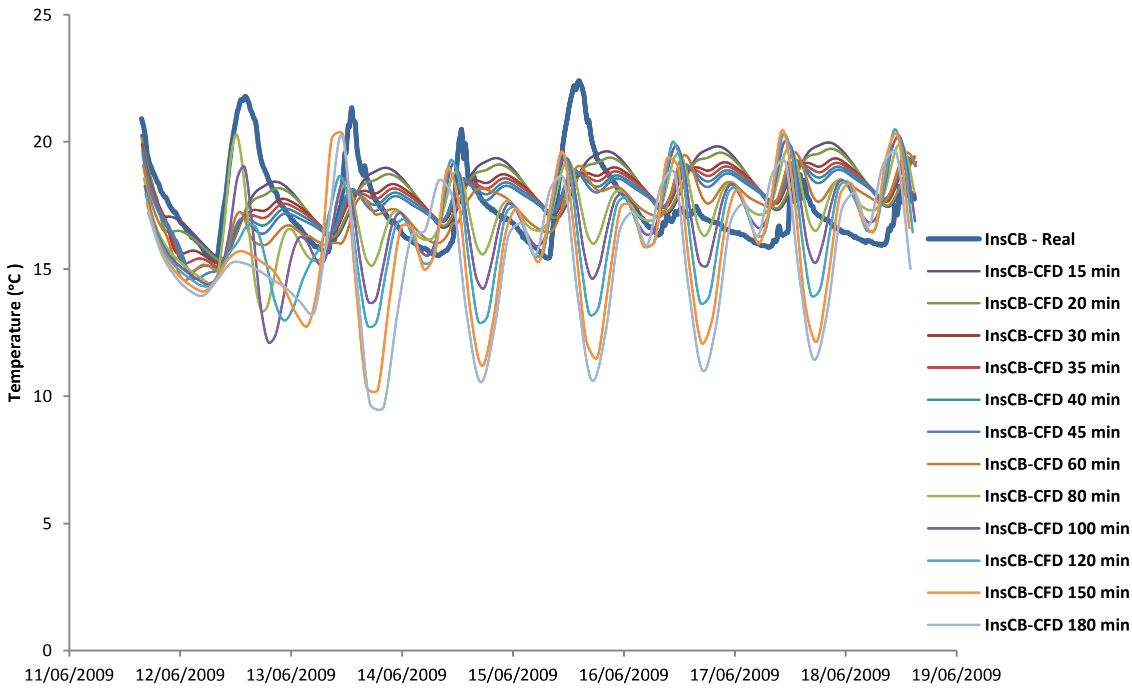

Figure 4.11e. Comparison between the real data and the CFD simulations with all-time steps for the InsCB module in winter week.

The average temperature fluctuation range for the real data was 4.58ºC, while the average temperature fluctuation ranges from the CFD analyses for the 15, 30, 60, 80, 100, 120, 150 and 180 minute time steps were 2.53ºC, 1.62ºC, 2.25ºC, 3.27ºC, 4.75ºC, 6.32ºC, 7.83ºC and 7.72ºC, respectively.

The average temperature fluctuation ranges were growing steadily with the larger time step sizes during the studied period, as shown in Figures 4.12.

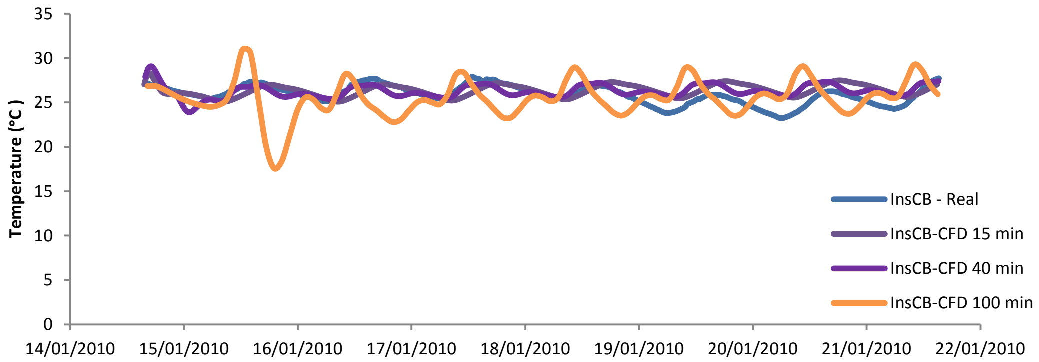

Figure 4.12a. Comparison between the real data and the CFD simulations with 15, 40 and 100 time steps for the InsCB module in the summer week.

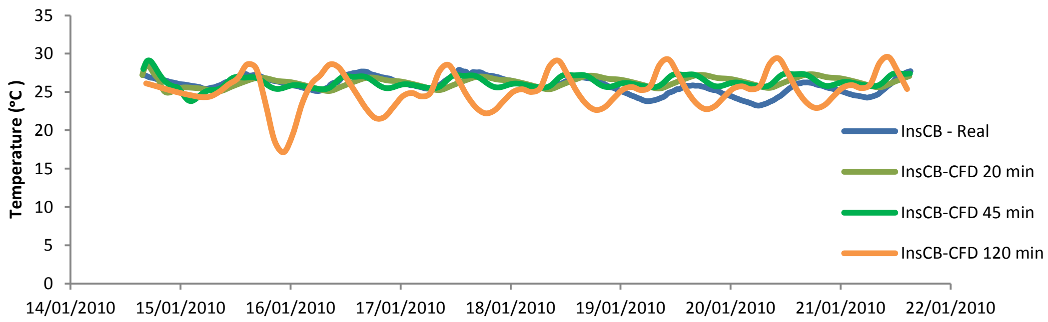

Figure 4.12b. Comparison between the real data and the CFD simulations with 20, 45 and 120 minutes time steps for the InsCB module in the summer week.

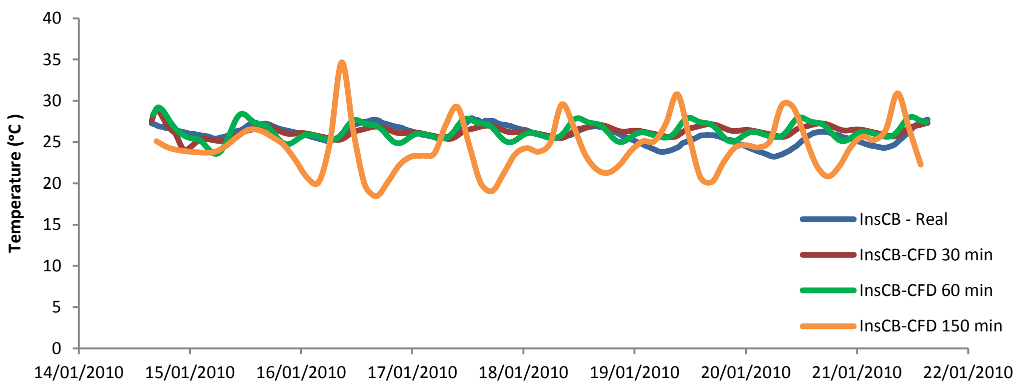

Figure 4.12c. Comparison between the real data and the CFD simulations with 30, 60 and 150 minutes time steps for the InsCB module in the summer week.

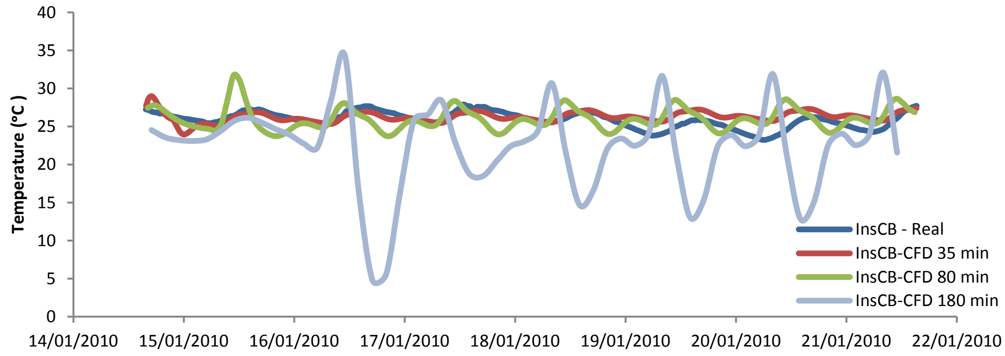

Figure 4.12d. Comparison between the real data and the CFD simulations with 35, 80 and 180 time steps for the InsCB module in the summer week.

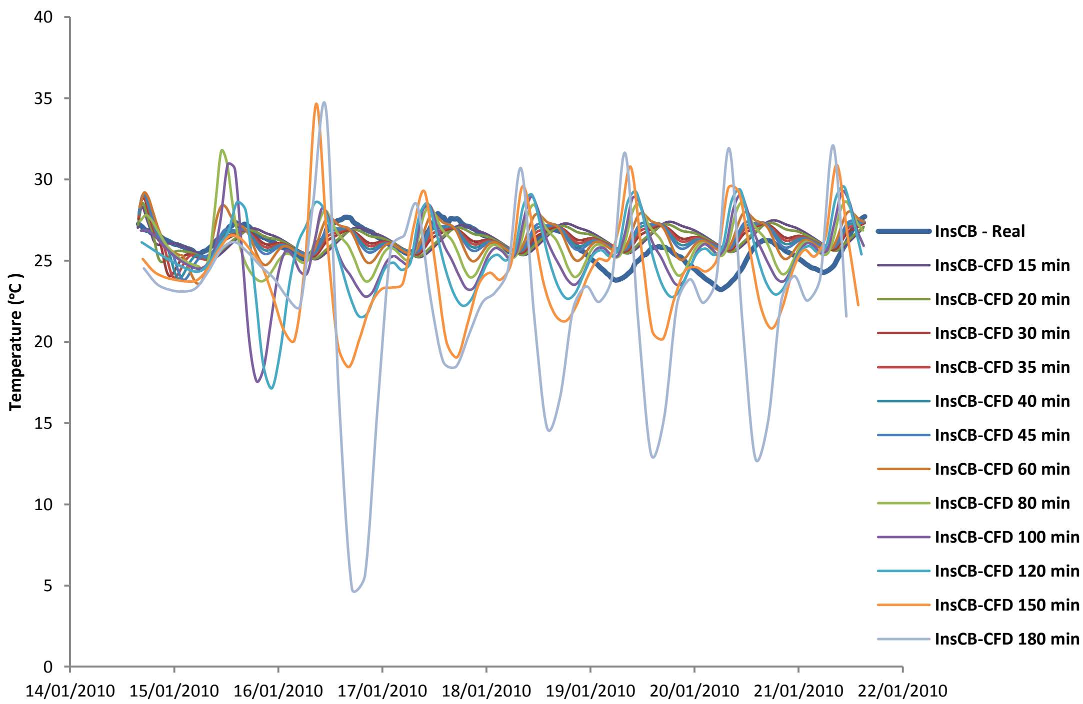

Figure 4.12e. Comparison between the real data and the CFD simulations with all the different time steps for the InsCB in the summer week.

The average internal temperature fluctuation range for the real data was 2.33ºC, while the average temperature fluctuation range from the CFD analyses for the 15, 30, 60, 80, 100, 120, 150 and 180 minute time steps were 1.94ºC, 1.60ºC, 2.89ºC, 4.40ºC, 5.32ºC, 6.45ºC, 9.42ºC and 19.07ºC, respectively, with the average temperature fluctuation range increasing steadily with the larger time step size.

The fluctuation ranges during the diurnal cycle were less than 4.6ºC, and the hourly changes were less than 0.5ºC for the InsCB module during the summer and winter weeks. This indicates that there were no rapid changes in temperature recorded inside the module.

It can also be seen from the above that the summer temperature fluctuation range for the real data was less than that for the winter, which allowed more sun to enter the modules due to the lower solar angle. This heated the building interiors during the day time, and also allowed the buildings to cool more quickly at night due to the lower external winter temperatures.

The simulations for all the modules indicated that there is direct relationship between the time step size and the temperature fluctuation range, where the temperature fluctuation range increased with a larger time step size, as shown Figures 4.13.

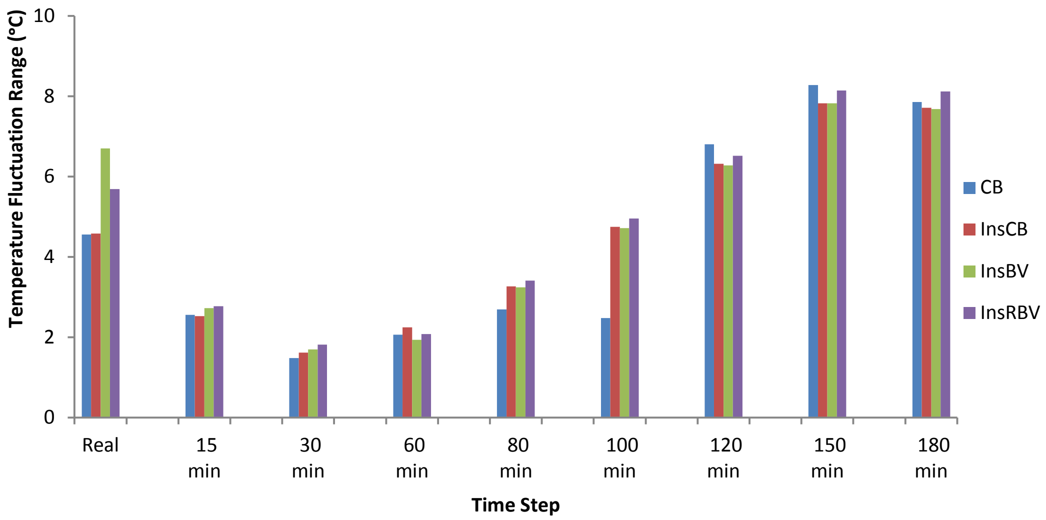

Figure 4.13a. Winter temperature fluctuation ranges for different time steps

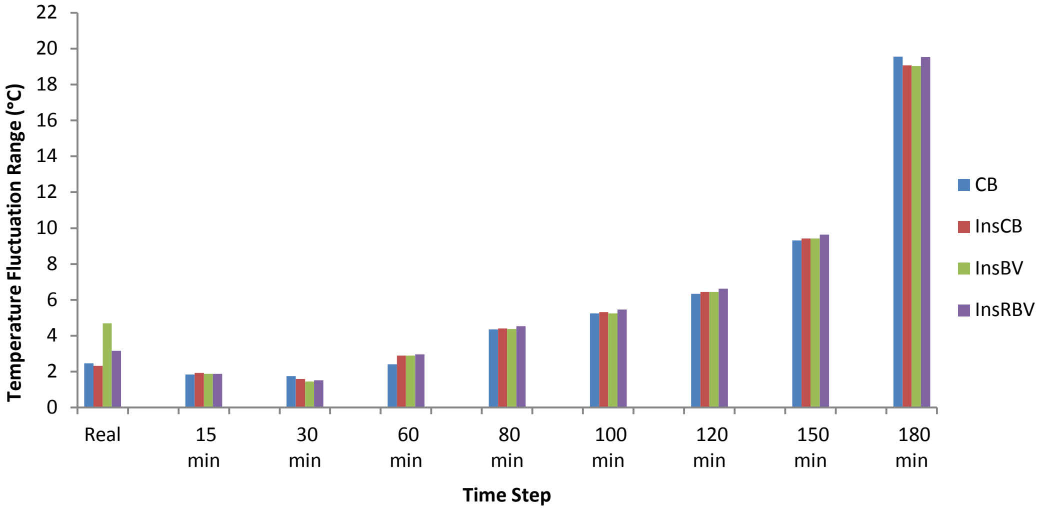

Figure 4.13b. Summer temperature fluctuation ranges for different time steps.

Smaller time steps provided lower temperature fluctuation ranges. The fluctuation ranges almost increased gradually and consistently (except for the 30 minute time step where it was constant or slightly lower) using the larger time steps.

The closest temperature fluctuation ranges occurred at the 60 minute time interval for the summer week and the 100 minute time interval for the winter week when compared to the real data. Applying larger time steps will accelerate the simulation process (less computing time) and will increase the temperature fluctuation range but will shift the peak temperature time inside the buildings (discrepancies in peak temperature between the real data and the CFD simulation results).

4.4 Discrepancies in Peak Temperatures

Increasing the time step size in the CFD simulation will affect the temperature fluctuation range and shift the peak temperature inside the buildings, as shown in Figure 4.14.

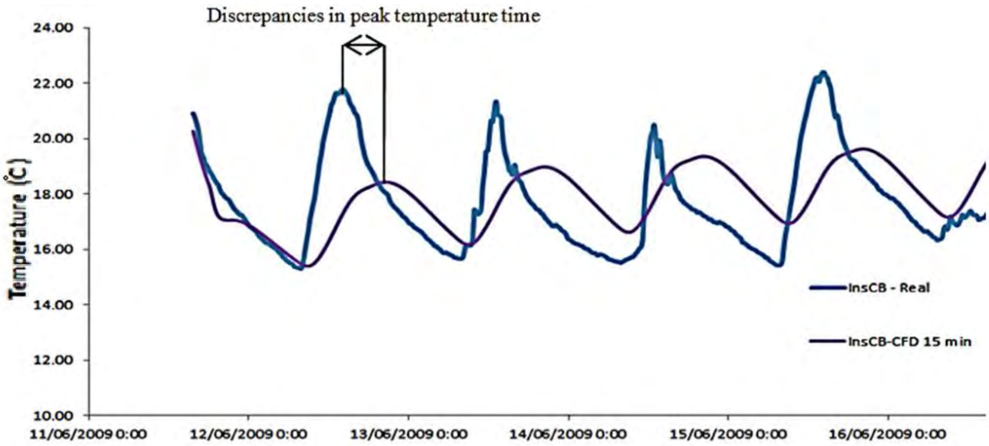

Figure 4.14. Discrepancies in the peak internal air temperature time between the real data and the CFD simulation for the InsCB.

In the real diurnal temperature cycle, the peak temperature inside the buildings depends on the outside weather conditions and does not occur at the same time every day (fluctuating by even 5 hours within the analysed period). The peak temperature time inside the buildings did not occur at the same time every day, and varied from day to day, and the peak temperature time varied between days, reaching 3 hours or more within the studied period. Tables 4.3a and 4.3b show the exact time when the internal air temperature reached its peak throughout the studied period.

Table 4.3a. Observed peak temperature time inside the buildings for the winter week.

	CB - Real	InsCB - Real	InsBV- Real	InsRBV- Real
Daily peak temperature time	12/06/2009 14:00	12/06/2009 14:10	12/06/2009 14:10	12/06/2009 14:10
Daily peak temperature time	13/06/2009 13:15	13/06/2009 13:10	13/06/2009 13:40	13/06/2009 13:05
Daily peak temperature time	14/06/2009 12:55	14/06/2009 12:55	14/06/2009 12:50	14/06/2009 13:00
Daily peak temperature time	15/06/2009 14:20	15/06/2009 14:20	15/06/2009 14:25	15/06/2009 14:15
Daily peak temperature time	16/06/2009 13:45	16/06/2009 15:30	16/06/2009 15:25	16/06/2009 15:30
Daily peak temperature time	17/06/2009 14:05	17/06/2009 12:15	17/06/2009 14:00	17/06/2009 12:20
Highest differences in peak temperature time	**1hr:25 min**	**3hr:15 min**	**2hr:30 min**	**3hr:10 min**

Table 4.3b. Observed peak temperature time inside the buildings for the summer week.

	CB - Real	InsCB - Real	InsBV- Real	InsRBV- Real
Daily peak temperature time	15/01/2010 16:10	15/01/2010 14:15	15/01/2010 14:10	15/01/2010 13:55
Daily peak temperature time	16/01/2010 16:40	16/01/2010 15:25	16/01/2010 15:35	16/01/2010 15:40
Daily peak temperature time	17/01/2010 15:50	17/01/2010 12:55	17/01/2010 13:05	17/01/2010 13:00
Daily peak temperature time	18/01/2010 14:40	18/01/2010 15:35	18/01/2010 16:05	18/01/2010 13:30
Daily peak temperature time	19/01/2010 16:50	19/01/2010 15:40	19/01/2010 15:30	19/01/2010 14:25
Daily peak temperature time	20/01/2010 17:40	20/01/2010 15:40	20/01/2010 15:50	20/01/2010 15:40
Highest differences in peak temperature time	**3 hr**	**2hr:45 min**	**3 hr**	**2hr:20 min**

Simulations were run for each model for the different time steps to monitor the discrepancies in peak temperature for each time step. The discrepancies are defined here as the differences in time between the simulated and real internal air temperature.

In this analysis, the daily peak temperature time also changed with the different time steps for the summer and winter weeks. For example, the highest discrepancies in peak temperature time occurred for the 15 minute time step, with a time lag of between 150 - 330 minutes compared with the real internal air temperature, as shown in Figures 4.15 for the winter week and Figures 4.16 for the summer week for each module.

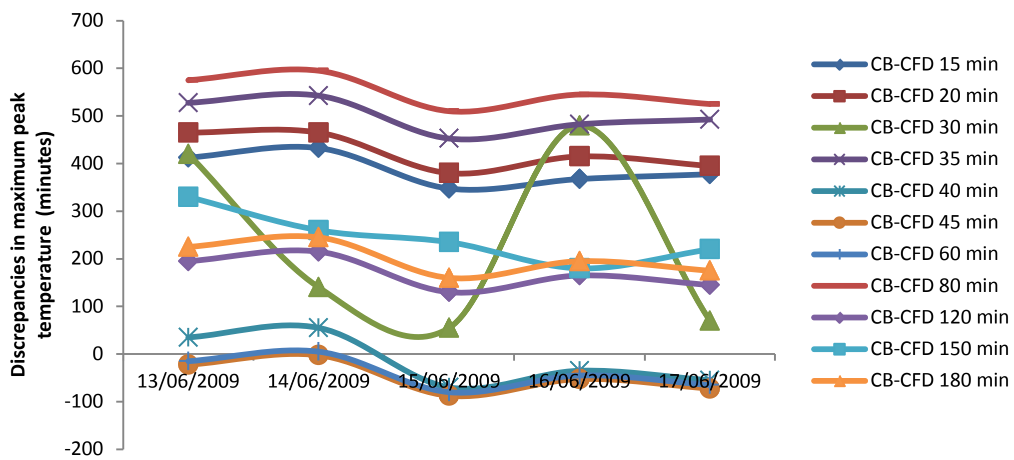

Figure 4.15a. Discrepancies in the peak temperatures for all modules in the winter week for the different time steps for the Cavity Brick Module.

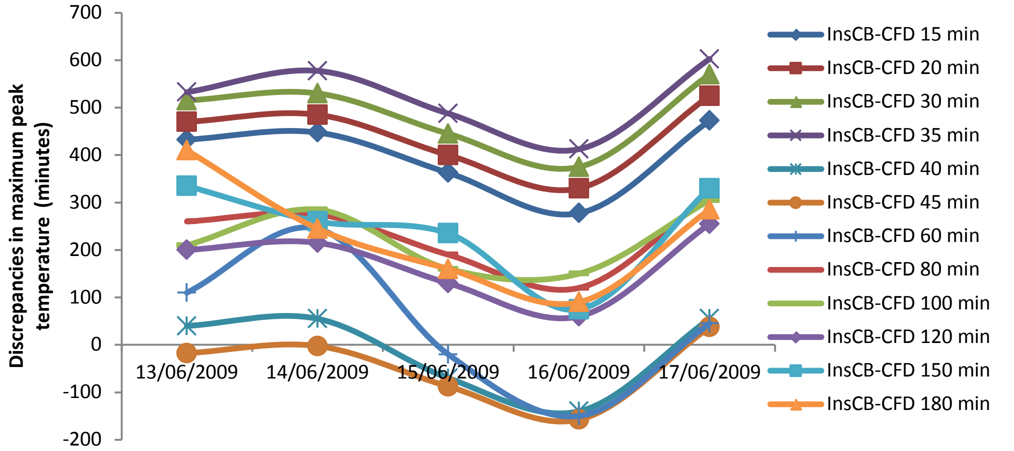

Figure 4.15b. Discrepancies in the peak temperatures for all modules in the winter week for the different time steps for the Insulated Cavity Brick Modul.

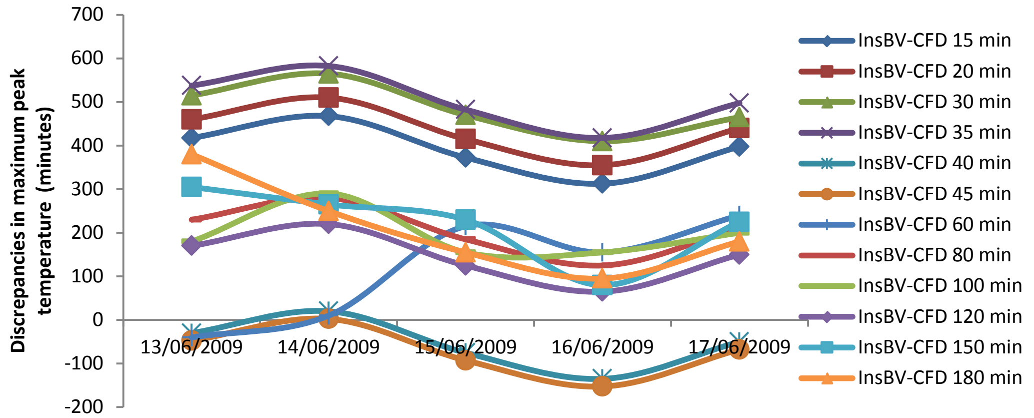

Figure 4.15c. Discrepancies in the peak temperatures for all modules in the winter week for the different time steps for the Insulated Brick Veneer Module.

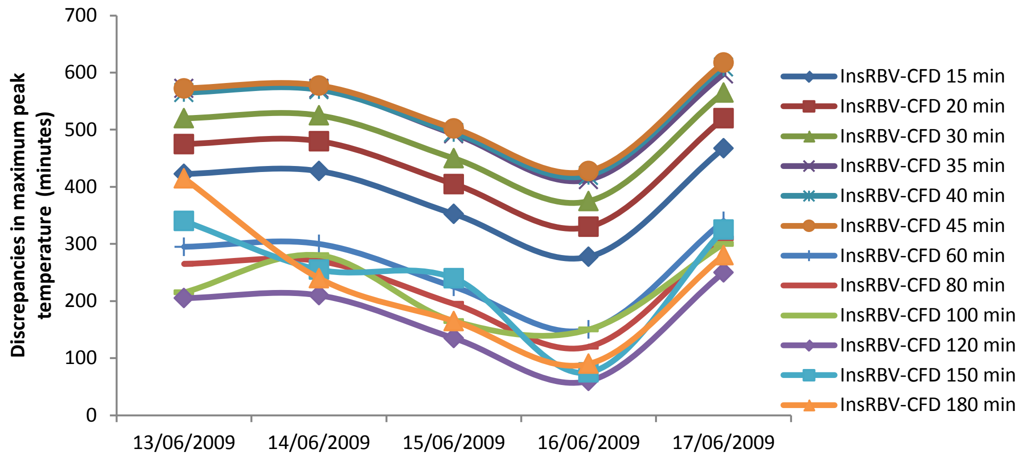

Figure 4.15d. Discrepancies in the peak temperatures for all modules in the winter week for the different time steps for the Insulated Reverse Brick Veneer Module.

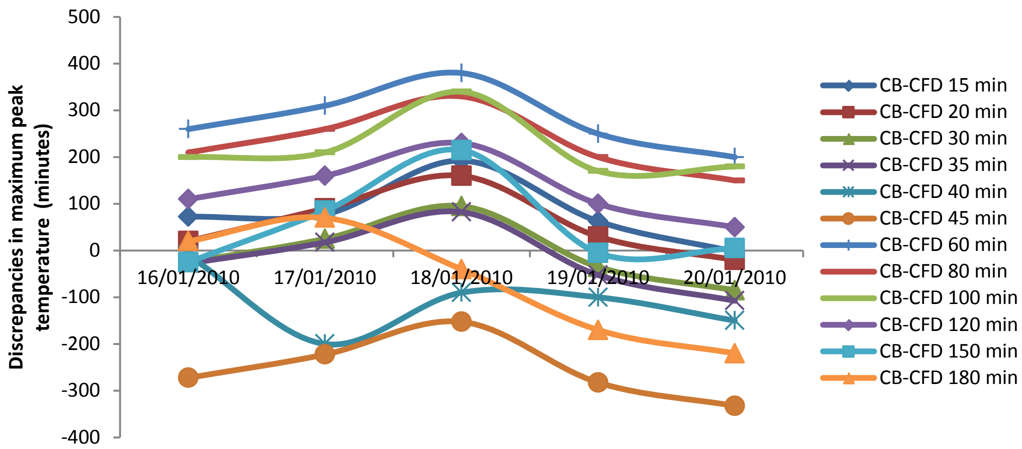

Figure 4.16a. Discrepancies in the peak temperatures for all modules in the summer week for the different time steps for the Cavity Brick Module.

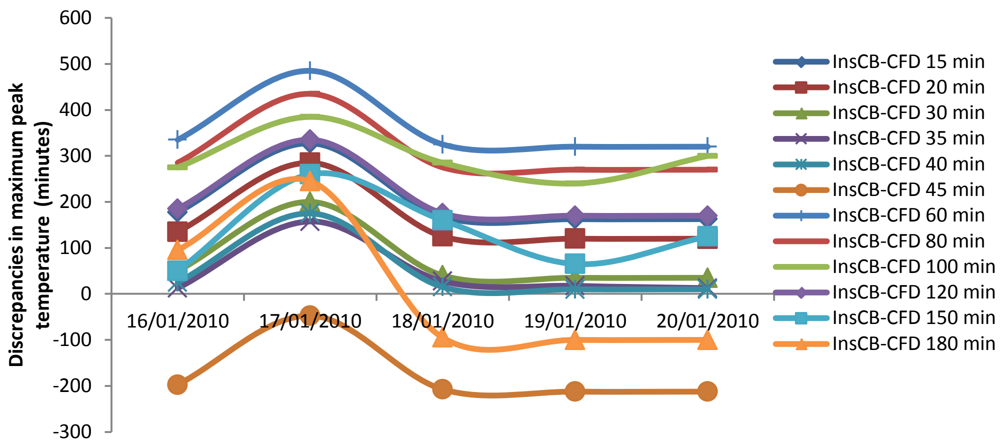

Figure 4.16b. Discrepancies in the peak temperatures for all modules in the summer week for the different time steps for the Insulated Cavity Brick Module.

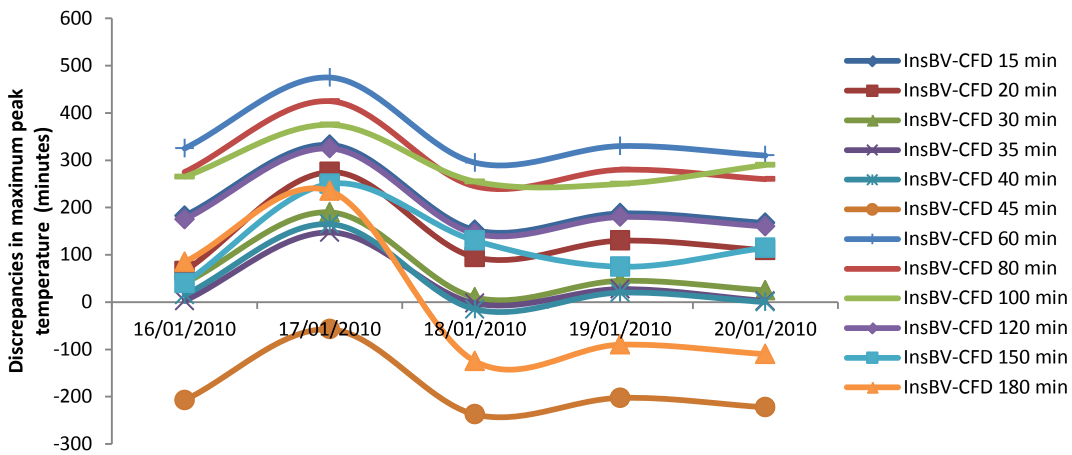

Figure 4.16c. Discrepancies in the peak temperatures for all modules in the summer week for the different time steps for the Insulated Brick Veneer Module

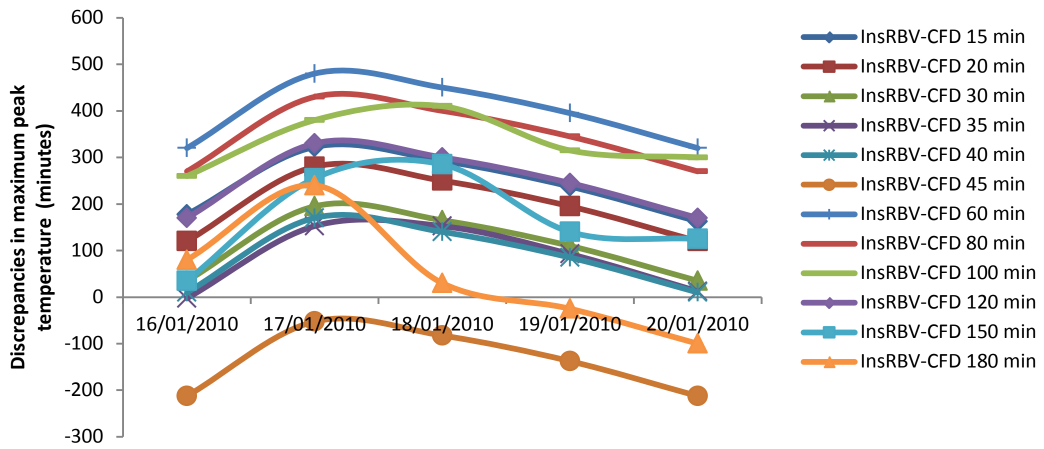

Figure 4.16d. Discrepancies in the peak temperatures for all modules in the summer week for the different time steps for the Insulated Reverse Brick Veneer Module

From the above, the discrepancies in peak temperature lagged by almost a fixed time for each time step, where the average discrepancies in the peak temperature for each time step for all the modules are shown in Figures 4.17.

The average discrepancies in peak temperature for all the modules shows that there were 3 - 5 hour discrepancies in the peak temperatures inside the buildings for most time steps compared to the real peak air temperature inside the buildings.

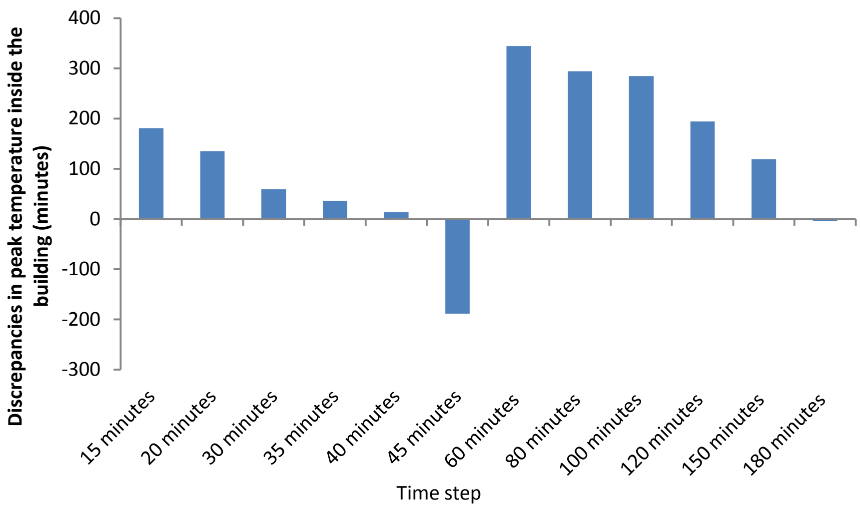

Figure 4.17a. Average discrepancies in peak temperature for all the modules for the summer week.

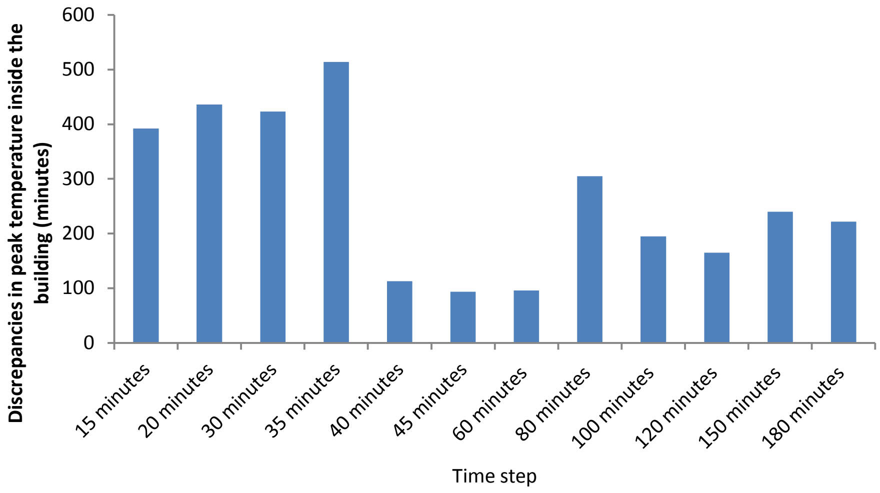

Figure 4.17b. Average discrepancies in peak temperature for all the modules for the different time steps in winter week.

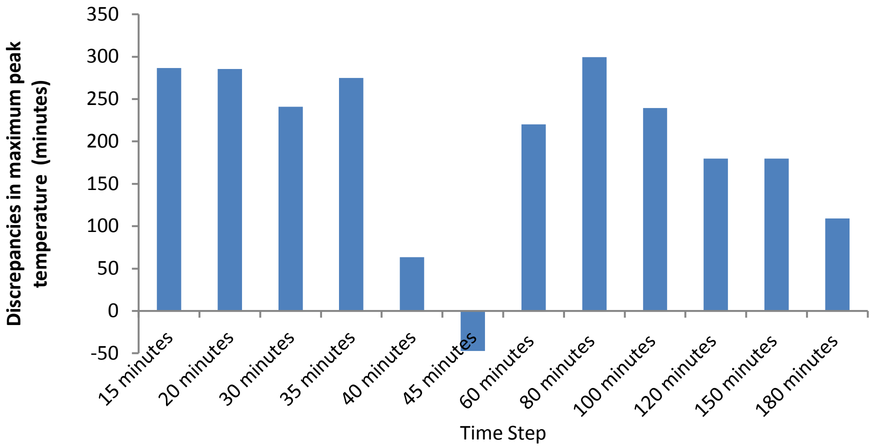

Figure 4.17c. Average discrepancies in peak temperature for all the modules for the different time steps (Average; winter + summer week)).

Peak temperature lagged (shifted) by an almost fixed time for each time step where the 80/100 minute time step lagged between 4 to 5 hours compared to real data for internal air temperature. The best results, in regards to the discrepancies in peak temperatures, come from the 40/45 minutes time step which was almost identical to the real data.

To examine the accuracy of the previous values the peak temperature will shift by certain period as shown in Table 4.4 (the recommended values were taken from Figure 4.17c.) where a positive value means shift backward and negative value means shift forward.

Table 4.4. Shifted time for the peak temperatures inside the buildings for each time step.

Time step (minutes)	15	30	40	45	60	80	100	120	150	180
Shifted time (hours)	4	4	1	-1	4	5	4	3	3	2

For example, for the 15minute time step for the InsCB, the discrepancy in the peak temperatures was 4 hours between the real data and the CFD simulation, so by shifting the curve back 4 hours the peak temperature time will match the real data peak time.

Applying larger time steps (60, 80, 100, 120, 150, 180 minutes) and shifting the peak temperature inside the building (according to the previous Table) results in better outcomes. By comparing the percentage of the number of hours where temperature difference falls within 3^{o}C between real data and CFD simulation for each module showed that shifted the peak temperature for 80 and 100 minutes provide more accurate results compared to the real data as shown in Table 4.5.

Table 4.5. Percentages of the number of hours between the real data and the CFD simulation for each module.

Time step/ model-season	CFD 60 min	CFD 60 min-shifted	CFD 80 min	CFD 80 min-shifted	CFD 100 min	CFD 100 min-shifted	CFD 120 min	CFD 120 min-shifted
CB summer	90.30%	94.55%	86.67%	93.79%	83.64%	88.34%	84.85%	85.37%
InsCB summer	98.79%	100.00%	95.15%	98.76%	88.48%	91.41%	87.27%	89.63%
InsBV summer	88.48%	90.91%	87.27%	93.79%	80.00%	91.41%	79.39%	84.15%
InsRBV summer	95.15%	95.15%	88.48%	95.65%	84.85%	88.96%	85.45%	87.20%
CB winter	96.36%	93.33%	93.33%	93.79%	94.55%	94.48%	84.85%	89.02%
InsCB winter	92.12%	89.70%	92.73%	92.55%	90.30%	90.80%	85.45%	89.63%
InsBV winter	50.91%	52.12%	70.30%	72.22%	80.61%	83.44%	83.03%	85.98%
InsRBV winter	76.97%	68.48%	87.88%	82.72%	94.55%	96.32%	89.70%	93.29%
Average	**86.14%**	**85.53%**	**87.73%**	**90.41%**	**87.12%**	**90.64%**	**85.00%**	**88.03%**

The fastest simulation with the most accurate results came from the 80/100 time step where 90% of the results fall within 3°C difference from the real data, with 1% of the computing time, compared to the 1minute time step. However this will shift the peak temperature time by an average of 2- 4 hours.

4.5 Wind Effect

The outside air temperature has an impact on heating and cooling loads. The CFD analysis can be used for long-term simulations (i.e., weeks and months) but including the wind effect in the CFD simulations requires very small time steps (seconds and milliseconds), which makes it impractical when using accessible personal computers.

Generally, the CFD predicts turbulent wind flows through Direct Numerical Simulation (DNS). However, the DNS method requires very small time steps, which makes the simulation extremely long (Zhai et al. 2007). In this section, a new method which includes the wind effects surrounding the buildings in the external air temperatures is developed. This new temperature (called here $T_{natural}$) causes the same rate of convection heat loss as is caused by the wind.

The Main Issues with Wind Simulations

- **Time Step Size**

For non-motion flow modelling, the time step size is at least a tenth of the mean flow velocity (0.1 of the time needed to travels the length of the device). In many cases, a much smaller time step size (1/20th) will be required to effectively determine the flow. In Autodesk CFD Simulation (2014), a good guideline for the time step size is approximately 1/20th the time required for a particle of fluid to cross the length of the device (Autodesk, solar heating 2014). For example, an average wind speed (V) 6m/s for 6m long building (L):

$$\textbf{Total travel time} = \mathbf{L/V} \quad (4.1)$$

The time required for the wind to cross the module is one second (6m / 6m/s = 1second)

$$\textbf{Time step size} = \mathbf{1s \times (1/20)} = 0.05\text{s} \quad (4.2)$$

Using a time step size of 0.05 second (0.000835 minutes) will take a very long computing time, which makes it impossible for the building analysis to include the wind effect and to simulate the results for long-term periods using available PCs, as is shown in the Table 4.6.

Table 4.6. Computing time for 0.05 second time step

Computing time for one day	Computing time for one week	Computing time for 30 days	Computing time for a season (120 days)
208 Days	1247 Days	5346 Days	21385 Days

➢ **Divergence**

The time step size for a typical solar heating simulation can be in the order of 100 seconds or more. Using larger time step sizes (1 or 5 minutes) to analyse for long-term periods will lead to divergence (i.e. when the solution no longer changes with additional iterations it is called divergence), because the iterative process is repeated until the variation becomes small, from one iteration to the next. If the transient simulation is diverging, the time step size should be decreased, which leads to longer computing times (Autodesk, Transient Flows 2014).

Most simulations are designed for shorter simulations (milliseconds, seconds, minutes and hours), so applying the wind effect required very small time steps otherwise the analysis will reach convergence. For example, the specified number of iterations is 750, which is the maximum number of iterations that will run. The Autodesk Simulation CFD 2014 stops the solution when either 750 iterations have been completed or when the solution reaches divergence, whichever comes first.
Wind changes the speed and direction all time. The wind speed and direction were recorded at the site every 5 minutes for one week from 14/01/2010 -21/01/2010, as shown in Figure 4.18 and Figure 4.19.

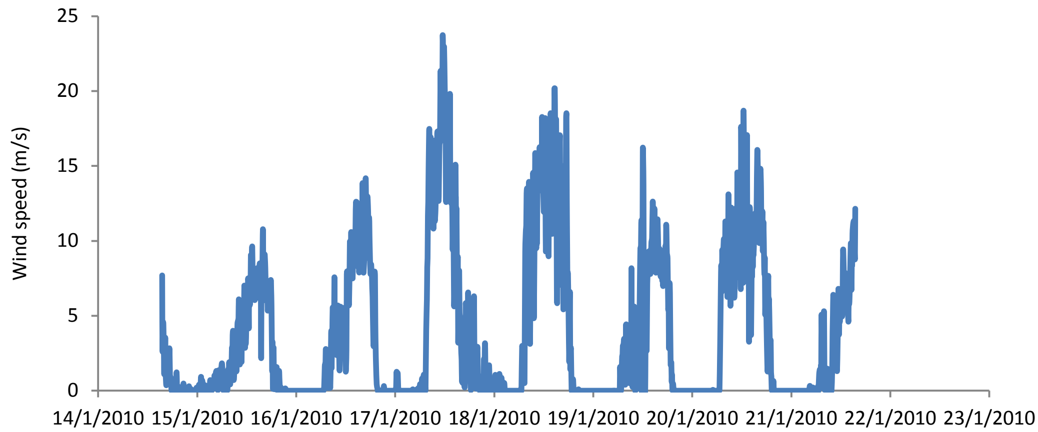

Figure 4.18. Wind speed for one week recorded on top of the building (4 metres from the ground).

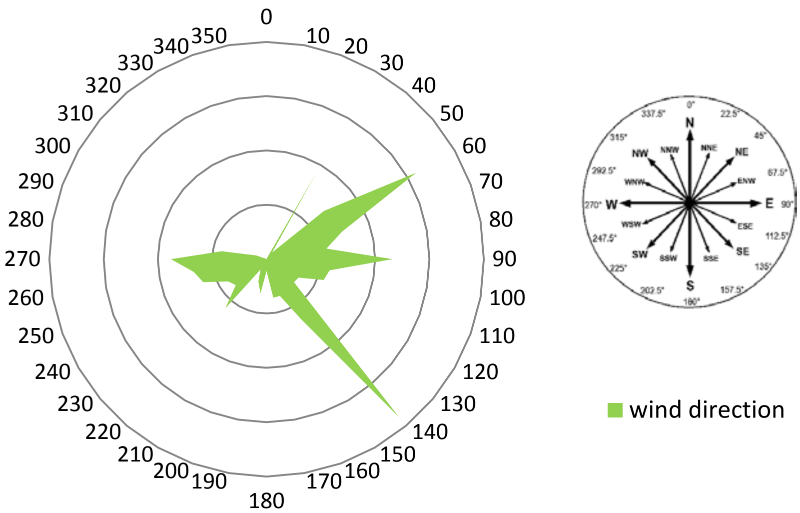

Figure 4.19. Frequency of wind direction (percentage of time wind came from each direction).

There have been many attempts at long-term wind simulation by coupling two software programs which still requires lengthy computing times. However, in this method one programme will be used to simulate wind by applying the wind effect to the external air temperature surrounding the building which will then allow the use of larger time steps (which mean faster computing time) without the simulation diverging.

To find a new external air temperature which causes the same rate of convection heat loss as with wind, the convective heat transfer equation was used (Cengel 2006):

$$\mathbf{q = h_c\, A_s\, (T_s - T_{air})} \tag{4.3}$$

Where;

q : Heat energy (W).
h_c : Convective heat transfer coefficient ($W/m^2.K$) .
A_s : Surface area (m^2).
T_s : Surface temperature (K).
T_{air}: Ambient air temperature (K).

The heat transfer coefficient varies with wind speed. To find the new air temperature $T_{natural}$ (no wind effect) which causes the same rate of convection heat loss as T_{total} (with wind effect) we can now rewrite the equation:

$$\mathbf{q = h_{natural}\, A_s\, (T_s - T_{natural}) = h_{total}\, A_s\, (T_s - T_{total})} \tag{4.4}$$

Which simplifies to:

$$\mathbf{T_{natural} = T_s - (h_{total} / h_{natural})(T_s - T_{total})} \qquad (4.5)$$

$T_{natural}$: Outside air temperature with wind speed equal zero (no wind effect)
T_{total} : Outside air temperature with wind speed of V_{actual}.
$h_{natural}$: Natural convection heat transfer coefficient with no wind (4.5W/m^2.K) (Luo C, 2010)
h_{total} : Total heat transfer coefficient (h_{forced} + $h_{natural}$).

To calculate the convective heat exchange at an external building surface, due to air flow along the surface (h_{forced}), is usually modelled by convective heat transfer coefficients which can be calculated through this equation (Defraeye et al. 2011):

$$\mathbf{h_{forced} = 5.01(U_{10})^{0.85} \text{ for WW}} \qquad (4.6)$$

$$\mathbf{h_{forced} = 2.27(U_{10})^{0.85} \text{ for LW}} \qquad (4.7)$$

Where;

h_{forced}: Forced convective heat transfer coefficients for exterior building surfaces.
U_{10} : Wind speed at a height of 10m above the ground, which is the typical arrangement for weather station anemometers.
WW: Windward incidence angles from -90 to 90.
LW : Leeward (remainder of incidence angles). Where incidence angles is the angle between approach flow wind direction and the normal to the windward surface.

The exterior total convection heat transfer coefficient as a quadratic summation of natural and forced convection components (Booten et al. 2010):

$$\mathbf{h_{total} = (h^2_{force} + h^2_{natural})^{0.5}} \qquad (4.8)$$

Where;

h_{total} : Total (forced + natural) exterior convective coefficient.
h_{forced}: Forced exterior convective coefficient.
$h_{natural}$: Natural exterior convective coefficient.

Finding the wind speed at 10m height (z) where the wind data is recorded at ~4m from the ground (z_r) will use the logarithmic law (Manwell et al. 2009):

$$\frac{u(Z)}{u(Zr)} = \frac{\ln(\frac{Z}{Zo})}{\ln(\frac{Zr}{Zo})} \qquad (4.9)$$

Where;

$u(z)$: Wind speed at 10m height.
$u(z_r)$: Available wind speed at 4m height (anemometer height over the building).
z_o : Surface roughness (Few trees z = 0.1m from Table 4.7). The landscape for the University of Newcastle, Australia.

At a height of 10 metres (z) ($U10 = 1.661 \times U_4$ at 4m height)

Note: The speed at 10 metres height equals 1.661 times the wind speed recorded on top of the modules (i.e., anemometer location).

Table 4.7. Values of the surface roughness for various types of terrain (Manwell et al. 2009).

Terrain Description	**z_0 (mm)**
Lawn grass	8
Rough pasture	10
Fallow field	30
Crops	50
Few trees	100
Many trees, hedges, few buildings	250
Forest and woodlands	500
Suburbs	1500
Centres of cities with tall buildings	3000

CFD analyses were used to analyse the modules after including the wind effect into the external air temperature surrounding the building which was developed in Section 4.2 and as shown in Figure 4.20.

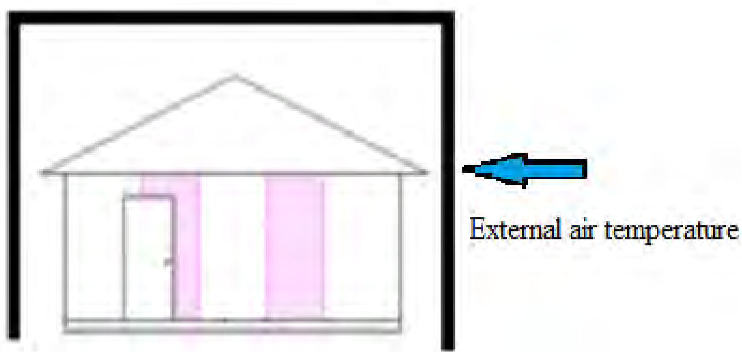

Figure 4.20. New external air boundary including the wind effect used in the CFD simulations.

The CFD analysis was run for each module using the new air temperature $T_{natural}$ (no wind effect), which causes the same rate of convection heat loss as T_{total} (with wind effect), then the simulation results were compared with the real data.

For the four sides of the new external boundary which were applied for all the modules (the roofs were fully insulted to eliminate any heat exchange), a new temperature was applied which included the wind effect for each side of the building. As an example, the results for the InsRBV are shown in Figures 4.21.

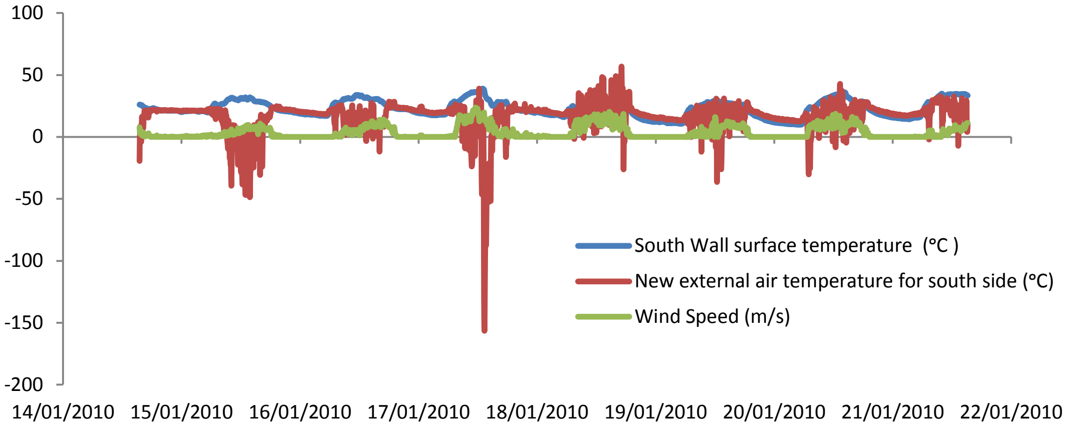

Figure 4.21a. The wall temperature, new air layer temperature and wind speed for the InsRBV external southern walls.

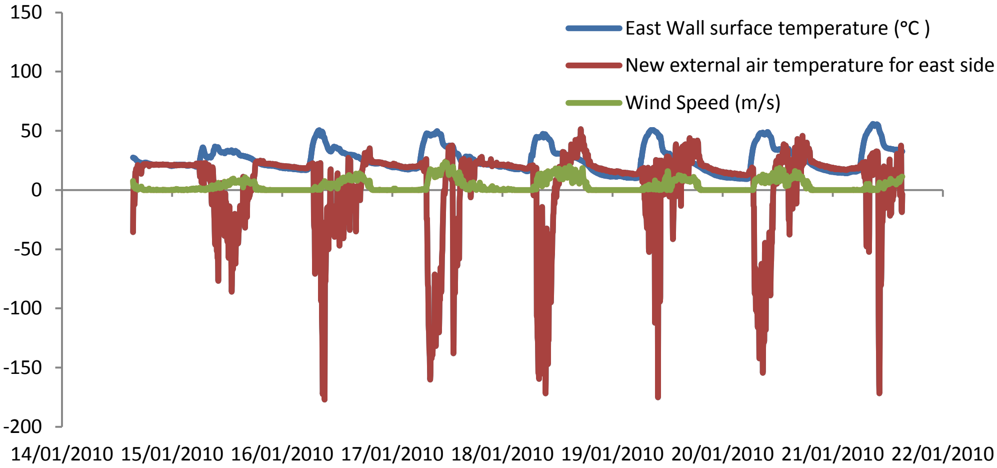

Figure 4.21b. The wall temperature, new air layer temperature and wind speed for the InsRBV external eastern walls.

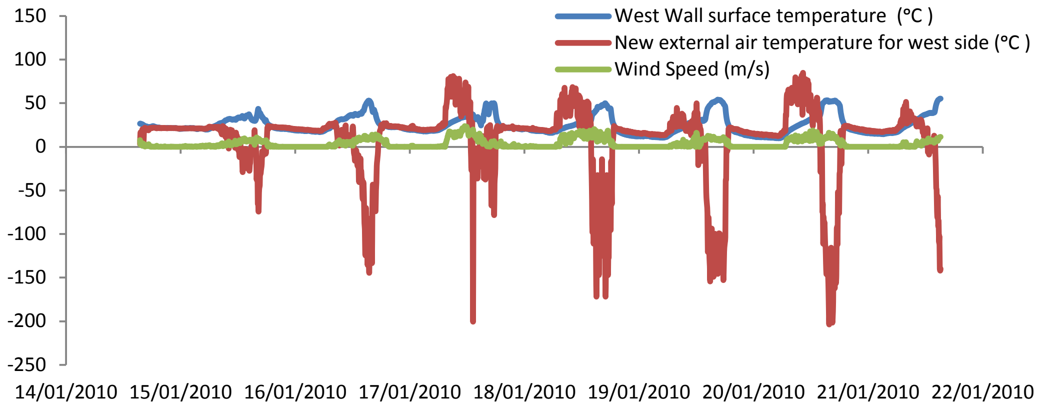

Figure 4.21c. The wall temperature, new air layer temperature and wind speed for the InsRBV external western walls.

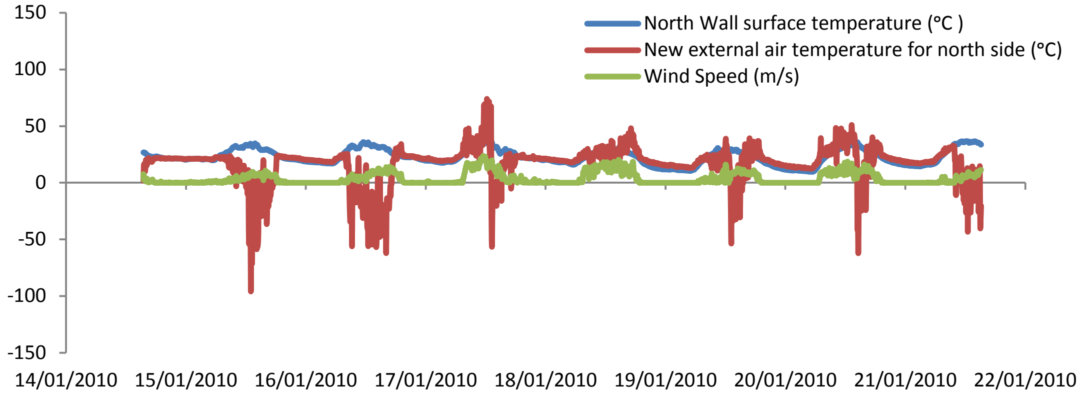

Figure 4.21d. The wall temperature, new air layer temperature and wind speed for the InsRBV external northern walls.

From the above, if the wall surface temperature is higher than the external air temperature, the new external air temperature with wind effect will be lower than the wall surface temperature, and if the wall surface temperature is lower than the external air temperature, the new external air temperature with wind effect will be higher than the wall surface temperature.

Higher wind speeds increased the wind effect, which resulted in an increase in the new external air temperature, while the wind direction increased the wind effect on the wall faced by the wind. Because most of the wind came from the east and west, the effect on the eastern and western walls was much higher compared with the northern and southern walls.

Figures 4.22 show the CFD simulation analyses, with the wind effect included in the external air boundary layer, compared to the real data for all the modules using an 80 minute time step size.

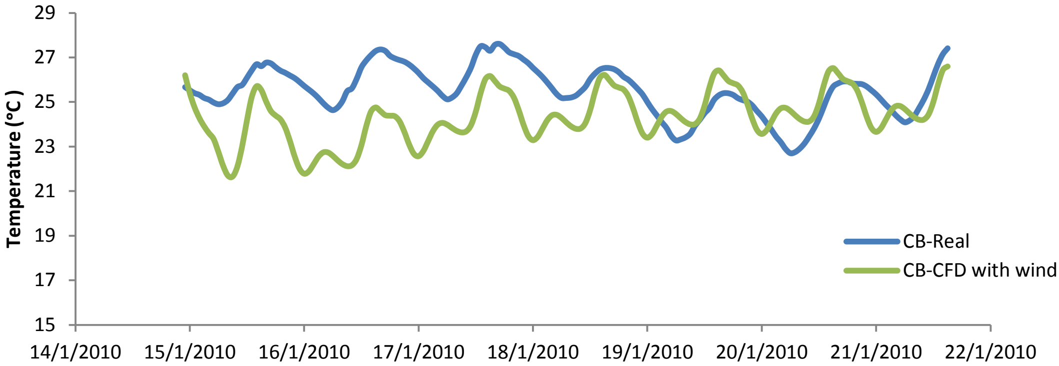

Figure 4.22a. The internal air temperature for the CFD simulations with the wind effect included and the real data for the Cavity Brick Module.

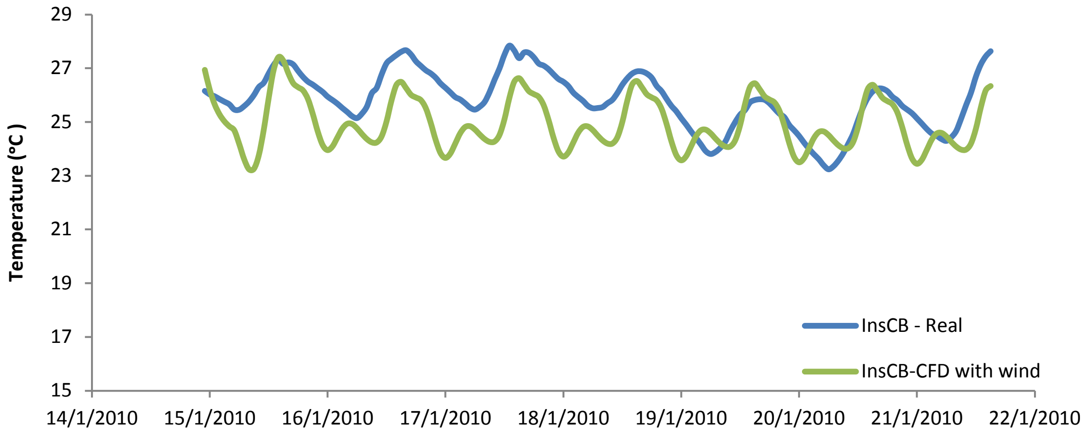

Figure 4.22b. The internal air temperature for the CFD simulations with the wind effect included and the real data for the Insulated Cavity Brick Module.

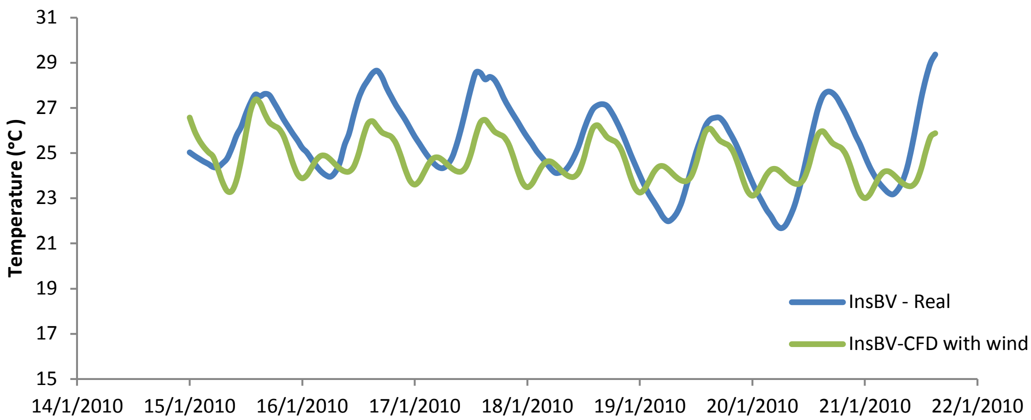

Figure 4.22c. The internal air temperature for the CFD simulations with the wind effect included and the real data for the Insulated Brick Veneer Module.

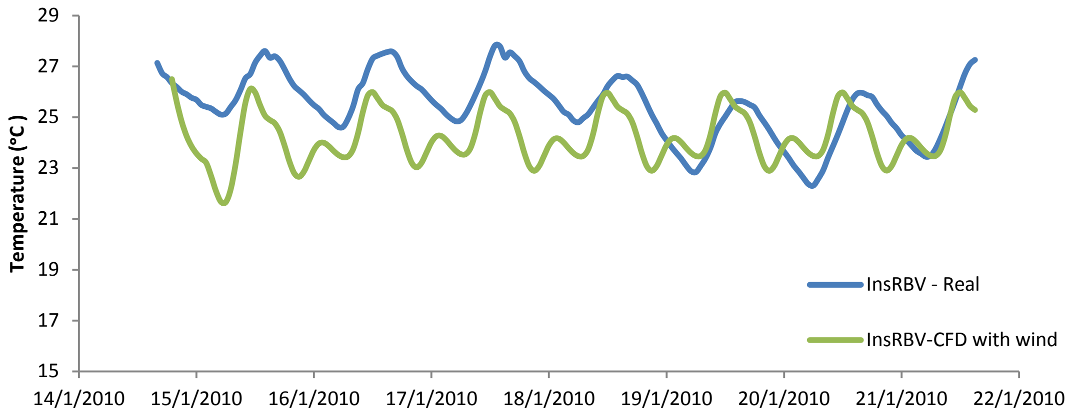

Figure 4.22d. The internal air temperature for the CFD simulations with the wind effect included and the real data for the Insulated Reverse Brick Veneer Module.

By comparing the number of hours that each module falls within the temperature difference (range) between the CFD simulation and the real internal air temperature, it is clear that applying wind to the external boundary will result in accurate internal air temperature calculations, where more than 90% of the simulated CFD results (91% for CB, 99% for InsCB, 94% for InsBV, 93% for InsRBV modules) fall within 0 - 3ºC difference compared to the real data, as shown in Table 4.8.

Table 4.8. Percentage of the number of hours for each temperature difference between the real data and the CFD simulation for the analysed period.

Temperature Range (ºC)	Cavity Brick Module	Insulated Cavity Brick Module	Insulated Brick Veneer Module	Insulated Reverse Brick Veneer Module
0-1	36%	51%	42%	32%
0-2	67%	84%	80%	74%
0-3	**91%**	**99%**	**94%**	**93%**
0-4	99%	100%	100%	100%

Neglecting the wind effect will lead to imprecise results compared with the results which included the wind effect, as is shown in Table 4.9. By including the wind effect, more than 90% of the results were within 0 - 3ºC difference compared to the real data, but when neglecting the wind effect the results drop to 83 - 88% difference compared to the real data. This illustrates the significance of adding the wind effect to precisely simulate the thermal performance of the modules.

Table 4.9. Percentage of the number of hours for each temperature difference between the real data and the CFD simulation for the analysed period (neglecting wind effect).

Temperature Range (ºC)	Cavity Brick Module	Insulated Cavity Brick Module	Insulated Brick Veneer Module	Insulated Reverse Brick Veneer Module
0-1	33%	48%	40%	30%
0-2	62%	77%	76%	69%
0-3	**87%**	**88%**	**85%**	**83%**
0-4	93%	96%	97%	99%

A building's internal air temperature can be calculated by adopting the new air temperature $T_{natural}$ which takes into account the same rates of convection heat losses created by the wind surrounding the building. Therefore, $T_{natural}$ enables a direct inclusion of the wind effect and considerably decreases the overall computing time.

Applying the wind effect to the external air temperature layer allows the use larger of time step sizes (60, 80 or 100 minutes) and the CFD simulation process will take a shorter computing time, from 20-30 minutes for a one week simulation compared to weeks when using smaller time step sizes.

The methods discussed above significantly reduce simulation time whilst still agrees well with the real internal air temperature data for the modules

4.6 Summary

By running the CFD simulations after adding the new boundary condition (new volume / external air layer enclosing the simulated module) the prolonged rise in the internal air temperature for the simulated modules was prevented. The CFD simulations with two external air boundary conditions provided more accurate results compared to the one external air boundary condition. It also provided a better representation of the real air temperatures inside the module, where more than 89% of results of the CFD simulated modules with two external air boundary conditions falling within 0 - 3ºC temperature difference compared with the real air temperatures measured inside the module.

Larger time steps were used to speed up the simulation time and give higher temperature fluctuation ranges but they increased the discrepancies in peak temperatures (the peak temperature inside the building will shift/lag compared with the real data). There is a direct relationship between the time step size and the temperature fluctuation range, where the temperature fluctuation range increased with a larger time step size. The fastest simulation with the most accurate results came from the 80/100 time step where 90% of the results within 3ºC of the real data, with 1% of the computing time compared to the 1 minute time step. However this may shift the results by up to 5 hours.

The building simulation requires very small time steps (seconds and milliseconds) when the wind effect is considered. This makes it unrealistic for long-term building analysis (i.e., weeks or months) using personal computers which may take years to process. For faster simulations and the maintenance of accurate results, the wind effect was accounted for by adjusting the external air temperature surrounding the building and the analysis was performed using larger time steps (minimizing computing times) without the simulation results diverging. A building's internal air temperature can be calculated by adapted the new air temperature $T_{natural}$ which takes into account the same rates of convection heat loss created by the wind surrounding the building. Therefore, $T_{natural}$ enables a direct inclusion of the wind effect and considerably decreases the overall computing time.

The techniques to enable the use of CFD analysis for prolonged simulations which have been developed and described in this chapter are now applied in the following chapters to develop the ATM for the assessment building thermal comfort.

To illustrate the applicability of the adjustments made for the CFD analysis for the complete structure, the analysis of actual Western Australia house in different climate zone is presented in Chapter 6.

Chapter Five:
Development of the Adaptive Thermal Metric (ATM)

5.1 Overview

In this chapter the thermal comfort ATM is developed using CFD simulations incorporating the adjustments described in Chapter 4. Analyses were carried out on the four modules, to find the module internal air temperature for the same point as was measured in the real house modules (at 1200mm height). The results were then verified by comparison with the results from the full-scale experimental housing test modules.

To find the thermal comfort ATM, the average volume internal temperatures inside the building need to be calculated. Simulations were carried out for one year for all modules using typical metrological year (TMY) data. The average internal air volume temperatures with the adaptive thermal comfort range were then used to evaluate the ATM.

Further assessment and validation of the ATM was carried out using the observed data from the housing test modules and with the results of the other AccuRate simulations of the same modules.

5.2 The ATM Development

After solving the CFD issues, the modified CFD simulations were carried out over a one year period to find the internal air temperature at 1200mm height for all the modules. For example, Figure 5.1 shows the results for the InsBV module from February 2012 to January 2013 compared with the real data (the data for December was unavailable). Appendixes E and F show the monthly CFD results and real data for the InsBV and InsCB modules.

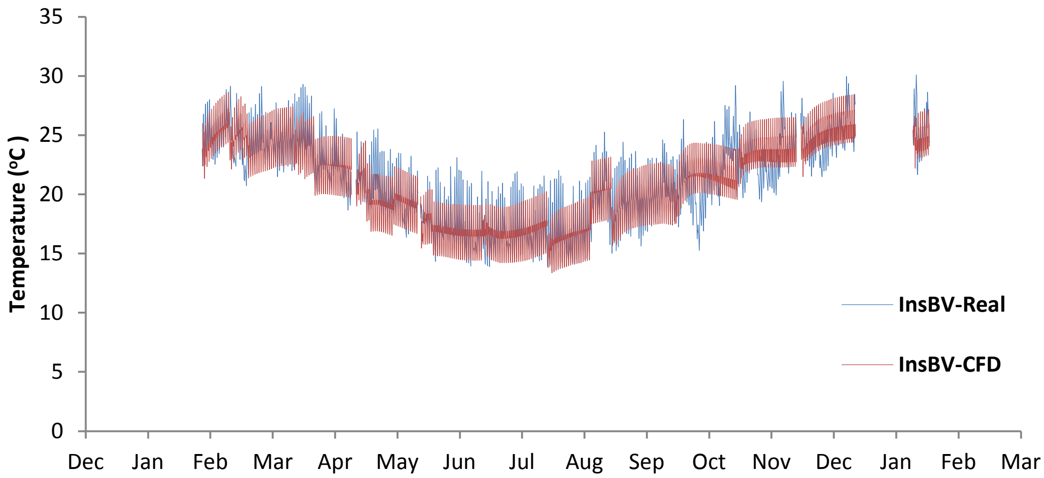

Figure 5.1. The real data and CFD simulations for the inside air temperature of the InsBV module.

The CFD simulation results are consistent and followed the trend of the outside air temperature over one year's analysis, which indicates the ability of this method to capture the dynamic external environment and predict the modules internal air temperature at reasonable degree of accuracy.

Comparison between the CFD simulations and the real data at 1200mm height inside each module showed that average accuracy at any given time during one year's simulations was approximately 93% for all modules, as is shown in Table 5.1. More than 90% of the results were within 3ºC difference compared with the real data for whole year's simulation, as is shown in Table 5.2.

Table 5.1. The average accuracy at any given time during one year's simulation.

CB	InsRBV	InsCB	InsBV
93.5%	93.7%	93.8%	92.7%

Table 5.2. Comparison between the CFD simulations and the real data.

Bin (ºC)	CB	InsRBV	InsCB	InsBV
0-1	43.20%	43.07%	45.08%	38.88%
0-2	74.98%	74.88%	78.56%	71.51%
0-3	**91.90%**	**91.26%**	**93.21%**	**90.16%**
0-4	97.47%	97.77%	98.10%	96.77%
0-5	99.38%	99.57%	99.51%	98.87%

Faster simulations for one year (using larger time steps, shifting peak temperatures and applying wind to the external volume) will be less accurate than simulating different time steps for each season, but this will take a longer computing time, so there is a compromise of some degree of accuracy for faster computing times.

After finding the temperatures inside the buildings using the CFD simulations, the next step is to find the ATM which characterises the thermal performance of the buildings using adaptive thermal comfort concepts. To find the ATM, the average volume internal temperatures inside the buildings need to be calculated (rather than the point temperature), using the CFD results (part) by selecting the internal air volume inside the module, to find the average air temperatures. Figures 5.2c and 5.2d show temperature variation through the InsCB module for different elevations during winter day and Figure 5.2e for summer day. Full details of the variation of temperature through the northern and western walls in Appendixes G and H.

Simulations were carried out for one year for all the modules using the TMY (Typical Meteorological Year), as shown in Figure 5.2b. To find the average internal air volume temperatures for all the modules, the average internal air volume temperatures is used to find the adaptive thermal comfort range.

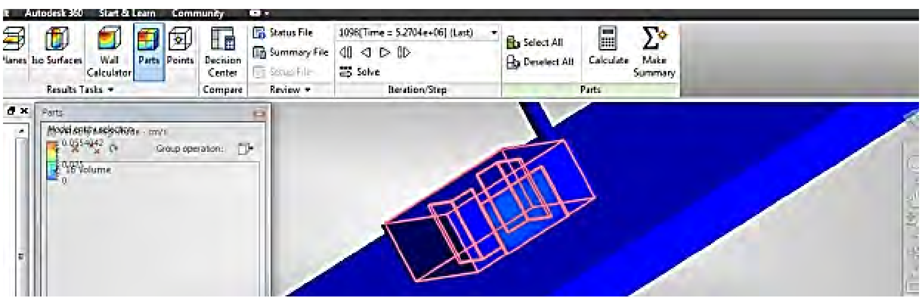

Figure 5.2a. Autodesk CFD screen shot for the average air temperature.

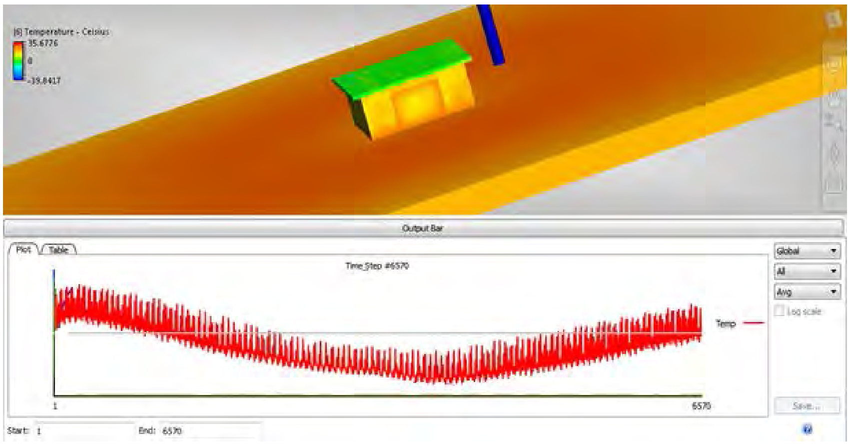

Figure 5.2b. Snapshot from the CFD simulation showing the temperature variations over one year inside the module.

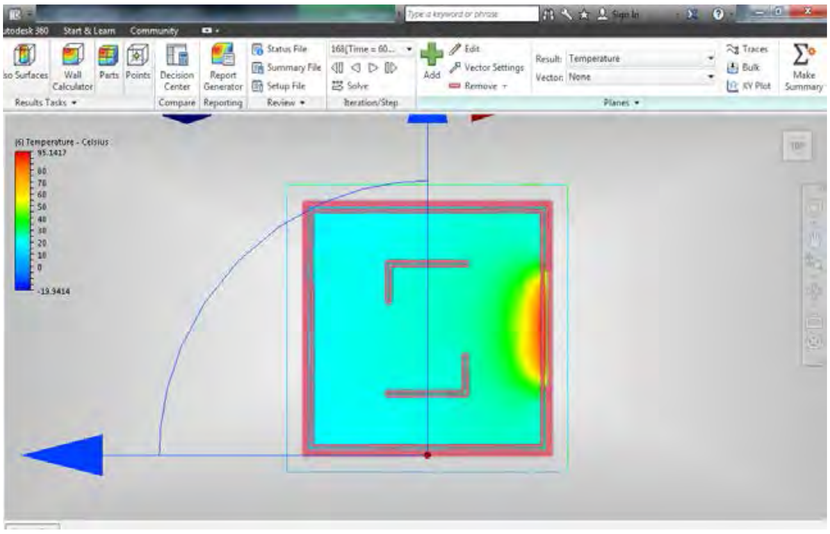

Figure 5.2c Horizontal plane inside the InsCB module during midday in winter on the floor (zero elevation).

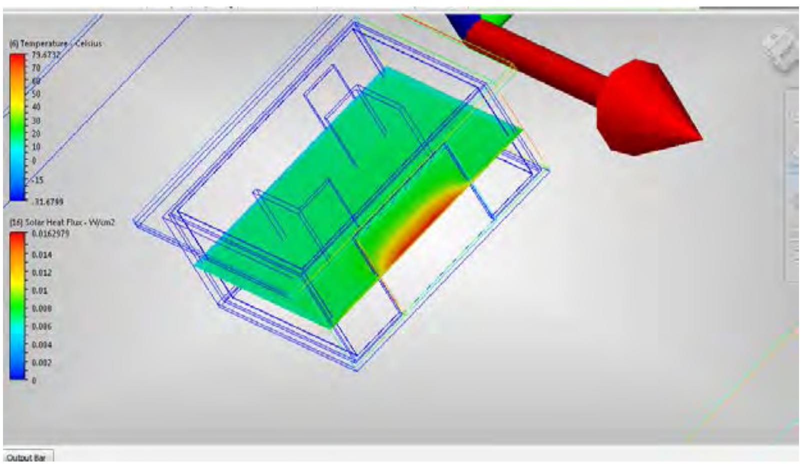

Figure 5.2d. Horizontal plane inside the InsCB module during midday in winter for 1200mm elevation.

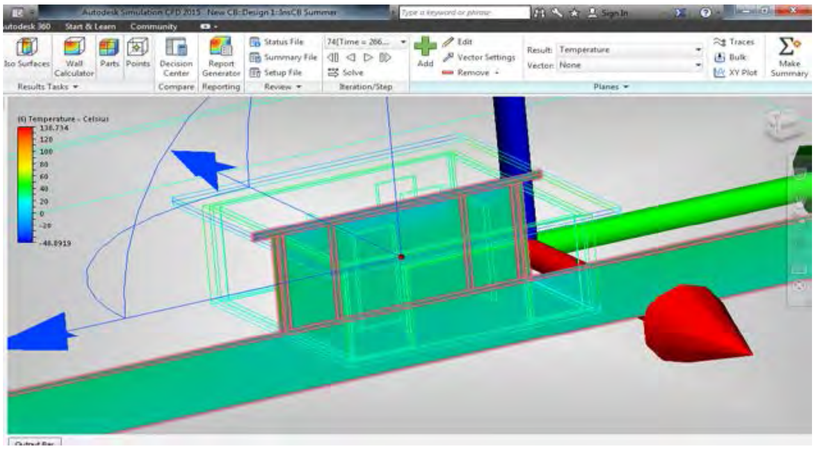

Figure 5.2e. Vertical plane inside the InsCB module during summer day.

To find the adaptive thermal comfort inside the building, the following equations will be used for the temperate climate in Australia (see Chapter 3 for Equations 3.1 to 3.3).

$$\mathbf{T_c = 17.8 + 0.31 \times T_o} \quad (3.1)$$

$$\textbf{\textit{90\% acceptability limits}} = \mathbf{T_c \pm 2.5\ ^oC} \quad \text{(ATM90)} \quad (3.2)$$

$$\textbf{\textit{80\% acceptability limits}} = \mathbf{T_c \pm 3.5\ ^oC} \quad \text{(ATM80)} \quad (3.3)$$

After finding the average volume internal air temperatures inside the buildings, the next step is to find the thermal comfort range over one year, which accounts for the percentage of time over which the internal temperatures of the buildings remain within the comfort range for all modules.

For the Cavity Brick (CB), Insulated Cavity Brick (InsCB), Insulated Brick Veneer (InsBV) and Insulated Reverse Brick Veneer (InsRBV) modules, the internal air temperatures inside the buildings using the CFD simulations and an adaptive thermal comfort range of 90% and 80% ***acceptability limits*** (ATM90; ATM80) are shown in Figures 5.3, 5.4, 5.5 and 5.6. These Figures show the outside air temperatures and the CFD simulated temperature fluctuations over one year. The green line represents the adaptive thermal comfort temperatures, the red and the black lines are for the higher and lower 90% and 80% ***acceptability limits***, respectively.

The adaptive thermal comfort temperatures varied over one year, peaking at 26.2ºC in summer and dropping to 23.1ºC in winter. The 90% ***acceptability limits*** (ATM90) will add 2.5ºC on both sides to expand the temperature range to 28.7 - 23.7ºC in summer and 25.6 - 20.6 ºC in winter. The 80% ***acceptability limits*** (ATM80) will expand the thermal comfort temperatures further to 29.7 - 22.7ºC in summer and 26.6 - 19.6ºC in winter. These wider ranges will potentially save massive amounts of imposed operational energy but will only make the occupants slightly more uncomfortable with the new temperatures.

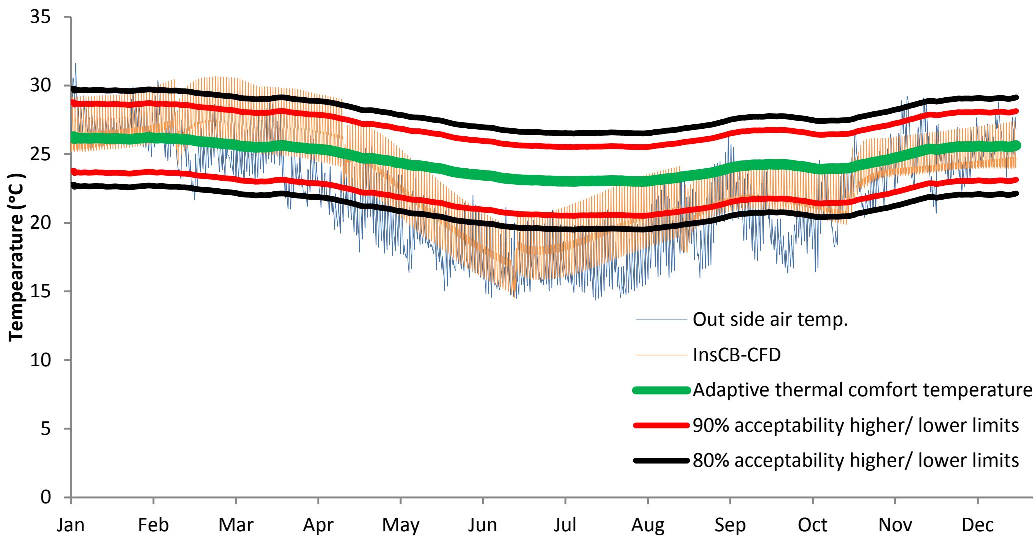

Figure 5.3. Internal air temperatures and thermal comfort ranges for the InsCB module for one year.

For the InsCB module the temperatures fall outside the thermal comfort ranges in part of the months of March, May, August and most of June and July, while in November and December the module's thermal performance was the best. The InsCB module has a high thermal mass so when the outside air temperature dropped the internal air temperature stabilised due to the thicker walls and remained within the acceptable thermal comfort range.

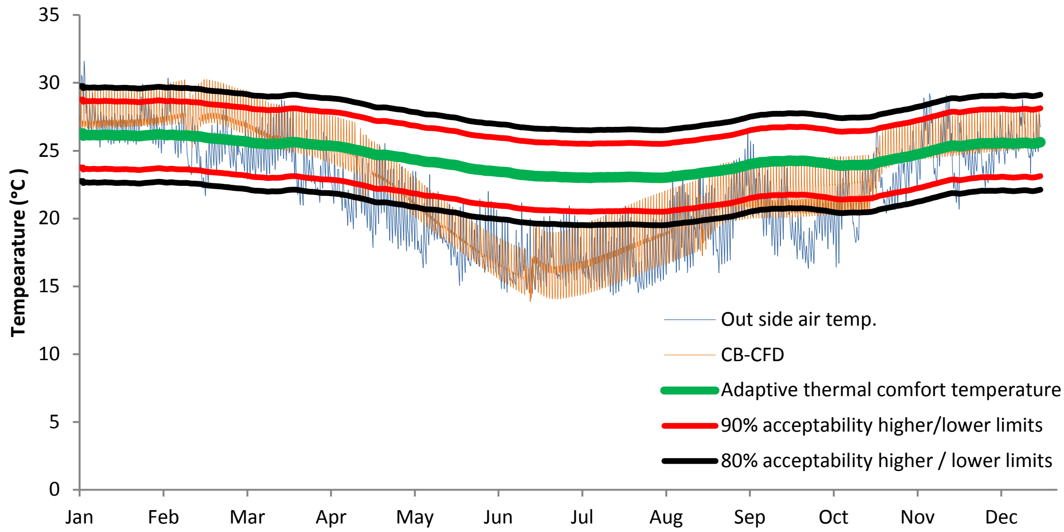

Figure 5.4. Average volume internal air temperatures inside the building and thermal comfort ranges for the CB module for one year.

For the CB module the temperatures fall outside the thermal comfort ranges in part of the months of May, August, September and October and most of June and July, while in November and December the temperatures remain within the comfortable range.

The CB module has a high thermal mass but no insulation, so when the outside air temperature decreases it is hard for the module to remain within the comfort range. Its thick brick walls release the outside cold inside the module which pushes the temperature outside the acceptable thermal comfort range.

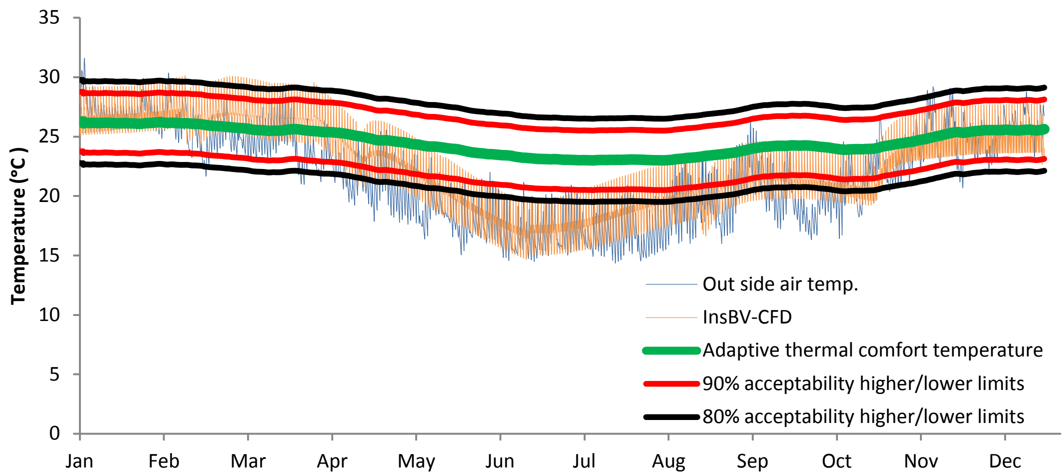

Figure 5.5. Internal air temperatures and thermal comfort ranges for the InsBV module for the whole year.

For the InsBV module, the temperatures fall outside the thermal comfort range in parts of the months of May to October and for most of June and July, while in November and December the module's thermal performance remains within the 90% acceptability limit. The internal air temperature fluctuations for the winter months are higher than the summer months due to the north-facing windows, which heat the module during the day and cool faster (due to greater heat loss through the glass) during the colder winter nights.

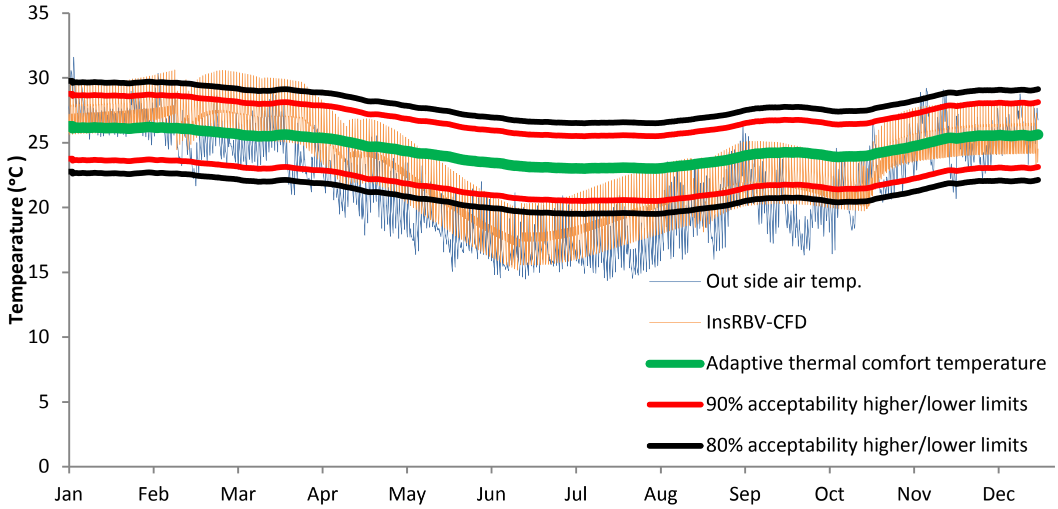

Figure 5.6. Internal air temperatures and thermal comfort ranges for the InsRBV module for the whole year.

The InsRBV module was one of the best thermal performing modules, where the temperatures fell outside the thermal comfort range in parts of the months of March, July and August and for most of June, while remaining within the thermal comfort limits for October, November and December.

For the ATM results to be comparable with other buildings, it should use:

- The Typical Metrological Year (TMY) data for external air temperature for each climate zone.
- The same CFD simulation procedures for all modules, as discussed above, to accurately capture the internal air temperature inside the building.

- The appropriate adaptive equation for the climate zone, which should be a fixed equation for each climate zone. To use the adaptive module it should have:
  - No mechanical cooling or heating systems.
  - Occupants considered as inactive inside the building, with metabolic rates of 1 - 1.3 Met (activity in winter will warm the body but in summer it will make them feel hotter).
  - Occupants are encouraged to adapt their clothing to the indoor and/or outdoor thermal conditions, within a range of 0.5 - 1.0 Clo.

The ATM used to characterise the whole building thermal performance confirmed that the best building thermal performance was observed for the InsCB module, followed by InsRBV, InsBV and CB modules.

5.3 Comparison of Module Performance Using the ATM

Microsoft Excel 2010 was used to compute the number of hours (expressed as a percentage) that the average internal air temperature of the building was in the zone defined by the thermal comfort ATM, compared to the total number of hours of observation (8760 hours (365 days)).

Comparison of the results of the modules, in terms of their thermal comfort for the 90% and 80% ***acceptability limits*** (ATM90; ATM80), showed that the InsCB module performed the best, followed by the InsRBV, then the InsBV, and finally the CB module, as shown in Table 5.3 and Figure 5.7.

Table 5.3. The ATM for all modules.

Acceptability limits / Module	CB	InsBV	InsRBV	InsCB
90% acceptability limits (ATM90)	56.8%	57.3%	61.2%	62.4%
80% acceptability limits (ATM80)	70.2%	71.7%	75.9%	78.2%

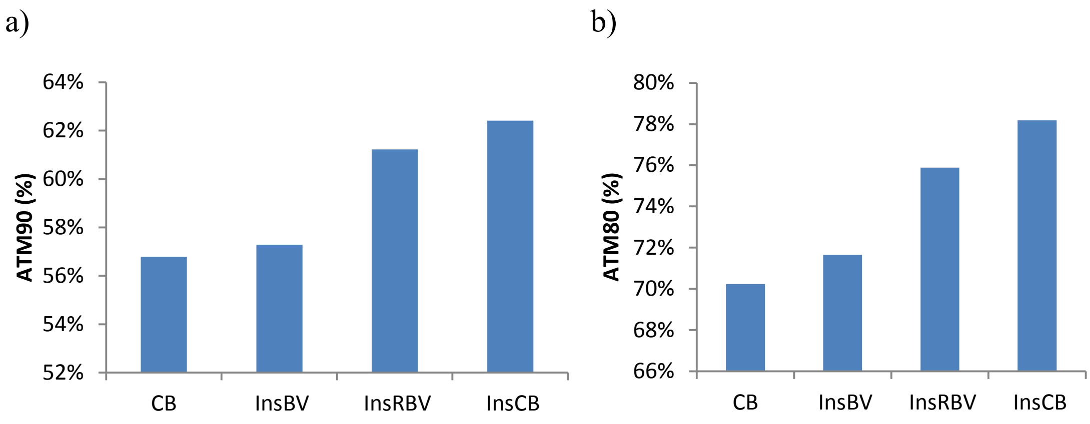

Figure 5.7. ATM results ((a) 90% acceptability limits, (b) 80% acceptability limits).

Overall, all the modules performed badly in the winter months (June, July and August). The monthly performance of each module, in terms of thermal comfort for the 90% and 80% ***acceptability limits*** (ATM90; ATM80 respectively), varies from month to month compared with other modules. For example, the CB building had the lowest thermal comfort in the winter months compared to the rest of the modules, while it performed best in only one month (April), as shown in Figures 5.8.

a)

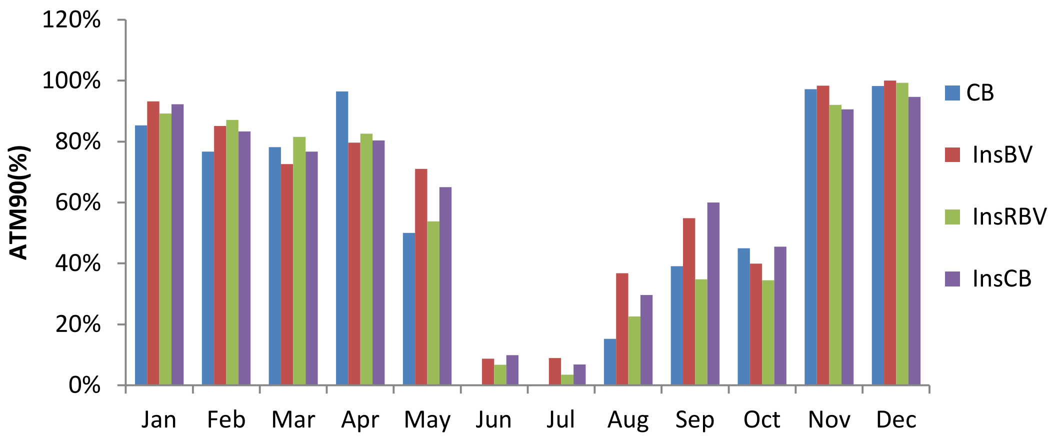

b)

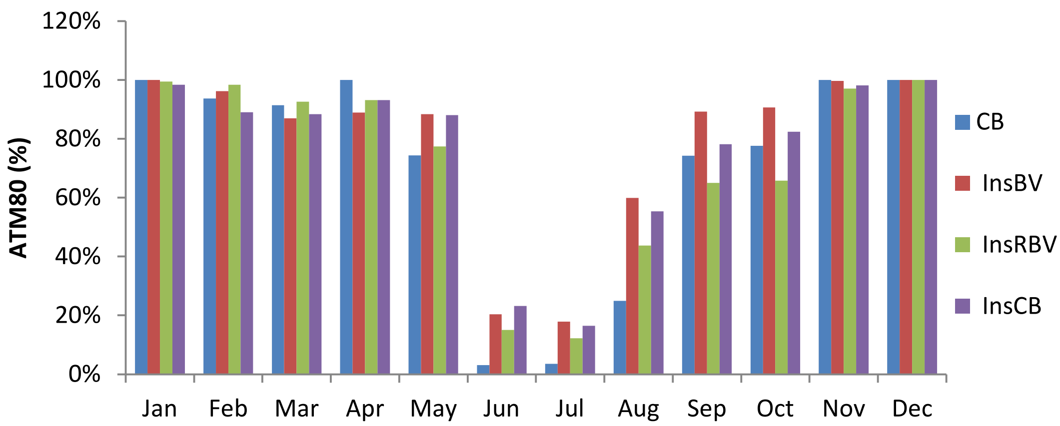

Figure 5.8. Monthly ATM for all modules for one year ((a) 90% acceptability limits, (b) 80% acceptability limits).

Most modules performed badly in the winter months, and this indicates where improvements would be needed. This will help the designer to improve the module design by using, for example, double glazed glass for the window. This will significantly improve the thermal performance of the modules in the winter months, as well as the modules' overall thermal performance.

The internal air temperature falls within the 80% acceptability limit for almost all of the months of January to May, November and December. This was because using the 80% acceptability limit provides wider ranges for the thermal comfort environment and it is easier for the internal air temperature to fall within that limit. However, this will compromise some degree of thermal comfort (80% of people will find it comfortable).

5.4 Simplified ways to Calculate the ATM

In this section representative months for faster CFD simulation to calculate the ATM are investigated. Instead of simulating the full 12 months, the minimum number of months which need to be simulated to result in the same ATM accuracy as the 12 months is determined. The possible monthly combinations are:

Seasonally: Using a representative month for each season results in 4 representative months per year. This will shorten the simulation process by one third of the 12 months simulation time. The average monthly results for summer (January), autumn (April), winter (July) and spring (October) are shown in Table 5.4.

The difference with 12 months calculated ATM can be defined as the ATM obtained from 12 months minus the ATM obtained by representative month for each season.

Table 5.4. ATM found using representative months for each season.

Season	Month	CB		InsCB		InsBV		InsRBV	
		Acceptability limits		Acceptability limits		Acceptability limits		Acceptability limits	
		90%	80%	90%	80%	90%	80%	90%	80%
summer	Jan	85%	100%	93%	100%	89%	99%	92%	98%
autumn	Apr	96%	100%	80%	89%	83%	93%	80%	93%
winter	Jul	0%	4%	9%	18%	3%	12%	7%	16%
spring	Oct	45%	78%	40%	91%	34%	66%	46%	82%
Average (%)		57%	70%	55%	74%	52%	68%	56%	73%
Difference with 12 months calculated ATM		-0.09%	0.05%	-6.98%	-3.80%	-4.87%	-4.01%	-4.97%	-3.28%

The results show that the CB module can be calculated using a representative month for each season, but the rest of the modules show higher variations compared with the 12 month period, which makes this approach less accurate.

Even / odd months: the monthly average results for the even months (February, April, June, August, October, December) and the odd months (January, March, May, July, September, November) are shown in Tables 4.5 and 5.6. This will take half of the simulation time of a full simulation for a 12 month period.

Table 5.5. ATM found using the even months for all modules.

Even months	CB		InsCB		InsBV		InsRBV	
	Acceptability limits		Acceptability limits		Acceptability limits		Acceptability limits	
	90%	**80%**	**90%**	**80%**	**90%**	**80%**	**90%**	**80%**
Feb	77%	94%	85%	96%	87%	98%	83%	89%
Apr	96%	100%	80%	89%	83%	93%	80%	93%
Jun	0%	3%	9%	20%	7%	15%	10%	23%
Aug	15%	25%	37%	60%	23%	44%	30%	55%
Oct	45%	78%	40%	91%	34%	66%	46%	82%
Dec	98%	100%	100%	100%	99%	100%	95%	100%
Average (%)	**55%**	**67%**	**58%**	**76%**	**55%**	**69%**	**57%**	**74%**
Difference with 12 months ATM	**-1.51%**	**-3.69%**	**-4.06%**	**-2.17%**	**-1.85%**	**-2.31%**	**-4.02%**	**-2.03%**

All modules show higher variations (from 1.5 - 4.06%) compared with a 12 month period, which makes this approach less precise.

Table 5.6. ATM found using the odd months for all models

Odd months	CB		InsCB		InsBV		InsRBV	
	Acceptability limits		Acceptability limits		Acceptability limits		Acceptability limits	
	90%	**80%**	**90%**	**80%**	**90%**	**80%**	**90%**	**80%**
Jan	85%	100%	93%	100%	89%	99%	92%	98%
Mar	78%	91%	73%	87%	82%	93%	77%	88%
May	50%	74%	71%	88%	54%	77%	65%	88%
Jul	0%	4%	9%	20%	7%	15%	10%	23%
Sep	39%	74%	37%	60%	23%	44%	30%	55%
Nov	97%	100%	98%	100%	92%	97%	91%	98%
Average (%)	**58%**	**74%**	**63%**	**76%**	**58%**	**71%**	**61%**	**75%**
Difference with 12 months ATM	**1.51%**	**3.69%**	**1.00%**	**-2.32%**	**0.35%**	**-0.77%**	**-0.55%**	**-0.66%**

The odd month results showed the least variation for most of the modules (~2% error) and this approach gave the closest results to the 12 month calculated ATM, as shown in Figure 5.9.

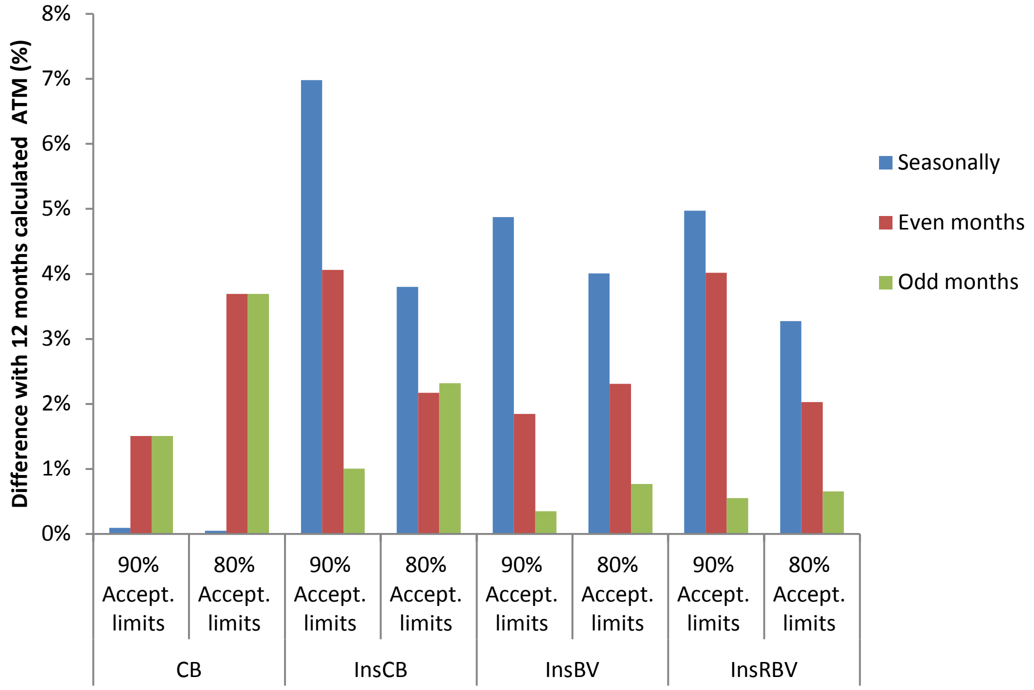

Figure 5.9. Difference between the seasonal, and even and odd months method compared to the 12 months calculated ATM.

Simulating for 6 odd months (January, March, May, July, September, November), resulting in the least variations with the 12 month calculated ATM.

5.5 Verification of the ATM

5.5.1 Comparison between the ATM Results and Previous Research at UON

Previous research on the modules containing the same walling systems for a period of one year was carried out between 2008 and 2009. The results were obtained under all seasonal conditions, with the interior of the modules "*free-floating*" with no ventilation.

Data was recorded over 6 week periods to represent each of the four seasons under free floating conditions. The average standard deviation of all the studied days (σ) represents the daily internal swing as a result of the external environment. The mean internal air temperatures and standard deviations for each of the modules and external air for each season are shown in Figure 5.10 (Page et al. 2011).

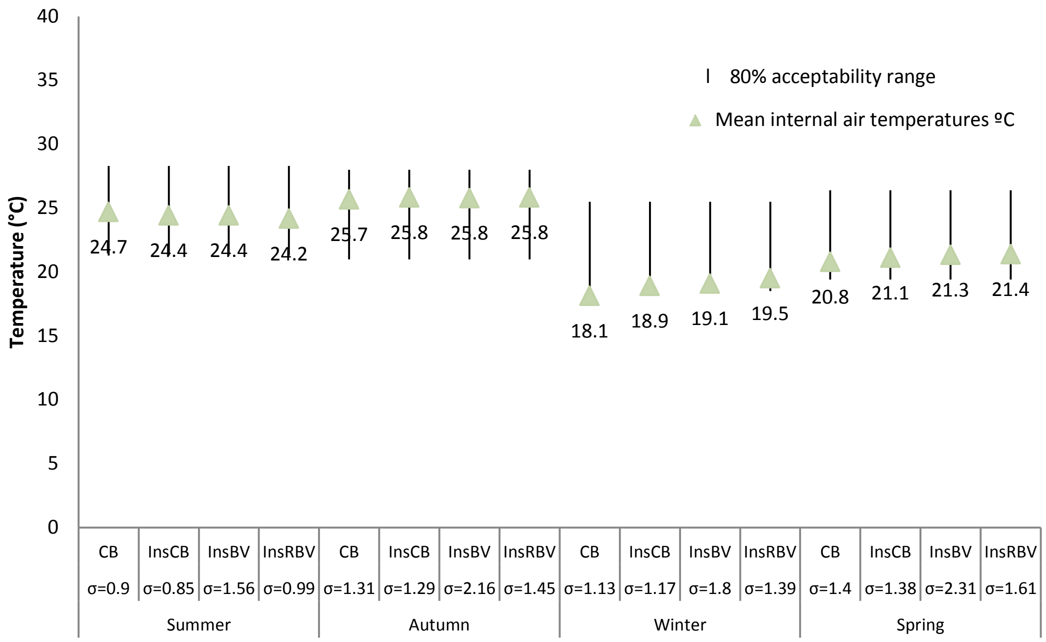

Figure 5.10. Mean module air temperatures, with 80% acceptability limits and standard deviations for each season.

From the above, the performance of each module can be assessed in several ways:

- The percentage of time that the internal air temperatures inside the building remain within the thermal comfort range for each season and close to the thermal comfort temperature, as shown in Table 5.7.

Table 5.7. Thermal comfort temperature and thermal comfort range.

Season	Average Outside air Temp. ºC	Comfort Temp. ºC	90% acceptability higher limits ºC	90% acceptability lower limits ºC	80% acceptability higher limits ºC	80% acceptability lower limits ºC
Summer	22.7	24.8	27.3	22.3	28.3	21.3
Winter	13.7	22.0	24.5	19.5	25.5	18.5
Autumn	21.7	24.5	27.0	22.0	28.0	21.0
Spring	16.5	22.9	25.4	20.4	26.4	19.4

All of the average internal air temperatures of the modules during all seasons lay inside the comfort zone except the Cavity Brick module, where in winter the average internal air temperature was outside the comfort zone.

- Assessment of the temperature swing range, where the better module performance has a lower internal diurnal swing (lower σ), since a larger σ will drive the temperature outside the thermal comfort zone.

The module thermal performances were ranked, with the best given an A rating, followed by B, C, and the worst performance with a D, based on the above measures and repeated for each season, as shown in Table 5.8.

Table 5.8. Average results for each ranking used in the comparison.

T	A	A	A	A	B	B	B	B	C	C	C	C	D	D	D	D
σ	A	B	C	D	A	B	C	D	A	B	C	D	A	B	C	D
Ave.	A	B	B	C	A	B	C	C	B	B	C	D	B	B	C	D

Note: T: the average internal air temperature and σ: the temperature swing range.

More weight will be given to the temperature swing range as the difference in the average internal air temperatures was minimal for most of the cases. The average results for each ranking (A for the best, followed by B then C and finally D for the worst thermal performance) are shown in Table 5.9.

Table 5.9. Module's performance for the different seasons, based on the UON research.

	Summer			Winter			Autumn			Spring		
	T	**σ**	**Overall performance**	**T**	**σ**	**Overall performance**	**T**	**σ**	**Overall performance**	**T**	**σ**	**Overall performance**
CB*	D	B	C	D	A	D*	A	B	B	D	B	C
InsCB	B	A	A	C	B	B	D	A	B	C	A	B
InsBV	B	D	D	B	D	C	B	D	C	B	D	C
InsRBV	A	C	B	A	C	B	C	C	C	A	C	B

* The Cavity Brick module average internal air temperature in winter was outside the comfort zone which makes it the worst performing module in the winter season.

In summary, the observed experimental results indicate that:

- For the summer season, the best overall thermal performance came from the InsCB module which had the coolest average temperature in summer and the lowest temperature swing, followed by the InsRBV, InsBV and CB modules. Despite the InsBV module having a cool temperature in summer, it had the largest temperature swing and the opposite was true for the CB module, which had a high average temperature but a lower σ.
- For the winter season, the best overall thermal performance was the InsRBV module, followed by the InsCB, InsBV and CB modules.
- For the autumn season, all the modules had an average internal air temperature close to the thermal comfort zone but the InsBV had the highest temperature swing.
- For the spring season, the best thermal performances were the InsCB and InsRBV modules, and worst performances were from the InsBV and CB modules.

The ATM is now used to characterise the thermal performance of the modules for each season, as shown in Table 5.10.

Table 5.10. ATM assessments for all modules during each season.

Season	CB		InsCB		InsBV		InsRBV	
	Acceptability limits		Acceptability limits		Acceptability limits		Acceptability limits	
	90%	**80%**	**90%**	**80%**	**90%**	**80%**	**90%**	**80%**
Summer	87%	98%	93%	99%	92%	99%	90%	96%
Winter	5%	11%	18%	33%	11%	24%	15%	32%
Autumn	75%	89%	74%	88%	73%	88%	74%	90%
Spring	60%	84%	64%	93%	54%	76%	65%	86%

The ATM values for each season indicate that:

- For the summer season, all modules performed well in the 80% acceptability limit and for the 90% acceptability limit, which is more challenging to meet. The best overall thermal performance came from the InsCB module, followed by the InsRBV, InsBV and CB modules.
- For the winter season, the best overall thermal performance was from the InsCB module, followed by the InsRBV, InsBV and CB modules.
- For the autumn season, all the module thermal performances were very close to each other, with a minimal advantage for the InsRBV and CB modules.
- For the spring season, the best module thermal performances were the InsRBV and InsCB modules, and the worst performances were from the CB and InsBV modules.

Comparing the previous findings from the University of Newcastle research on the walling systems to the ATM indicates that the ATM results almost match the previous research, as is shown in Table 5.11.

Table 5.11. Comparison between previous research and the ATM results.

Summer	ATM	Best performance	InsCB
		Worst performance	CB
	Previous research	Best performance	InsCB
		Worst performance	CB, InsBV
Winter	ATM	Best performance	InsCB
		Worst performance	CB
	Previous research	Best performance	InsRBV, InsCB
		Worst performance	CB
Autumn	ATM	Best performance	InsRBV, CB
		Worst performance	InsBV
	Previous research	Best performance	InsCB, CB
		Worst performance	InsBV
Spring	ATM	Best performance	InsCB
		Worst performance	InsBV
	Previous research	Best performance	InsCB, InsRBV
		Worst performance	InsBV, CB

There are some differences in assessing the thermal performance of the modules in autumn, but the differences between the modules from the previous research and using the ATM are marginal, with very minimal differences between the modules.
Finally, the InsCB and InsRBV modules had the best thermal performance, followed by the InsBV and CB modules. These results confirm the findings from the previous research on the walling systems.

5.5.2 Comparison of the ATM with AccuRate Results

The annual heating and cooling energy requirements and star ratings (bands) for the Newcastle area (Zone 15) based on house design, building site and climate zones for the CB module (as an example) are shown in Figure 4.11 (AccuRate Sustainability V2.3.3.13 SP1), where:

- Heating and cooling energy requirements are not the actual energy consumption and cannot be used to calculate the running costs for the buildings because the simulation does not characterize the consumption or lifestyle of the inhabitants.
- Heating and cooling are available at fixed time for example, for '*Living*', '*Living and Kitchen*', are available from 07:00 to 24:00 and in '*Bedroom*' from 16:00 to 09:00.
- The latent cooling load refers to the wet-bulb temperature of the building, where dehumidification happens when cooling is applied. The dehumidification energy is reported in AccuRate as the latent cooling energy (Bright Hub 2014).
- The sensible cooling load refers to the dry-bulb temperature of the building, where for cooling only the sensible heat of the air is removed, and there is no conversion in the moisture content. During a sensible cooling course the latent heat and the dew point temperature of the air remains constant, while the dry-bulb temperature and wet-bulb temperatures of the air decrease (Bright Hub 2014).

PROJECT DETAILS	
Postcode: 2308	Climate Zone: 15

CALCULATED ENERGY REQUIREMENTS*				
Heating	Cooling (sensible)	Cooling (latent)	Total Energy	Units
68	8	5	82	MJ/m².annum

* These energy requirements have been calculated using a standard set of occupant behaviours and so do not necessarily represent the usage pattern or lifestyle of the intended occupants. They should be used solely for the purposes of rating the building. They should not be used to infer actual energy consumption or running costs. The settings used for the simulation are shown in the building data report.

AREA-ADJUSTED ENERGY REQUIREMENTS				
Heating	Cooling (sensible)	Cooling (latent)	Total Energy	Units
48	6	4	58	MJ/m².annum
Floor area	conditioned: 36.0 m²	unconditioned: 0.0 m²	garage: 0.0 m²	

BAND RESULT
6.5

Figure 5.11. An example of AccuRate certificate showing the annual heating and cooling energy requirements and star ratings (bands) for the CB module.

Using the AccuRate results to compare the modules showed that the InsCB and InsRBV modules had the best thermal performances with the least annual heating and cooling energy requirements, followed by the InsBV and CB modules, as is shown in Figure 5.12.

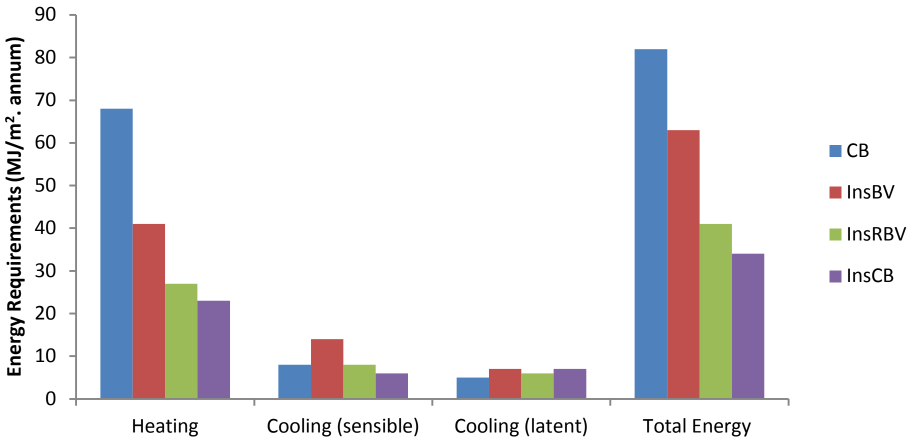

Figure 5.12. Annual heating and cooling energy requirements for all the modules.

Heating energy requirements are the main driver for the modules' thermal performance. For example, the CB module required the highest amount of energy for heating, which results in the highest total energy requirements. This explains why this module was rated last, compared with the other modules, as is shown in

Figure 5.13. The InsBV module required slightly higher sensible cooling, but still the main driver was the heating energy requirement.

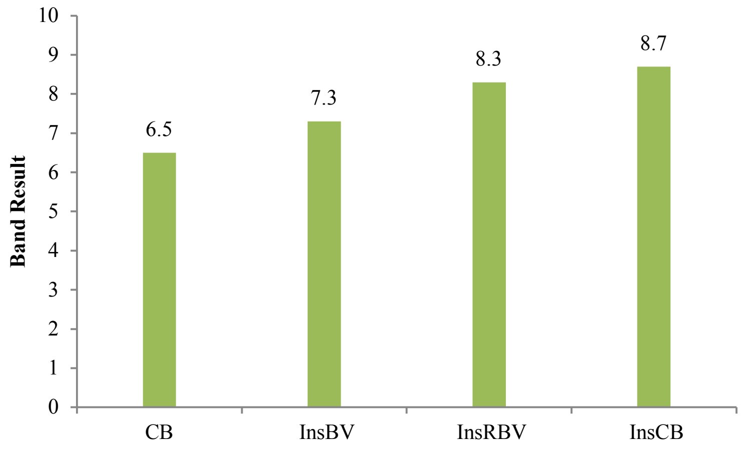

Figure 5.13. AccuRate band results for all modules.

Comparing the ATM with the AccuRate results indicate that the ATM results for the 90% and 80% ***acceptability limits*** (ATM90; ATM80) were consistent with the AccuRate results, as is shown in Figure 5.14.

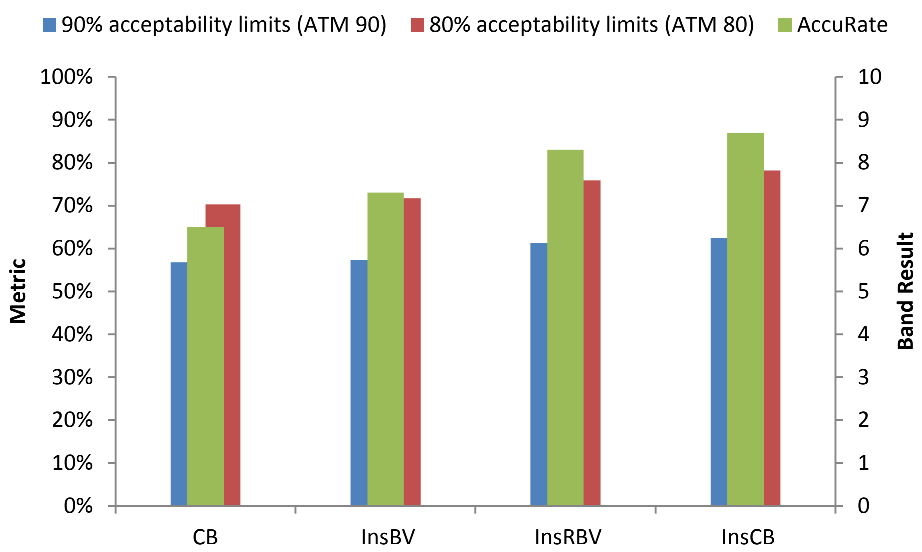

Figure 5.14. ATM and AccuRate band results for all modules.

The main advantages of the ATM approach over AccuRate are;

- In AccuRate, the inhabitants do not have a part in controlling their environment because the heating and cooling calculated is set from 07:00 to 24:00 in the 'Living' and 'Living and Kitchen' areas, and from 16:00 to 09:00

in the 'Bedroom', and it does not allow the user to modify the assumptions made regarding the occupant's behaviour.

- The heating and cooling thermostat settings are constant for winter and summer and do not interacted with the external environment. For example, for Zone 15, the Newcastle area, the thermostat is set constant for 20ºC in winter and 25ºC in summer, which consumes more energy, while the adaptive thermal comfort range is more flexible and use wider range for internal air temperature for example, in winter months the range from 19 - 25ºC.

- Assessing the building thermal performance using energy based software requires energy input (mechanical heating and cooling) to obtain thermal comfort (indirectly promoting for using more energy). In contrast, the ATM approach, based on free floating behaviour, promoting sustainable ways to obtain thermal comfort such as opening window for ventilation, changing clothes and shading instead of using energy.

5.6 Summary

The new thermal performance ATM results showed that the InsCB and InsRBV modules have the best thermal performance, followed by the InsBV and CB modules. These results confirm the findings from the research done at the University of Newcastle on the walling systems.

Comparing the ATM results with the AccuRate ratings indicates that the ATM results for the 90% and 80% ***acceptability limits*** (ATM90; ATM80) match the AccuRate results. The ATM approach has the potential to replace AccuRate as a new building thermal performance assessment system, and the ATM encouraging energy efficiency and sustainability compared to AccuRate.

Comparing the ATM with the AccuRate showed that the ATM able to:

- Characterise the thermal performance of representative housing modules, taking into account: thermal resistance, thermal mass of the building components and the influence of the dynamic external temperature environment.
- Compare a building's thermal performance. The ATM will be able to characterise and compare the thermal performances of representative housing modules, taking into consideration their construction materials, occupant's behaviour, orientation, shading and the weather at the site.
- Encourage sustainability by inspiring the use of adaptive techniques to obtain thermal comfort instead of mechanical heating or cooling which mainly come from fossil fuels.
- The ATM will be adaptable to future climate change by using minimum weather data (temperature and wind speed and direction) which can easily be modified when the weather changes.
- The ATM will integrate the occupants into the assessment process, which gives them more opportunities to control their environment and save more energy.

In the following chapter, the ATM is used to demonstrate its application to a complete house in Western Australia.

Chapter Six:
Case Study- Application of the Adaptive Thermal Metric (ATM)

6.1 Overview

In this chapter CFD simulations and the ATM will be calculated for a complete house rather than the housing test modules. The performance of a three bedroom house in suburban Perth, Western Australia (a different climate zone) is assessed. Detailed descriptions of the house have been given in Section 3.3 and Appendix B.

6.2 The ATM for the Western Australian House

CFD simulations were used to find the building's internal air temperatures and were compared to the results with the real data obtained from the site in order to assess the accuracy of the CFD simulations. TMY data was used to find the building's average internal air temperature to find the ATM.

The CFD module configurations described in in Chapter 4 were used to find the internal air temperature inside each room. From the real house, the external air temperatures were recorded over 9 months in 2009, with some data missing. The CFD analysis will use the external air temperatures for the simulation so the simulation is divided into four parts due to missing data, as shown in Figure 6.1.

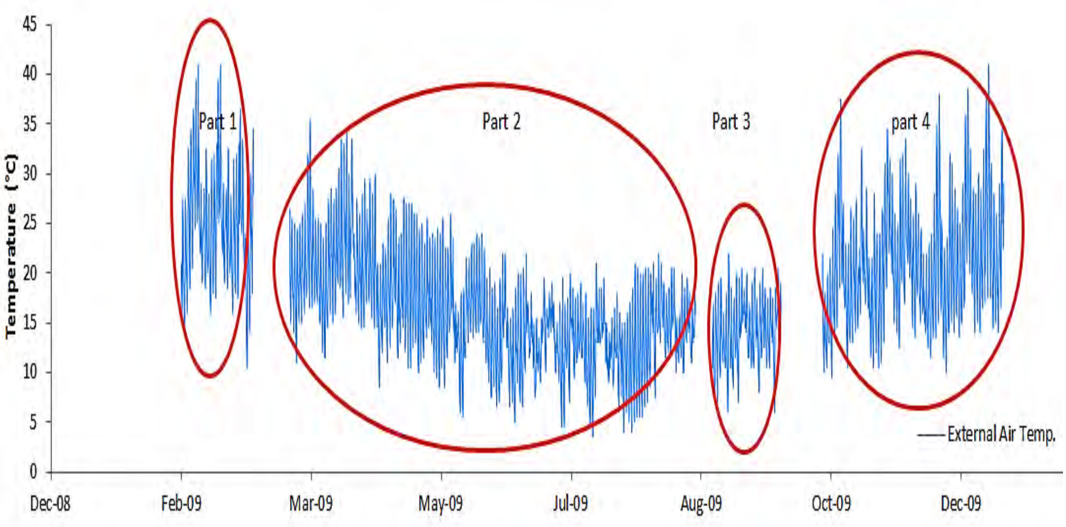

Figure 6.1. The CFD simulation parts used in this analysis.

Note: the period for part one was from 6/02/2009 until 5/03/2009. Part two was from 19/03/2009 until 22/08/2009. Part three was from 29/08/2009 until 24/09/2009. Part four was from 10/10/2009 until 19/12/2009.

CFD simulations were carried out for each part during the simulation period, where the temperature variations outside the house changed with the time of the day and the season, as shown in Figure 6.2.

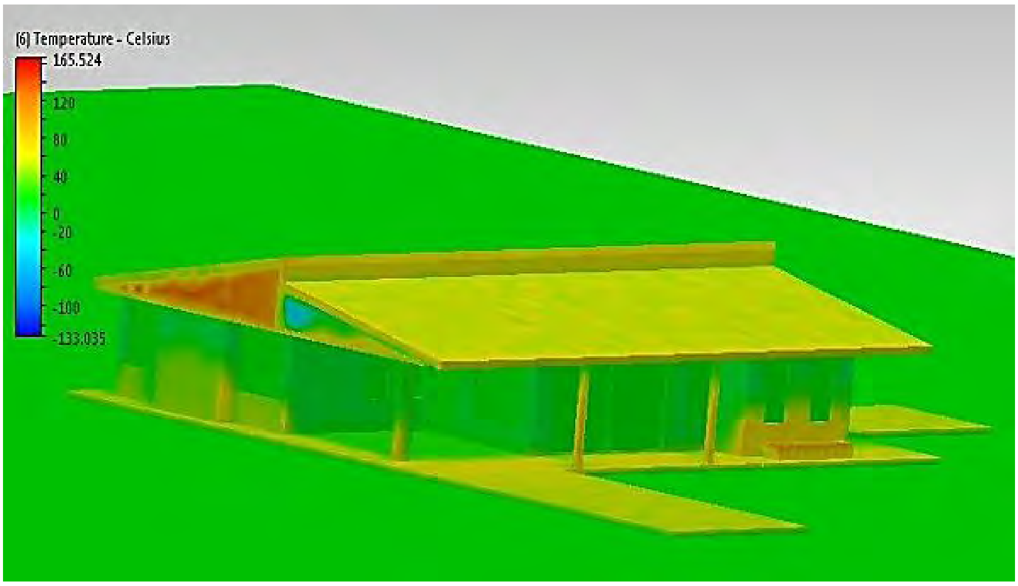

Figure 6.2a. Snapshots from the CFD simulations showing temperature variations on the external surfaces during sunny morning spring day (15/10/2009).

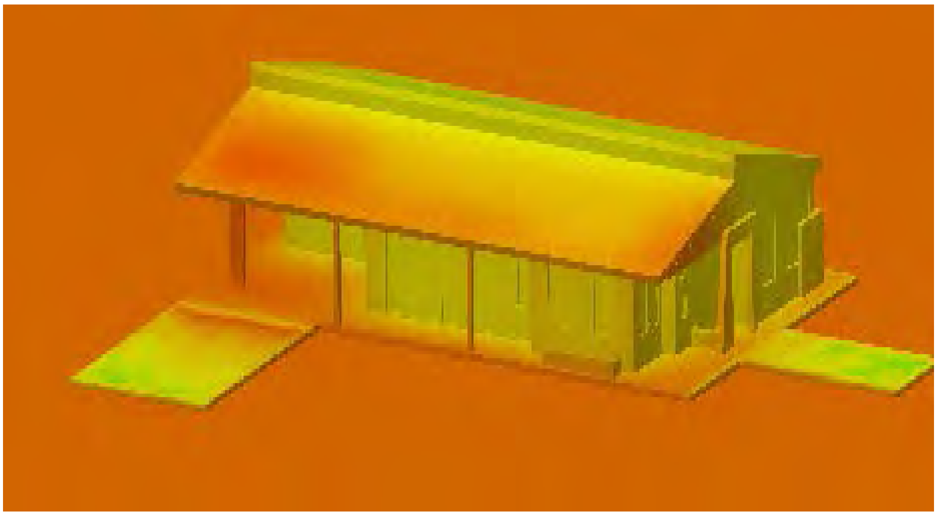

Figure 6.2b. Snapshots from the CFD simulations showing temperature variations on the external surfaces during midday for cloudy winter day (24/06/2009).

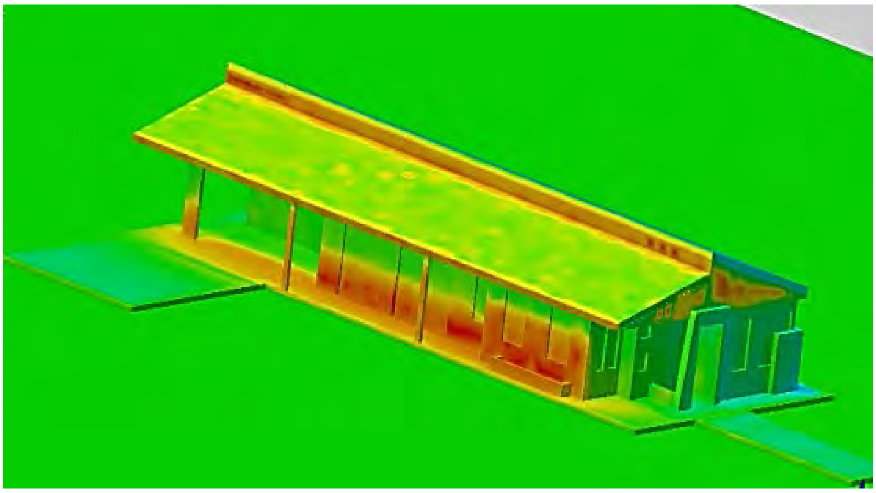

Figure 6.2c. Snapshots from the CFD simulations showing temperature variations on the external surfaces during the evening for sunny winter day (18/06/2009).

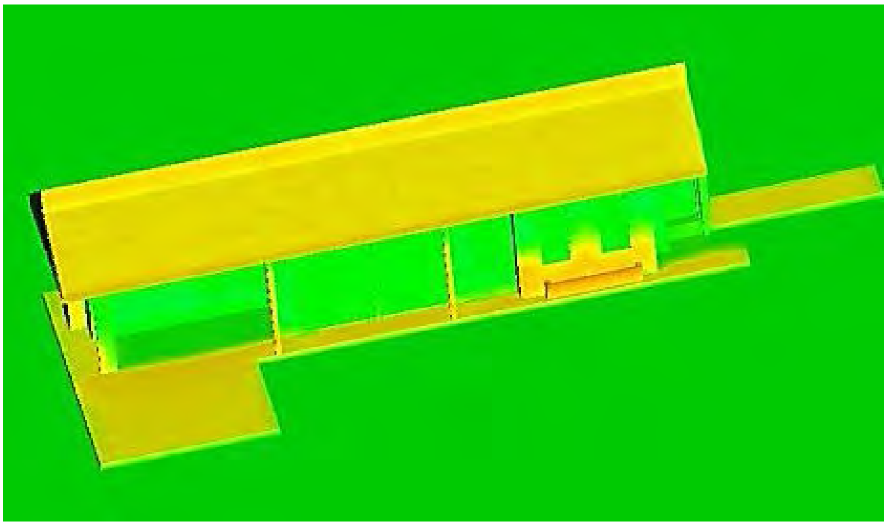

Figure 6.2d. Snapshots from the CFD simulations showing temperature variations on the external surfaces during a night for autumn day (08/04/2009)

To determine the accuracy of the CFD simulations, the variations of the internal air temperatures for each room between the simulated CFD results and the real house data were compared, as shown in Figure 6.3.

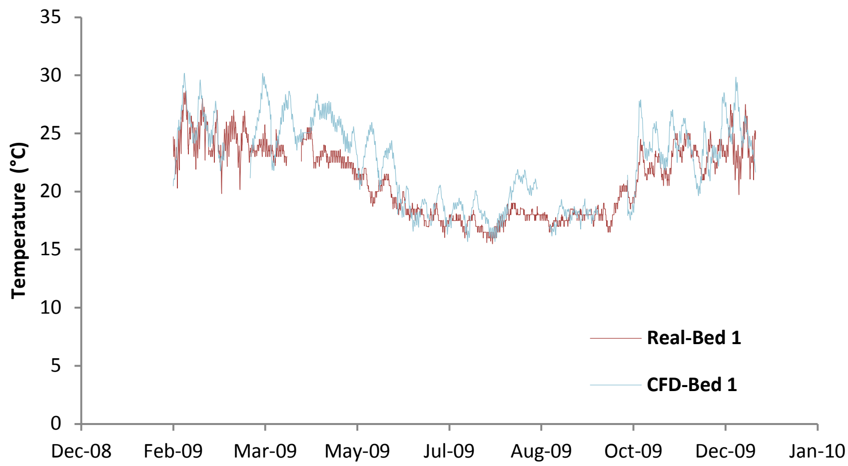

Figures 6.3a. Variations of the internal air temperatures between the CFD simulation results and the real data for bedroom 1.

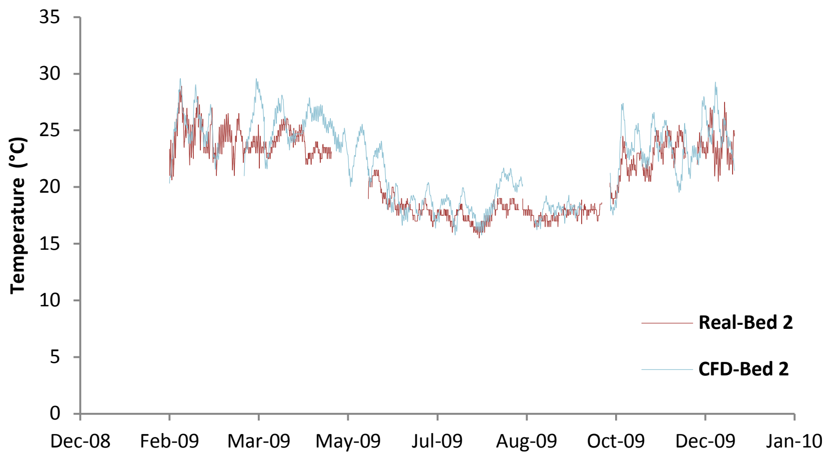

Figures 6.3b. Variations of the internal air temperatures between the CFD simulation results and the real data bedroom 2.

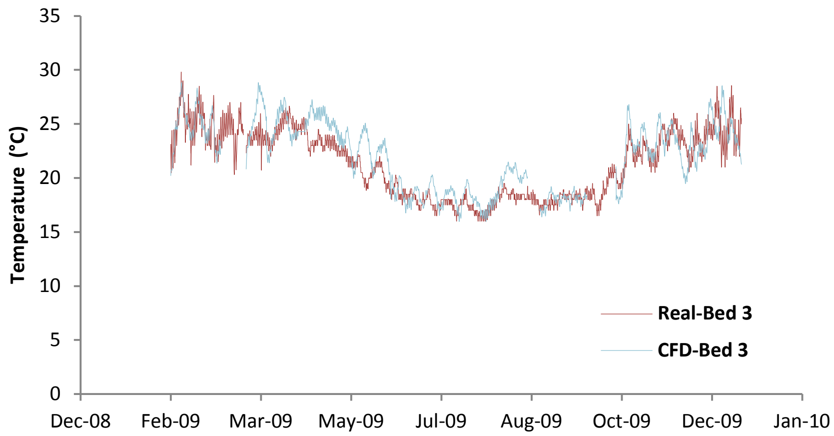

Figures 6.3. Variations of the internal air temperatures between the CFD simulation results and the real data for bedroom 3.

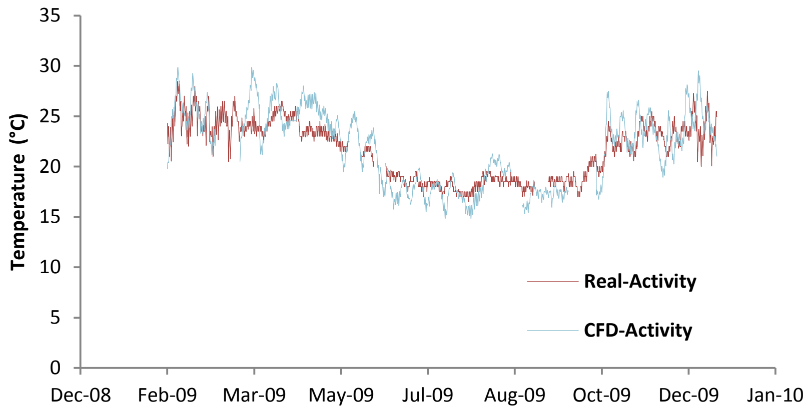

Figures 6.3d. Variations of the internal air temperatures between the CFD simulation results and the real data for the activity room.

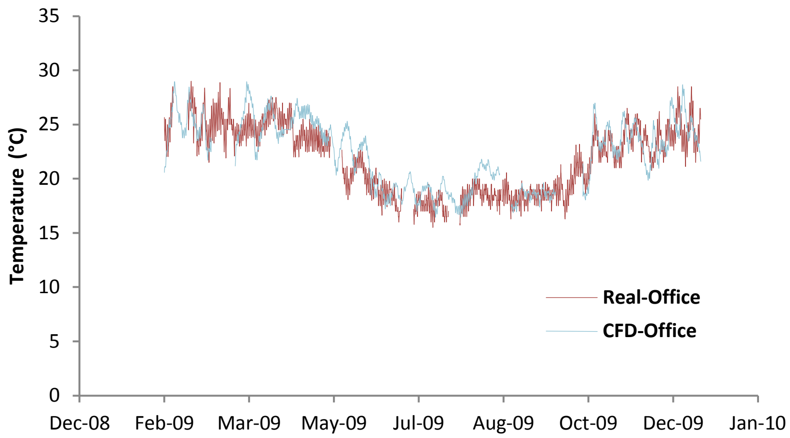

Figures 6.3e. Variations of the internal air temperatures between the CFD simulation results and the real data for the office.

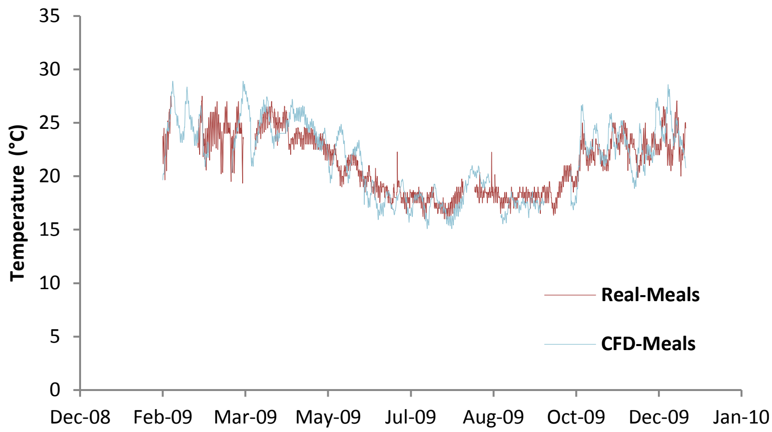

Figures 6.3f. Variations of the internal air temperatures between the CFD simulation results and the real data for the meals room.

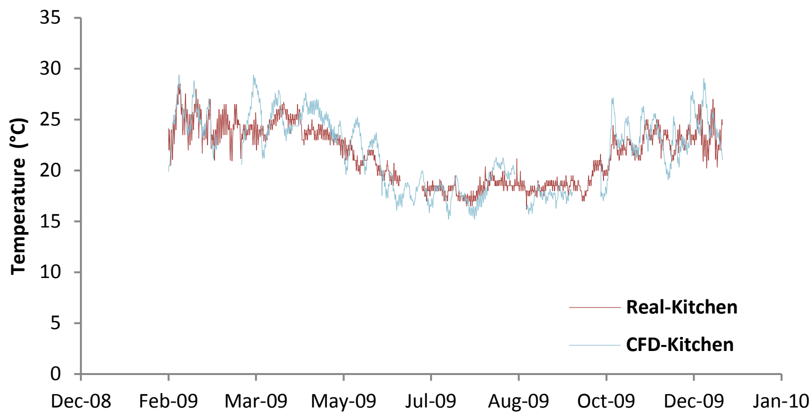

Figures 6.3g. Variations of the internal air temperatures between the CFD simulation results and the real data for the kitchen.

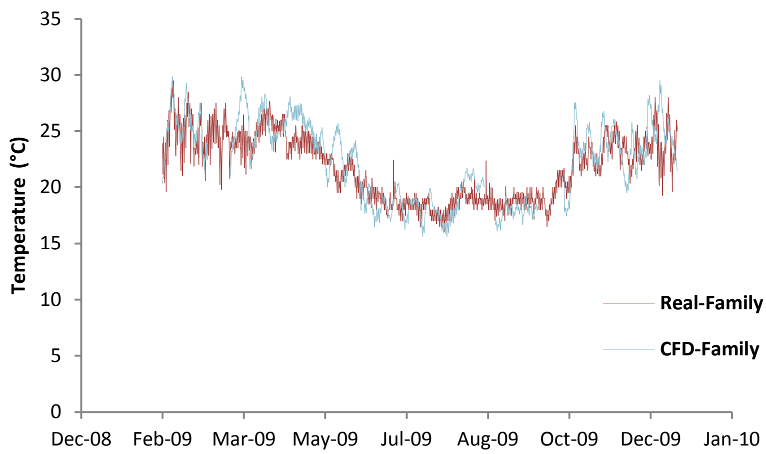

Figures 6.3h. Variations of the internal air temperatures between the CFD simulation results and the real data for the family room.

Comparison between the CFD simulations and the real data for each room inside the house showed that the average accuracy, at any given time during one year's simulation, was around 92.26% for all rooms, as shown the Table 6.1.

Table 6.1. The average accuracy (%) between the real data and the CFD simulated data during the simulation period.

Bed 1	Bed 2	Bed 3	Office	Meals	Kitchen	Family	Activity	Average
88.66%	92.14%	93.71%	90.05%	93.89%	94.72%	93.48%	91.45%	92.26%

Using the CFD results (part) for the internal air to find the average volume internal air temperatures inside the house are shown in Figure 6.4. Simulations were carried out using TMY data and then the average internal air volume temperatures were used to find the adaptive thermal comfort range.

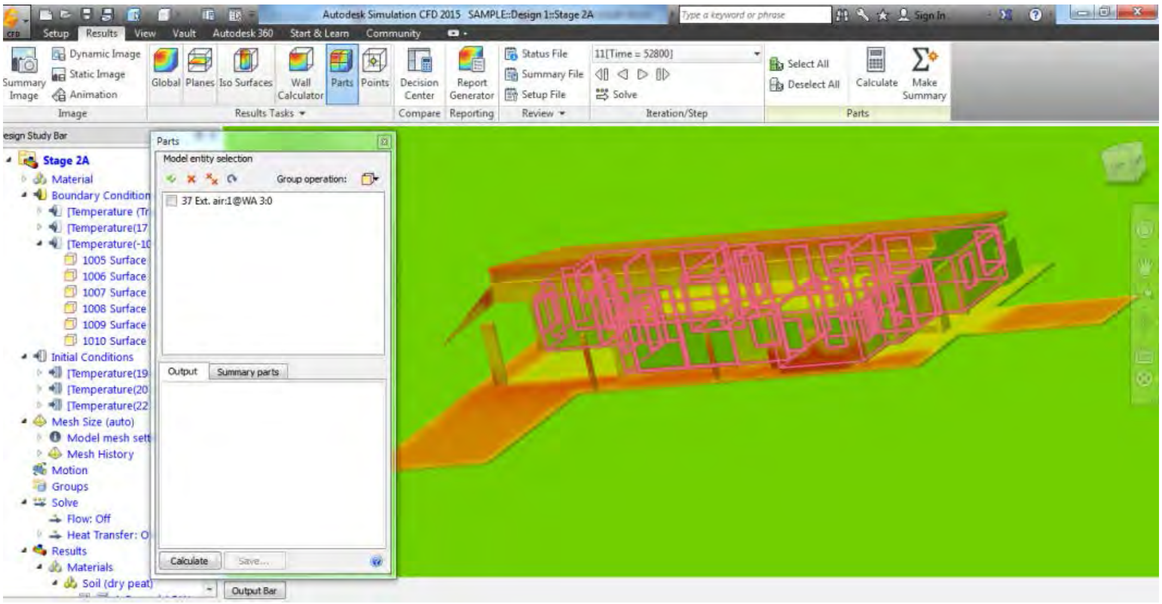

Figure 6.4 Autodesk CFD screenshot to find the average volume air temperatures inside the house. Note: the ATM encapsulates the average volume air temperature for one year to assess the thermal performance.

After finding the temperatures inside the building using CFD simulations, the next step is to find the ATM which characterises the thermal performance of the building using the thermal comfort concepts. To find the adaptive thermal comfort inside the building, the same temperate climate equation for the Newcastle area was used (Eq. 3.1 to 3.3).

To be consistent with AccuRate, and to standardize the ATM, TMY will be used to find the average volume internal air temperatures inside the building. After that, the adaptive thermal comfort range over one year will be calculated to find the ATM for the WA house. The internal air temperatures inside the building using the CFD simulations and the adaptive thermal comfort range for the 90% and 80% ***acceptability limits*** (ATM90; ATM80) are shown in Figure 6.5.

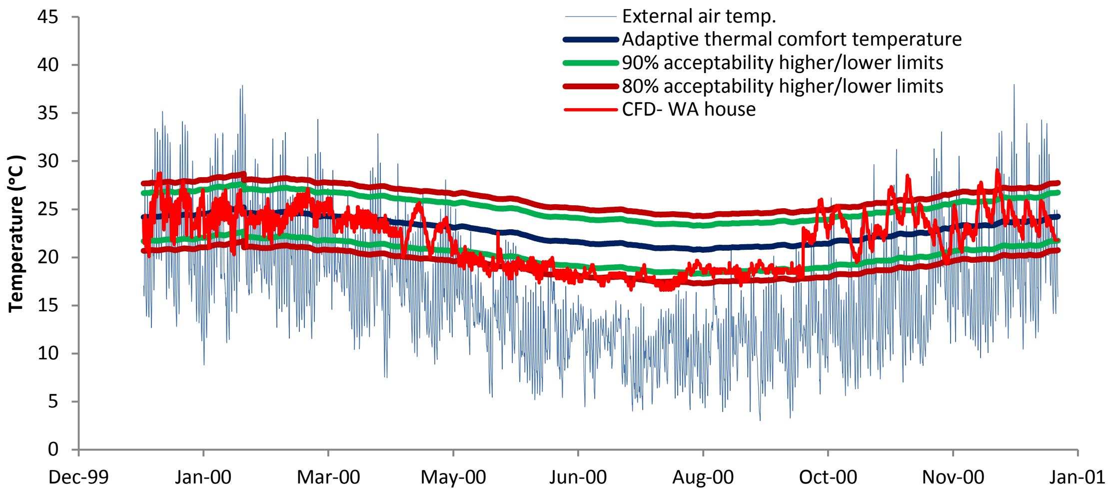

Figure 6.5. Internal and external air temperatures and thermal comfort ranges for the WA house.

The average thermal performance over a year is 60.2% for the 90% ***acceptability limit*** (ATM90) and 84.9% for the 80% ***acceptability limit*** (ATM80). There are significant differences between 90% and 80% ***acceptability limits*** due to the building's average internal air temperature of just under the 90% acceptability limit for most of the winter months, as shown in Figure 6.6. The overall internal air temperatures fall outside the 90% acceptability limit for most of the time in winter months.

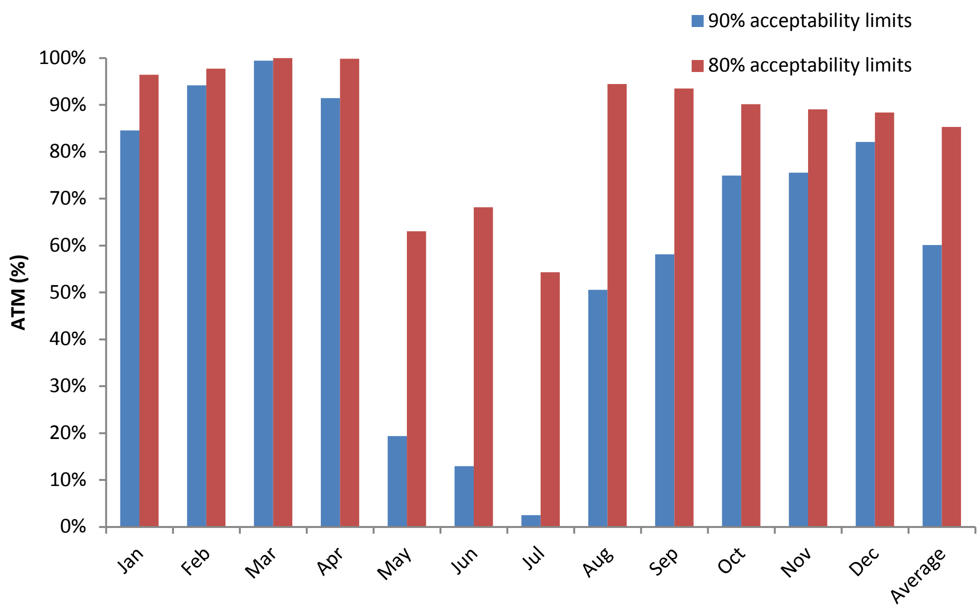

Figure 6.6. Monthly 90% and 80% ***acceptability limits*** for the WA house over the studied period.

6.3 Comparison of the ATM with AccuRate

The AccuRate band result is 7 where most of the energy required is for heating (64 MJ/m^2. annum compared to 6 MJ/m^2. annum for cooling). This AccuRate result falls within the range for 90% ***acceptability limits*** (ATM90) and is higher than for the 80% ***acceptability limits*** (ATM80) as discussed above, also this result accurately matches the ATM to indicate that most of the energy was required in winter months.

6.4 Summary

Comparison between the CFD simulations for different housing types in different climate zones and the real data at any given time during one year's simulation indicated that the average accuracy was in the order of 92%. This is consistent with the previous CFD simulations for the housing test modules in Newcastle area.

The ATM was calculated for a complete WA house in a different location (Western Australia climate zone). The results show that the ATM was able to characterise the thermal performance of the complete housing. This illustrates the capability of the ATM which may be used as a new universal metric.

In the following chapter the ATM is used to assess various techniques to improve the thermal performance of the modules.

Chapter Seven: Application of the ATM to Study Energy Enhancement Techniques

7.1 Overview

Improving a building's thermal performance will lead to a more energy efficient building with lower running costs. This chapter describes some of the cost effective strategies to enhance the energy efficiency of a building, using the ATM as a measure of assessing the thermal performance of the housing modules with various modifications to improve their thermal performance.

Initially the characteristics of each building component and its influence on the thermal performance of an overall building is considered to determine the best possible strategies to improve the housing test modules design and reach more energy efficient modules. Additional techniques which could be used to achieve an almost 100% thermally comfortable module without using any form of energy from fossil fuels are then considered (e.g.; using renewable energy techniques). A feasibility study to compare the effectiveness of the various components of the module or the renewable energy systems is performed to determine which strategies could provide the greatest energy savings with the least cost.

7.2 The Influence of the Module Components on Thermal Performance

Since the testing modules have fully insulated roofs and doors, the performance of the modules can only be improved by changing the walls, floors, and the window glass materials and properties.

7.2.1 External Walls

As described in Chapter two the external walling system directly influences the thermal performance of a building as it acts as a barrier between the internal environment and the changing weather outside and by storing heat in the walls (thermal mass) which is beneficial in many instances. Using the appropriate walling system can enhance the module's thermal performance. For example, changing the walls from cavity brick to insulated cavity brick improved the ATM (80% acceptability limit) by 8% and the AccuRate star rating (bands) by 2.2. Changing the walls from insulated brick veneer to insulated reverse brick veneer enhanced the thermal performance by 4% for the ATM and 1 for the AccuRate star rating, as shown in Table 7.1.

Table 7.1. AccuRate ratings and the ATM results for the various walling systems

Walling System	ATM80 (80% acceptability limits)	AccuRate Star rating
CB	70%	6.5
InsBV	72%	7.3
InsRBV	76%	8.3
InsCB	78%	8.7

The best walling system, in terms of thermal performance in a temperate climate (Newcastle area), is insulated cavity brick (InsCB) in comparison to the rest of the walling systems. For this reason, the InsCB module will be used as a base module for the rest of the improvements.

7.2.2 Floor

Measurements of the ground temperature beneath the module floor slab at a depth of 1m for one year are shown in Figure 7.1 (Page et al. 2011). This indicates that the ground temperature in summer (20 - 24ºC) was cooler than the building itself, resulting in heat transfer between the building and the ground (heat sink) and lower cooling energy being required. In winter, the ground temperature ranged between 16 - 20ºC, which was higher than the outside air temperature, but was close to the building's internal air temperature, so the effect of the ground temperature on the cost of heating the building will be insignificant.

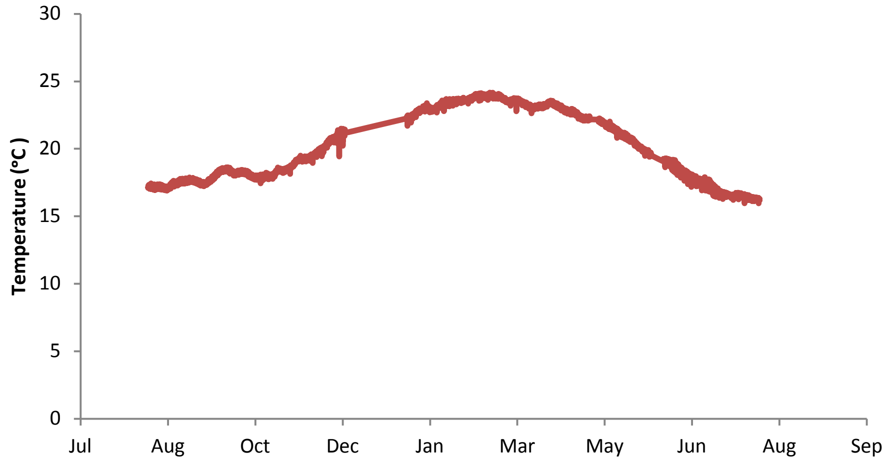

Figure 7.1. Ground temperatures at 1m under the modules in 2009/10.

Appropriate floor insulation to produce a thermal resistance (R-value) of 1.0 for the InsCB module will trap the heat in the summer months inside the building resulting in higher cooling energy being required, but with no change in the cooling energy required. This will decrease the AccuRate star rating by 0.3 (8.7 to 8.4).

A simulation for one year to find the ATM for the InsCB module after insulating the floor with R1 insulation resulted in a slight increase in temperatures outside the thermal comfort range in February and March, as is shown in Figure 7.2.

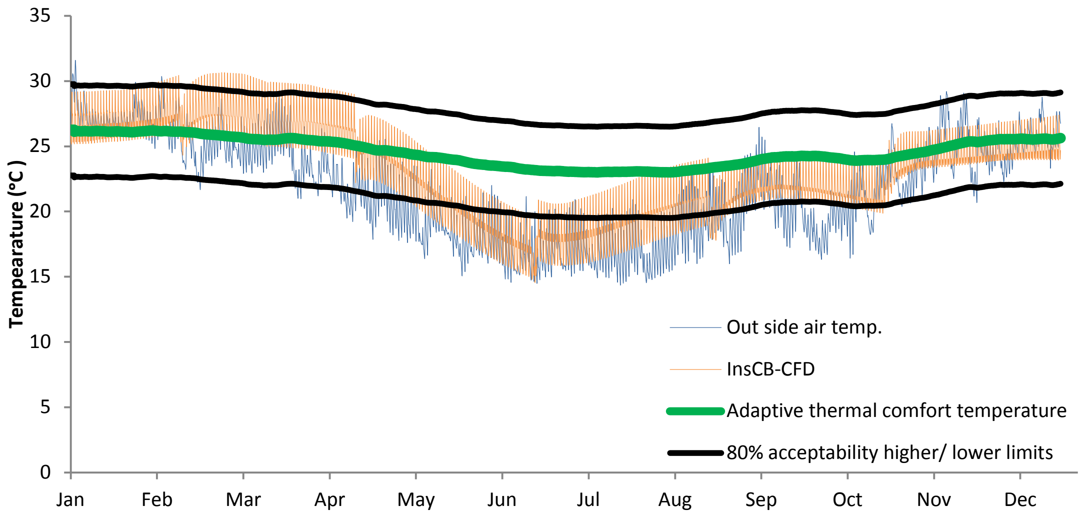

Figure 7.2. Internal and external air temperatures and thermal comfort range limits for the InsCB module.

The ATM (80% acceptability limit) decreases from 78% to 76% after insulating the floor for InsCB module as shown in Table 7.2.

Table 7.2. The ATM results and AccuRate ratings for insulated/uninsulated floors.

Modifications	**ATM80** (80% acceptability limits)	**AccuRate Star Rating**
Uninsulated floor for InsCB	78%	8.7
Insulated floor for InsCB	76%	8.4

Insulating the floor will cost more and will not significantly improve the overall thermal performance of the module, so insulating the floors will not be considered in the next module improvements.

7.2.3 Window

A perfect window design is to gain and keep heat inside the modules in winter and to eliminate heat and solar gain from entering in summer (more details in Section 2.1.1.1). To achieve this will require different types of windows, such as double glazed windows which do not block solar heat gain and allow winter sun penetration but still require appropriate summer shading.

The still layer of air between the glass surfaces in double glazed window helps to minimise convective heat transfer. Replacing the air with a heavier inert gas (Argon) reduces the convection loss further.

From the AccuRate results, the most energy is required for heating (16 out of 24 MJ/m^2. annum) in the winter months, and the lowest values for the ATM are for the winter months. Thus improving the building design to be warmer in winter will improve the overall thermal performance of the modules.

In the modules, heat losses in winter mainly occur through the windows and improving the window design will have a direct impact on the building's thermal performance. Using ALM-006-01 A Aluminium B DG Argon Fill Clear-Clear with two 4mm thick glass and an air gap of 12 mm will improve the AccuRate star rating by 0.6 (from 8.7 to 9.3) and reduce the heating energy from 16 to 9 MJ/m^2. annum

Changing the glass properties in the CFD analysis and simulation to find the ATM improves the ATM from 78% to 87%, which is a significant rise in the thermal performance. By changing the windows glass to double glazing, the number of hours for the InsCB module within the thermal comfort range increased from 6,831 hours to 7,359 hours per year. Window frame material, such as aluminium, is a good conductor and causes more rapid heat loss/gain, while timber is a better insulator, but it will have an insignificant effect due to the small frame area, as shown in Table 7.3.

Table 7.3. The ATM results and AccuRate ratings for the different window glazing and framing materials.

Modifications	**ATM80** (80% acceptability limits)	**AccuRate Star rating**
Single glazed for InsCB	78%	8.7
Double glazed for InsCB	87%	9.3
Single glazed for InsCB with Aluminium frame	78%	8.7
Double glazed for InsCB with Aluminium frame	87%	9.3
Single glazed for InsCB with Timber frame	78%	8.7
Double glazed for InsCB with Timber frame	87%	9.3

7.2.4 Internal Walls and Thermal Mass

The thermal mass effect is described in Section 2.1.1.2. From the AccuRate ratings, the modules required more heating energy than cooling energy and the ATM results showed the lowest values for the winter months, indicating that the worst thermal performance for the buildings occurred in the winter months. Therefore, to improve the overall thermal performance in the buildings focus should be on the winter months. One of the methods to increase the thermal mass inside the building is to use high thermal mass materials which store winter sun/heat entering the modules during the day time and release it at night time as shown in Figure 7.3.

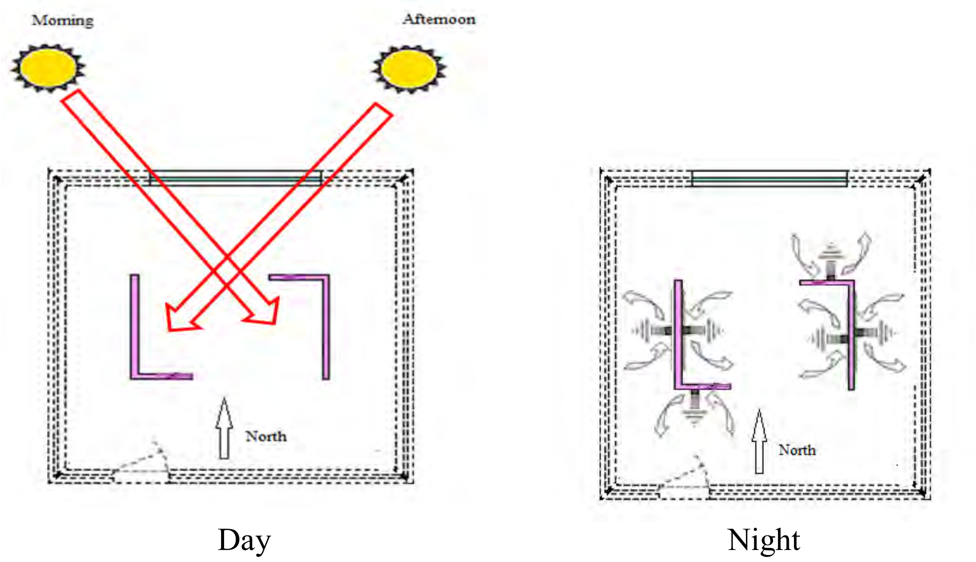

Figure 7.3. Illustrative picture of the internal walls and the thermal mass inside the module during one day in winter.

Thermal mass is useful in environments with a high diurnal range, which causes the internal temperature to stay closer to the mean temperature, but if the mean temperature is too cold or hot, thermal mass will not be sufficient.

Using a material with a high thermal mass will store more heat in winter and improve the overall building's thermal performance. For example, in Rammed Earth 300mm walls with a thermal lag of 10 - 12 hours the high daytime temperatures will reach the internal surfaces and store the heat in the internal walls and release it at night after 10 - 12 hours (Your Home 2010).

For illustrative purposes, higher thermal mass material will be applied to improve the thermal performance (e.g.; Rammed Earth 300mm). This will improve the overall ratings for the buildings from 8.7 to 8.9 stars and minimize the cooling energy. On the other hand, using lower thermal mass materials (such as plasterboard on stud walling) will reduce the overall thermal performance from 8.7 to 8.4 stars.

For the ATM, using a higher thermal mass material (Rammed Earth 300mm) enhances the thermal performance of the modules and increases the ATM to 84%, as shown in Table 7.4.

Table 7.4. ATM results and AccuRate ratings for different internal wall materials.

Modifications	**ATM80** (80% acceptability limits)	**AccuRate Star rating**
Brick Internal wall for InsCB (original module)	78%	8.7
Rammed Earth 300mm internal wall for InsCB	84%	8.9
Plasterboard on stud internal wall for InsCB	76%	8.4

7.3 Influence of Design Concepts on the Module Thermal Performance

7.3.1 Orientation

As described in Section 2.1.3 an appropriate building orientation will allow the desirable winter sun to enter the building and allow ventilation in summer by facing the summer wind stream.

In the modules the windows face north, which allows the winter sun to enter the building and heat it up. Changing the building's orientation to either the east or west will heat the building in summer because the east and west windows lose more heat than they gain in winter and gain more heat in summer. A southern orientation results in a little solar gain and heat losses through the window in winter.

The orientation for the InsCB module with an uninsulated floor was changed to determine the effect of orientation on the AccuRate star rating and the ATM. Changing the module orientation from north to any another direction showed a significant decrease in the AccuRate ratings and the ATM, as is shown in Table 7.5.

Table 7.5. Effect of orientation on the AccuRate star ratings and the ATM.

Modifications	ATM80 (80% acceptability limits)	AccuRate star ratings
Base design (North window)	78%	8.7
Window facing West	55%	6.2
Window facing South	49%	5.4
Window facing East	57%	6.4

7.3.2 Internal Colour

Different physical properties affect the thermal performance of building (see Section 2.1.14). Using darker colours for internal surfaces will increase the absorptivity from 50% for a medium colour to 96% for the colour black, and painting the internal walls and the floor will increase the heat absorbed from the north-facing window and will reduce the heating required for colder months.

Changing the internal brick walls' colour to a darker colour will result in the same star rating in AccuRate as changing the internal wall material to 300mm of

Rammed Earth. Therefore, painting is a lower cost option. For the ATM, changing the internal colour to a darker colour will increase the ATM to 83% and the AccuRate rating increased to 8.9. The full results are shown in Table 7.6.

In this research, the darker colour option was used to study the effect on the thermal performance, but in real life darker colours have issues, such as:

- Not visually pleasing for most people.
- Required more lighting than lighter colours, which results in more energy consumption.

Table 7.6. The ATM results and AccuRate ratings for different internal colours.

Modifications	ATM80 (80% acceptability limits)	AccuRate star rating
Brick Internal wall for InsCB (absorptivity = 50%)	78%	8.7
Internal wall for InsCB (absorptivity = 96%)	83%	8.9

7.3.3 Building Location

Design for the climate is important because each location requires different design techniques as discussed in detail in Chapter 2 (Building Design for the Climate).

For example for the same InsCB module if its location is changed from Newcastle to Perth in Western Australia the star rating will increase from 8.9 to 9.2 and if it is changed to Darwin it drops to 7.7 as shown in Table 7.7.

Colder climates such Melbourne and Hobart will result in a greater need for heating energy because of the large uninsulated window. On the other hand, in hot climates such as Darwin this will result in lower thermal performance because of the large cooling energy required caused by the high thermal mass of the walls and the radiation entering the module through the north facing window.

Table 7.7. Star rating for InsCB module in different locations in Australia

Location	Star rating
Newcastle, NSW	8.9
Sydney, NSW	9.2
Melbourne, Vic	6.5
Adelaide, SA	7.9
Brisbane, QLD	9.3
Hobart, TAS	5.9
Perth, WA	9.2
Darwin, NT	6.7

Note: Newcastle located 170 km north of Sydney with almost similar climate

7.4 Best Design Improvements for the Original Modules

Changing the window materials from single clear glass to double glazing and the internal wall material to a higher thermal mass material with a darker colour will improve the overall thermal performance of the buildings from 8.7 to 9.5 stars and reduce the heating load by half (from 34 to 17 MJ/m^2. annum) full details of the materials and sizes are given in Appendix C.

For the thermal performance ATM the same changes will improve the ATM from 78% to 91% where the internal air temperature inside the modules increased for the final design compared with the based design as shown in Figure 7.4.

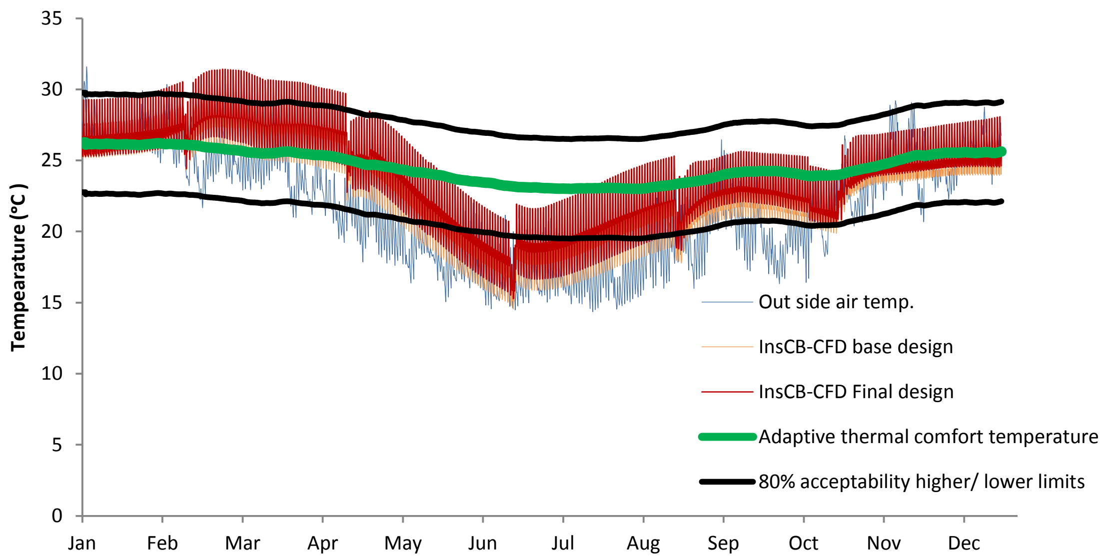

Figure 7.4. Base and final CFD simulation results for the internal air temperature for the InsCB module.

7.5 Best Design Improvements for the Western Australia House

Improvements to the design (as investigated in the previous Sections 7.1 to 7.4) are then applied to assess the accuracy and applicability of the ATM. The uses of the optimum design techniques for the modules are investigated in this section to potentially improve the thermal performance of the Western Australia house. Because the main problem arise for this house in the winter months, the improvements will focus on increasing the house's thermal performance in these months by changing the external wall insulation from R1.5 to R2.5, the window materials from single clear glass pane to double glazing, the internal wall materials to a higher thermal mass material and a darker colour applied to the external northern surfaces to absorb more heat for the winter months. The main living room with two sliding glass doors is already facing north which is ideally orientated to allow winter sun to warm the house.

These modifications significantly reduced the heating requirements for the winter months from 64 to 28 MJ/m^2. annum and improved the overall thermal performance of the building from 7 to 8.5 stars. For the ATM, the same changes improve the ATM from 60% to 81.9% for the 80% acceptability limit, as shown in Figures 7.5 and 7.6 Full details are given in Appendix I for the final design materials and the sizes taken from the AccuRate final report.

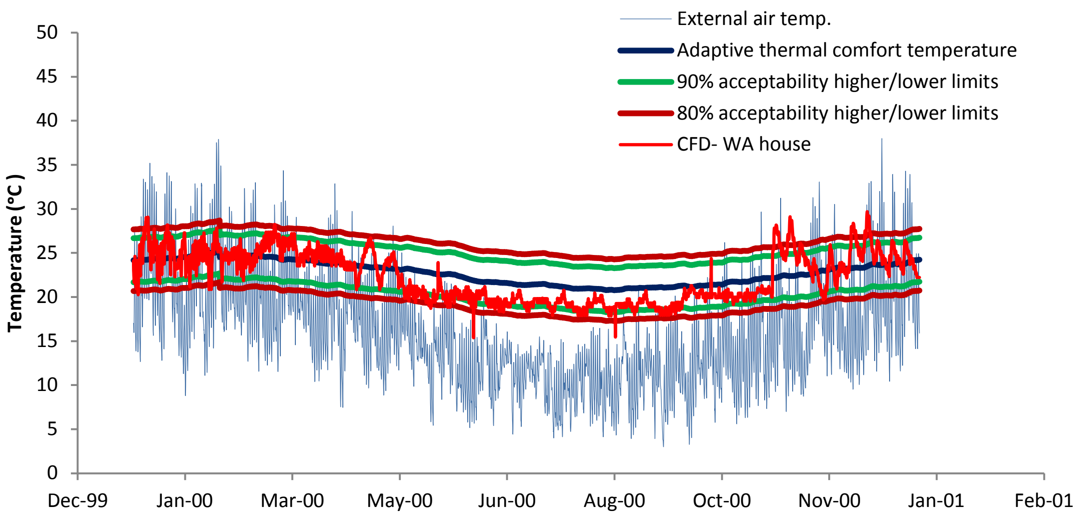

Figure 7.5. Internal and external air temperatures and thermal comfort ranges for the WA house.

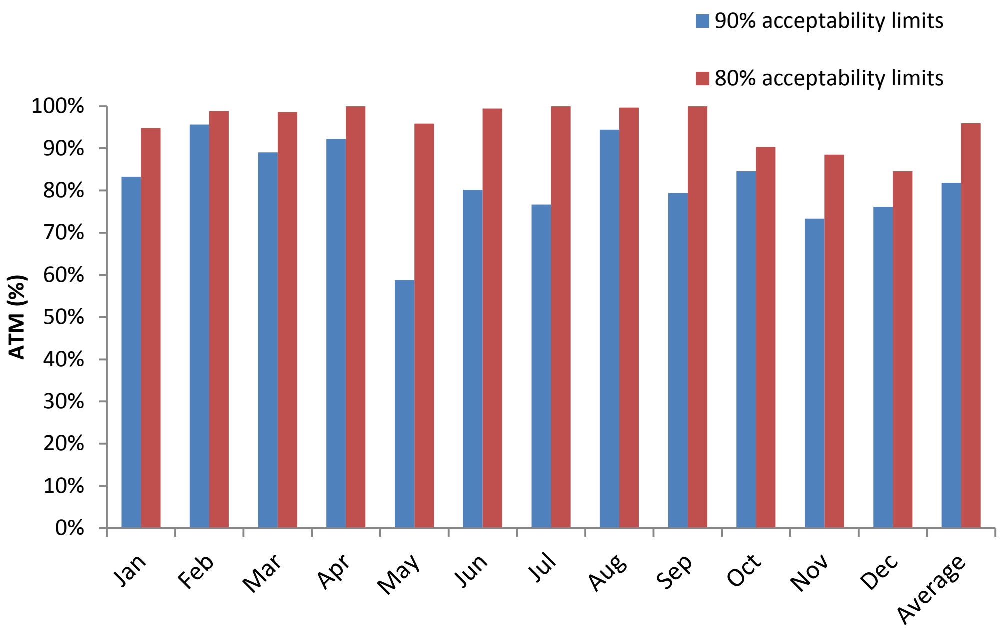

Figure 7.6. Monthly 90% and 80% monthly acceptability limits for the WA house over one year.

7.6 Relationship between the ATM and AccuRate Bands

To study the relationship between the ATM and the AccuRate rating system, a comparison between the AccuRate results and the ATM for each improvement is shown in Table 7.8.

Table 7.8. The AccuRate ratings and ATM results for the various module modifications.

Design Attempt	Modifications	ATM (80% acceptability) limits)	AccuRate Star rating
1	South window for InsCB	49%	5.4
2	West window for InsCB	55%	6.2
3	East window for InsCB	57%	6.4
4	CB walls	70%	6.5
5	InsBV walls	72%	7.3
6	InsRBV walls	76%	8.3
7	Insulated floor for InsCB	76%	8.4
8	InsCB walls	78%	8.7
9	North facing window for InsCB	78%	8.7
10	Darker colour for internal walls and floor for InsCB	83%	8.9
11	Rammed Earth 300mm for internal wall for InsCB	84%	8.9
12	Double glazed window for InsCB	87%	9.3
13	Double glazed window + Rammed Earth for internal walls+ darker internal colour for InsCB	91%	9.5

Comparing the thermal assessment results from the AccuRate ratings and the ATM shows that there is a direct relationship between the AccuRate ratings and the ATM results with consistent trend, as is shown in Figure 7.7.

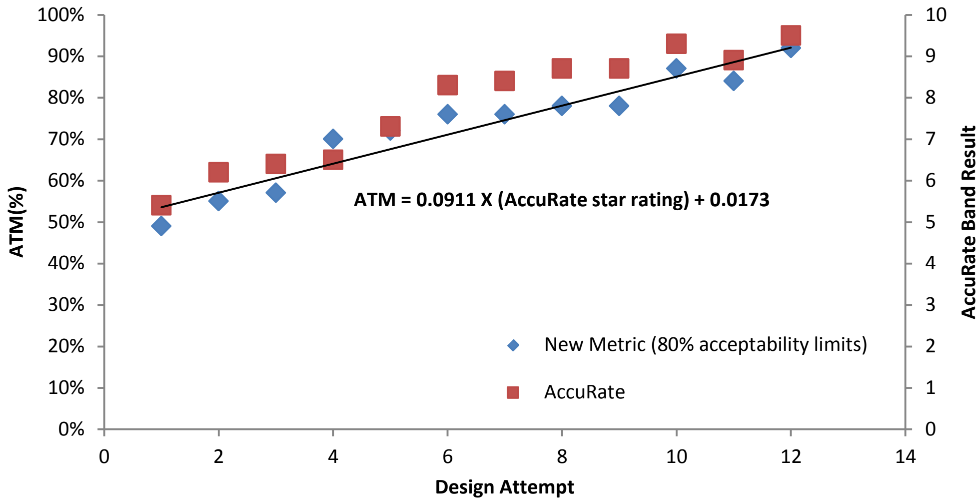

Figure 7.7. Relationship between the AccuRate ratings and the ATM results.

From the above Figure and using Excel to find the linear equation which represents this relationship;

$$\textbf{ATM} = \textbf{0.0911 X (AccuRate star rating)} + \textbf{0.0173} \qquad (7.1)$$

R^2 = 0.922 is the proportion of the variance in the ATM can be attributed to the variance in AccuRate star rating.

These results confirm that the proposed thermal performance ATM has the potential to replace the AccuRate system as a building thermal performance assessment tool. An addition advantage is that the ATM embraces sustainable principles, which encourages greater energy efficiency and sustainability.

7.7 Costs of Improvements to the Original Module Design

Building construction costs vary, depending on the location, level of finish (low, medium and high) and the construction type, whether residential (houses, townhouses and units) or commercial. This section focuses on the costs of the improvements discussed in the previous section.

The analysis is based on the assumption that there is no extra labour cost to change the module components as they would form part of the original construction. The comparisons are therefore based only on the materials costs.

7.7.1 Replacement of Walling Systems

The average construction and building component costs for the walling systems are shown in Table 7.9. The cheapest option is InsBV, so all the modules will be compared with cheapest option (where the total wall area is 67.2 m^2).

Table 7.9. Average walling system costs (ACCEL design).

Walling system	Average cost	Cost difference compared with InsBV
Cavity Brick	$220/m^2$	$2,016
Insulated Cavity Brick	$240/m^2$	$3,360
Insulated Brick Veneer	$190/ m^2$	$0.00
Insulated Reverse Brick Veneer	$200/m^2$	$672.0

The use of insulated cavity brick walls will cost an extra $3,360, compared to the cheapest option of InsBV, but InsCB will improve the building's thermal performance by 6%.

7.7.2 Replacement of Window Type

Double glazed windows are better insulators than single glazed windows but the price of a double glazed window will depend on its quality, and will be at least 25% more expensive than single glazed windows. Double glazing window for new buildings can add up to a price difference of between $3,000 and $5,000, as compared to single glazing windows (Home Improvement).

Using double glazed windows for the modules will cost around $600, compared to using single glazed windows, and will improve the ATM results by 9%, which is a more feasible option compared to changing the walling systems.

7.7.3 Introduction of the Thermal Mass

For illustrative purposes only, changing the internal walls to Rammed Earth 300mm will cost, on average, $275/m^2$ (Unique Earth), which is an extra of $1260 compared to the brick walls of 16.8m^2, and this will improve the ATM for the InsCB module from 78% to 84%.

7.7.4 Introduction of the Thermal Resistance

Insulation depends on R-values where the higher the R-value the better the insulation but with higher cost as shown in Table 7.10. The roofs were insulated for all modules.

Table 7.10. Average insulation cost, based on R-values without installation (Feel Good Insulation)

R-value	Average cost
R1	\$7/m^2
R2	\$10/m^2
R3	\$13/m^2
R4	\$16/m^2
R5	\$27/m^2

7.7.5 Total Costs of Improvements to the Original Module Design

The InsCB module was already fully insulated so there was no need to calculate the cost for extra insulation. Table 7.10 summarizes the improvements needed to enhance the thermal performance of the other modules and the associated costs.

Table 7.10. Cost for each improvement.

Modifications	ATM80 (80% acceptability limits)	Cost $
CB walls	70%	$2,016
InsRBV walls	76%	$672
InsCB walls	78%	$3,360
Insulated floor for InsCB	76%	$300
North facing window for InsCB	78%	$0.00
Darker colour for internal walls and floor for InsCB	83%	$150
Rammed Earth 300mm for internal wall for InsCB	84%	$1260
Double glazed window for InsCB	87%	$600

The final improvements will cost around $5,370, and will improve the thermal performance from 70% to 91%. The next section will determine how much energy is saved by the improvements and which renewable energy system provides the modules with the best performance and the least cost.

7.8 Introduction of Renewable Energy Systems to Achieve the Complete Thermal Comfort for the Modules

To find suitable renewable energy system the modules' energy requirements for heating and cooling over the 12 month study period need to be calculated first.

The main issue which reduces the performance is the heating during the winter months. The average winter temperature was 12ºC, and the amount of energy required to heat the system from 12ºC to 19ºC (a comfortable temperature in winter) is shown below:

$$\mathbf{U = m\ C_p\ dT} \tag{7.2}$$

Where;

U: Energy required to heat the air inside the module (kJ)
m: Mass of air at 12 ºC = 1.225 kg (The Engineering Toolbox) for each module, the total volume = 86.4 m^3 and the total mass of air inside each module = 105.84 kg.
C_p : Specific heat capacity of the air =1 (kJ/kg ^{o}C)
dT: Temperature difference = 7 ºC

The energy required to heat each module equals to 0.21 kWh (105.84 kg x 1 kJ/kg^{o}C x 7 ºC = 740.8kJ = 0.21 kWh).

This is in steady-state condition, but in transient conditions the heating energy required for each month can be calculated easily though Autodesk Ecotect. For example, the calculation of the energy required for the InsBV module (the basic design with no improvements, where the thermal performance was just 70%) is shown in Table 7.12, and for the improved design InsCB module (91%) is shown in Table 7.13.

Table 7.12. Monthly heating/cooling energy required (loads) for the basic InsBV module.

Loads (kWh)	Jan	Feb	Mar	Apr	May	Jun	Jul	Aug	Sep	Oct	Nov	Dec	Total
Heating	0	8.16	33.04	32	73.5	286.8	325.2	129.9	67.9	26.88	0.9	0	984.3
Cooling	18	22	16	0	0	0	0	0	0	0	0	5	61

Table 7.13. Monthly heating/cooling energy required (loads) for the improved InsCB design.

Loads (kWh)	Jan	Feb	Mar	Apr	May	Jun	Jul	Aug	Sep	Oct	Nov	Dec	Total
Heating	0.0	3.4	11.8	10.0	10.5	71.7	73.9	36.1	9.7	8.4	0.3	0.0	235.7
Cooling	2	7	6	0	0	0	0	0	0	0	0	0	15

Large amounts of energy are used for heating in winter compared to small amounts of energy required in summer months to attain thermal comfort inside all modules.

The improvements will save \$149.7/year (984.3 – 235.7 = 748.6 kWh/year heating energy, the energy cost = \$0.2/kWh, the energy bill will be around \$149.7/year).

Assuming that the lifetime of the module is 20 years, the current cost (present value) of the energy required to maintain thermal comfort through the lifetime of the building can be calculated and compared with the new sustainable system to find the most economical way to obtain thermal comfort.

Money in the future is worth less than 'today's money' because money available today can be used immediately. Discounting is the process whereby an amount of money in the future is converted to a present day value, or Present Value (PV). The discount rate is basically the interest rate at which money can be borrowed for a project, or if the money is available, it is the rate of interest that would be earned on a competing project or investment.

Net Present Value (NPV): is used where there are a number of payments throughout the life of the project. It is the sum of the Present Value of all the costs and benefits.

$$\mathbf{NPV = PWF\ (i,f,n) \times S} \tag{7.3}$$

S: Annual cost or value into the future (cost –ve, saving +ve)

PWF: Present Worth Factor (The University of Texas website):

$$\boldsymbol{PWF} = \frac{\mathbf{1} - \left(\frac{\mathbf{1}+\boldsymbol{f}}{\mathbf{1}+\boldsymbol{i}}\right)^{\boldsymbol{n}}}{\left(\frac{\mathbf{1}+\boldsymbol{i}}{\mathbf{1}+\boldsymbol{f}}\right) - \mathbf{1}} \tag{7.4}$$

Where;

i : Discount rate

f : Inflation rate

n : Number of years

Assuming that the interest rate is around 6%, the inflation rate around 3% and the lifetime for the building is 20 years, the PWF is 15 and the net present value is \$2245.8.

The cost to improve the module from InsBV (70%) to the improved InsCB (91%) will cost around \$5,370 and will save just \$2245.8 on energy bills. New ways to improve the thermal performance of the modules, with the least cost, such as renewable energy systems, will be examined in the next section.

Reaching 100% of the time where the internal air temperature inside the building remain within the thermal comfort range by using appropriate design, materials and renewable energy systems without using energy come from fossil fuel.

This section will discuss some of the sustainable systems which can be used to improve the thermal comfort inside the building without significantly increasing the cost, such as:

- Heating systems (solar heating system).
- Cooling systems (evaporative cooling).
- Heating and cooling systems (PV systems, wind turbines, hybrid systems).

Choosing the right system depends on the climate and the solar/wind availability. For example, for dry hot climates an evaporative cooling system will work effectively and for humid environments ventilation will work better. For cold climates a solar heating system will work efficiently. Wind turbines and PV systems can be used for most climates, depending on the wind and solar availability to power the cooling and heating systems installed inside the buildings.

Selecting the right building components will improve a building's thermal performance to 91%. To reach an almost 100% thermal performance, with no need for heating and cooling energy (from fossil fuels) to obtain thermal comfort, a renewable system will be used.

Heating energy consumes 235.7 kWh/year for the improved InsCB module, which will cost (based on \$0.2/kWh) \$47.14/year for heating and assuming interest rate of 6%, 3% inflation and the lifetime of the building is 20 years, PWF equal 15 and the cost for 20 years = \$707.13.

July required the highest amount of heating energy (73.9 kWh/month) so we need a renewable system which can provide heating energy of around 70 kWh/month to maintain thermal comfort in the winter months and will cost less than \$707.13. The cost for the various renewable energy systems are shown in Table 7.14.

Table 7.14. Renewable system costs.

Renewable systems	Average cost
Solar Air Heater	\$600/m^2 (Nenergy)
Wind turbine	\$6000/kW (Solar online Australia)
Photovoltaics system	\$1200/kW (Energy matter)
Evaporative cooling	\$120/ kW cooling power (Gstore)

Solar air heater efficiency reach up to 75% assuming the system efficiency=70% and the average solar radiation fell on the module shown in Table 7.16. Using 1m^2 of solar heater can provide almost enough heating energy as shown in Table 7.15.

Table 7.15 .Amount of solar energy absorbed by $1m^2$ solar heater system.

	Jan	Feb	Mar	Apr	May	Jun	Jul	Aug	Sep	Oct	Nov	Dec
Monthly average solar radiation (kWh/m^2 day)	6.7	5.8	5.7	4.4	3.6	3.4	3.3	4.4	5.2	5.8	6.3	6.9
Absorbed by solar heater (eff.=0.7) ($kWh\ /m^2day$)	4.69	4.06	3.99	3.08	2.52	2.38	2.31	3.08	3.64	4.06	4.41	4.83
$1m^2$ Solar heater provide per month (kWh/month)	140.7	121.8	119.7	92.4	75.6	71.4	69.3	92.4	109.2	121.8	132.3	144.9

Using a 0.7kW photovoltaic system (which is equivalent to a $1m^2$ solar air heater) can provide enough energy for heating in winter and cooling in summer, as shown in Table 7.16.

Table 7.16. Energy supplied by 0.7kW PV system.

	Jan	Feb	Mar	Apr	May	Jun	Jul	Aug	Sep	Oct	Nov	Dec
Monthly average solar radiation (kWh/m^2. day)	6.7	5.8	5.7	4.4	3.6	3.4	3.3	4.4	5.2	5.8	6.3	6.9
1kW PV system (kWh/month)	140.7	121.8	119.7	92.4	75.6	71.4	69.3	92.4	109.2	121.8	132.3	144.9

The modules required more heating energy than cooling energy and a PV system will provide more energy in summer months due to higher solar radiation and this energy can be used inside the module to run appliances, for example.

For the modules, it required a system cost of less than $707 to be economically feasible, which applies for the solar air heater and photovoltaics systems. The rest of the systems are too expensive or do not suit the module's climate, as is shown in Table 7.17.

Table 7.17. Cost comparison for the various renewable energy systems.

Renewable systems	Average cost	Feasibility
Solar Air Heater	$600/$m^2$	Economically feasible
Wind turbine	$6000/kW	Too expensive
Photovoltaics system	$1200/kW $840/0.7kW	Slightly more expensive but can be applied
Evaporative cooling	$120/kW cooling power	Heating required for the existing modules not cooling

To reach close to 100% self-sufficient energy, the solar air heater and photovoltaics systems are economically feasible, whereas a wind system is an expensive option to provide energy to the modules. The next step will find the best combination of materials and renewable energy systems to achieve thermal comfort inside the modules with the least amount of energy.

7.9 Optimum Design Options

The improved InsCB module was more energy efficient but significantly more expensive than the InsBV module. Using insulation and double glazed windows for the basic InsBV will cost $600 and will improve the thermal performance to 79% of the time within the thermal comfort zone. The energy required for heating the improved InsBV module is shown in Table 7.18.

Table 7.18. Monthly heating/cooling energy required (loads) for the improved InsBV module (79%).

Loads (kWh)	Jan	Feb	Mar	Apr	May	Jun	Jul	Aug	Sep	Oct	Nov	Dec	Total
Heating	0	2.1	15.5	21.4	53.6	224.7	287.1	87.6	43.1	12.5	0	0	747
Cooling	7	12	10	0	0	0	0	0	0	0	0	5	34

Using 2m^2 solar air heaters will provide much needed heating energy in the winter months 142.8 kWh in June and 138.6kWh in July and that will improve the module's thermal performance. The total cost for the improvements (double glazed windows and 2m^2 solar air heater) almost $1800 and the saving on heating energy bills equal $1750 (582.6 kWh/year X $0.2/kWh X 15(PWF) = $1747.8). That is almost cost the same as using electricity for heating but it is more environmentally friendly.

If the modules connected to the grid, the PV system can export extra energy in summer and import some of the energy in winter PV system is preferred. The total cost for the improvements (double glazed windows and 0.7PV system) almost $1440 and the saving on energy bills equal $2000 (1146.6 kWh/year X $0.2/kWh X 15(PWF) = $3439.8.This option costs significantly less than the other design options. Using Photovoltaic systems provide less heating energy in winter but more energy in summer months due to higher solar radiation and this energy can be used inside the module to run appliances and this depends on the occupants need for energy.

7.10 Summary

Changing the walling system can improve the ATM80 (80% ***acceptability limits***) by 8%. Changing the walls from cavity brick to insulated cavity brick improves the ATM by 8% and improves the AccuRate star rating (bands) by 2.2 (from 6.5 to 8.7, see table 7.1).

Changing the walls from insulated brick veneer to insulated reverse brick veneer improves the ATM by 4% and improves the AccuRate star rating (bands) by 1. Insulating the ground floor will cost more and will not improve the overall thermal performance of the modules because it will trap the heat in the summer months inside the building which requires higher cooling energy and the floor insulation has an insignificant effect in the winter months.

The best orientation is when the windows face the north. Changing the building's orientation to the east and west will heat the building in summer because the east and west windows gain more heat in summer and lose more heat than they gain in winter. A southern orientation results in small solar gains and heat losses through the windows in winter.

Double glazed windows insulate the windows from the external environment and will improve the ATM from 78% to 87%, which is a significant improvement in the thermal performance.

Applying higher thermal mass material (Rammed Earth 300mm) to the internal walls will improve the overall thermal performance of the building by 6%. Painting the original internal walls with a darker colour (black) will give the same results as changing the wall material but darker colours require more lighting and are not visually pleasing.

To reach 100% self-sufficient energy, solar air heaters and photovoltaic systems are economically feasible whereas a wind system is an expensive option to provide energy to the modules.

The above (selective) study has illustrated the use of the ATM in investigating techniques to improve energy efficiency ratings by facilitating the assessment of the thermal performance of whole building envelopes and finding ways to thermally improve house designs and reduce energy consumption.

The next Chapter summarises the main conclusions of this research and makes recommendations for future work.

Chapter Eight: Conclusions and Recommendations for Future Research

8.1 Conclusions

Energy efficient buildings are essential for sustainable development; this requires a realistic and accurate prediction of the performance of the building under a wide range of weather conditions to capture the impact of all the physical parameters and occupant behaviour influencing the thermal performance of the building. This in turn requires an effective metric to accurately predict the thermal performance of the buildings.

The principal goal of this research was to develop a new universal Adaptive Thermal Metric (ATM) to characterise the thermal performance of complete buildings. The proposed ATM facilitates the assessment of the thermal performance of whole building envelopes by determining the internal air temperatures of a building using CFD simulation and then accounting for the percentage of time over which the internal air temperatures of a building remain within the adaptive thermal comfort range (90% and 80% ***acceptability limits***).

The Adaptive Thermal Metric (ATM) can be used to characterise and compare the thermal performance of complete buildings taking into consideration occupant behaviour, building materials, weather at the site, shading, orientation, and the environment surrounding the building using the adaptive thermal comfort range for temperate climate and the average internal air volume temperatures for a building.

8.2 Major Findings

8.2.1 CFD Simulations

This is the first research to use CFD simulation alone to determine the internal air temperature of buildings for long periods (one year), without the assistance of any additional software, with fast computing times and an acceptable degree of accuracy for the simulation results. CFD simulations over long periods face issues, such as: the simulated internal air temperature warming with time; long computing times; smaller fluctuation range discrepancies in peak temperature time; and wind effects on the external surface. These issues were resolved as follow;

- It was found that adding a new boundary condition/layer surrounds the module with the ambient external air temperature without affecting the solar radiation received by the module. This new boundary layer prevented the long term rise in the internal air temperature, which resulted in more than 89% of the results falling within 0 - 3ºC temperature difference compared with the real air temperatures measured inside the module.

- Larger time steps were used (80/100 minutes) in the CFD analysis to speed up the simulation time by 99% compared to 1 minute time step computing time. This resulted in higher temperature fluctuation ranges but increased the discrepancies in peak temperature.

- It was proven that wind effect can be simulated in CFD modelling for long periods by adapting the new air temperature $T_{natural}$ which takes into account the same rates of convection heat losses created by the wind surrounding the building. $T_{natural}$ enables the direct inclusion of the wind effect and considerably decreases the overall computing time.

- After solving CFD simulating issues, simulations were carried out for four full scale housing test modules for a one year period, with an average accuracy of 93% when compared with the real data at any given time during the year. Performing CFD analysis after applying the measures (discussed in Chapter four) resulted in faster computing times, with 1% of the computing time compared to that for a 1 minute time step, and with 90% of the results lying within 3°C of the real (observed) data.

8.2.2 Development of the Adaptive Thermal Metric (ATM)

The ATM has the potential to characterise and compare the thermal performances of complete buildings, taking into consideration their aspect and shading environment. The characteristics of the new ATM are:

- ✓ The ATM can be applied universally.
- ✓ Since adaptive techniques are used to obtain thermal comfort rather than energy usage, sustainability and energy saving are encouraged.
- ✓ Fast calculation time.
- ✓ Minimum weather data requirements.
- ✓ Ability to compare the thermal performance of complete buildings.
- ✓ Consideration of the various building components and the shading environment of the buildings are included.

- The ATM results for the thermal performance of the housing modules indicated that the InsCB module had the best thermal performance, followed by the InsRBV, InsBV and CB modules. These results are reliable and in the line with previous findings from the research undertaken at the University of Newcastle on the walling systems and the results from AccuRate.

8.2.3 Applications of the ATM

- To examine the capability of the ATM to reproduce the thermal performance of different housing types in different locations, as a case study, the ATM was calculated for a three bedroom house in a different climate zone. The final results illustrated the possibility of using the ATM as a new universal metric which could be applied anywhere around the world.

- Current energy thermal assessment tools do not account for the occupants' behaviour and make various assumptions about the physical and material properties which lead to great differences between the theoretical and real results. However, this ATM is based on wider ranges of internal air temperatures (a temperature-based approach not energy based) and the occupants have more options to obtain thermal comfort (e.g; adapting to a wider range of internal temperature, changing clothes, opening windows, or employing low energy solutions, such as fans). This results in lower energy usage and running costs, therefore enhancing the economic and environmental performance of the building.

8.2.4 Enhancement of the Thermal Performance for Selected Modules

The ATM was used to investigate some techniques to improve energy efficiency ratings by finding ways to thermally improve house designs and reduce energy consumption. By simulating the performance of the modules with various energy enhancement strategies the following was concluded;

- Insulating the cavity brick walls improve the ATM80 by 8% and improve the AccuRate star rating (bands) by 2.2. On the other hand insulating the ground floor cost more but did not improve the overall thermal performance of the modules.

- The best orientation is when the windows face the north and using double glazed windows will improve the ATM80 by 9%, which is a significant improvement with least cost.

- In this research for illustrative purposes, using a higher thermal mass material or painting the internal walls with darker colour will improve the overall thermal performance of the building by the same level but darker colours require more energy for lighting and are not visually appealing.

- To reach 100% self-sufficient energy for the modules, solar air heaters are economically feasible whereas photovoltaic systems and wind turbine are more expensive options to provide energy to the modules.

- The feasibility study showed that by using the appropriate building components, with the assistance of renewable energy systems, 98% of the thermal comfort inside the modules could be achieved with the least amount of energy consumption.

These promising results may facilitate the use of this ATM as an assessment tool for new buildings to accurately predict the thermal performance of any building envelop to sustain an appropriate thermal comfort level.

8.3 Recommendations for Future Research

The accuracy of the CFD analyses was in the order of 93% at any given time during the studied year. The CFD analysis could be further refined to increase the accuracy and reduce the simulation time by finding the appropriate sky temperature for each month for more accurate and precise simulations.

Determine the adaptive equation for each climate zone in Australia. In this research there are two adaptive equations for Australia, one for the temperate climate and the other for the hot and humid climate but there are no adaptive equations for colder climates or dry and hot Australian climates.

The cost analysis should include the embodied energy for the modules and the renewable energy systems to find the total amount of energy required for the module's life cycle.

A wider examination of the ATM using different building types, materials, locations and for different climates is needed, as well as comparison of the thermal assessment ATM results with more building assessment tools used in different countries.

References

ACCEL design (2015). Elements of smarter construction. Retrieved April 2015. available on: www.accel.com.au/base_tl/Smarter%20Construction%20Book.pdf

AccuRate Sustainability (V2.3.3.13 SP1). (2013) tool helps manual.

Ajmire, S., Nilesh, S. (2013). Greenchem: Recent developments in chemical engineering. Dumore International E Publication. ISBN;9383520183.

Albatayneh A., Alterman A., Page A., Moghtaderi B. (2015). The Significance of Time Step Size in Simulating the Thermal Performance of Buildings. Advances in Research; Vol. 5, Issue: 6. ISSN: 2348-0394.

Alterman, D., Moffiet, T., Hands, S., Page, A., Luo, C., Moghtaderi, B. (2012). A concept for a potential ATM to characterise the dynamic thermal performance of walls. Energy and buildings; 54; 52-60.

American Society of Heating, Refrigerating and Air-Conditioning Engineers (ASHRAE). (2010). Standard 55. Thermal environment conditions for human occupancy, USA.

American Society of Heating, Refrigerating and Air-Conditioning Engineers (ASHRAE). (2004). Standard 55. Thermal environment conditions for human occupancy, USA.

American Society of Heating, Refrigerating and Air-Conditioning Engineers (ASHRAE). (1992). Standard 55. Thermal environment conditions for human occupancy. USA.

ANSI/ASHRAE Standard 55. (2013). Thermal Environmental Conditions for Human Occupancy.

Auliciems, R., de Dear. (1986). Air conditioning in Australia: human thermal factors. Architectural Science Review; 29 67–75.

Australian Greenhouse Office (AGO), (2004). Australian Residential Building Sector. Greenhouse Gas Emissions 1990-2010. Executive Summary Report 2004. Canberra.

Australian Solar Energy Society. (2006). Australian solar radiation data handbook. 4th edition. Retrieved October 2014. Available on: www.exemplary.com.au.

Autodesk Ecotect. Analysis sustainable design analysis software. Ecotect & Vasari: Climate Analysis. Retrieved November 2014. Available on: http://sustainabilityworkshop.autodesk.com/buildings/ecotect-vasari-climate-analysis

Autodesk Ecotect. Analysis sustainable design analysis software. PsychroATM charts. Retrieved October 2014. Available on: http://sustainabilityworkshop.autodesk.com/buildings/psychroATM-charts.

Autodesk Simulation CFD. (2014). CFD user manual, quick guide. Retrieved October 2014. Available on: http://help.autodesk.com/view/SCDSE/2014/ENU/?guid=GUID-C1E9EBEA-B7DF-478A-A795-24F337C93DF3. Accessed 2014.

Autodesk Simulation CFD. (2014). Solar Heating. Retrieved October 2014. Available on: http://help.autodesk.com/view/SCDSE/2014/ENU/?guid=GUID-EBC7C1DC-11F8-4BC2-8D0D-D49AB3106848.

Autodesk Simulation CFD. (2014). Solar Heating. Retrieved October 2014. Available on: http://help.autodesk.com/view/SCDSE/2014/ENU/?guid=GUID-7BE54C33-D7CE-4F95-81B0-FD3B5517E9B3. Accessed Sep 2014.

Autodesk Simulation CFD. (2014). Solar Heating. Retrieved October 2014. Available on: http://help.autodesk.com/view/SCDSE/2014/ENU/?guid=GUID-7BE54C33-D7CE-4F95-81B0-FD3B5517E9B3).

Autodesk Simulation CFD. (2014). Transient Flows. Retrieved August 2014. Available on: http://help.autodesk.com/view/SCDSE/2014/ENU/?guid=GUID-384EC529-309C-426C-B036-93ADDB842F0E

Autodesk Simulation CFD. (2014). Transient Parameters. Retrieved October 2014. Available on: http://help.autodesk.com/view/SCDSE/2014/ENU/?guid=GUID-7BE54C33-D7CE-4F95-81B0-FD3B5517E9B3

Azhar, S., et al. (2012). Building information modeling (BIM): now and beyond. Australasian Journal of Construction Economics and Building; 12 (4) 15-28.

Basix. Building sustainability index. The Department of Planning and Environment. Evaporative cooling. Retrieved April 2015. Available on: http://www.basix.nsw.gov.au/basixcms/basix-help-notes/energy/heating-and-cooling/evaporative-cooling.html.

Bhattacharya, y. (2010). PsychroATM chart tutorial: a tool for understanding human thermal comfort conditions. University of California Los Angeles, Dept. of Architecture and Urban Design.

Big Ladder. Climate Calculations. Retrieved December 2014. Available on: http://bigladdersoftware.com/epx/docs/8-0/engineering-reference/page-031.html

BINQ. world standard, Double Glazing, Triple Glazing, Low E. Retrieved October 2014. available on: http://www.binq.com.au/#!binq-glass/c18ge

BMT Group. built environment CFD. Retrieved January 2015. Available on:http://www.bmtwbm.com.au/markets/water-and-environment/environmental-cfd/built-environment-cfd/

BMW Group, available on: http://www.bmw-welt.com/en/visitor_information/

Bodycote testing group. Retrieved October 2014. Available on:: http://www.bodycote.com/

BOM (Bureau of Meteorology). Newcastle university (site number: 061390). Retrieved October 2014. Available on: http://www.bom.gov.au/climate/averages/tables/cw_061390.shtml

Booten, C., Kruis, N., Christensen, C. national laboratory of the U.S. Department of Energy. Office of Energy Efficiency & Renewable Energy. Identifying and Resolving Issues in EnergyPlus and DOE-2 Window Heat Transfer. Calculations National Renewable Energy Laboratory NREL Task No. BE120104.

Borge-Diez, D., Colmenar-Santos, A., Mur-Pérez, F., Castro-Gil, M. (2013) Impact of passive techniques and clean conditioning systems on comfort and economic feasibility in low-cost shelters. Energy and Buildings; Volume 62, 414-426, ISSN 0378-788.

Bouden, H., Ghrab. (2005). An adaptive thermal comfort model for Tunisian contest: a field study results. Energy and Buildings; 37 (1) 952–963.

Brager, G.S., R.J., de Dear. (2001). Climate, Comfort & Natural Ventilation: A new adaptive comfort standard for ASHRAE Standard 55. Proceedings, Moving Thermal Comfort Standards into the 21st Century, Windsor, UK.

BREEAM, BREEAM: What is BREEAM?. Building Research Establishment. Retrieved May 2015. Available on: . http://www.breeam.org/about.jsp?id=66.

Bright hub. PsychroATM Processes: Sensible Cooling and Sensible Heating of Air. Retrieved March 2015. Available on: http://www.brighthubengineering.com/hvac/41436-psychroATM-processes-sensible-cooling-and-sensible-heating-of-air/.

Brundtland Commission. (1987). Report of the World Commission on Environment and Development. United Nations.

Castilla, M., Álvarez, J., Berenguel, M., Rodríguez, F., Guzmán, J., Pérez M. (2011). A comparison of thermal comfort predictive control strategies. Energy and Buildings; Volume 43, Issue 10, 2737-2746, ISSN 0378-7788.

CEAE. Engineering Center. Predicting Thermal Comfort. University of Colorado at Boulder. Civil, Environmental, and Architectural Engineering ECCE 246, 428 UCB.

Retrieved May 2015. Available on: http://ceae.colorado.edu/~brandem/aren3050/docs/ThermalComfort.pdf

Cengel, Y.A., Cengel, Y. (2006). Heat and Mass Transfer: A Practical Approach. McGraw-Hill.

Clayton, Crowe. (2012). E-Study Guide for: Engineering Fluid Mechanics. Cram101 Textbook Reviews; ISBN 9780470259771.

Crawley, B., Lawrie, K., Pedersen, O., Winkelmann, C. (2000). EnergyPlus: energy simulation program. ASHRAE Journal; 42 (4) 49–56.

Crawley, D., Hand, J., Kummert, M., Griffith, B. (2008). Contrasting the capabilities of building energy performance simulation programs. Building and Environment; 43 661–673.

Daniel, L, Soebarto, V., Williamson, T. (2013). Assessing the simulation capability of the accurate engine in modelling massive construction elements. 13th Conference of International Building Performance Simulation Association. Chambéry, France.

Daniel, P., Loucks, Eelco, Van Beek. (2005). Water Resources Systems Planning and Management: An Introduction to Methods, Models and Applications. UNESCO; Page 255-261.

DCCEE. (2010). Department of Climate Change and Energy Efficiency 2010. Australia's emissions projections. Canberra, ACT.

DCCEE. (2010). Your Home Technical Manual. Department of Climate Change and Energy Efficiency. Australia's guide to environmentally sustainable homes. 4th Edition. Retrieved March 2014. Available on: http://yourhome.gov.au/technical/index.html.

de Dear, R., J., Auliciems, A. (1985). Validation of the predicted mean vote model of thermal comfort in six Australian field studies. ASHRAE Transactions; 91 (2B) 452–468.

de Dear, R., J., Brager, G., S. (1998). Developing an adaptive model of thermal comfort and preference. ASHRAE Transactions; 104 (1) 145–167.

de Dear, R., J., Leow, K., G., Foo, S., C. (1991). Thermal comfort in the humid tropics: field experiments in air conditioned and naturally ventilated buildings in Singapore. International Journal of Biometeeorology; 34, 1991, pp. 259-265.

De Dear, R.J., & G.S., Brager. (1998) . Towards an adaptive model of thermal comfort and preference. ASHRAE Transactions; Vol 104 (1), pp. 145-167.

De Paula, A., Xavier, L., Roberto. (2000). Indices of thermal comfort developed from field survey in Brazil. ASHRAE Transactions; 106 (1) 45–58.

Defraeye, T., Blocken, B., Carmeliet, J. (2011). Convective heat transfer coefficients for exterior building surfaces: Existing correlations and CFD modelling. Energy conversion and management; 52:512-522.

Delsante, A. (2005). Is the new generation of building energy rating software up to the task? – a review of AccuRate'. ABCB Conference Building Australia's Future. Surfers Paradise Queensland.

DEWHA. (2008). Department of the Environment, Water, Heritage and the Arts. Energy use in the Australian residential sector. Retrieved March 2014. Available on: http://ee.ret.gov.au/energy-efficiency/strategies-and-initiatives/national-construction-code/energy-use-australian-residential-sector-1986-2020.

DEWHA. (2008). Energy use in the Australian residential sector 1986-2020. Energy Efficient Strategies for the Department of Environment. Water, Heritage and the Arts, Australian Government. Retrieved March 2014. Available on: http://www.energyrating.gov.au/wp-content/uploads/Energy_Rating_Documents/Library/Energy_Consumption/2008-energy-use-aust-res-sector-full.pdf

Driscoll, M. P. (2005). Psychology of Learning for Instruction, Pearson Education. Florida State University.

EN 15251 Standards. (2007). Indoor environmental input parameters for design and assessment of energy performance of buildings addressing indoor air quality. Thermal environment, lighting and acoustics.

Enerconcept Technologies inc. (2012). Lubi Collector Technical manual Version 1.2-En-March 2012. Retrieved May 2015. Available on: http://www.enerconcept.com/en/

Energy matter. Sydney and NSW solar power deals. Retrieved April 2015. Available on: http://www.energymatters.com.au/specials/nsw-solar-power-deals/

Feel good insulation. Knauf Insulation Price List - Feel good insulation. Retrieved March 2015. Available on: www.feelgoodinsulation.com.au/.../Knauf_Insulation_Price_List_LR.pdf

Fergus, N. (2004). Adaptive thermal comfort standards in the hot–humid tropics. Energy and Buildings; Volume 36, Issue 7, 628-637, ISSN 0378-7788.

Feriadi, Henry, Wong, Nyuk, Hien. (2004). Thermal comfort for naturally ventilated houses in Indonesia, Energy and Buildings; Volume 36, Issue 7, 614-626, ISSN 0378-7788.

Ferreira, P., Ruano, A., Silva, S., Conceição, E. (2012). Neural networks based predictive control for thermal comfort and energy savings in public buildings. Energy and Buildings; Volume 55, 238-251, ISSN 0378-7788.

Fraas, L., Partain, L. (2010). Solar Cells and their Applications Second Edition, Wiley; ISBN 978-0-470-44633-1.

Frankl, P. (2002). Life Cycle Assessment (LCA) of Photovoltaic Systems. 18th European Photovoltaic Solar Energy Conference. Rome, Italy.

Fraunhofer Insitute for Solar Energy Systems (ISE). (2015). Photovoltaics Report. Retrieved July 2015. Available on: http://www.ise.fraunhofer.de/en/downloads-englisch/pdf-files-englisch/photovoltaics-report-slides.pdf.

G., E., Schiller, E., A., Arens, F., S., Bauman, et al. (1988). A field study of thermal environment in office buildings. ASHRAE Transactions 94 (2) 280–308.

Geard, D. (2011). An empirical validation of the house energy rating software AccuRate for residential buildings in cool temperate climates of Australia, PhD thesis, University of Tasmania; 281-283.

Givoni, B. (1998) .Climate Considerations in Building and Urban Design, John Wiley and Sons, New York.

Goudling, J., R., Lewis, J., O., & Steemers, T., C. (1992) .Energy Conscious Design: A Primer for Architects, B.T. Batsford Ltd., London.

Govt. of Australia. (2008). Climate change programs. Retrieved 15th May 2008. Available on: http://www.greenhouse.gov.au/resources/energy.html.

Govt. of Australia. (2008). Energy efficiency. Retrieved May 2008. Available on: http://www.environment.gov.au/settlements/energyefficiency/index.html.

Green remodelling. Benefits of a Home Wind Generator. Retrieved May 2015. Available on: http://cnw8.net/home-wind-power.

GreenBuildingAdvisor. All About Thermal Mass. Retrieved July 2015. Available on: http://www.greenbuildingadvisor.com/blogs/dept/musings/all-about-thermal-mass

Gstore, Brivis. Advance F35D Dump Evaporative Cooler. Retrieved March 2015. Available on: http://www.gstore.com.au/brivis-advance-f35d-evaporative-cooler.html?gclid=CIv0toL7zcICFVUHvAodyAwA0w

H., Feriadi, N., H., Wong. (2004). Thermal comfort for naturally ventilated houses in Indonesia, Energy and Buildings; 36 (7) 614–626.

Haapio, A., P., Viitaniemi. (2008). A critical review of building environmental assessment tools, Environmental Impact Assessment Review; 28 469–482.

Hamza, N. (2007). Double versus single skin facades in hot arid areas. Energy and Buildings; 40 (2008) 240–248.

Heidari, S., Sharples, S. (2002). A comparative analysis of short-term and long-term thermal comfort surveys in Iran. Energy and Buildings; Volume 34, Issue 6, July, 607-614, ISSN 0378-7788.

Heidari, S., Sharples, S. (2002). A comparative analysis of short-term and long-term thermal comfort surveys in Iran. Energy and Buildings; 34 (6) 607–614.

Helwan University. (2006). Bioclimatic design Department of Architect, Egypt. Retrieved March 2015. Available on: http://www.shadyattia.net/academic/BioclimaticDesign/Lecture%2007.html.

Holopainen, R., Tuomaala, P., Hernandez, P., Häkkinen, T., Piira, K., Piippo, J. (2014). Comfort assessment in the context of sustainable buildings: Comparison of simplified and detailed human thermal sensation methods. Building and Environment; Volume 71, January, 60-70, ISSN 0360-1323.

Home Improvement , Hi. How Much Does Double Glazing Cost?. Retrieved May 2015. Available on: http://www.homeimprovement.com.au/article/how_much_does_double_glazing_cost

Hong, T., Chou, S. K., & Bong, T. Y. (2000). Building simulation: an overview of developments and information sources. Building and environment, 35(4), 347-361.

Hulme, I., Clavelle, E., van der Lee, L., & Kantzas, A. (2005). CFD modeling and validation of bubble properties for a bubbling fluidized bed. Industrial & engineering chemistry research; 44(12), 4254-4266.

Humphreys, M., A., J., F., Nicol. (2000). Outdoor temperature and indoor thermal comfort: rising the precision on the relationship for the 1998 ASHRAE database of fields studies. ASHRAE Transactions; 38 (2) 485–492.

Humphreys, M.,A. (1975). Field studies of thermal comfort compared and applied. Journal of Institution of Heating and Ventilation Engineer; 44- 527.

Hwang, Ruey-Lung, Tzu-Ping, Lin., Nai-Jung, Kuo. (2006). Field experiments on thermal comfort in campus classrooms in Taiwan. Energy and Buildings; Volume 38, Issue 1, 53-62, ISSN 0378-7788.

IEA. (2009). Trends in photovoltaic applications. Survey report of selected IEA countries between 1992 and 2008. Report IEA-PVPS T1-18:2009, International Energy Agency PVPS Task 1.

IndiaMART, Louvre Windows,available on: http://trade.indiamart.com/details.mp?offer=6955256848

Interacademy Council. (2007). Lighting the way toward a sustainable energy future.

IPCC. (2007). Intergovernmental Panel on Climate Change. Retrieved March 2015. Available on: https://www.ipcc.ch/publications_and_data/publications_and_data_reports.shtml.

ISO 7726. (1998). Ergonomics of the thermal environment - Instrument for measuring physical quantities. Geneva, Switzerland: International Organization for Standardization.

J., Han, G., Q., Zhang, Q., Zhang, et al. (2007). Field study on occupants' thermal comfort and residential thermal environment in a hot-humid climate of China. Building and Environment; 42 4043–4050.

J.,F., Busch. (1990). Thermal responses to the Thai office environment, ASHRAE Transactions; 96 (1) 859–872.

J.,F., Nicol, I., A., Raja, A., Allaudin, G., N., Jamy. (1999). Climatic variation in comfortable temperatures: the Pakistan projects. Energy and buildings; 30 (2) 261–279.

Jacobsson, S., B., A., Andersson, et al. (2002). Transforming the energy system - the evolution of the German technological system for solar cells. SPRU Electronic Working Paper Series Paper No. 84. Brighton, U.K., Science and Technology Research, University of Sussex.

Jing, Liu, Runming, Yao, Rachel, McCloy. (2012). A method to weight three categories of adaptive thermal comfort. Energy and Buildings; Volume 47, 312-320, ISSN 0378-7788.

Jones, W. (2002). Capabilities and limitations of thermal models for use in thermal comfort standards. Energy and Buildings; Volume 34, Issue 6, July, 653-659, ISSN 0378-7788.

K.,J., Mc Cartney, J., F., Nicol. (2002). Developing an adaptive control algorithm for Europe. Energy and Buildings; 34 (1) 623–635.

K.,W., H., Mui, W., T., D., Chan. (2003). Adaptive comfort temperature model of air-conditioned building in Hong Kong. Building and Environment; 38 (2) 837–852.

Kordjamshidi, M. (2010). House rating schemes: from energy to comfort base green energy and technology springer series in green energy and technology. ISBN 3642157904. Springer, Page 8.

Kordjamshidi, M., King, S. (2009). Overcoming problems in house energy ratings in temperate climates: a proposed new rating framework. Energy and Buildings; 41(1) 125–132.

Kwok. A., G. (1998). Thermal comfort in tropical classrooms. ASHRAE Transactions; 104 (1B) 1031–1047.

Kwong, Qi, Jie., Adam, Nor, Mariah, Sahari, B. (2014). Thermal comfort assessment and potential for energy efficiency enhancement in modern tropical buildings: A review. Energy and Buildings; Volume 68, Part A, January, 547-557, ISSN 0378-7788.

Larsen, L., Rajkovich, N., Leighton, C., McCoy, K., Calhoun, K., Mallen, E., Bush, K., Enriquez, J., Pyke, C., McMahon, S., and Kwok, A. (2010). Green Building and Climate Resilience: Understanding Impacts and Preparing for Changing Conditions. University of Michigan; U.S. Green Building Council, 2011. 1663–1682.

Leftheriotis, G., P., Yianoulis. (2000). Thermal properties of building materials evaluated by a dynamic simulation of a test cell. Solar Energy; 69 (4) 295–304.

Luo, C., Moghtaderi, B., Page, A. (2010).Determining the Thermal Capacitance, Conductivity and the Convective Heat Transfer Coefficient of a Brick Wall by Annually Monitored Temperatures and Total Heat Fluxes. Energy & Buildings; pp.7-86.

M., Indraganti, K., D., Rao. (2010). Effect of age, gender, economic group and tenure on thermal comfort: a field study in residential buildings in hot and dry climate with seasonal variations. Energy and Buildings; 42 (3) 273–281.

M., Indraganti. (2010). Thermal comfort in naturally ventilated apartments in summer: findings from a field study in Hyderabad, India. Applied Energy; 87 (3) 866–883.

Manwell, J., G., McGowan, A., L., Rogers. (2009). Wind Energy Explained: Theory. Design and Application. John Wiley & Sons Ltd p 47.

Maohui, L., Bin, C., Xiang, Z., Min, L., Jingsi, Z., Qin, O., Yingxin Z. (2014). Can personal control influence human thermal comfort? A field study in residential buildings in China in winter. Energy and Buildings; Volume 72, 411-418, ISSN 0378-7788.

Morrissey, J., Moore, T. (2011). Horne Affordable passive solar design in a temperate climate: An experiment in residential building orientation. Renewable Energy; 36 568e577.

Moujalled, B., Cantin, R., Guarracino, G. (2008). Comparison of thermal comfort algorithms in naturally ventilated office buildings. Energy and Buildings; Volume 40, Issue 12, 2215-2223, ISSN 0378-7788.

Nanjing Oulu Electric Transmission. Wind- PV (Solar) Hybrid Power System. Retrieved March 2015. Available on: http://www.njoulu.com/

Nenergy. Solar powered solar air heater. Retrieved March 2015. Available on: http://negergy.com.au/products/solar-air-heater?gclid=CLD7wuP1zcICFUoGvAodDGwAqA

Nicol, J., F., Humphreys, M., A. (2002). Adaptive thermal comfort and sustainable thermal standards for buildings. Energy and Buildings; Volume 34, Issue 6, 563-572, ISSN 0378-7788.

Olesen, B., Parsons, K., C., (2002). Introduction to thermal comfort standards and to the proposed new version of EN ISO 7730. Energy and Buildings; 34 (6) 537–548.

Page, A., Moghtaderi, B., Alterman, D., Hands S. (2011). A study of the thermal performance of Australian housing. Priority Research Centre for Energy, the University of Newcastle. Retrieved March 2014. Available on: http://www.thinkbrick.com.au/thermalperformance-and-climate-design.

Parsons, K., C. (2003). Introduction to thermal comfort standards. (T. & Francis, Ed.) (2nd Ed.). London: Taylor & Francis Group.

PMC, (2004). Securing Australia's Energy Future. Australian Government, Department of Prime Minister and Cabinet, Canberra. Retrieved March 2014. Available on: http://www.efa.com.au/Library/CthEnergyWhitePaper.pdf.

Praznik, M., Butala, V., Senegačnik, M. (2013). Simplified evaluation method for energy efficiency in single-family houses using key quality parameters. Energy and Buildings; Volume 67, 489-499, ISSN 0378-7788.

Preston, L., Jones, R. (2006). Climate Change Impacts on Australia and the Benefits of Early Action to Reduce Global Greenhouse Gas Emissions. A consultancy report for the

Australian Business Roundtable on Climate Change. CSIRO. Canberra, Australian Capital Territory.

Rabah, K. (2005). Development of energy-efficient passive solar building design in Nicosia Cyprus, Renewable Energy; 30(6):937e56.

Reilly, D., Duffy, A., Willis, D., Conlon, M. (2013). Development and implementation of a simplified residential energy asset rating model. Energy and Buildings; Volume 65, 159-166, ISSN 0378-7788.

Richalet V., Neirac F.P., Tellez F., Marco J., Bloem J.J., (2001), HELP (house energy labeling procedure): methodology and present results, Energy and Buildings, Volume 33, Issue 3, , 229-233, ISSN 0378-7788.

Roaf, S., Nicol, F., Humphreys, M., Tuohy, P., Boerstra, A. (2010). Twentieth century standards for thermal comfort: promoting high energy buildings. Architectural Science Review; 53:1, 65-77.

Sala, J.,M., Urresti, K., Martin, I., Flores, A., Apaolaza. (2008). Static and dynamic thermal characterisation of a hollow brick wall: tests and numerical analysis. Energy and Buildings; 40 1513–1520.

Soebarto, V., Bennetts, H. (2014). Thermal comfort and occupant responses during summer in a low to middle income housing development in South Australia. Building and Environment; Volume 75, 19-29, ISSN 0360-1323.

Solar online Australia. Wind turbines. Retrieved May 2015. Available on: https://www.solaronline.com.au/wind-turbines.html.

Solar retrofit for weatherization and remodel. Retrieved March 2014. Available on: http://www.pasolar.ncat.org/lesson02.php

Sourbron, M., Helsen, L. (2011). Evaluation of adaptive thermal comfort models in moderate climates and their impact on energy use in office buildings, Energy and Buildings; Volume 43, Issues 2–3, 423-432, ISSN 0378-7788.

Spanos, I., Simons, M., Holmes, K. (2005). Cost savings by application of passive solar heating. Structural Survey; 23(2):111e30.

Sproul, A., (2012). Lecture notes from SOLA3010 / 9009 University of New South Wales – Topic: Climate and Passive Solar A. Prof. A.B. Sproul.

Stein, J., Meier, A. (2000). Accuracy of home energy rating systems. Energy; 25 339–354.

Strachan, P. (2011). Validation of dynamic thermal simulation programs. International workshop: whole building testing, evaluation and modelling for energy assessment. Lyngby, Denmark.

Sydney weather. Climate statistics for Australian locations. Bureau of Meteorology. Retrieved February 2015.

Taiwan Solar Energy, available on: http://www.twsolarenergy.com/tc/TSE_newenergy-2-sp.html

Tan, G., & Glicksman, L. (2005). Application of integrating multi-zone model with CFD simulation to natural ventilation prediction. Energy and Buildings; 37(10), 1049-1057.

Terés-Zubiaga, J., Martín, K., Erkoreka, A., Sala, J. (2013). Field assessment of thermal behaviour of social housing apartments in Bilbao, Northern Spain. Energy and Buildings; Volume 67, 118-135, ISSN 0378-7788.

The engineering toolbox. Air Properties. Retrieved May 2015. Available on: http://www.engineeringtoolbox.com/air-properties-d_156.html.

The University of Hong Kong. MEBS6006 Environmental Services. PsychroATM Chart. Retrieved April 2015. Available on: http://www.mech.hku.hk/bse/MEBS6006/psychart-cibse.gif.

The University of Texas at Austin. Factor Formulas. Department of Mechanical Engineering and Faculty Innovation. Centre Cockrell School of Engineering. Retrieved May 2015. Available on: http://www.me.utexas.edu/~me353/lessons/S2_Evaluation/L02_Equivalence/factor_formulas.html

The World Commission on Environment and Development. (1987a). Our Common Future (the 'Brundtland Commission report').

Toe, D., Kubota, T. (2013). Development of an adaptive thermal comfort equation for naturally ventilated buildings in hot–humid climates using ASHRAE RP-884 database.Frontiers of Architectural Research; Volume 2, Issue 3, 278-291, ISSN 2095-2635.

Tyler, H., Stefano, S., Alberto, P., Dustin, M., Kyle, S. (2013) CBE Thermal Comfort Tool. Center for the Built Environment, University of California Berkeley. Retrieved April 2014. Available on: http://cbe.berkeley.edu/comforttool/

U.S. Dept. of Energy. (2008). Energy Efficiency & Renewable Energy. Buildings Energy Data Book.

UNIDO. (2011). United Nations Industrial Development Organization. Industrial Development Report .Industrial energy efficiency for sustainable wealth creation capturing environmental, economic and social dividends. Retrieved November 2014. Available on: http://www.onu.org.br/rio20/img/2012/01/UNIDO_FULL_REPORT_EBOOK.pdf.

Unique earth. Rammed Earth construction. Retrieved April 2015. Available on: http://www.uniqueearth.com.au/.

USGCRP. (2009). Global Climate Change Impacts in the United States. A report of the U.S. Global Change Research Program.

USGCRP. (2013). National Climate Assessment and Development Advisory Committee (NACDAC) Report. US Global Change Research Program. Retrieved April 2014. Available on: http://ncadac.globalchange.gov.

Van der, Linden, A., C., Boerstra, A., C., Raue, A., K., Kurvers, S., R., de Dear, R., J. (2006). Adaptive temperature limits: A new guideline in The Netherlands: A new approach for the assessment of building performance with respect to thermal indoor climate. Energy and Buildings; Volume 38, Issue 1, 8-17, ISSN 0378-7788.

Wagner, E., Gossauer, C., Moosmann, et al. (2007). Thermal comfort and workplace occupant satisfaction—results of field studies in German low energy office buildings. Energy and Buildings; 39 (7) 758–769.

Walton, G., N. (1983). Thermal Analysis Research Program Reference Manual. NBSSIR 83-2655. National Bureau of Standards; p. 21.

Wang, L., & Wong, N. H. (2009). Coupled simulations for naturally ventilated rooms between building simulation (BS) and computational fluid dynamics (CFD) for better prediction of indoor thermal environment. Building and Environment; 44(1), 95-112.

Wang, S., Yan, C., Xiao, F. (2012). Quantitative energy performance assessment methods for existing buildings. Energy and Buildings; Volume 55, 873-888, ISSN 0378-7788.

Wang, X., Chen, D., Ren, Z. (2010). Assessment of climate change impact on residential building heating and cooling energy requirement in Australia. Building and Environment; 45 663–1682.

Wang, Z., Zhang, L., Zhao, J., He, Y. (2010). Thermal comfort for naturally ventilated residential buildings in Harbin. Energy and Buildings; Volume 42, Issue 12, 2406-2415, ISSN 0378-7788.

Weather in Perth. (2010). Australian tourism website.. Retrieved April 2015. Available on: http://www.australia.com/en/facts/weather/perth-weather.html

Wind power program. Power curve. Retrieved April 2014. Available on: http://www.wind-power-program.com/popups/powercurve.htm

Window Sash, Window Sash Picture, available on: http://windowsashokosh.blogspot.com.au/2015/04/window-sash-picture.html

Wong, N., H., Feriadi, H., P.,Y., Lim, et al. (2002). Thermal comfort evaluation of naturally ventilated public housing in Singapore. Building and Environment; 37 (12).

Wong, N., H., S., S., Khoo. (2003). Thermal comfort in classrooms in the tropics. Energy and Buildings; 35 (4) 337–351.

Worldwatch Institute. (2011). A Building Revolution: How Ecology and Health Concerns Are Transforming Construction. Retrieved April 2014. Available on: http://www.worldwatch.org/node/866 . Accessed. 5/10/2013.

X.,J., Ye, Z.,P., Zhou, Z.,W., Lian, et al. (2006). Field study of thermal environment and adaptive model in Shanghai. Indoor Air; 16 (4) 320–326.

Y., Z., Xia, R., Y., Zhao, Y., Jiang. (1999). Thermal comfort in naturally ventilated houses in Beijing. HV&AC; 29 (2) 1–5.

Yi, Y., K., & Feng, N. (2013). Dynamic integration between building energy simulation (BES) and computational fluid dynamics (CFD) simulation for building exterior surface. In Building Simulation. Springer Berlin Heidelberg; Vol. 6, No. 3, pp. 297-308.

Young, Hugh, D. (1992). University Physics. Table 15-5. Values for diamond and silica aerogel from CRC Handbook of Chemistry; 7th Ed. Addison Wesley.

Your Home. Rammed Earth 300mm. Retrieved April 2014. Available on: http://www.yourhome.gov.au/materials/rammed-earth.

Your solar energy home. Retrieved April 2014. Available on: http://www.your-solar-energy-home.com/Solar-hot-air.html

Zhai, Z. (2006). Application of Computational Fluid Dynamics in Building Design: Aspects and Trends. Indoor and Built Environment; 15; 305.

Zhai, Z., Chen, Q. (2003). Solution characters of iterative coupling between energy simulation and CFD programs. Energy and Buildings; 35 (5) 493–505.

Zhai, Z., Chen, Q. (2006). Sensitivity analysis and application guides for integrated building energy and CFD simulation. Energy and Buildings; 38 1060–1068.

Zhai, Z., Chen, Q., Haves, P., Klems, H. (2002). On approaches to couple energy simulation and computational fluid dynamics programs. Building and Environment; 37 857–864.

Zhai, Z., Chen, Q., Klems, J., H., & Haves, P. (2001). Strategies for coupling energy simulation and computational fluid dynamics programs. Lawrence Berkeley National Laboratory.

Zhai, Z., J., & Chen, Q., Y. (2005). Performance of coupled building energy and CFD simulations. Energy and buildings; 37(4), 333-344.

Zhai, Z., J., Zhang, Z., Zhang, W., & Chen, Q., Y. (2007). Evaluation of various turbulence models in predicting airflow and turbulence in enclosed environments by CFD: Part 1—Summary of prevalent turbulence models. Hvac&R Research; 13(6), 853-870.

Zhai, Z., Q., Chen, P., Haves, J., H., Klems. (2002). On approaches to couple energy simulation and CFD programs. Building and Environment; Vol. 37.

Zhu, L., Hurt, R., Correia, D., Boehm, R. (2009). Detailed energy saving performance analyses, on thermal mass walls demonstrated in a zero energy house. Energy and Buildings; 41 303e310.

Appendix A. Thermocouple and heat flux layout in all modules (Page et al. 2011).

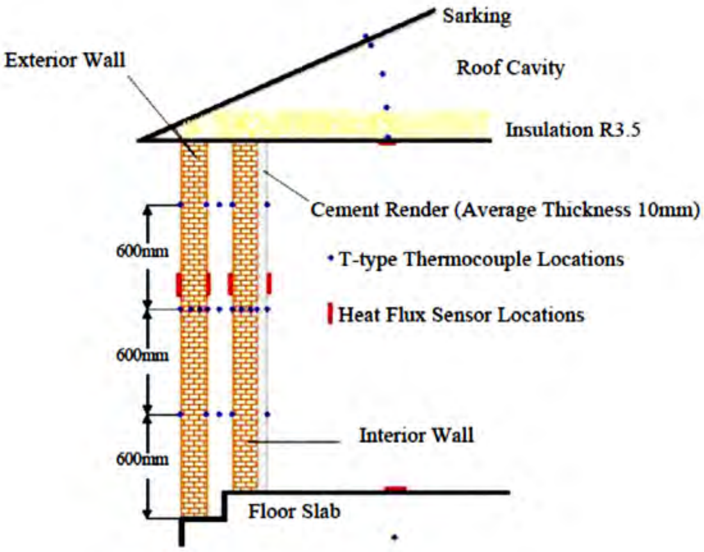

Figure A1. Cavity brick module

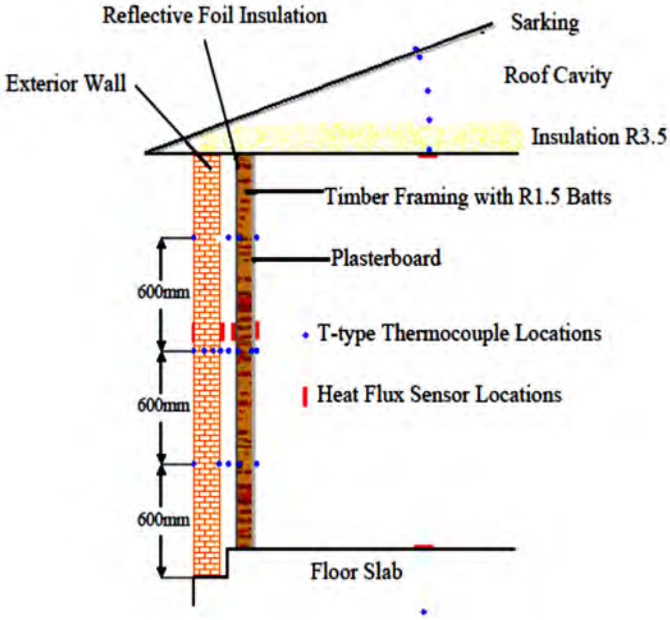

Figure A2. Insulated brick veneer module.

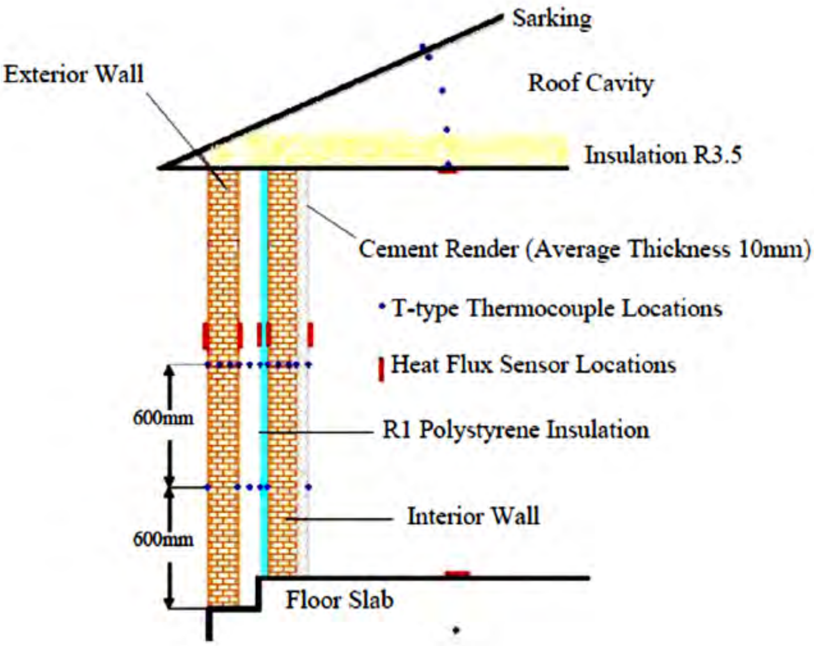

Figure A3. Insulated cavity brick module

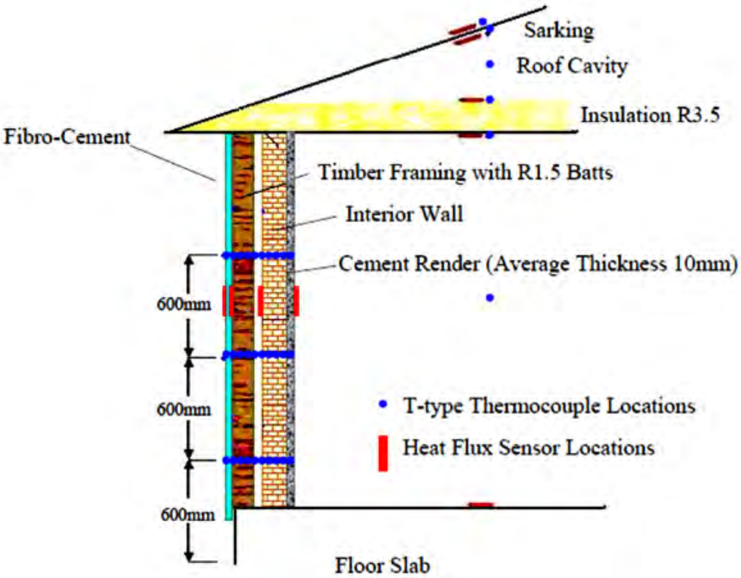

Figure A4. Insulated reverse brick veneer module

Appendix B. Western Australia house layout

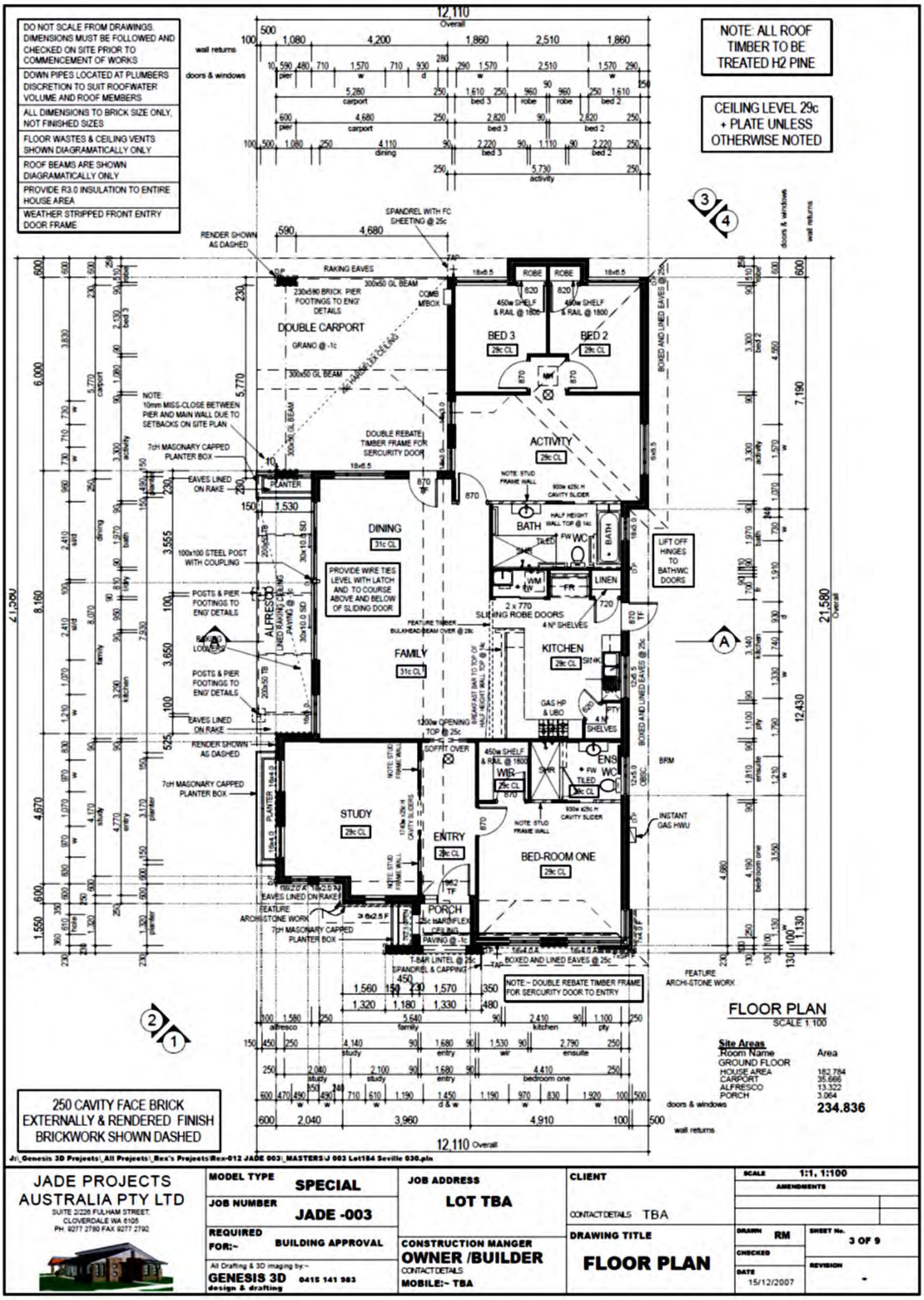

Appendix C. Construction materials and sizes taken from AccuRate final report

AccuRate Sustainability V2.3.3.13 SP1

Nationwide House Energy Rating Scheme

Project Name: WA		
File Name: C:\literature review\PhD\WA House\Aiman\AccuRate\WA new base desing.PRO		
Postcode: 6112	**Climate Zone:** 47	**Exposure:** Suburban
Client Name: verdant Circuit, Armadale WA 6112		
Site Address:		
Design Option: Base Design		
Date: 02/08/2015	**Time:** 20:21:02	**Page:** 1

Construction details: External Walls		
Description: Cavity Brick (R1.5 polystyrene) + plasterboard		
External colour: Medium	**Internal colour:** Medium	**Area:** 159.9 m²
External absorptance (%): 50	**Internal absorptance (%):** 50	
Layer	**Material**	**Thickness (mm)**
1	Brickwork: generic extruded clay brick (typical density)	110
2	Air gap vertical 17-30 mm (20 nominal) unventilated non-reflective (0.9/0.9; E = 0.82)	20
3	Polyester or polyester/wool blanket: R4.0)	180
4	Brickwork: generic extruded clay brick (typical density)	110
5	Plasterboard	10

Description: Fibro-cement (uninsulated)		
External colour: Medium	**Internal colour:** Medium	**Area:** 19.8 m²
External absorptance (%): 50	**Internal absorptance (%):** 50	
Layer	**Material**	**Thickness (mm**
1	Fibre-cement sheet (compressed)	6
2	Air gap vertical 31-65 mm (40 nominal) unventilated non-reflective (0.9/0.9; E = 0.82)	40
3	Plasterboard	10

Construction details: Windows		
Description: ALM-006-01 A Aluminium B DG Argon Fill Clear-Clear		
Manufacturer: DEFAULTS		
Version: 2.3.3.13.0.9	**Expiry Date:** 15/06/2019	
System U-value (NFRC): 4.50	**SHGC (NFRC):** 0.61	**Area:** 33.2 m²
Frame type: Custom	**Frame colour:** Medium	
Frame fraction (%): 28	**Frame absorptance (%):** 50	
Layer	**Material**	**Thickness (mm**
1	Glass	4
2	Glazing air gap (generic)	12
3	Glass	4

AccuRate Sustainability V2.3.3.13 SP1

Nationwide House Energy Rating Scheme

Project Name: WA		
File Name: C:\literature review\PhD\WA House\Aiman\AccuRate\WA new base desing.PRO		
Postcode: 6112	**Climate Zone:** 47	**Exposure:** Suburban
Client Name: verdant Circuit, Armadale WA 6112		
Site Address:		
Design Option: Base Design		
Date: 02/08/2015	**Time:** 20:21:02	**Page:** 2

Construction details: Floor/Ceilings

Description: Concrete Slab 100 mm: cork tiles/bare		
Top colour: Medium	**Bottom colour:** Medium	**Area:** 168.4 m²
Top absorptance (%): 50	**Bottom absorptance (%):** 50	

Layer	Material	Thickness (mm
1	Cork tile	6
2	Concrete: standard (2400 kg/m³)	100

Description: Plasterboard 13 mm + R2.5 bulk insulation		
Top colour: Paint: white	**Bottom colour:** Medium	**Area:** 163.5 m²
Top absorptance (%): 23	**Bottom absorptance (%):** 50	

Layer	Material	Thickness (mm
1	Polystyrene expanded: R4.0	156
2	Plasterboard	13

Construction details: Internal Walls

Description: Rammed earth 300 mm		
First colour: Paint: black	**Last colour:** Paint: black	**Area:** 100.1 m²
First absorptance (%): 96	**Last absorptance (%):** 96	

Layer	Material	Thickness (mm
1	Rammed earth	300

Construction details: Roofs

Description: Tiles (concrete)		
External colour: Paint: black	**Internal colour:** Paint: black	**Area:** 210.4 m²
External absorptance (%): 96	**Internal absorptance (%):** 96	

Layer	Material	Thickness (mm
1	Roof tiles (concrete)	20

	AccuRate Sustainability V2.3.3.13 SP1 Nationwide House Energy Rating Scheme	

Project Name: WA		
File Name: C:\literature review\PhD\WA House\Aiman\AccuRate\WA new base desing.PRO		
Postcode: 6112	**Climate Zone:** 47	**Exposure:** Suburban
Client Name: verdant Circuit, Armadale WA 6112		
Site Address:		
Design Option: Base Design		
Date: 02/08/2015	**Time:** 20:21:02	**Page:** 3

Habitable zones

Name	Type	Volume (m³)	Floor height (m)	Ceiling height above floor (m)	Heated	Cooled
BD1	Bedroom	66.9	0.1	2.5	Y	Y
BD2	Bedroom	24.1	0.1	2.5	Y	Y
BD3	Bedroom	24.1	0.1	2.5	Y	Y
Activity	Living	47.1	0.1	2.5	Y	Y
BW	Other (daytime usage)	19.6	0.1	2.5	N	N
Entry	Other (daytime usage)	20.0	0.1	2.5	Y	Y
Office	Other (daytime usage)	46.5	0.1	2.5	Y	Y
Family/Dining	Living/Kitchen	158.4	0.1	2.5	Y	Y

Habitable zones (continued)

Name	Chimneys		Wall/Ceiling vents	Exhaust fans		Vented downlights	Unflued gas heaters	Ceiling fans	Type
	U/S	S		U/S	S				
BD1	0	0	0	0	0	0	0	0	-
BD2	0	0	0	0	0	0	0	0	-
BD3	0	0	0	0	0	0	0	0	-
Activity	0	0	0	0	0	0	0	0	-
BW	0	0	0	0	0	0	0	0	-
Entry	0	0	0	0	0	0	0	0	-
Office	0	0	0	0	0	0	0	0	-
Family/Dining	0	0	0	0	0	0	0	0	-

Roofspace zones

Name	Volume (m³)	Reflective	Sarking	Roof surface	Openness
Attic	198.0	N	Sarked	Discontinuous	

	AccuRate Sustainability V2.3.3.13 SP1 Nationwide House Energy Rating Scheme	
Project Name: WA		
File Name: C:\literature review\PhD\WA House\Aiman\AccuRate\WA new base desing.PRO		
Postcode: 6112	**Climate Zone:** 47	**Exposure:** Suburban
Client Name: verdant Circuit, Armadale WA 6112		
Site Address:		
Design Option: Base Design		
Date: 02/08/2015	**Time:** 20:21:02	**Page:** 4

BD1: External walls main data

Wall	Construction	Azi (deg.)	L (m)	H (m)	Area (gross) (m²)	Area (net) (m²)	Fixed shade	Opening (m²)	Opening Type
1	Cavity Brick (R1.5 polystyrene) + plaste	90	6.18	2.49	15.39	14.15	600	0.00	Controlled
2	Cavity Brick (R1.5 polystyrene) + plaste	180	5.00	2.49	12.45	9.46	100	0.00	Controlled
3	Cavity Brick (R1.5 polystyrene) + plaste	270	1.36	2.49	3.39	3.39	2000	0.00	Controlled

BD1: External walls horizontal shading data

		Eaves				Other fixed shading				
Wall	Name	Projection (m)	Horizontal Offset (m)	Vertical Offset (m)	Length (m)	Projection (m)	Horizontal Offset (m)	Vertical Offset (m)	Length (m)	Monthly blocking factors (%)
1	600	0.60	0.00	499.00	999.00	0.00	0.00	0.00	0.00	100,100,100,100,100,100,100,100,100,100,100,100
2	100	0.10	0.00	499.00	999.00	0.00	0.00	0.00	0.00	100,100,100,100,100,100,100,100,100,100,100,100
3	2000	2.00	0.00	499.00	999.00	0.00	0.00	0.00	0.00	100,100,100,100,100,100,100,100,100,100,100,100

BD1: Windows in walls

Wall	Window Name	Type	Construction		Azi. (deg.)	H (m)	W (m)	Area (m²)
1	Ensuite Window	Awning	ALM-006-01 A	Aluminium B DG Argon Fill Clear-Clear	90	1.03	1.20	1.24
2		Awning	ALM-006-01 A	Aluminium B DG Argon Fill Clear-Clear	180	1.54	0.97	1.49
2	Bed 1 Window Left	Awning	ALM-006-01 A	Aluminium B DG Argon Fill Clear-Clear	180	1.54	0.97	1.49

BD1: Windows in walls (continued)

Wall	Window Name	Indoor covering	Outdoor covering	Fixed shade	HH (m)	HO (m)	Opening (%)	Weather stripped	Gap size
1	Ensuite Window	Hollandblinds	None		2.20	0.00	45.00	Y	
2		Hollandblinds	None	600	2.20	0.00	60.00	Y	
2	Bed 1 Window Left	Hollandblinds	None	600	2.20	0.00	60.00	Y	

BD1: Windows in wall horizontal shading data

			Eaves				Other fixed shading				
Wall	Window Name	Name	Projection (m)	Horizontal Offset (m)	Vertical Offset (m)	Length (m)	Projection (m)	Horizontal Offset (m)	Vertical Offset (m)	Length (m)	Monthly blocking factors (%)
2		600	0.60	0.00	499.00	999.00	0.00	0.00	0.00	0.00	100,100,100,100,100,100,
											100,100,100,100,100,100
2	Bed 1 Window Left	600	0.60	0.00	499.00	999.00	0.00	0.00	0.00	0.00	100,100,100,100,100,100,
											100,100,100,100,100,100

BD1: Internal walls

Wall	Construction	L (m)	H (m)	Area (gross) (m²)	Area (net) (m²)	Adjacent Zone	Opening (m²)	Opening Type
1	Rammed earth 300 mm	6.10	2.49	15.19	13.4	Entry	1.80	Controlled
2	Rammed earth 300 mm	4.40	2.49	10.96	11.0	Family/Dining	0.00	Controlled

BD1: Floors

Floor	Construction	Area (gross) (m²)	Area (net) (m²)	Under the floor	Edge Ins.	Opening (m²)	Opening Type
1	Concrete Slab 100 mm: cork tiles/bare	26.9	26.9	Ground		0.00	Controlled

BD1: Ceilings

Ceiling	Construction	Area (gross) (m²)	Area (net) (m²)	Above the ceiling	Opening (m²)	Opening Type
1	Plasterboard 13 mm + R2.5 bulk insulation	26.9	26.9	Attic	0.00	Controlled

	AccuRate Sustainability V2.3.3.13 SP1 Nationwide House Energy Rating Scheme	
Project Name: WA		
File Name: C:\literature review\PhD\WA House\Aiman\AccuRate\WA new base desing.PRO		
Postcode: 6112	**Climate Zone:** 47	**Exposure:** Suburban
Client Name: verdant Circuit, Armadale WA 6112		
Site Address:		
Design Option: Base Design		
Date: 02/08/2015	**Time:** 20:21:02	**Page:** 5

BD2: External walls main data

Wall	Construction	Azi (deg.)	L (m)	H (m)	Area (gross) (m²)	Area (net) (m²)	Fixed shade	Opening (m²)	Opening Type
1	Cavity Brick (R1.5 polystyrene) + plaste	180	3.40	2.49	8.47	8.47	600	0.00	Controlled
2	Cavity Brick (R1.5 polystyrene) + plaste	90	1.70	2.49	4.23	1.82	600	0.00	Controlled
3	Cavity Brick (R1.5 polystyrene) + plaste	180	0.60	2.49	1.49	1.49	1600	0.00	Controlled
4	Cavity Brick (R1.5 polystyrene) + plaste	90	1.10	2.49	2.74	2.74	100	0.00	Controlled

BD2: External walls horizontal shading data

		Eaves				Other fixed shading				
Wall	Name	Projection (m)	Horizontal Offset (m)	Vertical Offset (m)	Length (m)	Projection (m)	Horizontal Offset (m)	Vertical Offset (m)	Length (m)	Monthly blocking factors (%)
1	600	0.60	0.00	499.00	999.00	0.00	0.00	0.00	0.00	100,100,100,100,100,100,100,100,100,100,100,100
2	600	0.60	0.00	499.00	999.00	0.00	0.00	0.00	0.00	100,100,100,100,100,100,100,100,100,100,100,100
3	1600	1.60	0.00	499.00	999.00	0.00	0.00	0.00	0.00	100,100,100,100,100,100,100,100,100,100,100,100
4	100	0.10	0.00	499.00	999.00	0.00	0.00	0.00	0.00	100,100,100,100,100,100,100,100,100,100,100,100

BD2: Windows in walls

Wall	Window Name	Type	Construction	Azi. (deg.)	H (m)	W (m)	Area (m²)
2	Bed 2 Window	Sliding	ALM-006-01 A Aluminium B DG Argon Fill Clear-Clear	90	1.54	1.57	2.42

BD2: Windows in walls (continued)

Wall	Window Name	Indoor covering	Outdoor covering	Fixed shade	HH (m)	HO (m)	Opening (%)	Weather stripped	Gap size
2	Bed 2 Window	Hollandblinds	None		2.00	0.00	30.00	Y	

BD2: Internal walls

Wall	Construction	L (m)	H (m)	Area (gross) (m²)	Area (net) (m²)	Adjacent Zone	Opening (m²)	Opening Type
1	Rammed earth 300 mm	2.60	2.49	6.47	6.5	BD3	0.00	Controlled
2	Rammed earth 300 mm	2.80	2.49	6.97	5.2	Activity	1.80	Controlled

BD2: Floors

Floor	Construction	Area (gross) (m²)	Area (net) (m²)	Under the floor	Edge Ins.	Opening (m²)	Opening Type
1	Concrete Slab 100 mm: cork tiles/bare	9.8	9.8	Ground		0.00	Controlled

BD2: Ceilings

Ceiling	Construction	Area (gross) (m²)	Area (net) (m²)	Above the ceiling	Opening (m²)	Opening Type
1	Plasterboard 13 mm + R2.5 bulk insulation	9.8	9.8	Attic	0.00	Controlled

AccuRate Sustainability V2.3.3.13 SP1

Nationwide House Energy Rating Scheme

Project Name: WA		
File Name: C:\literature review\PhD\WA House\Aiman\AccuRate\WA new base desing.PRO		
Postcode: 6112	**Climate Zone:** 47	**Exposure:** Suburban
Client Name: verdant Circuit, Armadale WA 6112		
Site Address:		
Design Option: Base Design		
Date: 02/08/2015	**Time:** 20:21:02	**Page:** 6

BD3: External walls main data

Wall	Construction	Azi (deg.)	L (m)	H (m)	Area (gross) (m²)	Area (net) (m²)	Fixed shade	Opening (m²)	Opening Type
1	Cavity Brick (R1.5 polystyrene) + plaste	0	3.40	2.49	8.47	8.47	6800	0.00	Controlled
2	Cavity Brick (R1.5 polystyrene) + plaste	90	1.70	2.40	4.08	1.66	600	0.00	Controlled
3	Cavity Brick (R1.5 polystyrene) + plaste	0	0.60	2.49	1.49	1.49	6800	0.00	Controlled
4	Cavity Brick (R1.5 polystyrene) + plaste	90	1.10	2.49	2.74	2.74	100	0.00	Controlled

BD3: External walls horizontal shading data

		Eaves				Other fixed shading				
Wall	Name	Projection (m)	Horizontal Offset (m)	Vertical Offset (m)	Length (m)	Projection (m)	Horizontal Offset (m)	Vertical Offset (m)	Length (m)	Monthly blocking factors (%)
1	6800	6.80	0.00	499.00	999.00	0.00	0.00	0.00	0.00	100,100,100,100,100,100,100,100,100,100,100,100
2	600	0.60	0.00	499.00	999.00	0.00	0.00	0.00	0.00	100,100,100,100,100,100,100,100,100,100,100,100
3	6800	6.80	0.00	499.00	999.00	0.00	0.00	0.00	0.00	100,100,100,100,100,100,100,100,100,100,100,100
4	100	0.10	0.00	499.00	999.00	0.00	0.00	0.00	0.00	100,100,100,100,100,100,100,100,100,100,100,100

BD3: Windows in walls

Wall	Window Name	Type	Construction	Azi. (deg.)	H (m)	W (m)	Area (m²)
2	Bed 3 Window	Sliding	ALM-006-01 A Aluminium B DG Argon Fill Clear-Clear	90	1.54	1.57	2.42

BD3: Windows in walls (continued)

Wall	Window Name	Indoor covering	Outdoor covering	Fixed shade	HH (m)	HO (m)	Opening (%)	Weather stripped	Gap size
2	Bed 3 Window	Hollandblinds	None		2.00	0.00	30.00	Y	

BD3: Internal walls

Wall	Construction	L (m)	H (m)	Area (gross) (m²)	Area (net) (m²)	Adjacent Zone	Opening (m²)	Opening Type
1	Rammed earth 300 mm	2.60	2.49	6.47	6.5	BD2	0.00	Controlled
2	Rammed earth 300 mm	2.80	2.49	6.97	5.2	Activity	1.80	Controlled

BD3: Floors

Floor	Construction	Area (gross) (m²)	Area (net) (m²)	Under the floor	Edge Ins.	Opening (m²)	Opening Type
1	Concrete Slab 100 mm: cork tiles/bare	9.8	9.8	Ground		0.00	Controlled

BD3: Ceilings

Ceiling	Construction	Area (gross) (m²)	Area (net) (m²)	Above the ceiling	Opening (m²)	Opening Type
1	Plasterboard 13 mm + R2.5 bulk insulation	9.8	9.8	Attic	0.00	Controlled

	AccuRate Sustainability V2.3.3.13 SP1 Nationwide House Energy Rating Scheme	

Project Name: WA		
File Name: C:\literature review\PhD\WA House\Aiman\AccuRate\WA new base desing.PRO		
Postcode: 6112	**Climate Zone:** 47	**Exposure:** Suburban
Client Name: verdant Circuit, Armadale WA 6112		
Site Address:		
Design Option: Base Design		
Date: 02/08/2015	**Time:** 20:21:02	**Page:** 7

Activity: External walls main data

Wall	Construction	Azi (deg.)	L (m)	H (m)	Area (gross) (m²)	Area (net) (m²)	Fixed shade	Opening (m²)	Opening Type
1	Cavity Brick (R1.5 polystyrene) + plaste	0	3.40	2.49	8.47	7.67	600	0.00	Controlled
2	Cavity Brick (R1.5 polystyrene) + plaste	0	2.30	2.49	5.73	2.60	5200	0.00	Controlled
3	Cavity Brick (R1.5 polystyrene) + plaste	270	0.60	2.49	1.49	1.49	13600	0.00	Controlled

Activity: External walls horizontal shading data

		Eaves				Other fixed shading				
Wall	Name	Projection (m)	Horizontal Offset (m)	Vertical Offset (m)	Length (m)	Projection (m)	Horizontal Offset (m)	Vertical Offset (m)	Length (m)	Monthly blocking factors (%)
1	600	0.60	0.00	499.00	999.00	0.00	0.00	0.00	0.00	100,100,100,100,100,100,100,100,100,100,100,100
2	5200	5.20	0.00	499.00	999.00	0.00	0.00	0.00	0.00	100,100,100,100,100,100,100,100,100,100,100,100
3	13600	13.60	0.00	499.00	999.00	0.00	0.00	0.00	0.00	100,100,100,100,100,100,100,100,100,100,100,100

Activity: Windows in walls

Wall	Window Name	Type	Construction	Azi. (deg.)	H (m)	W (m)	Area (m²)
1	ActivityWindow	Awning	ALM-006-01 A Aluminium B DG Argon Fill Clear-Clear	0	0.51	1.57	0.80
2	ctivity Carport Windo w	Awning	ALM-006-01 A Aluminium B DG Argon Fill Clear-Clear	0	2.14	1.46	3.12

Activity: Windows in walls (continued)

Wall	Window Name	Indoor covering	Outdoor covering	Fixed shade	HH (m)	HO (m)	Opening (%)	Weather stripped	Gap size
1	ActivityWindow	Hollandblinds	None		2.20	0.00	45.00	Y	
2	ctivity Carport Windo w	Hollandblinds	None		2.20	0.00	30.00	Y	

Activity: Internal walls

Wall	Construction	L (m)	H (m)	Area (gross) (m²)	Area (net) (m²)	Adjacent Zone	Opening (m²)	Opening Type
1	Rammed earth 300 mm	2.80	2.49	6.97	5.2	BD2	1.80	Controlled
2	Rammed earth 300 mm	2.80	2.49	6.97	5.2	BD3	1.80	Controlled
3	Rammed earth 300 mm	4.00	2.49	9.96	8.2	BW	1.80	Controlled
4	Rammed earth 300 mm	2.00	2.49	4.98	3.2	Family/Dining	1.80	Controlled

Activity: Floors

Floor	Construction	Area (gross) (m²)	Area (net) (m²)	Under the floor	Edge Ins.	Opening (m²)	Opening Type
1	Concrete Slab 100 mm: cork tiles/bare	18.9	18.9	Ground		0.00	Controlled

Activity: Ceilings

Ceiling	Construction	Area (gross) (m²)	Area (net) (m²)	Above the ceiling	Opening (m²)	Opening Type
1	Plasterboard 13 mm + R2.5 bulk insulation	18.9	18.9	Attic	0.00	Controlled

AccuRate Sustainability V2.3.3.13 SP1

Nationwide House Energy Rating Scheme

Project Name: WA		
File Name: C:\literature review\PhD\WA House\Aiman\AccuRate\WA new base desing.PRO		
Postcode: 6112	**Climate Zone:** 47	**Exposure:** Suburban
Client Name: verdant Circuit, Armadale WA 6112		
Site Address:		
Design Option: Base Design		
Date: 02/08/2015	**Time:** 20:21:02	**Page:** 8

BW: External walls main data

Wall	Construction	Azi (deg.)	L (m)	H (m)	Area (gross) (m²)	Area (net) (m²)	Fixed shade	Opening (m²)	Opening Type
1	Cavity Brick (R1.5 polystyrene) + plaste	180	1.97	2.49	4.91	3.78	600	0.00	Controlled

BW: External walls horizontal shading data

		Eaves				Other fixed shading				
Wall	Name	Projection (m)	Horizontal Offset (m)	Vertical Offset (m)	Length (m)	Projection (m)	Horizontal Offset (m)	Vertical Offset (m)	Length (m)	Monthly blocking factors (%)
1	600	0.60	0.00	499.00	999.00	0.00	0.00	0.00	0.00	100,100,100,100,100,100,100,100,100,100,100,100

BW: Windows in walls

Wall	Window Name	Type	Construction	Azi. (deg.)	H (m)	W (m)	Area (m²)
1	Bath Window	Sliding	ALM-006-01 A Aluminium B DG Argon Fill Clear-Clear	180	1.54	0.73	1.12

BW: Windows in walls (continued)

Wall	Window Name	Indoor covering	Outdoor covering	Fixed shade	HH (m)	HO (m)	Opening (%)	Weather stripped	Gap size
1	Bath Window	Hollandblinds	None		2.20	0.00	30.00	Y	

BW: Internal walls

Wall	Construction	L (m)	H (m)	Area (gross) (m²)	Area (net) (m²)	Adjacent Zone	Opening (m²)	Opening Type
1	Rammed earth 300 mm	4.00	2.49	9.96	8.2	Activity	1.80	Controlled
2	Rammed earth 300 mm	2.00	2.49	4.98	5.0	Family/Dining	0.00	Controlled
3	Rammed earth 300 mm	4.00	2.49	9.96	10.0	Family/Dining	0.00	Controlled

BW: Floors

Floor	Construction	Area (gross) (m²)	Area (net) (m²)	Under the floor	Edge Ins.	Opening (m²)	Opening Type
1	Concrete Slab 100 mm: cork tiles/bare	8.3	8.3	Ground		0.00	Controlled

BW: Ceilings

Ceiling	Construction	Area (gross) (m²)	Area (net) (m²)	Above the ceiling	Opening (m²)	Opening Type
1	Plasterboard 13 mm + R2.5 bulk insulation	7.9	7.9	Attic	0.00	Controlled

	AccuRate Sustainability V2.3.3.13 SP1 Nationwide House Energy Rating Scheme	

Project Name: WA		
File Name: C:\literature review\PhD\WA House\Aiman\AccuRate\WA new base desing.PRO		
Postcode: 6112	**Climate Zone:** 47	**Exposure:** Suburban
Client Name: verdant Circuit, Armadale WA 6112		
Site Address:		
Design Option: Base Design		
Date: 02/08/2015	**Time:** 20:21:02	**Page:** 9

Entry: External walls main data

Wall	Construction	Azi (deg.)	L (m)	H (m)	Area (gross) (m²)	Area (net) (m²)	Fixed shade	Opening (m²)	Opening Type
1	Cavity Brick (R1.5 polystyrene) + plaste	270	1.68	2.49	4.18	3.39	1600	0.00	Controlled

Entry: External walls horizontal shading data

		Eaves				Other fixed shading				
Wall	Name	Projection (m)	Horizontal Offset (m)	Vertical Offset (m)	Length (m)	Projection (m)	Horizontal Offset (m)	Vertical Offset (m)	Length (m)	Monthly blocking factors (%)
1	1600	1.60	0.00	499.00	999.00	0.00	0.00	0.00	0.00	100,100,100,100,100,100,100,100,100,100,100,100

Entry: Windows in walls

Wall	Window Name	Type	Construction	Azi. (deg.)	H (m)	W (m)	Area (m²)
1	Front Glass	Awning	ALM-006-01 A Aluminium B DG Argon Fill Clear-Clear	270	2.19	0.36	0.79

Entry: Windows in walls (continued)

Wall	Window Name	Indoor covering	Outdoor covering	Fixed shade	HH (m)	HO (m)	Opening (%)	Weather stripped	Gap size
1	Front Glass	Hollandblinds	None		2.20	0.00	60.00	Y	

Entry: Internal walls

Wall	Construction	L (m)	H (m)	Area (gross) (m²)	Area (net) (m²)	Adjacent Zone	Opening (m²)	Opening Type
1	Rammed earth 300 mm	6.10	2.49	15.19	13.4	BD1	1.80	Controlled
2	Rammed earth 300 mm	4.77	2.49	11.88	8.3	Office	3.60	Controlled
3	Rammed earth 300 mm	1.70	2.49	4.23	2.4	Family/Dining	1.80	Controlled

Entry: Floors

Floor	Construction	Area (gross) (m²)	Area (net) (m²)	Under the floor	Edge Ins.	Opening (m²)	Opening Type
1	Concrete Slab 100 mm: cork tiles/bare	8.4	8.4	Ground		0.00	Controlled

Entry: Ceilings

Ceiling	Construction	Area (gross) (m²)	Area (net) (m²)	Above the ceiling	Opening (m²)	Opening Type
1	Plasterboard 13 mm + R2.5 bulk insulation	8.0	8.0	Attic	0.00	Controlled

	AccuRate Sustainability V2.3.3.13 SP1 Nationwide House Energy Rating Scheme	
Project Name: WA		
File Name: C:\literature review\PhD\WA House\Aiman\AccuRate\WA new base desing.PRO		
Postcode: 6112	**Climate Zone:** 47	**Exposure:** Suburban
Client Name: verdant Circuit, Armadale WA 6112		
Site Address:		
Design Option: Base Design		
Date: 02/08/2015	**Time:** 20:21:02	**Page:** 10

Office: External walls main data

Wall	Construction	Azi (deg.)	L (m)	H (m)	Area (gross) (m²)	Area (net) (m²)	Fixed shade	Opening (m²)	Opening Type
1	Cavity Brick (R1.5 polystyrene) + plaste	270	2.10	2.49	5.23	4.61	100	0.00	Controlled
2	Cavity Brick (R1.5 polystyrene) + plaste	90	0.60	2.49	1.49	1.49	2600	0.00	Controlled
3	Cavity Brick (R1.5 polystyrene) + plaste	270	2.04	2.40	4.90	3.39	600	0.00	Controlled
4	Cavity Brick (R1.5 polystyrene) + plaste	0	4.85	2.49	12.08	9.42	600	0.00	Controlled
5	Cavity Brick (R1.5 polystyrene) + plaste	90	1.10	2.49	2.74	2.74	14000	0.00	Controlled

Office: External walls horizontal shading data

		Eaves				Other fixed shading				
Wall	Name	Projection (m)	Horizontal Offset (m)	Vertical Offset (m)	Length (m)	Projection (m)	Horizontal Offset (m)	Vertical Offset (m)	Length (m)	Monthly blocking factors (%)
1	100	0.10	0.00	499.00	999.00	0.00	0.00	0.00	0.00	100,100,100,100,100,100,100,100,100,100,100,100
2	2600	2.60	0.00	499.00	999.00	0.00	0.00	0.00	0.00	100,100,100,100,100,100,100,100,100,100,100,100
3	600	0.60	0.00	499.00	999.00	0.00	0.00	0.00	0.00	100,100,100,100,100,100,100,100,100,100,100,100
4	600	0.60	0.00	499.00	999.00	0.00	0.00	0.00	0.00	100,100,100,100,100,100,100,100,100,100,100,100
5	14000	14.00	0.00	499.00	999.00	0.00	0.00	0.00	0.00	100,100,100,100,100,100,100,100,100,100,100,100

Office: Windows in walls

Wall	Window Name	Type	Construction	Azi. (deg.)	H (m)	W (m)	Area (m²)
1	Office Square Windows Fro nt 1	Awning	ALM-006-01 A Aluminium B DG Argon Fill Clear-Clear	270	0.51	0.61	0.31
1	Off ce Square Window Fro nt 2	Awning	ALM-006-01 A Aluminium B DG Argon Fill Clear-Clear	270	0.51	0.61	0.31
3	Front Office Left	Awning	ALM-006-01 A Aluminium B DG Argon Fill Clear-Clear	270	1.54	0.49	0.75
3	Front Office Right	Awning	ALM-006-01 A Aluminium B DG Argon Fill Clear-Clear	270	1.54	0.49	0.75
4	Office Side 1	Sliding	ALM-006-01 A Aluminium B DG Argon Fill Clear-Clear	0	1.37	0.97	1.33
4	Office Side2	Sliding	ALM-006-01 A Aluminium B DG Argon Fill Clear-Clear	0	1.37	0.97	1.33

Office: Windows in walls (continued)

Wall	Window Name	Indoor covering	Outdoor covering	Fixed shade	HH (m)	HO (m)	Opening (%)	Weather stripped	Gap size
1	Office Square Windows Fro nt 1	Hollandblinds	None		2.20	0.00	90.00	Y	
1	Off ce Square Window Fro nt 2	Hollandblinds	None		2.20	0.00	90.00	Y	
3	Front Office Left	Hollandblinds	None		2.20	0.00	60.00	Y	
3	Front Office Right	Hollandblinds	None		2.20	0.00	60.00	Y	
4	Office Side 1	Hollandblinds	None		2.20	0.00	45.00	Y	
4	Office Side2	Hollandblinds	None		2.20	0.00	45.00	Y	

Office: Internal walls

Wall	Construction	L (m)	H (m)	Area (gross) (m²)	Area (net) (m²)	Adjacent Zone	Opening (m²)	Opening Type
1	Rammed earth 300 mm	4.77	2.49	11.88	8.3	Entry	3.60	Controlled
2	Rammed earth 300 mm	3.05	2.49	7.59	7.6	Family/Dining	0.00	Controlled

Office: Floors

Floor	Construction	Area (gross) (m²)	Area (net) (m²)	Under the floor	Edge Ins.	Opening (m²)	Opening Type
1	Concrete Slab 100 mm: cork tiles/bare	22.7	22.7	Ground		0.00	Controlled

Office: Ceilings

Ceiling	Construction	Area (gross) (m²)	Area (net) (m²)	Above the ceiling	Opening (m²)	Opening Type
1	Plasterboard 13 mm + R2.5 bulk insulation	18.7	18.7	Attic	0.00	Controlled

	AccuRate Sustainability V2.3.3.13 SP1 Nationwide House Energy Rating Scheme	

Project Name: WA		
File Name: C:\literature review\PhD\WA House\Aiman\AccuRate\WA new base desing.PRO		
Postcode: 6112	**Climate Zone:** 47	**Exposure:** Suburban
Client Name: verdant Circuit, Armadale WA 6112		
Site Address:		
Design Option: Base Design		
Date: 02/08/2015	**Time:** 20:21:02	**Page:** 11

Family/Dining: External walls main data

Wall	Construction	Azi (deg.)	L (m)	H (m)	Area (gross) (m²)	Area (net) (m²)	Fixed shade	Opening (m²)	Opening Type
1	Cavity Brick (R1.5 polystyrene) + plaste	0	8.16	2.49	20.32	10.05	1600	0.00	Controlled
2	Cavity Brick (R1.5 polystyrene) + plaste	90	4.30	2.49	10.71	8.79	6600	0.00	Controlled
3	Cavity Brick (R1.5 polystyrene) + plaste	180	5.10	2.49	12.70	11.40	600	0.00	Controlled

Family/Dining: External walls horizontal shading data

		Eaves				Other fixed shading				
Wall	Name	Projection (m)	Horizontal Offset (m)	Vertical Offset (m)	Length (m)	Projection (m)	Horizontal Offset (m)	Vertical Offset (m)	Length (m)	Monthly blocking factors (%)
1	1600	1.60	0.00	499.00	999.00	0.00	0.00	0.00	0.00	100,100,100,100,100,100,100,100,100,100,100,100
2	6600	6.60	0.00	499.00	999.00	0.00	0.00	0.00	0.00	100,100,100,100,100,100,100,100,100,100,100,100
3	600	0.60	0.00	499.00	999.00	0.00	0.00	0.00	0.00	100,100,100,100,100,100,100,100,100,100,100,100

Family/Dining: Windows in walls

Wall	Window Name	Type	Construction		Azi. (deg.)	H (m)	W (m)	Area (m²)
1	Side Glass Doors	Sliding	ALM-006-01 A	Aluminium B DG Argon Fill Clear-Clear	0	2.14	4.80	10.27
2	Dining Carport	Sliding	ALM-006-01 A	Aluminium B DG Argon Fill Clear-Clear	90	1.20	1.60	1.92
3	Kitchen Window	Sliding	ALM-006-01 A	Aluminium B DG Argon Fill Clear-Clear	180	1.00	1.30	1.30

Family/Dining: Windows in walls (continued)

Wall	Window Name	Indoor covering	Outdoor covering	Fixed shade	HH (m)	HO (m)	Opening (%)	Weather stripped	Gap size
1	Side Glass Doors	Hollandblinds	None		2.20	0.00	20.00	Y	
2	Dining Carport	Hollandblinds	None		2.20	0.00	45.00	Y	
3	Kitchen Window	Hollandblinds	None		2.20	0.00	45.00	Y	

Family/Dining: Internal walls

Wall	Construction	L (m)	H (m)	Area (gross) (m²)	Area (net) (m²)	Adjacent Zone	Opening (m²)	Opening Type
1	Rammed earth 300 mm	4.40	2.49	10.96	11.0	BD1	0.00	Controlled
2	Rammed earth 300 mm	2.00	2.49	4.98	3.2	Activity	1.80	Controlled
3	Rammed earth 300 mm	2.00	2.49	4.98	5.0	BW	0.00	Controlled
4	Rammed earth 300 mm	4.00	2.49	9.96	10.0	BW	0.00	Controlled
5	Rammed earth 300 mm	1.70	2.49	4.23	2.4	Entry	1.80	Controlled
6	Rammed earth 300 mm	3.05	2.49	7.59	7.6	Office	0.00	Controlled

Family/Dining: Floors

Floor	Construction	Area (gross) (m²)	Area (net) (m²)	Under the floor	Edge Ins.	Opening (m²)	Opening Type
1	Concrete Slab 100 mm: cork tiles/bare	63.6	63.6	Ground		0.00	Controlled

Family/Dining: Ceilings

Ceiling	Construction	Area (gross) (m²)	Area (net) (m²)	Above the ceiling	Opening (m²)	Opening Type
1	Plasterboard 13 mm + R2.5 bulk insulation	63.6	63.6	Attic	0.00	Controlled

	AccuRate Sustainability V2.3.3.13 SP1 Nationwide House Energy Rating Scheme	
Project Name: WA		
File Name: C:\literature review\PhD\WA House\Aiman\AccuRate\WA new base desing.PRO		
Postcode: 6112	**Climate Zone:** 47	**Exposure:** Suburban
Client Name: verdant Circuit, Armadale WA 6112		
Site Address:		
Design Option: Base Design		
Date: 02/08/2015	**Time:** 20:21:02	**Page:** 12

Attic: External walls main data

Wall	Construction	Azi (deg.)	L (m)	H (m)	Area (gross) (m²)	Area (net) (m²)	Fixed shade	Opening (m²)	Opening Type
1	Fibro-cement(uninsulated)	270	6.30	1.15	7.24	7.24	100	0.00	Controlled
2	Fibro-cement(uninsulated)	0	15.10	0.50	7.55	7.55	600	0.00	Controlled
3	Fibro-cement(uninsulated)	270	5.60	0.90	5.04	5.04	100	0.00	Controlled

Attic: External walls horizontal shading data

		Eaves				Other fixed shading				
Wall	Name	Projection (m)	Horizontal Offset (m)	Vertical Offset (m)	Length (m)	Projection (m)	Horizontal Offset (m)	Vertical Offset (m)	Length (m)	Monthly blocking factors (%)
1	100	0.10	0.00	499.00	999.00	0.00	0.00	0.00	0.00	100,100,100,100,100,100,100,100,100,100,100,100
2	600	0.60	0.00	499.00	999.00	0.00	0.00	0.00	0.00	100,100,100,100,100,100,100,100,100,100,100,100
3	100	0.10	0.00	499.00	999.00	0.00	0.00	0.00	0.00	100,100,100,100,100,100,100,100,100,100,100,100

Attic: Floors

Floor	Construction	Area (gross) (m²)	Area (net) (m²)	Under the floor	Edge Ins.	Opening (m²)	Opening Type
1	Plasterboard 13 mm + R2.5 bulk insulation	18.9	18.9	Activity		0.00	Controlled
2	Plasterboard 13 mm + R2.5 bulk insulation	7.9	7.9	BW		0.00	Controlled
3	Plasterboard 13 mm + R2.5 bulk insulation	26.9	26.9	BD1		0.00	Controlled
4	Plasterboard 13 mm + R2.5 bulk insulation	8.0	8.0	Entry		0.00	Controlled
5	Plasterboard 13 mm + R2.5 bulk insulation	18.7	18.7	Office		0.00	Controlled
6	Plasterboard 13 mm + R2.5 bulk insulation	63.6	63.6	Family/Dining		0.00	Controlled
7	Plasterboard 13 mm + R2.5 bulk insulation	9.8	9.8	BD3		0.00	Controlled
8	Plasterboard 13 mm + R2.5 bulk insulation	9.8	9.8	BD2		0.00	Controlled

Attic: Roofs

Roof	Construction	Area (gross) (m²)	Area (net) (m²)	Azi (deg.)	Pitch (deg.)	Exposure
1	Tiles (concrete)	116.30	116.30	180	20	Normal
2	Tiles (concrete)	15.30	15.30	90	20	Normal
3	Tiles (concrete)	78.80	78.80	0	18	Normal

AccuRate Sustainability V2.3.3.13 SP1

Nationwide House Energy Rating Scheme

Project Name: WA		
File Name: C:\literature review\PhD\WA House\Aiman\AccuRate\WA new base desing.PRO		
Postcode: 6112	**Climate Zone:** 47	**Exposure:** Suburban
Client Name: verdant Circuit, Armadale WA 6112		
Site Address:		
Design Option: Base Design		
Date: 02/08/2015	**Time:** 20:21:02	**Page:** 13

Shading Schemes

	Eaves				Other fixed shading				
Name	Projection (m)	Vert Offset (m)	Horiz Offset (m)	Length (m)	Projection (m)	Vert Offset (m)	Horiz Offset (m)	Length (m)	Monthly blocking factors (%)
600	0.60	0.00	499.00	999.00	0.00	0.00	0.00	0.00	100,100,100,100,100,100,100,100,100,100,100,10(
5200	5.20	0.00	499.00	999.00	0.00	0.00	0.00	0.00	100,100,100,100,100,100,100,100,100,100,100,10(
6600	6.60	0.00	499.00	999.00	0.00	0.00	0.00	0.00	100,100,100,100,100,100,100,100,100,100,100,10(
100	0.10	0.00	499.00	999.00	0.00	0.00	0.00	0.00	100,100,100,100,100,100,100,100,100,100,100,10(
1600	1.60	0.00	499.00	999.00	0.00	0.00	0.00	0.00	100,100,100,100,100,100,100,100,100,100,100,10(
6800	6.80	0.00	499.00	999.00	0.00	0.00	0.00	0.00	100,100,100,100,100,100,100,100,100,100,100,10(
13600	13.60	0.00	499.00	999.00	0.00	0.00	0.00	0.00	100,100,100,100,100,100,100,100,100,100,100,10(
2000	2.00	0.00	499.00	999.00	0.00	0.00	0.00	0.00	100,100,100,100,100,100,100,100,100,100,100,10(
2600	2.60	0.00	499.00	999.00	0.00	0.00	0.00	0.00	100,100,100,100,100,100,100,100,100,100,100,10(
14000	14.00	0.00	499.00	999.00	0.00	0.00	0.00	0.00	100,100,100,100,100,100,100,100,100,100,100,10(

Ventilation

Footprint: vertical dimension (m)	Footprint: horizontal dimension (m)	Azimuth of highlighted facade (degrees)	Insect screens
21.6	12.1	0	N

Appendix D. Sensors location in Western Australia house.

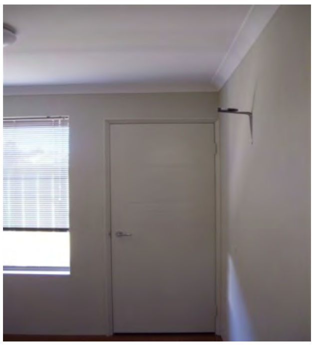

Figure D1. Bedroom 3

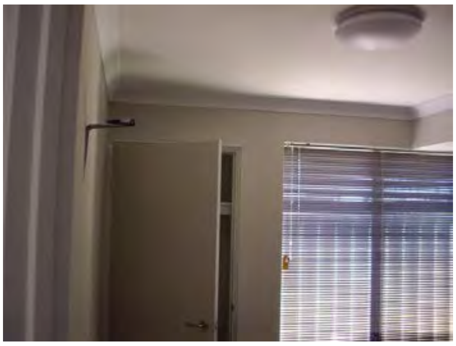

Figure D2. Office

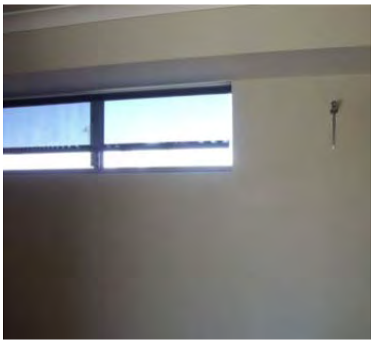

Figure D3. Family room

Figure D4. Kitchen

Figure D5. Bedroom 1

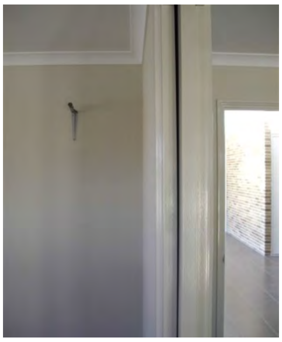

Figure D6. Bedroom 2

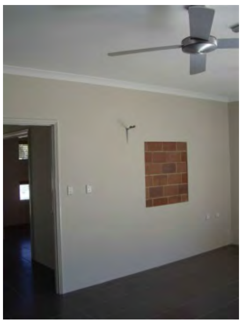

Figure D7. Activity room

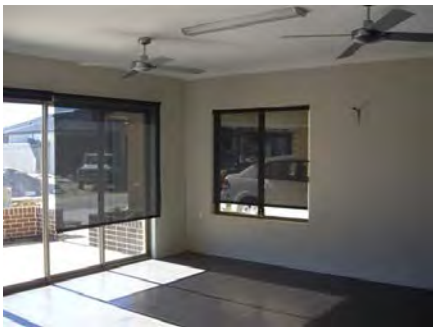

Figure D8. Meals room

Appendix E; Monthly CFD results and the real data for the InsBV module from Feb 2012 to Jan 2013 (Note; the data for December and most of January 2013 are missing).

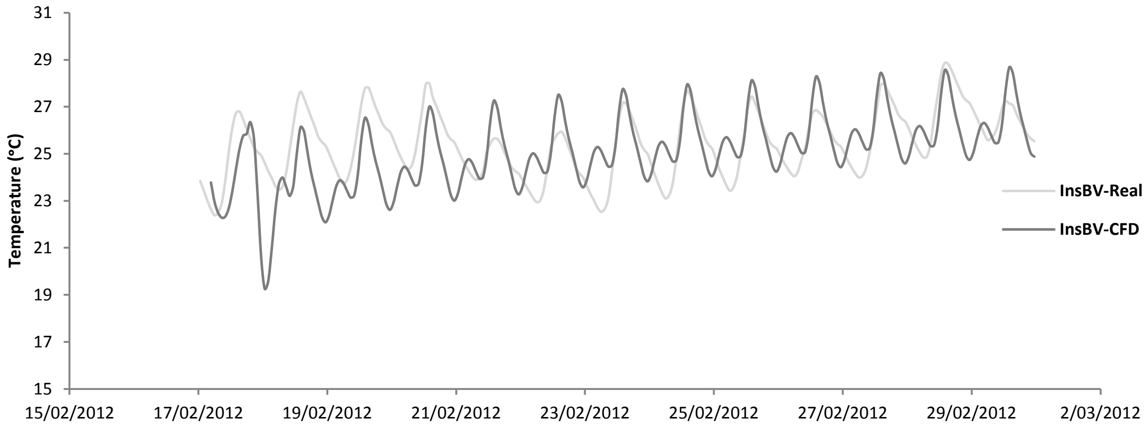

Figure E1. Monthly CFD results and the real data for the InsBV module for February 2012.

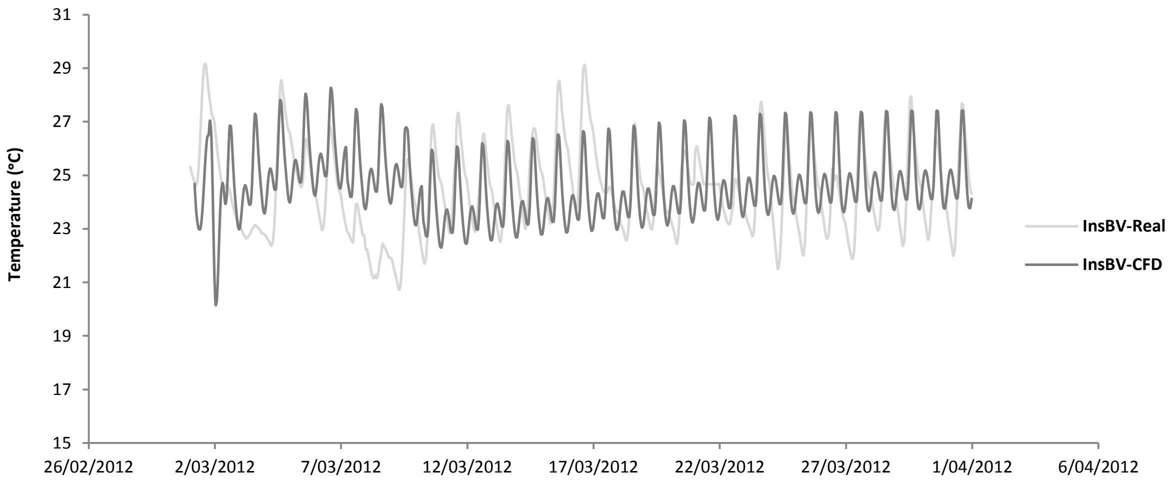

Figure E2. Monthly CFD results and the real data for the InsBV module for March 2012.

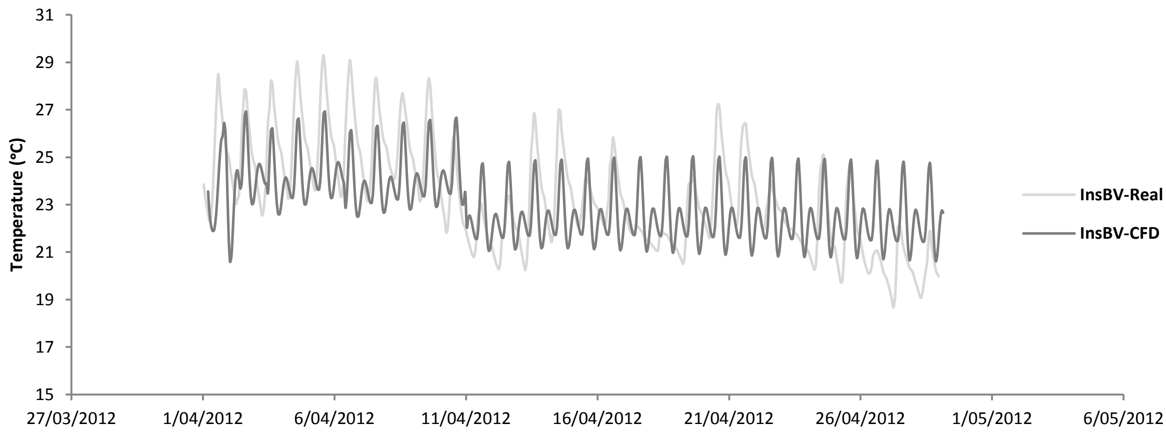

Figure E3. Monthly CFD results and the real data for the InsBV module for April 2012.

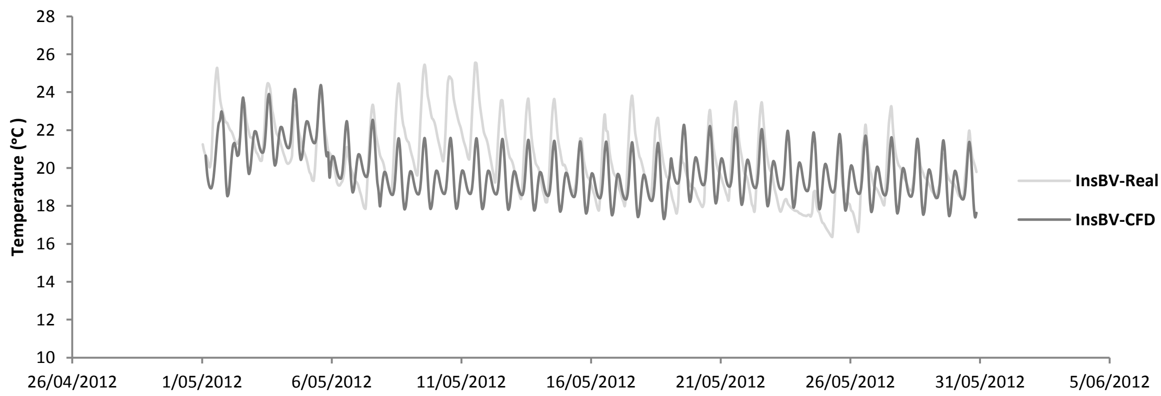

Figure E4. Monthly CFD results and the real data for the InsBV module for May 2012.

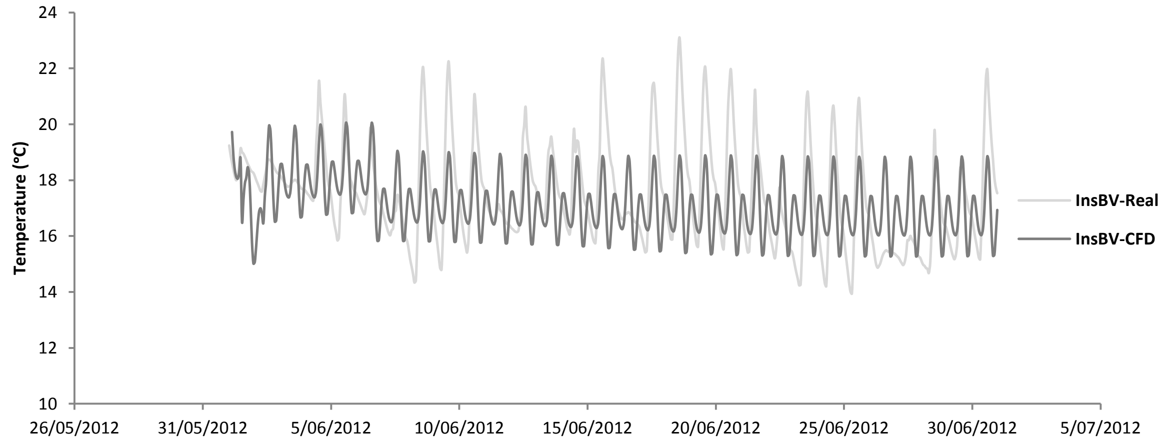

Figure E5. Monthly CFD results and the real data for the InsBV module for June 2012.

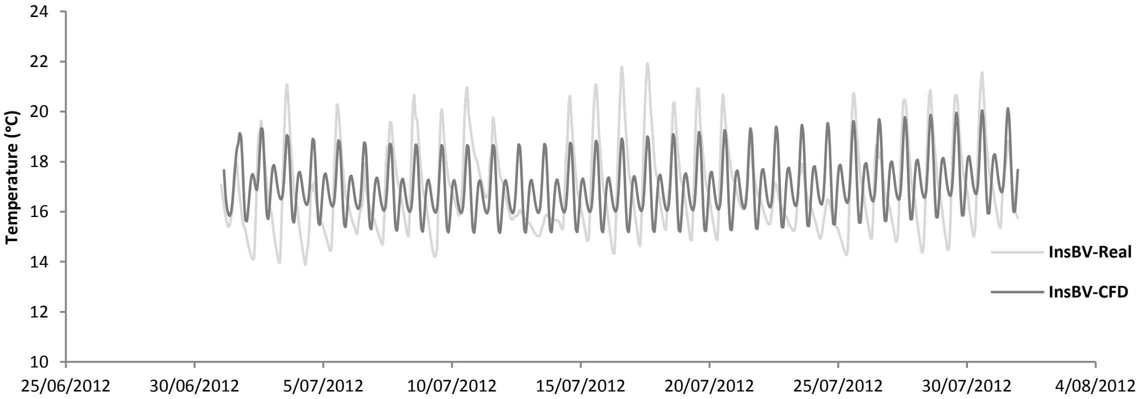

Figure E6. Monthly CFD results and the real data for the InsBV module for July 2012.

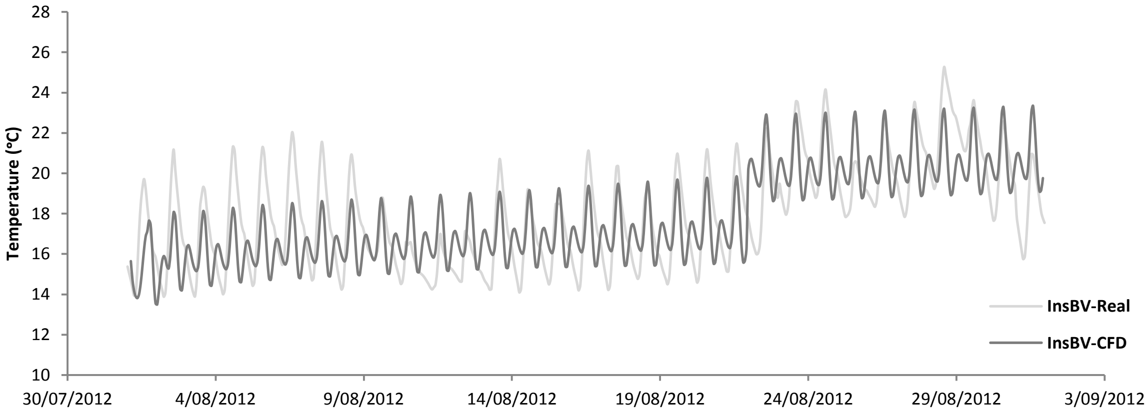

Figure E7. Monthly CFD results and the real data for the InsBV module for August 2012.

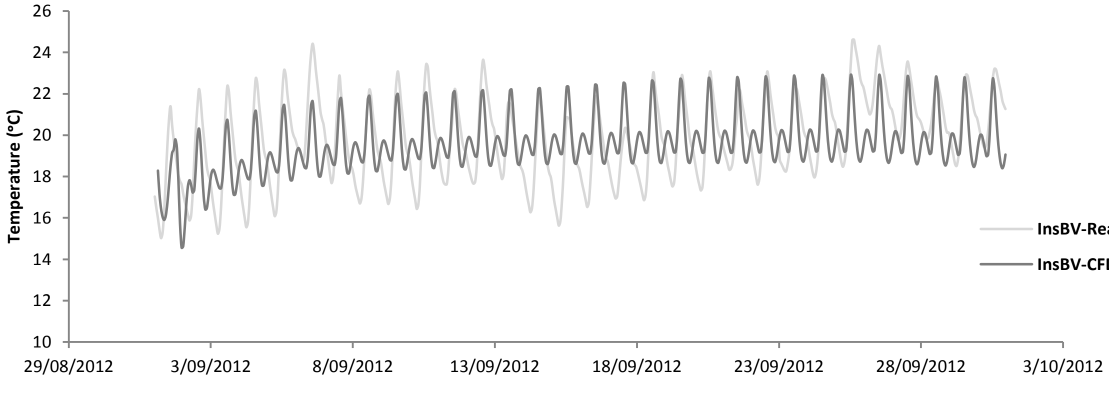

Figure E8. Monthly CFD results and the real data for the InsBV module for September 2012.

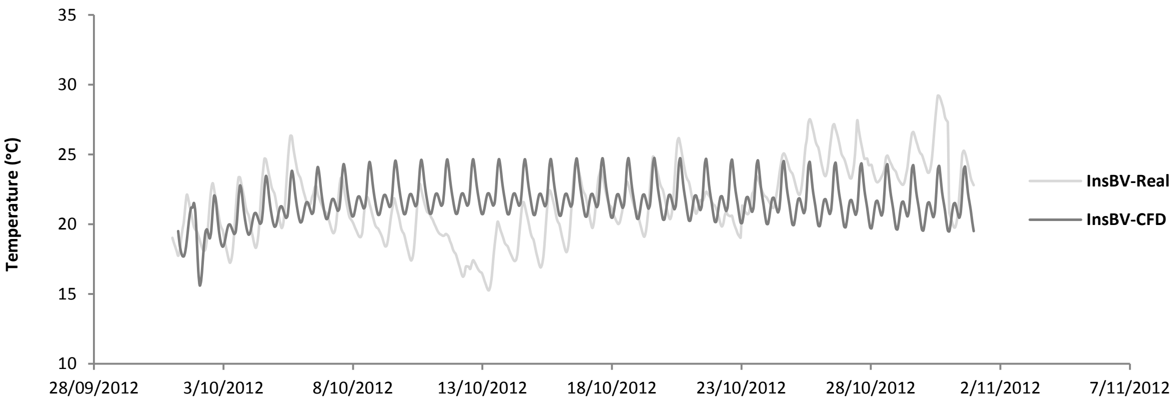

Figure E9. Monthly CFD results and the real data for the InsBV module for October 2012.

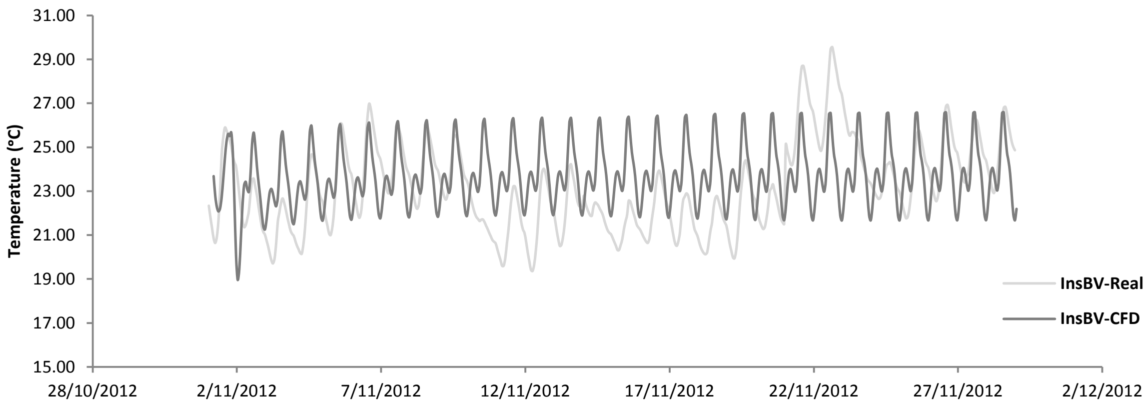

Figure E10. Monthly CFD results and the real data for the InsBV module for November 2012.

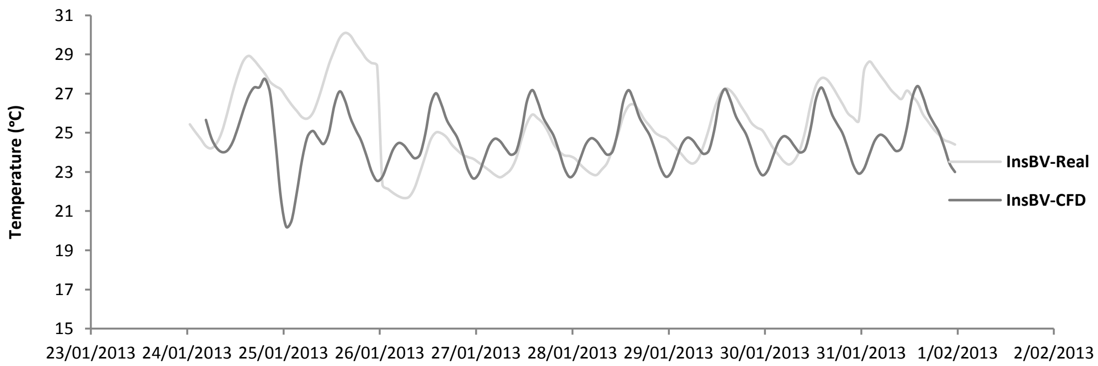

Figure E11. Monthly CFD results and the real data for the InsBV module for January 2013.

Appendix F; Monthly CFD results and real data for the InsCB module from February 2012 to Jan 2013 (Note; the data for December and most of January 2013 are missing).

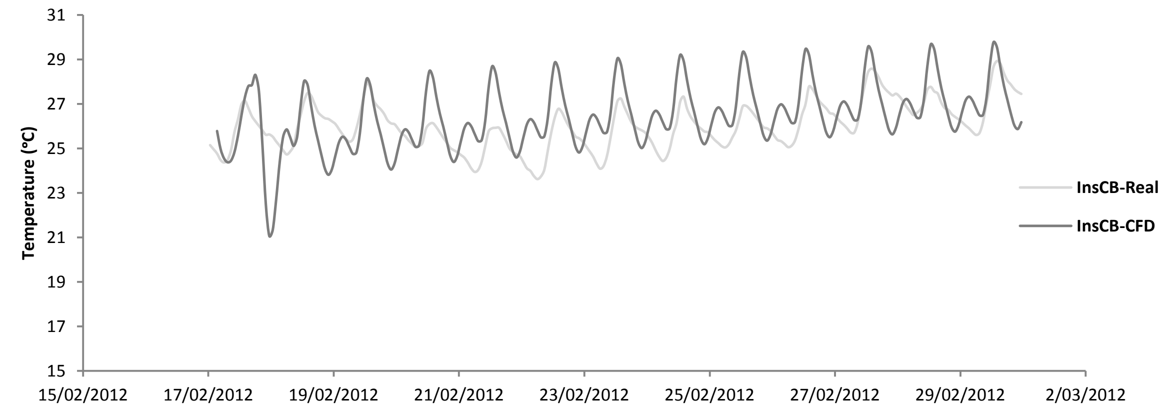

Figure F1. Monthly CFD results and the real data for the InsCB module for February 2012.

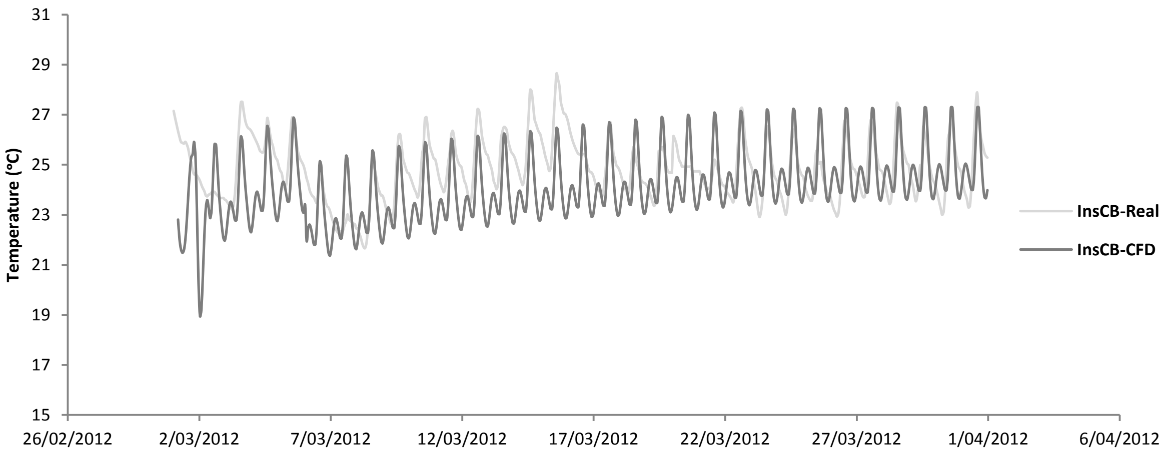

Figure F2. Monthly CFD results and the real data for the InsCB module for March 2012.

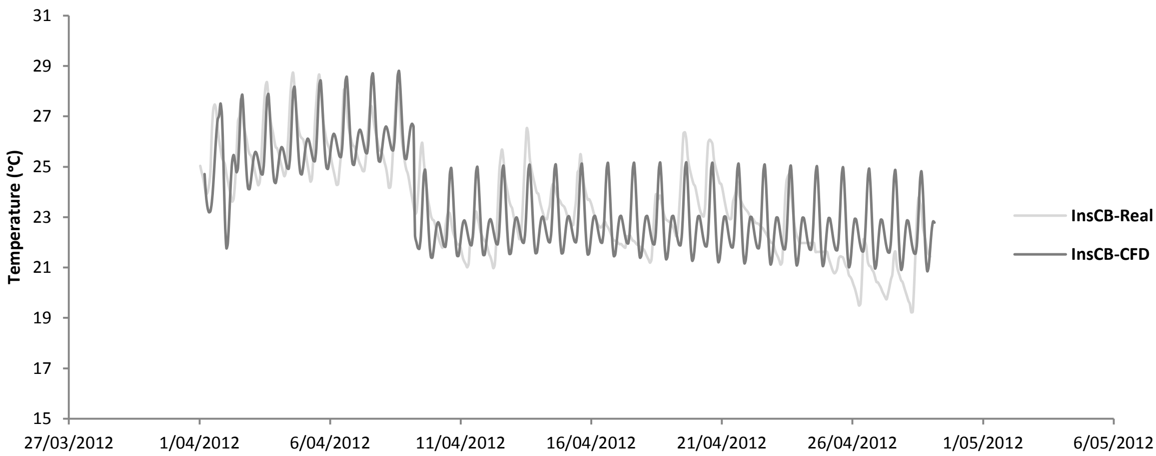

Figure F3. Monthly CFD results and the real data for the InsCB module for April 2012.

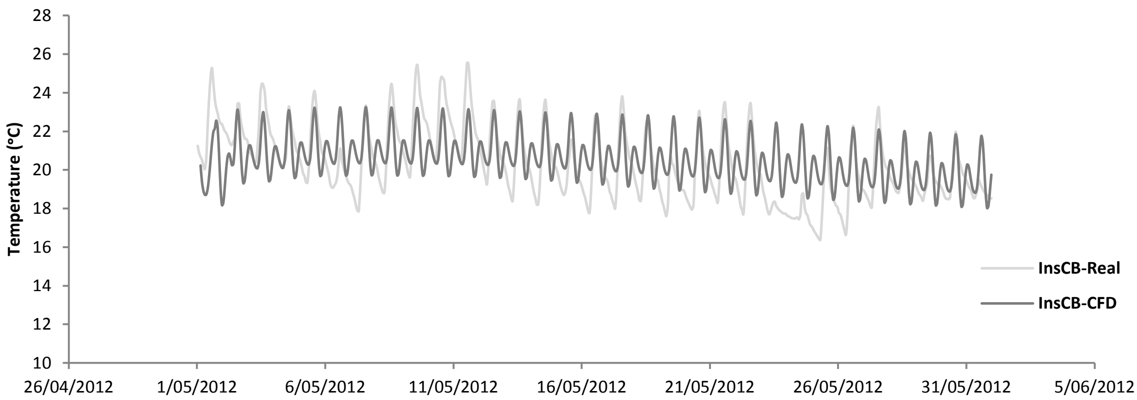

Figure F4. Monthly CFD results and the real data for the InsCB module for May 2012.

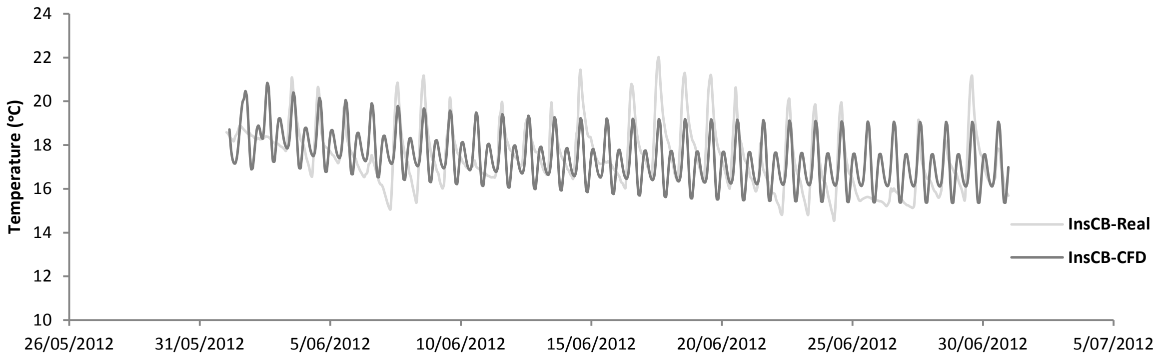

Figure F5. Monthly CFD results and the real data for the InsCB module for June 2012.

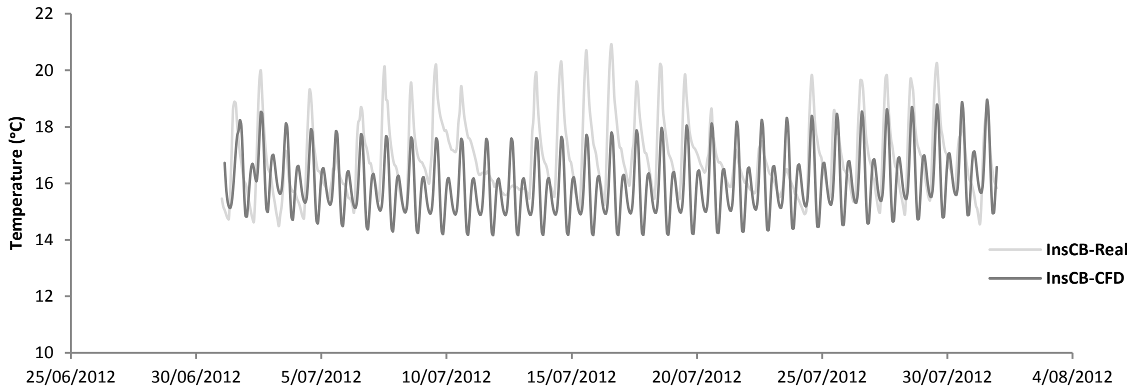

Figure F6. Monthly CFD results and the real data for the InsCB module for July 2012.

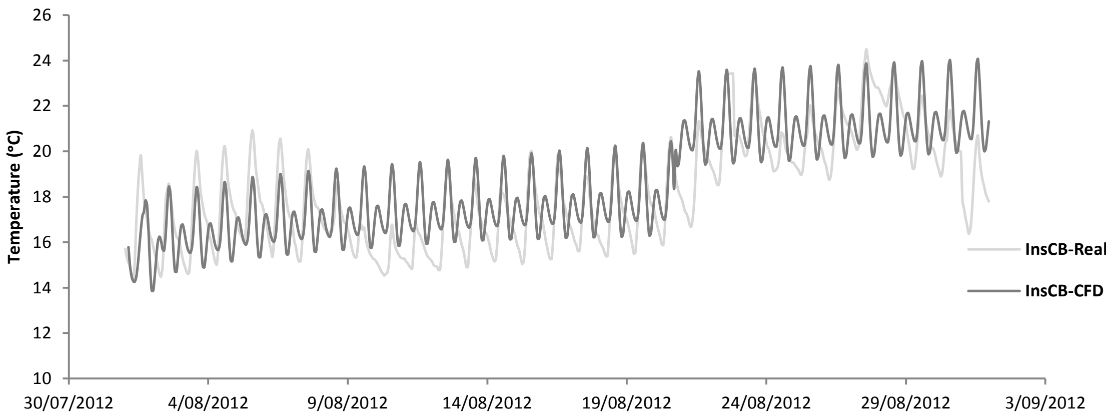

Figure F7. Monthly CFD results and the real data for the InsCB module for August 2012.

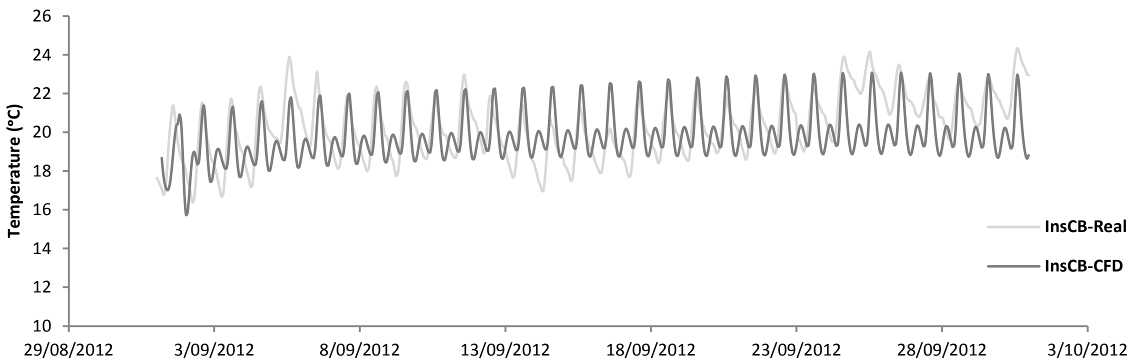

Figure F8. Monthly CFD results and the real data for the InsCB module for September 2012.

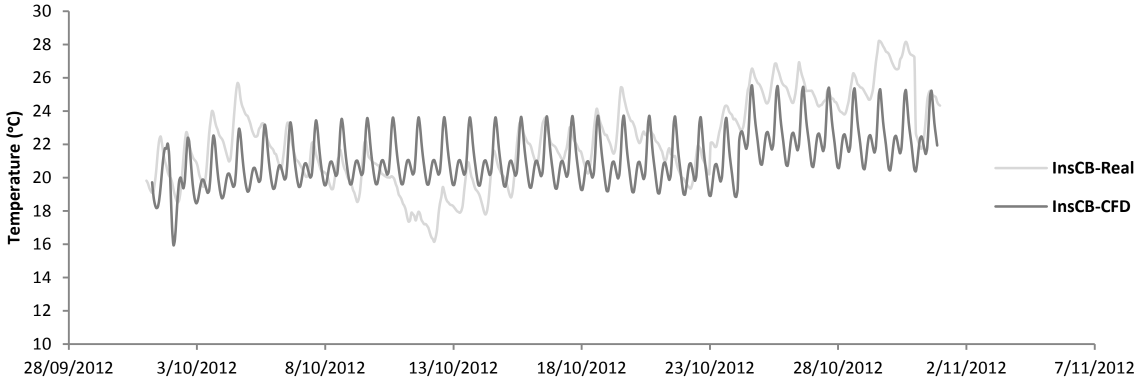

Figure F9. Monthly CFD results and the real data for the InsCB module for October 2012.

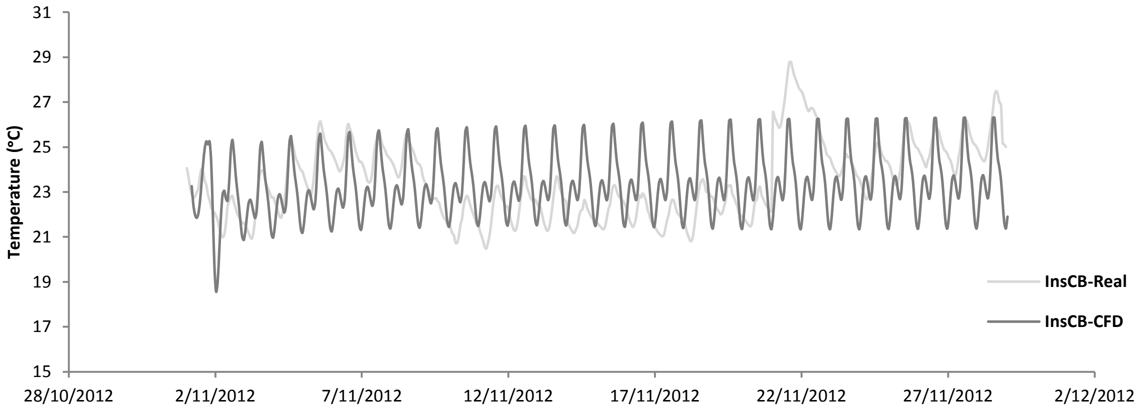

Figure F10. Monthly CFD results and the real data for the InsCB module for November 2012.

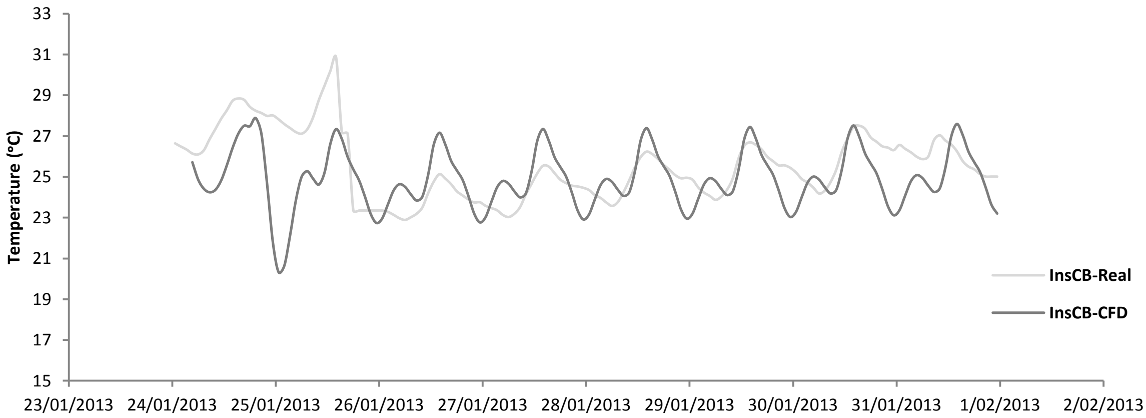

Figure F11. Monthly CFD results and the real data for the InsCB module for January 2013.

Appendix G; Hourly temperature variations throughout the northern wall of the InsCB module during winter day (14/06/2009) started at 2:30:00 PM.

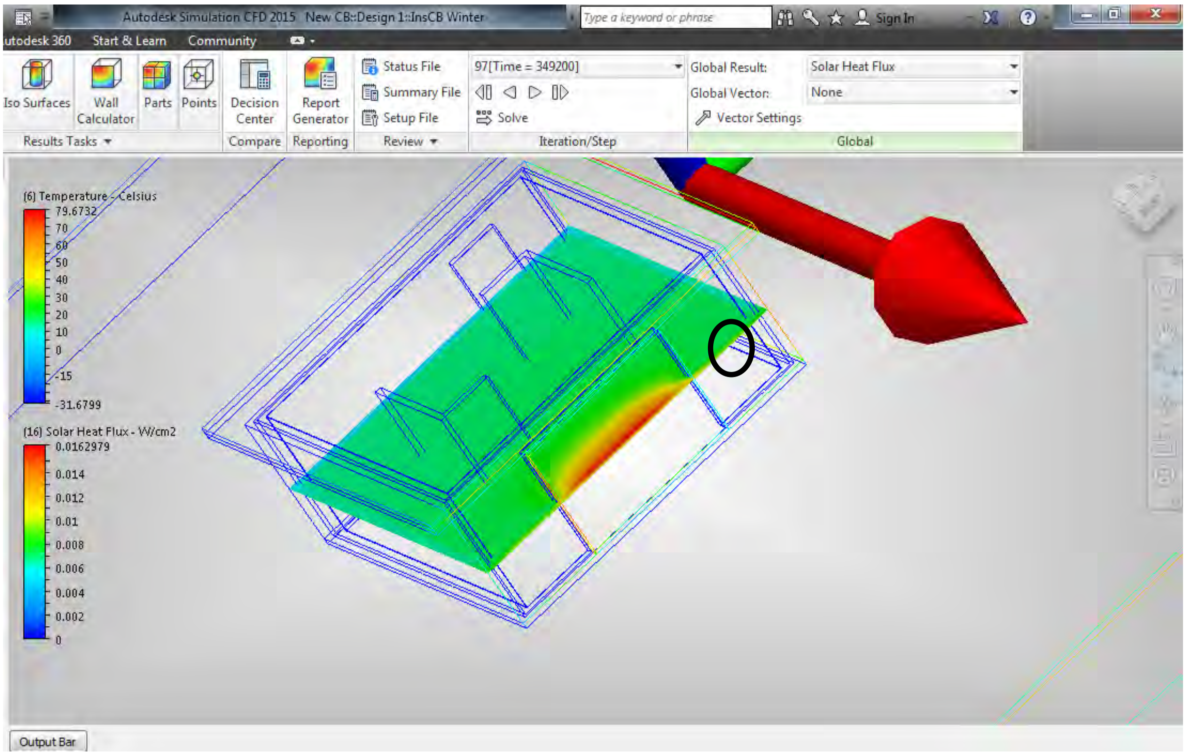

Figure G1. Horizontal plane at 1200mm elevation from the floor where the black circle shows the location of the temperature variations for the next Figures (C2-C26).

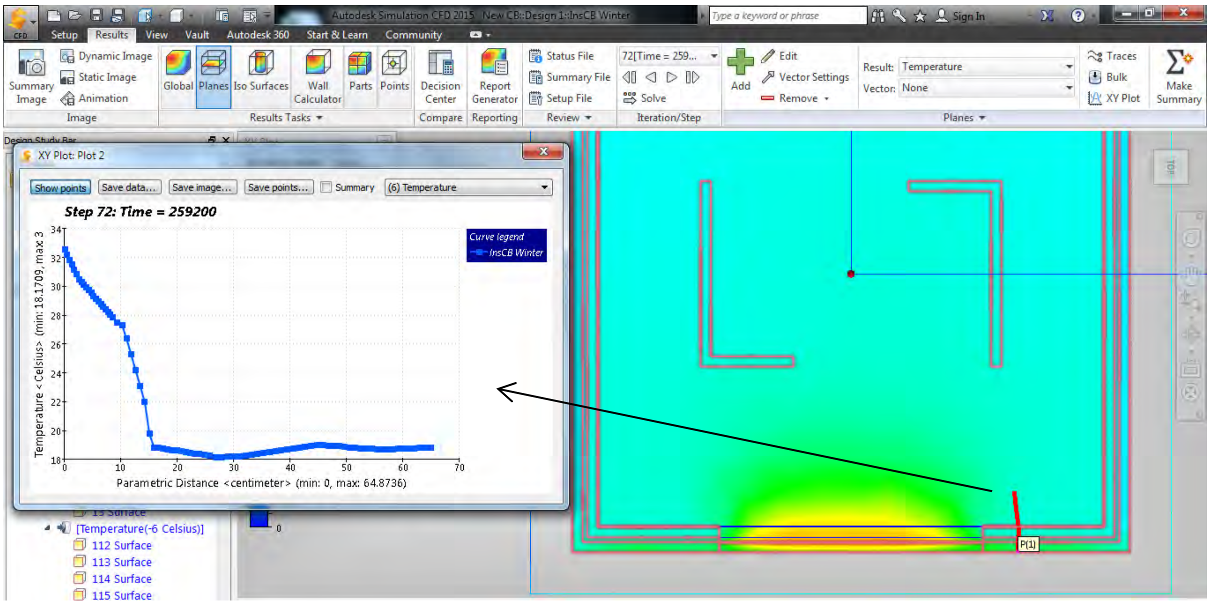

Figure G2. Temperature variation throughout northern wall at: 2:30 PM. (Note; the red line shows the temperature changes location across the wall).

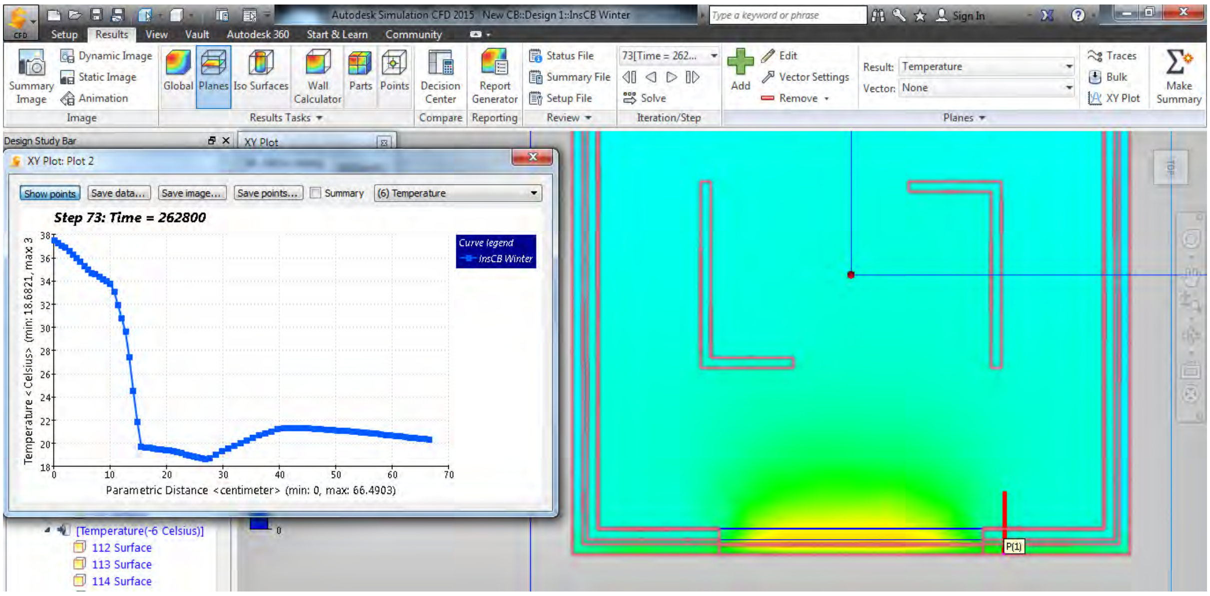

Figure G3. Temperature variation throughout northern wall at: 3:30 PM. (Note; the red line shows the temperature changes location across the wall).

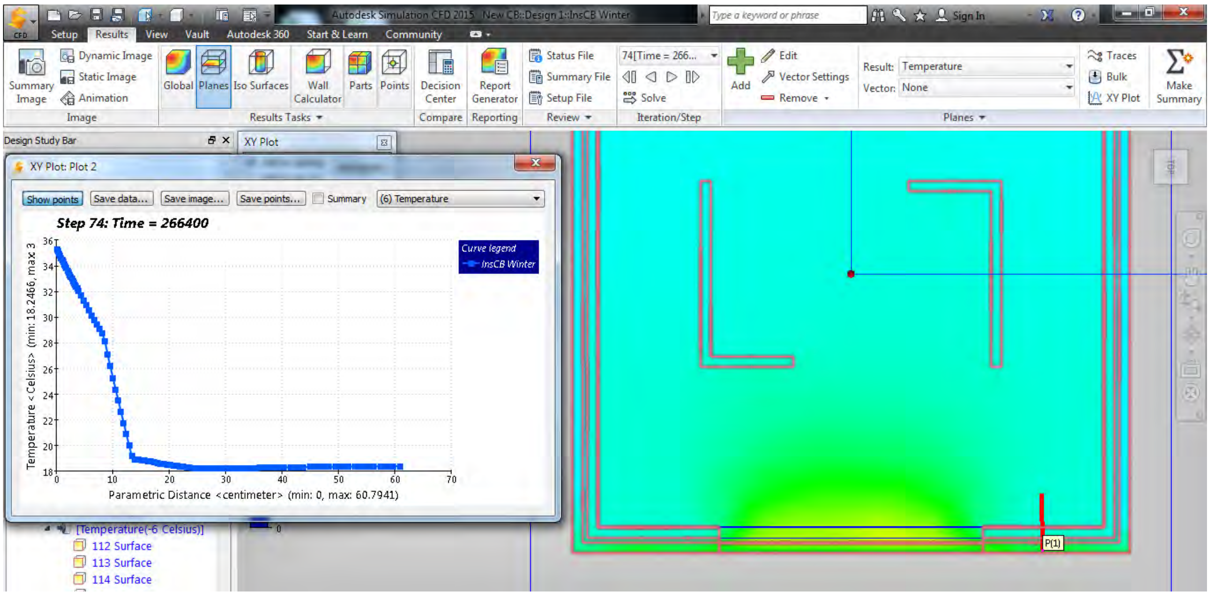

Figure G4. Temperature variation throughout northern wall at: 4:30 PM. (Note; the red line shows the temperature changes location across the wall).

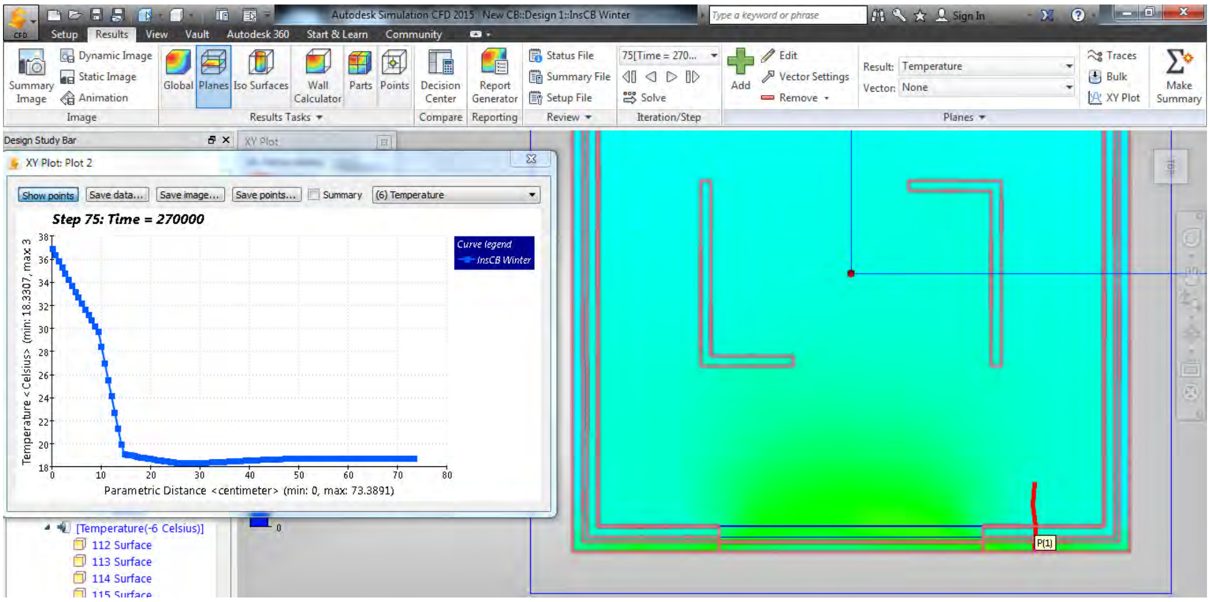

Figure G5. Temperature variation throughout northern wall at: 5:30 PM. (Note; the red line shows the temperature changes location across the wall).

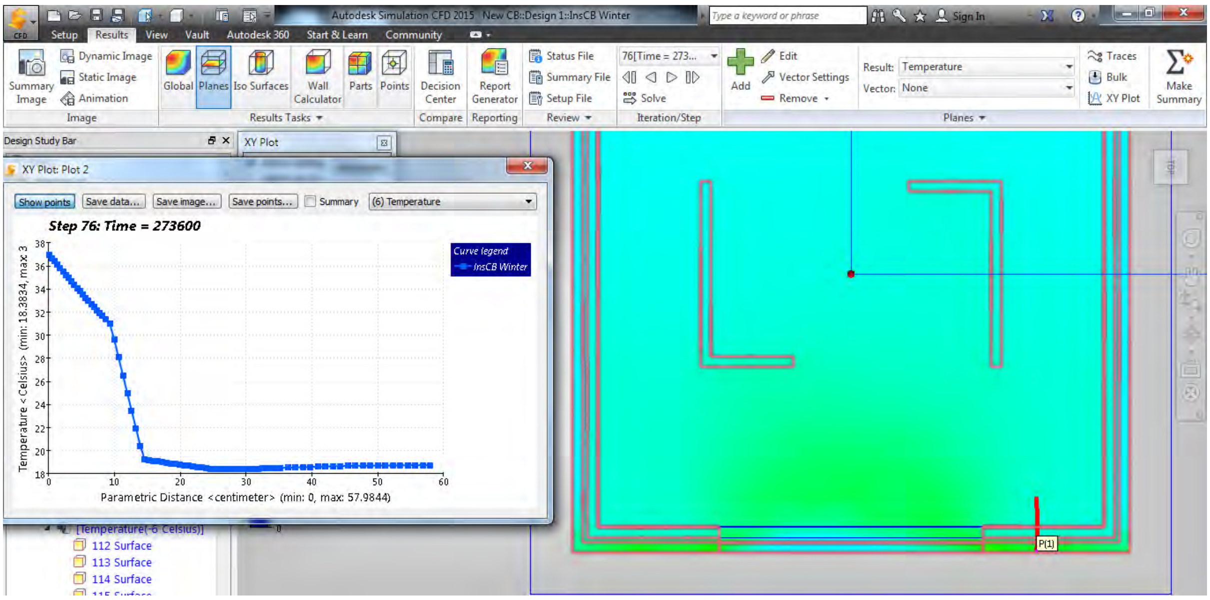

Figure G6. Temperature variation throughout northern wall at: 6:30 PM. (Note; the red line shows the temperature changes location across the wall).

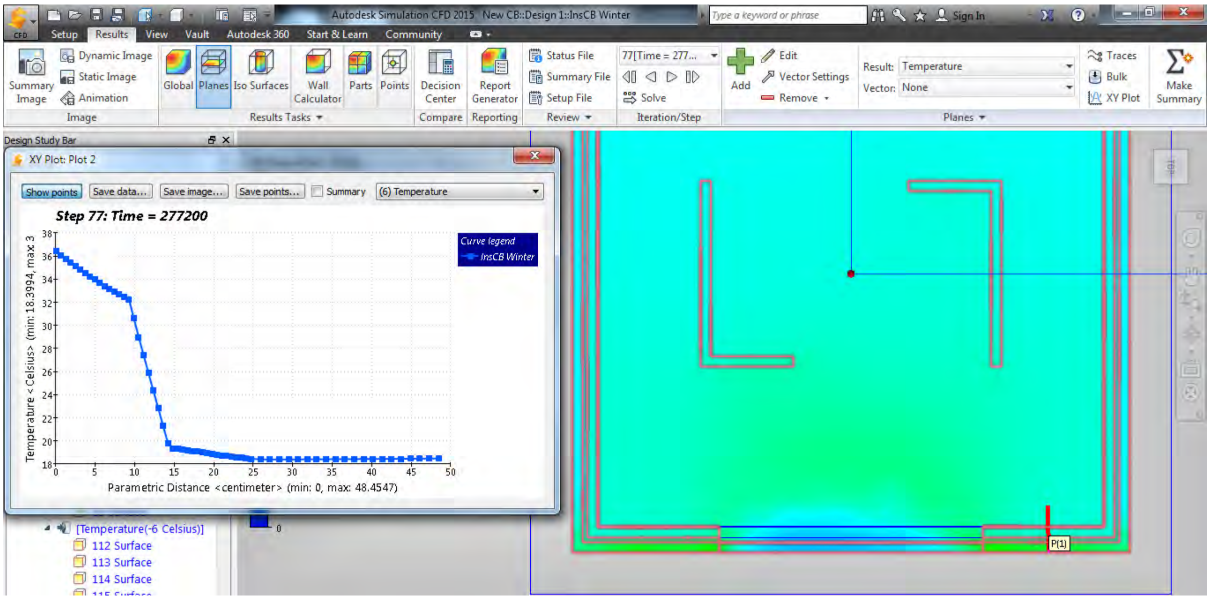

Figure G7. Temperature variation throughout northern wall at: 7:30 PM. (Note; the red line shows the temperature changes location across the wall).

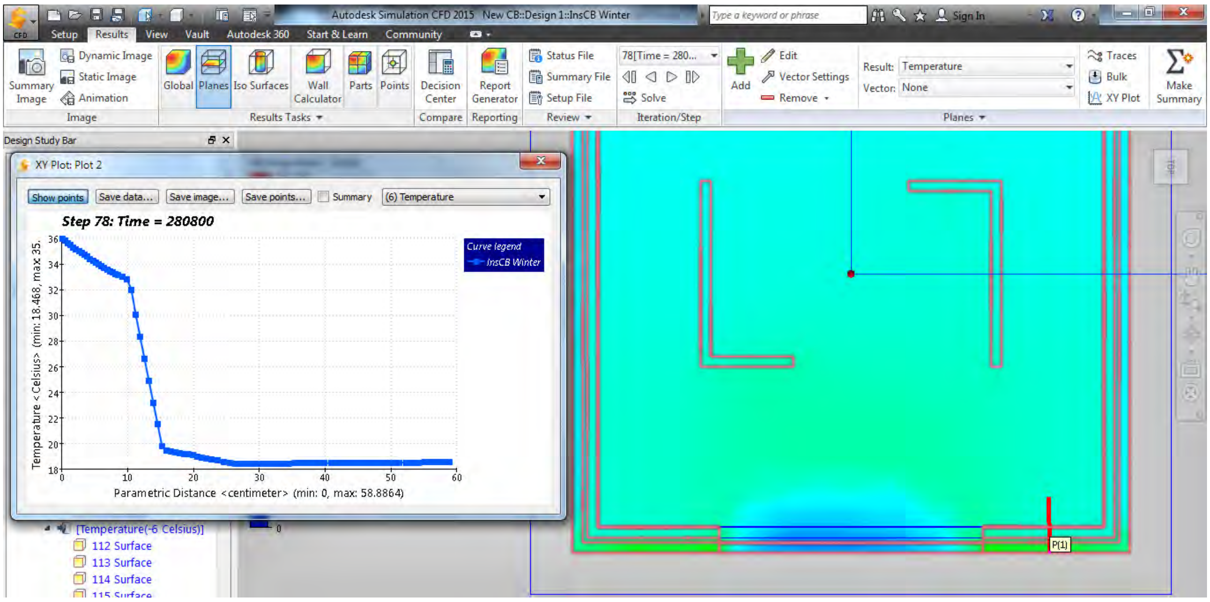

Figure G8. Temperature variation throughout northern wall at: 8:30 PM. (Note; the red line shows the temperature changes location across the wall).

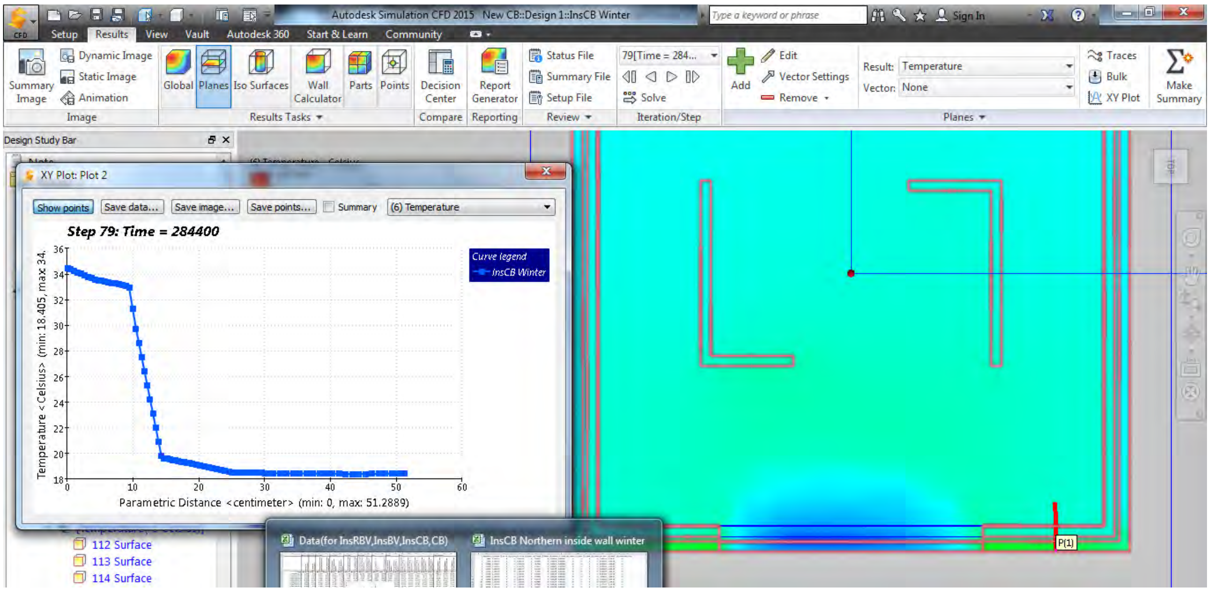

Figure G9. Temperature variation throughout northern wall at: 9:30 PM. (Note; the red line shows the temperature changes location across the wall).

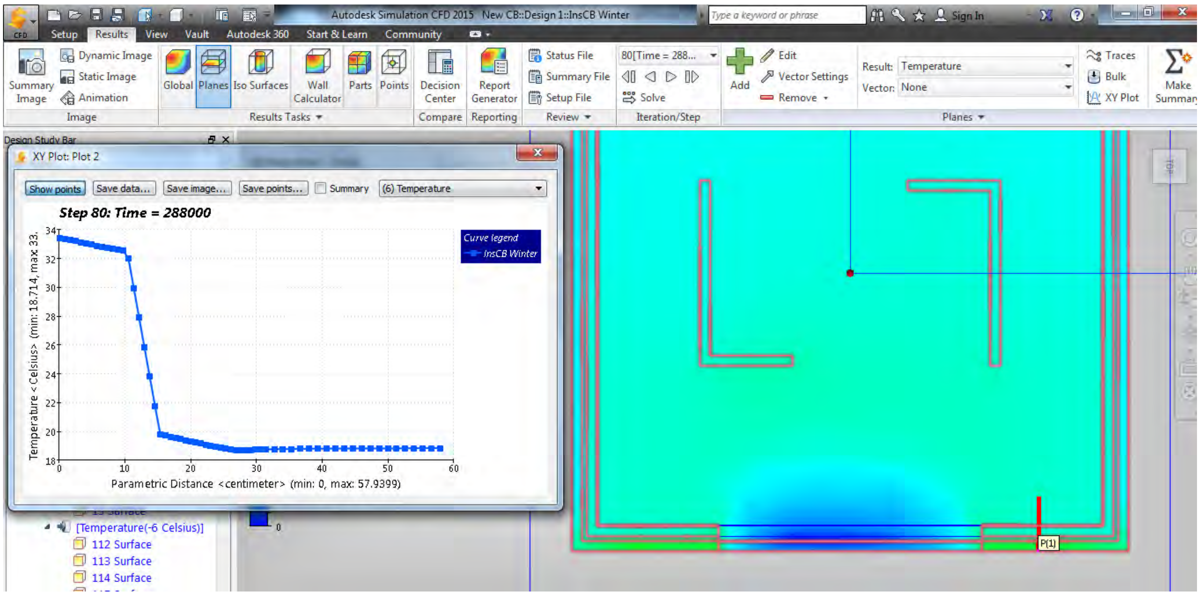

Figure G10. Temperature variation throughout northern wall at: 10:30 PM. (Note; the red line shows the temperature changes location across the wall).

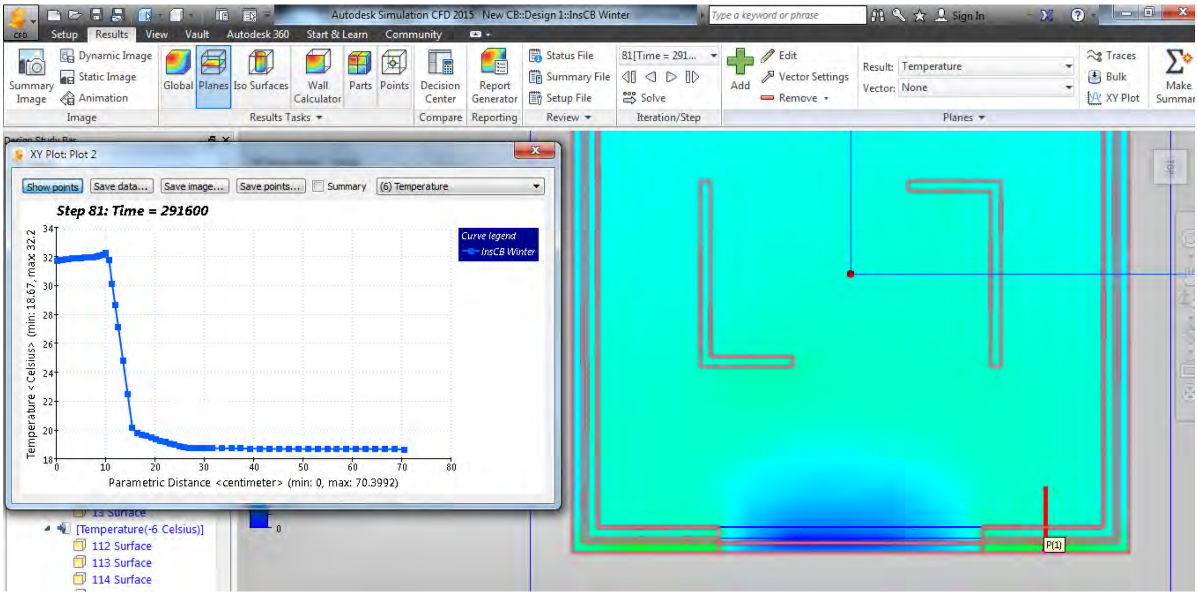

Figure G11. Temperature variation throughout northern wall at: 11:30 AM. (Note; the red line shows the temperature changes location across the wall).

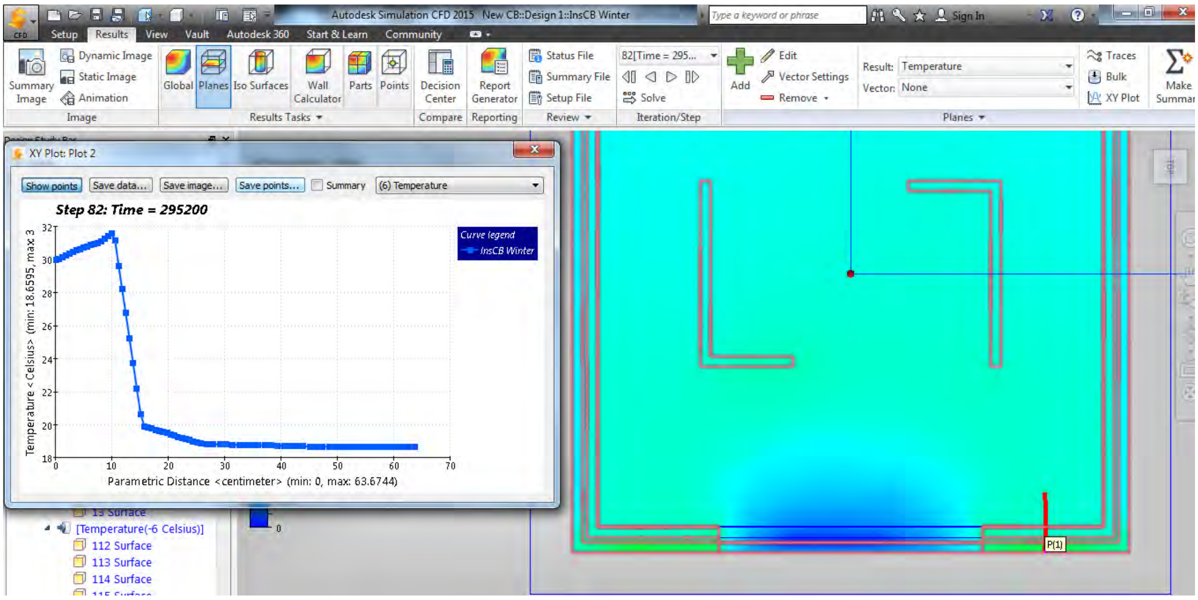

Figure G12. Temperature variation throughout northern wall at: 12:30 PM. (Note; the red line shows the temperature changes location across the wall).

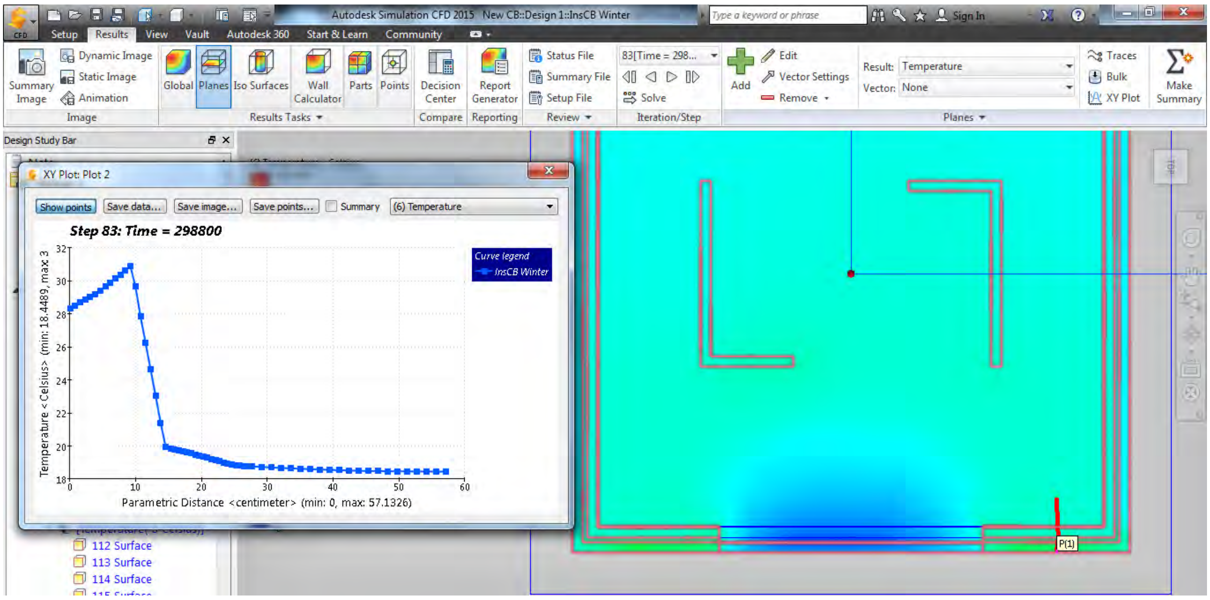

Figure G13. Temperature variation throughout northern wall at: 1:30 AM. (Note; the red line shows the temperature changes location across the wall).

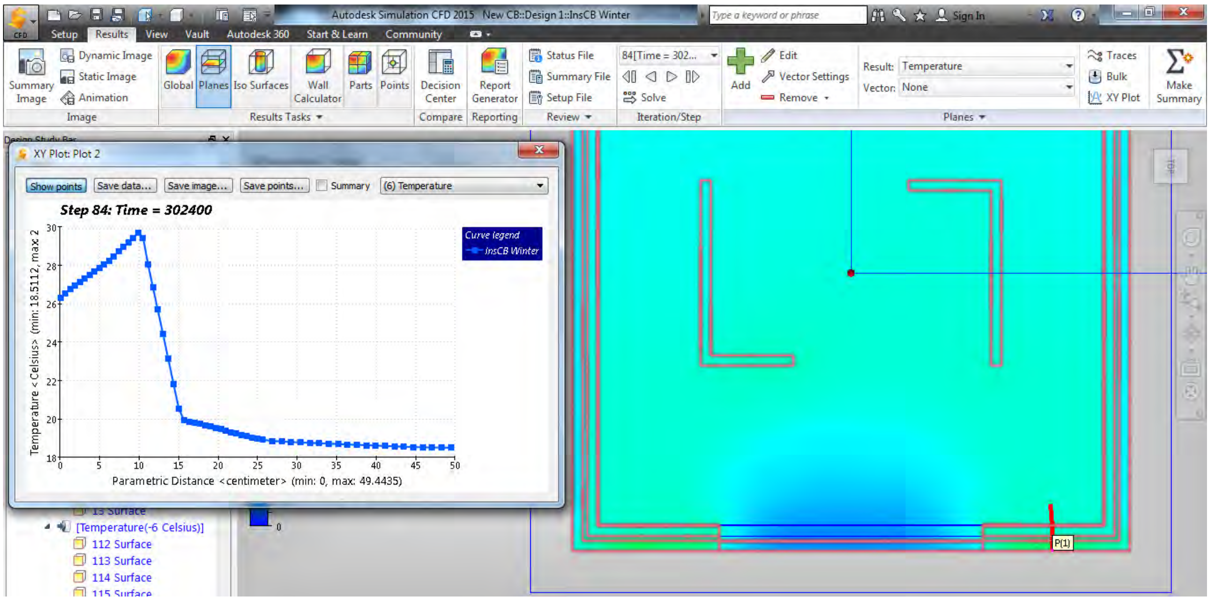

Figure G14. Temperature variation throughout northern wall at: 2:30 AM. (Note; the red line shows the temperature changes location across the wall).

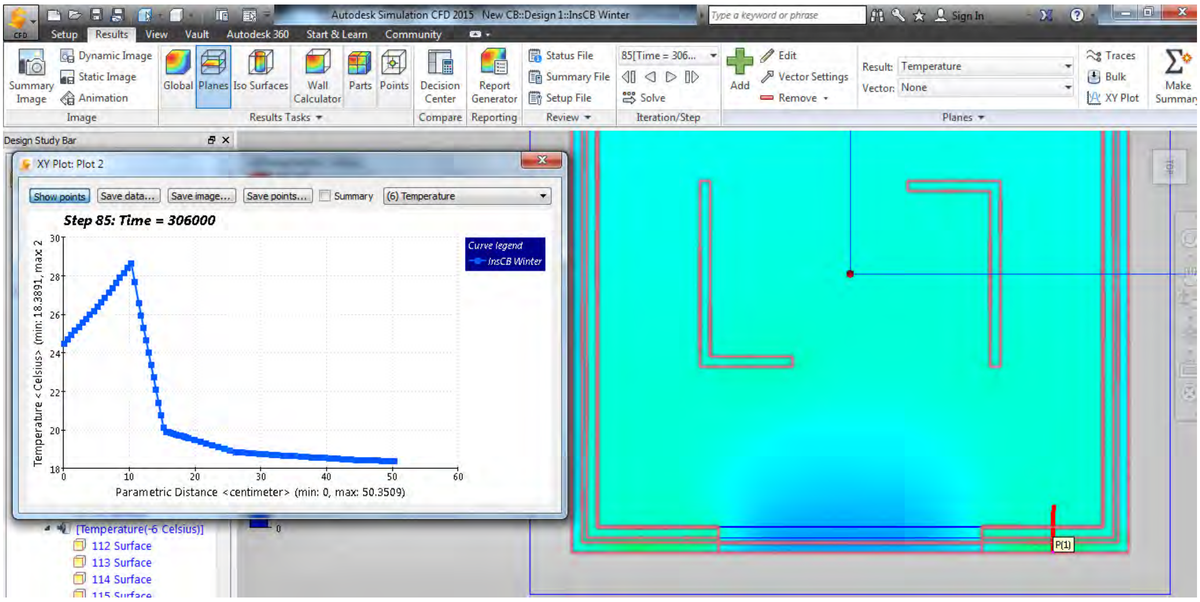

Figure G15. Temperature variation throughout northern wall at: 3:30 AM. (Note; the red line shows the temperature changes location across the wall).

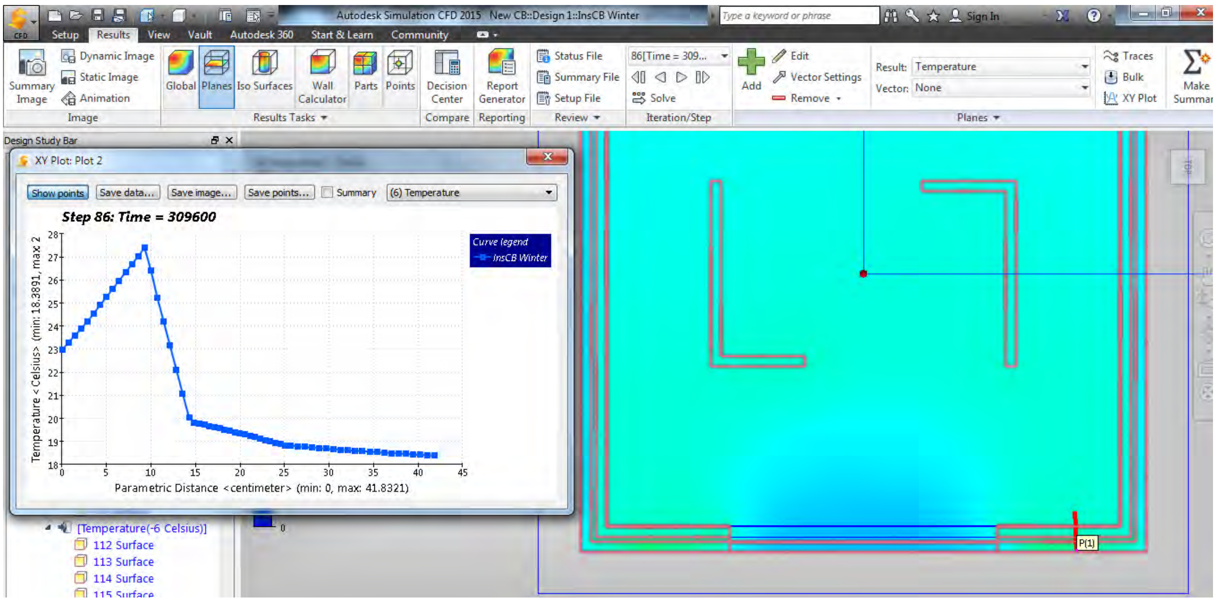

Figure G16. Temperature variation throughout northern wall at: 4:30 AM. (Note; the red line shows the temperature changes location across the wall).

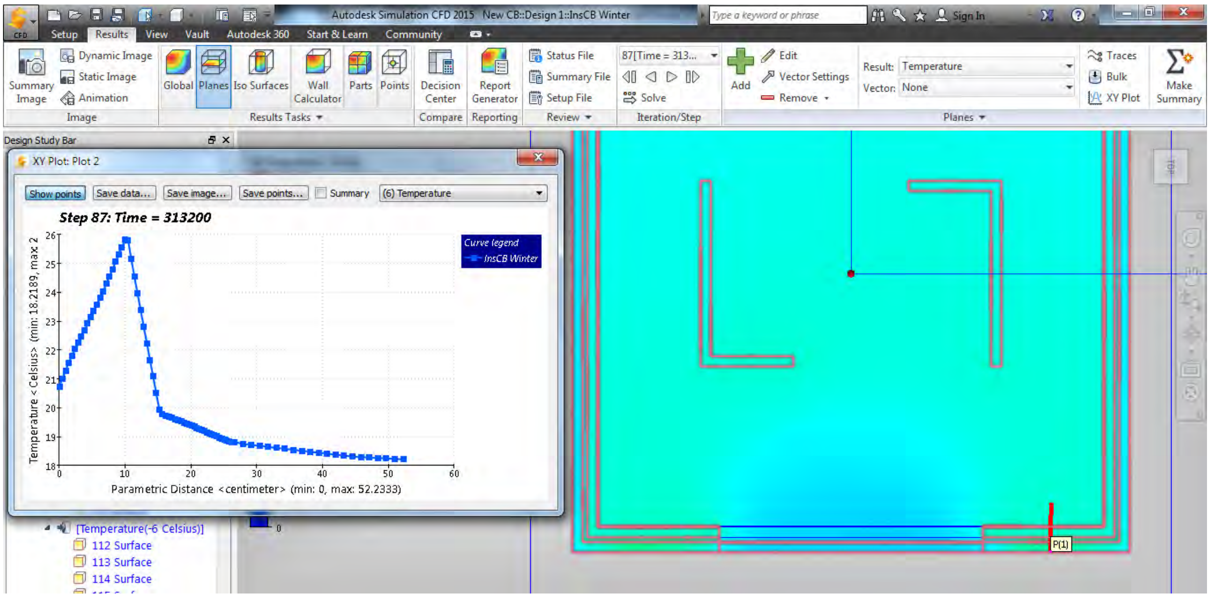

Figure G17. Temperature variation throughout northern wall at: 5:30 AM. (Note; the red line shows the temperature changes location across the wall).

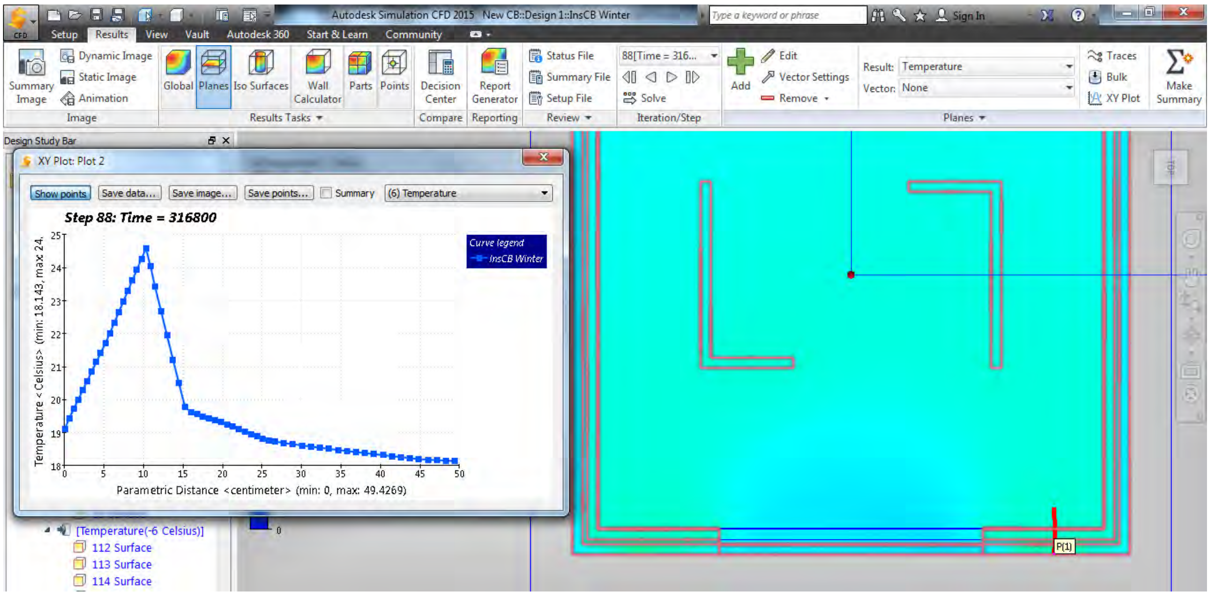

Figure G18. Temperature variation throughout northern wall at: 6:30 AM. (Note; the red line shows the temperature changes location across the wall).

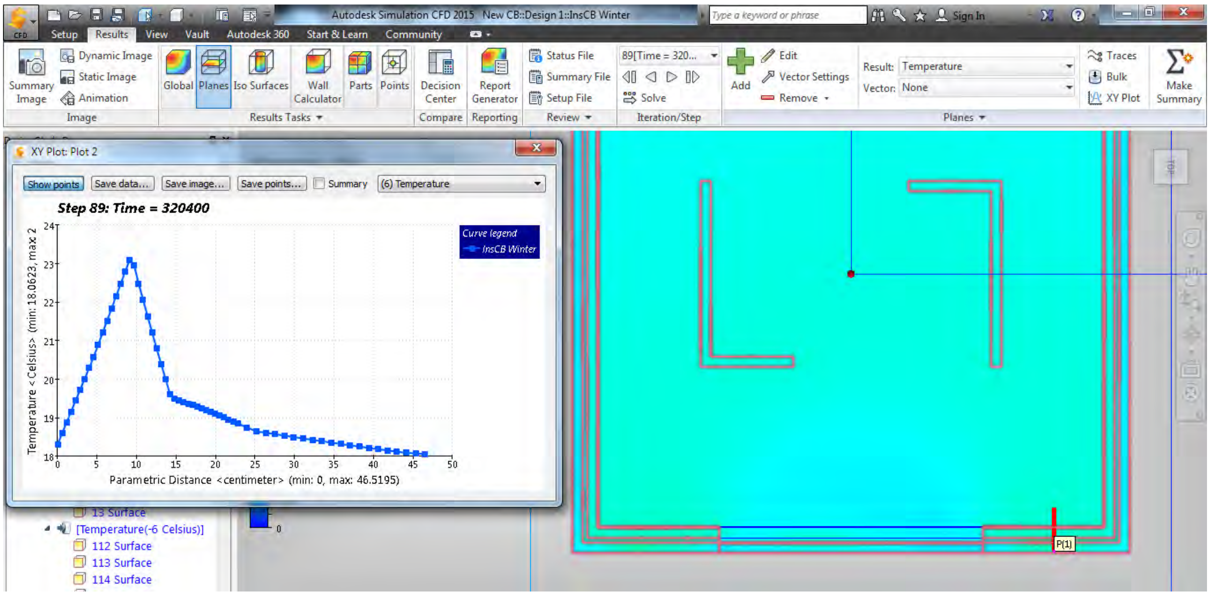

Figure G19. Temperature variation throughout northern wall at: 7:30 AM. (Note; the red line shows the temperature changes location across the wall).

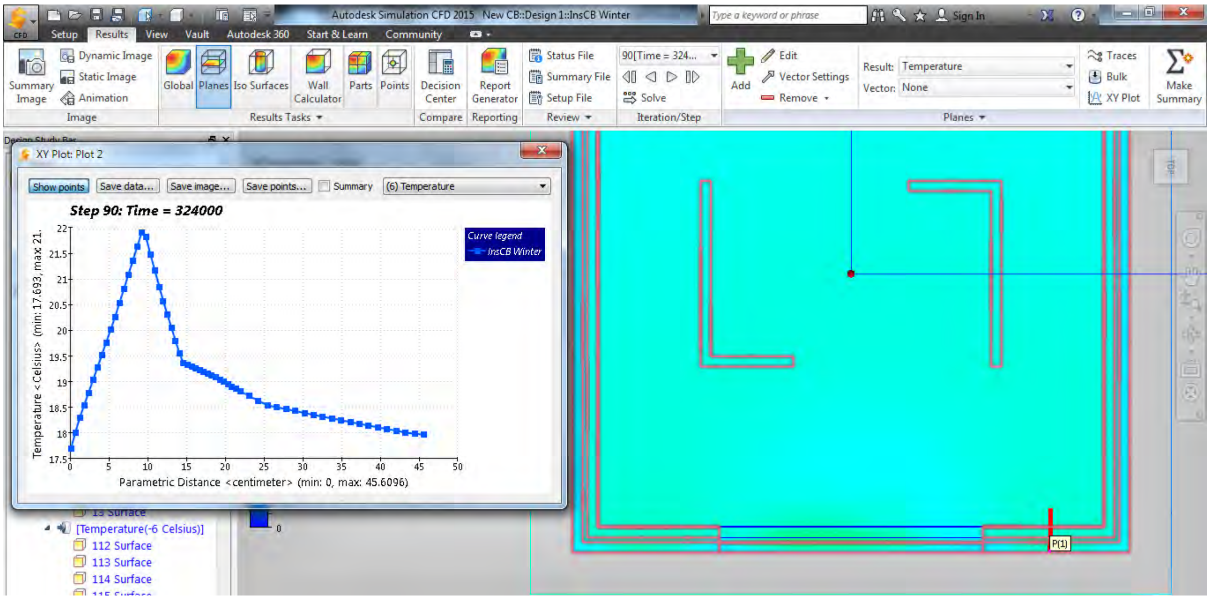

Figure G20. Temperature variation throughout northern wall at: 8:30 AM. (Note; the red line shows the temperature changes location across the wall).

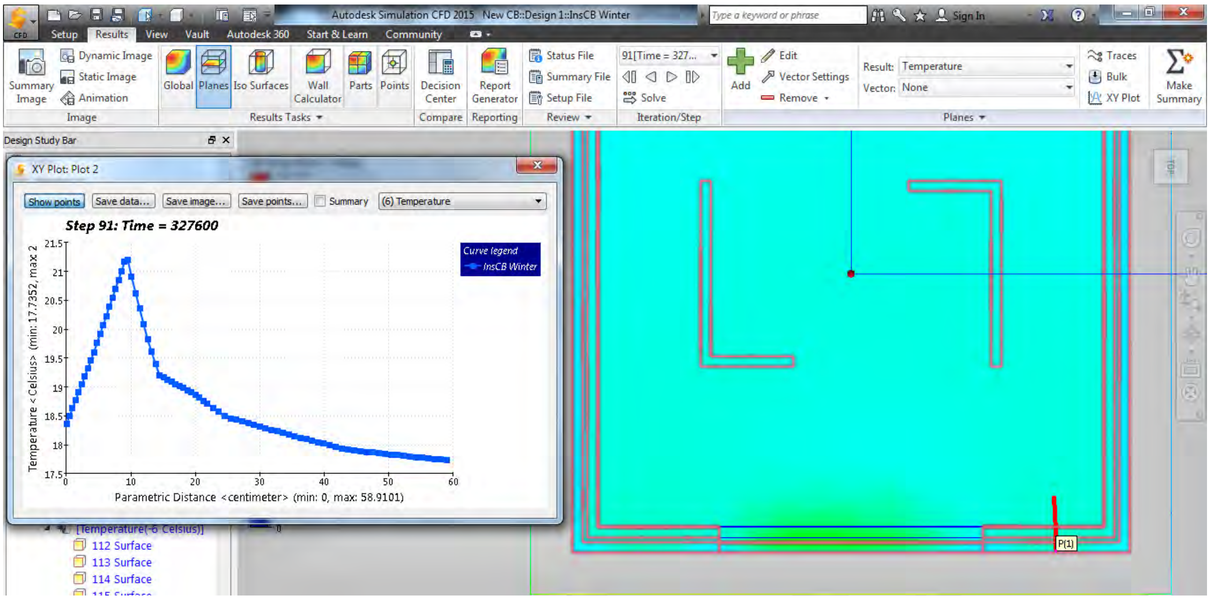

Figure G21. Temperature variation throughout northern wall at: 9:30 AM. (Note; the red line shows the temperature changes location across the wall).

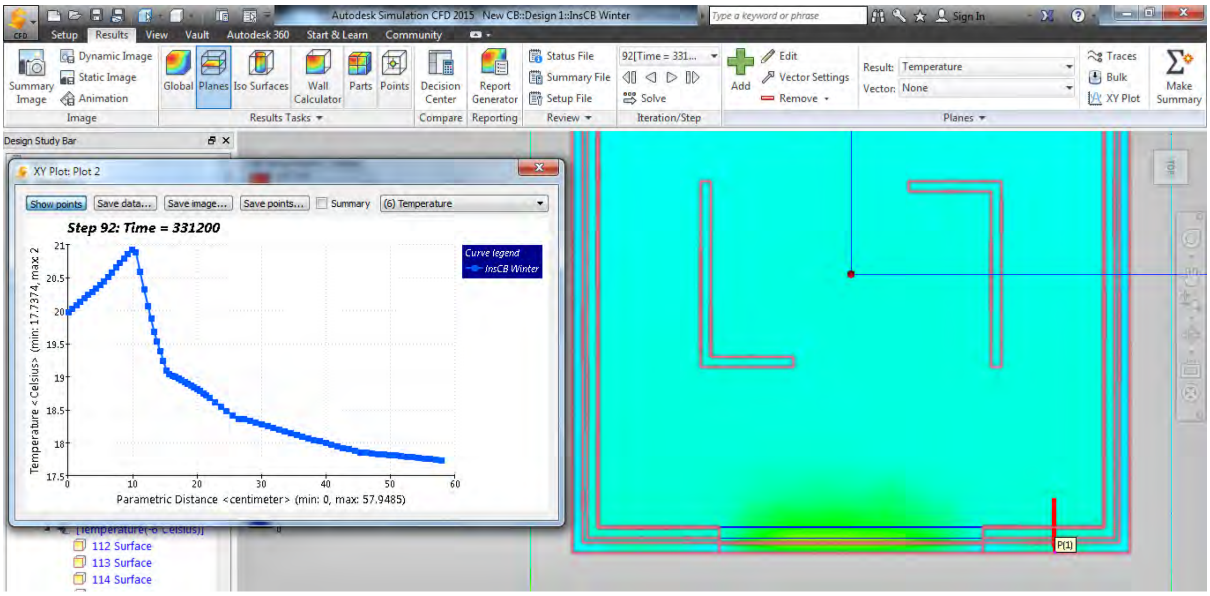

Figure G22. Temperature variation throughout northern wall at: 10:30 AM. (Note; the red line shows the temperature changes location across the wall).

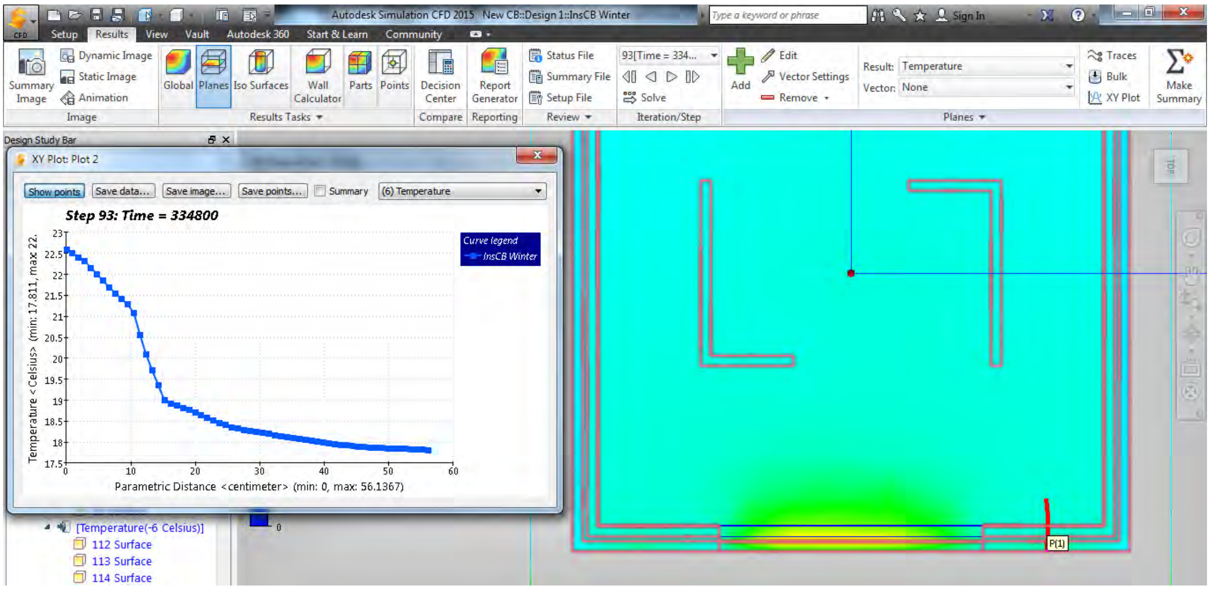

Figure G23. Temperature variation throughout northern wall at: 11:30 AM. (Note; the red line shows the temperature changes location across the wall).

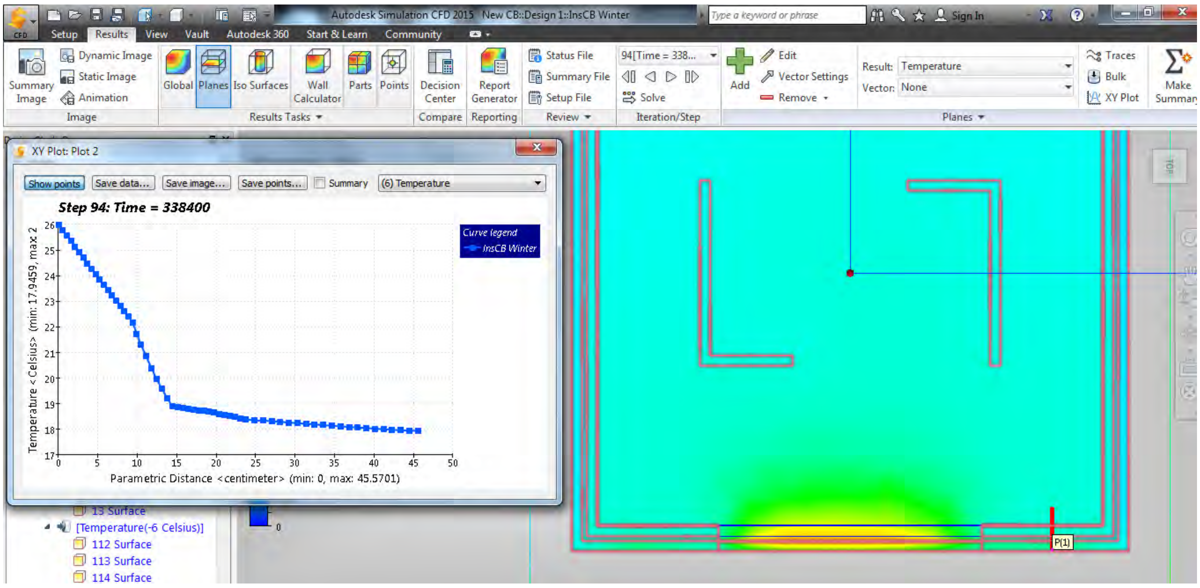

Figure G24. Temperature variation throughout northern wall at: 12:30 PM. (Note; the red line shows the temperature changes location across the wall).

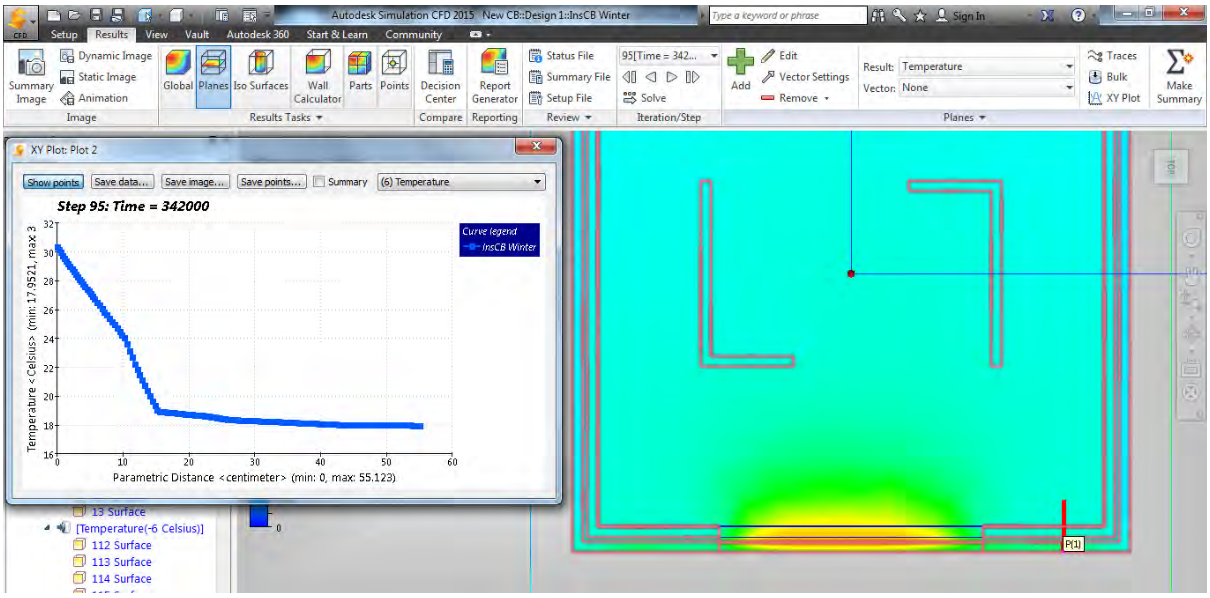

Figure G25. Temperature variation throughout northern wall at: 1:30 PM. (Note; the red line shows the temperature changes location across the wall).

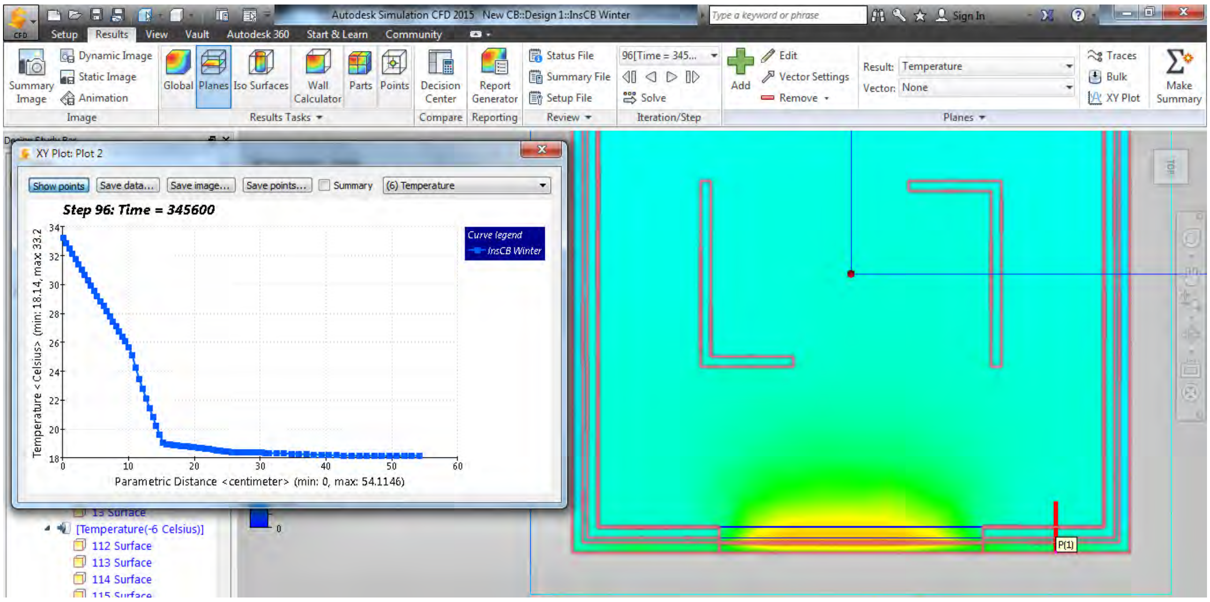

Figure G26. Temperature variation throughout northern wall at: 2:30 PM. (Note; the red line shows the temperature changes location across the wall).

Appendix H; Hourly temperature variation throughout the western wall for the InsCB module during one summer day 17/01/2010 started at 4:30:00 PM.

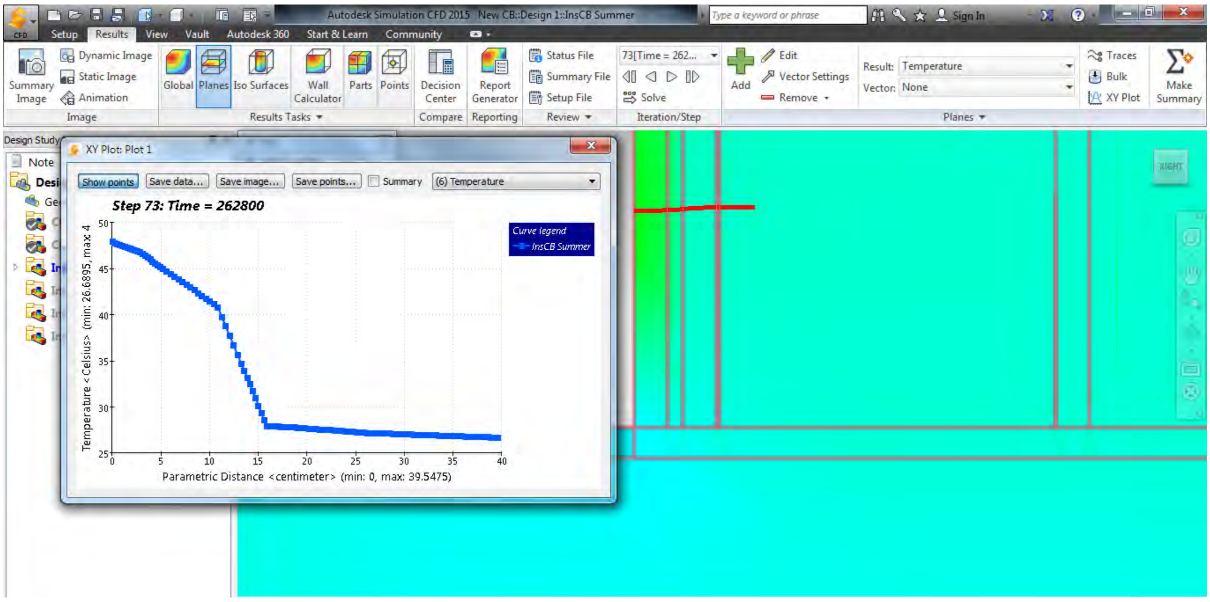

Figure H1. Temperature variation throughout western wall at: 4:30 PM. (Note; the red line shows the temperature changes location across the wall).

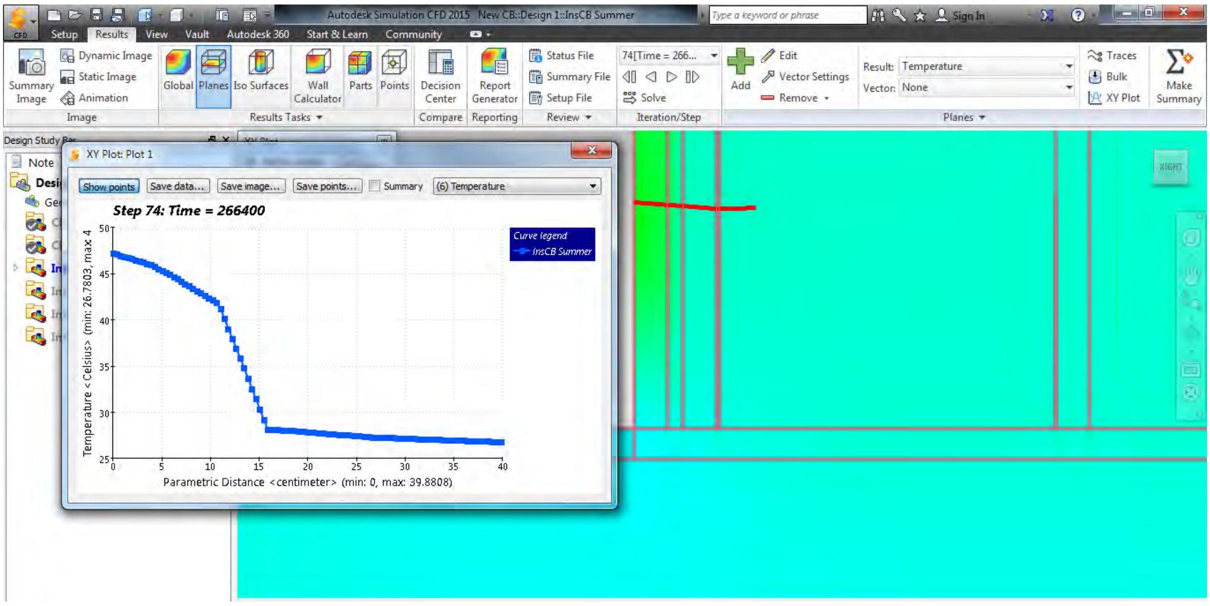

Figure H2. Temperature variation throughout western wall at: 5:30 PM. (Note; the red line shows the temperature changes location across the wall).

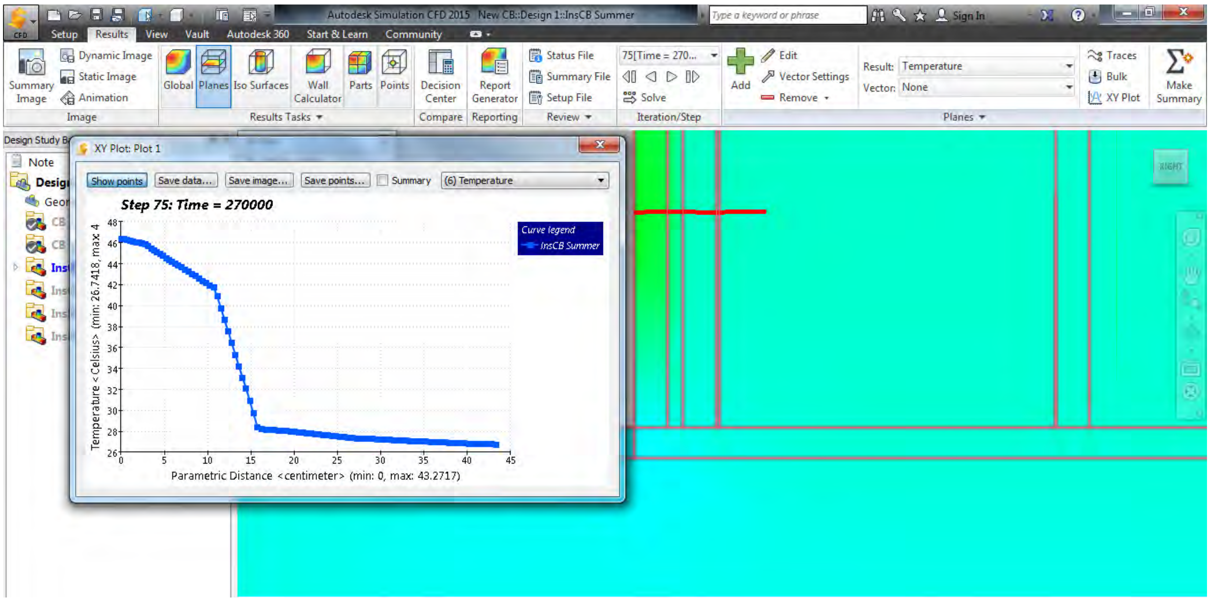

Figure H3. Temperature variation throughout western wall at: 6:30 PM. (Note; the red line shows the temperature changes location across the wall).

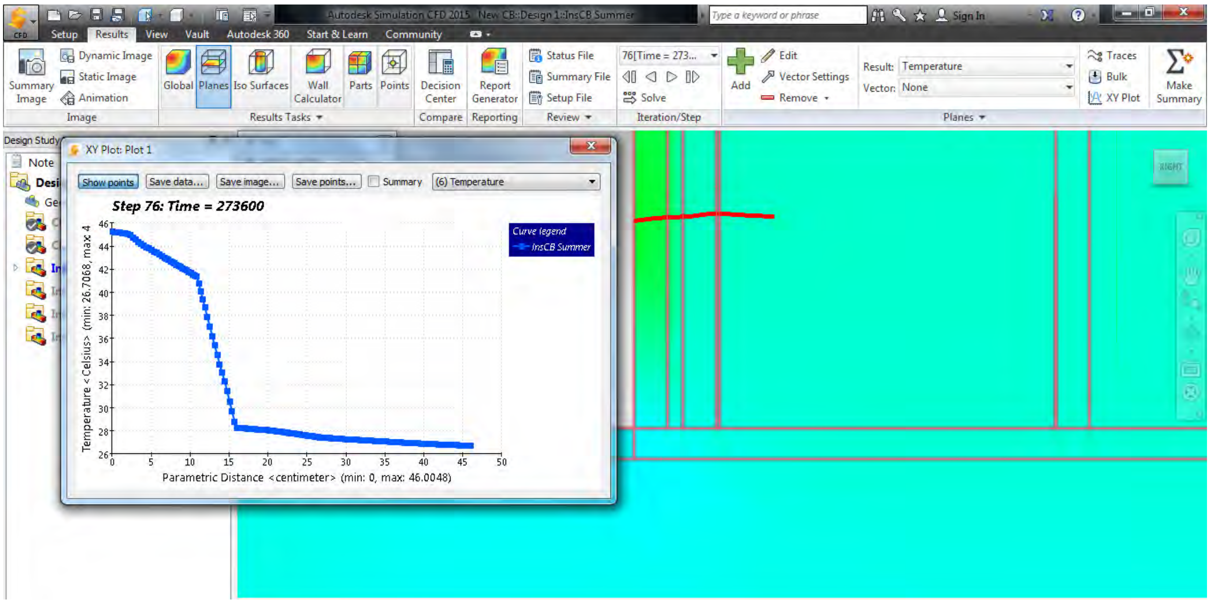

Figure H3. Temperature variation throughout western wall at: 7:30 PM. (Note; the red line shows the temperature changes location across the wall).

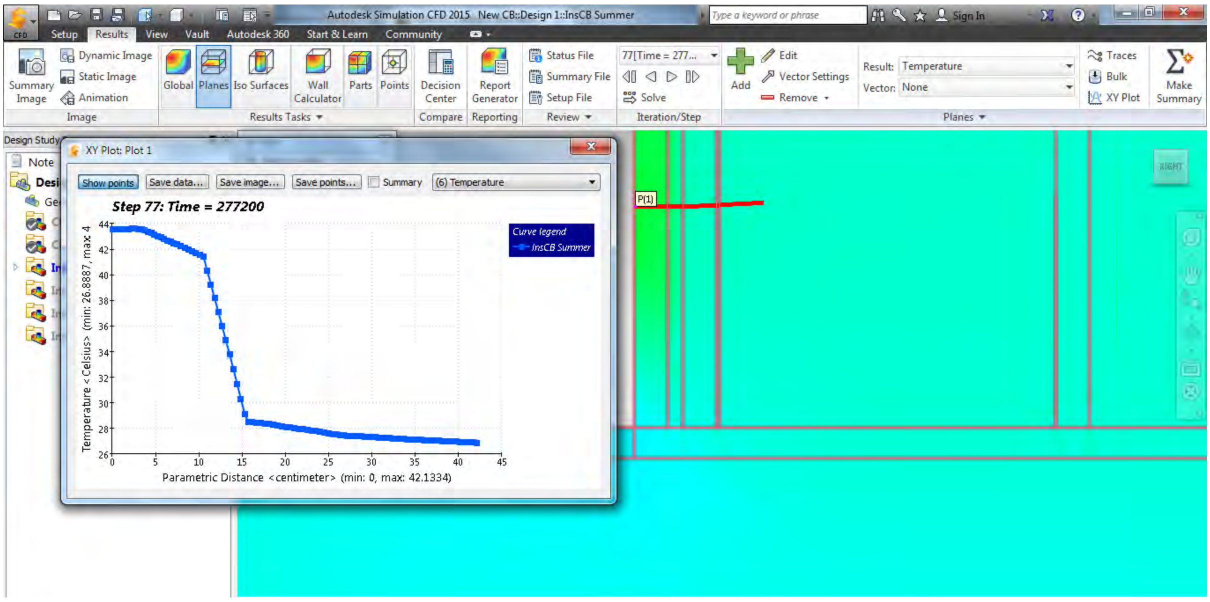

Figure H4. Temperature variation throughout western wall at: 8:30 PM. (Note; the red line shows the temperature changes location across the wall).

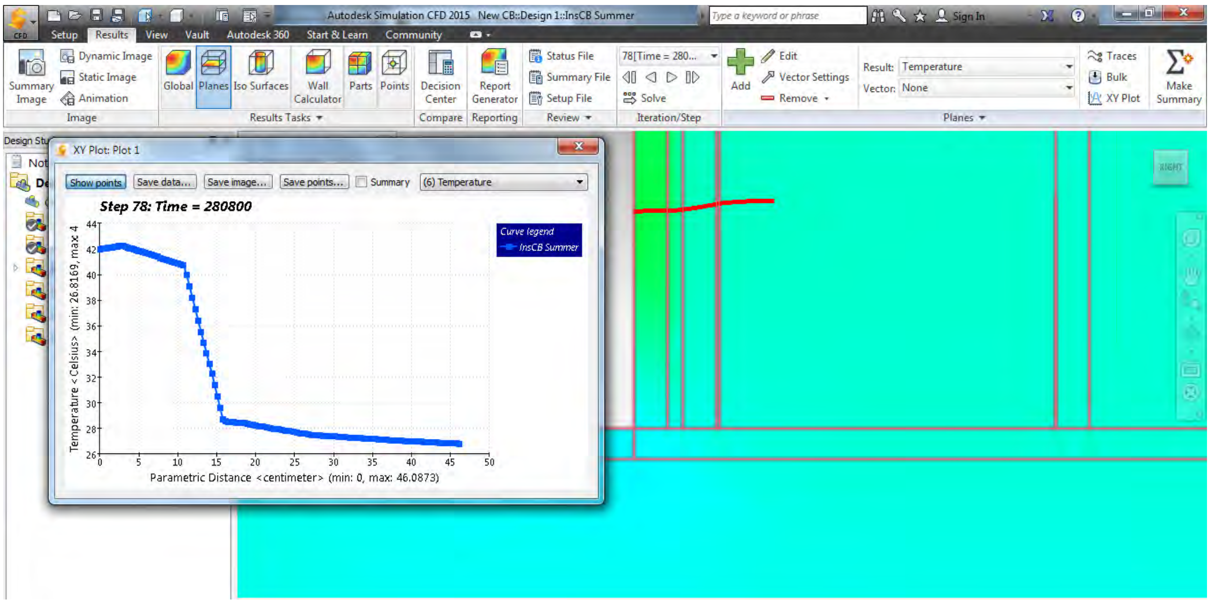

Figure H5. Temperature variation throughout western wall at: 9:30 PM. (Note; the red line shows the temperature changes location across the wall).

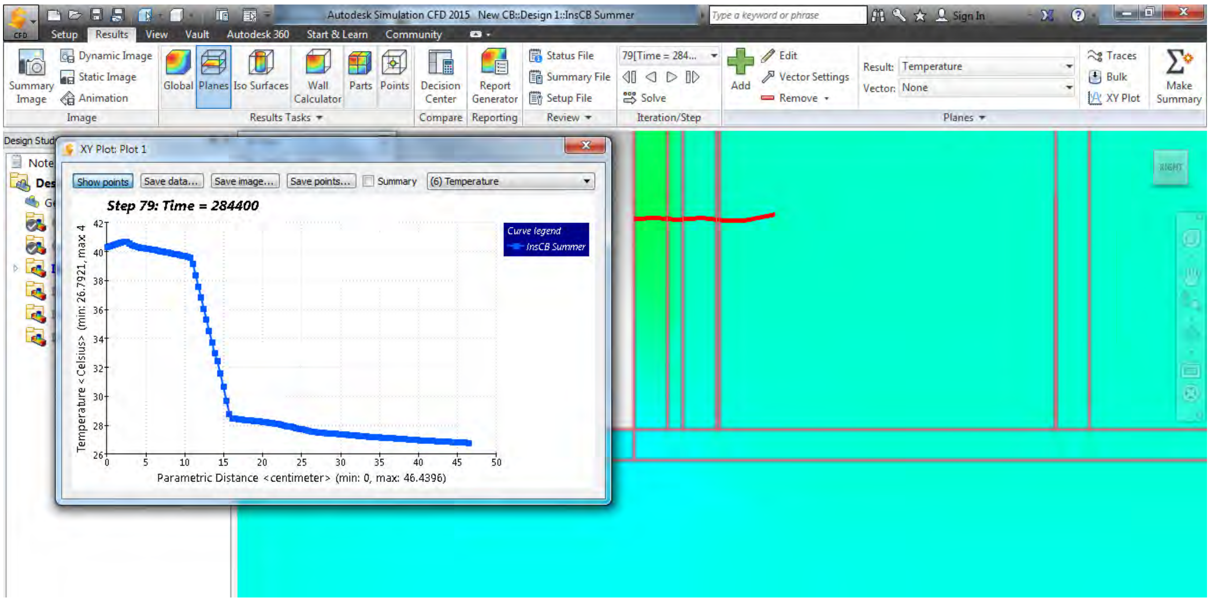

Figure H6. Temperature variation throughout western wall at: 10:30 PM. (Note; the red line shows the temperature changes location across the wall).

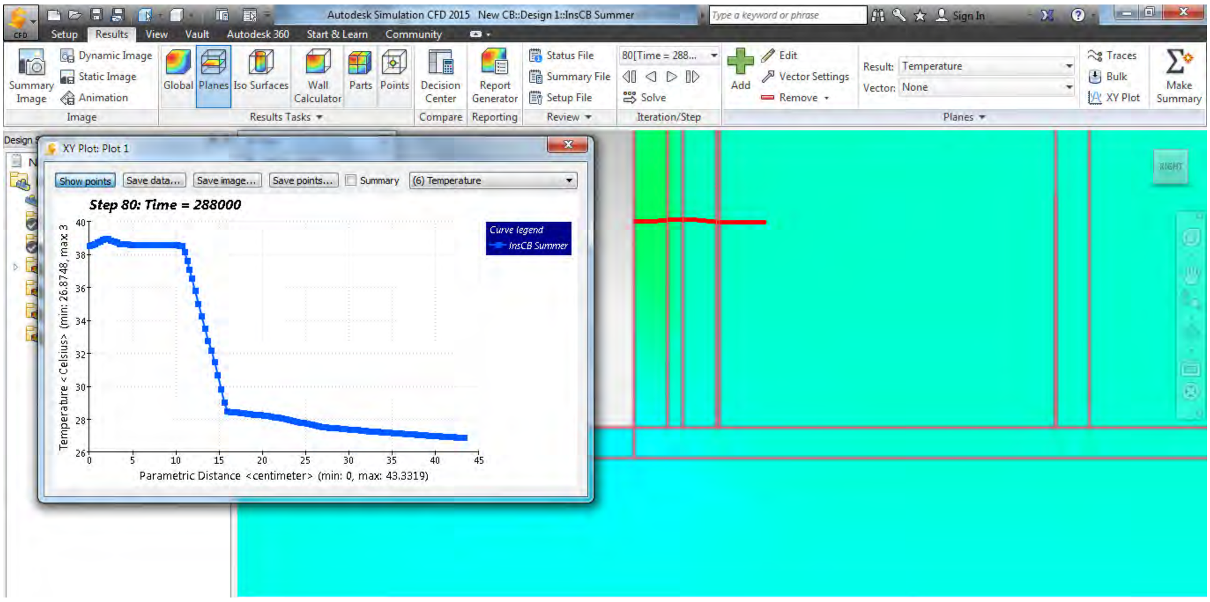

Figure H7. Temperature variation throughout western wall at: 11:30 PM. (Note; the red line shows the temperature changes location across the wall).

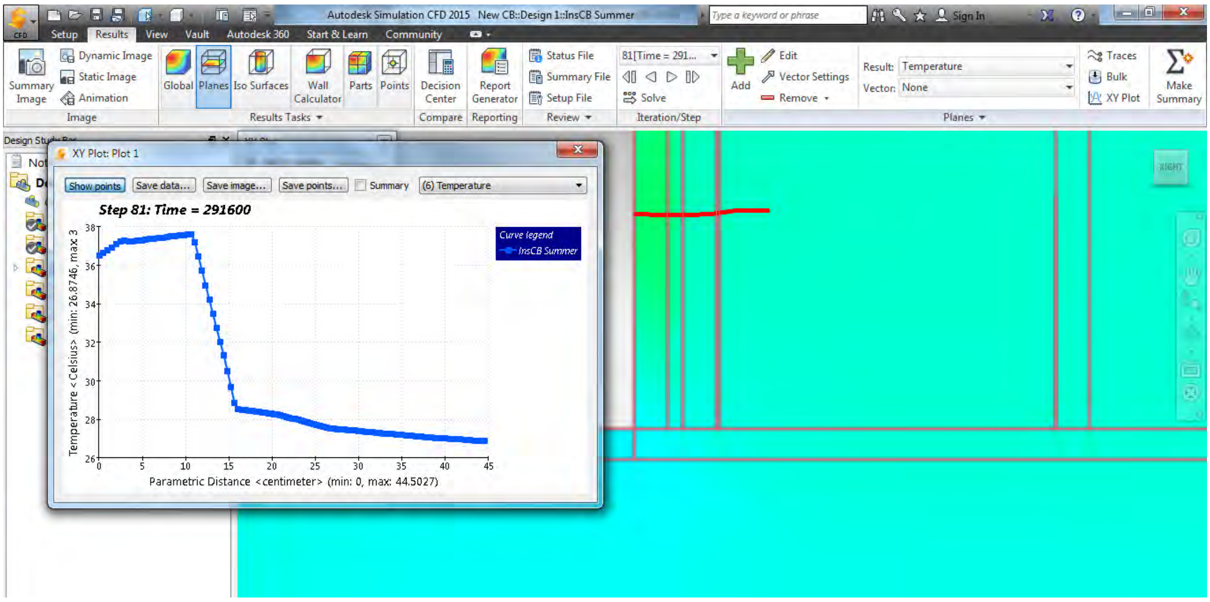

Figure H8. Temperature variation throughout western wall at: 12:30 AM. (Note; the red line shows the temperature changes location across the wall).

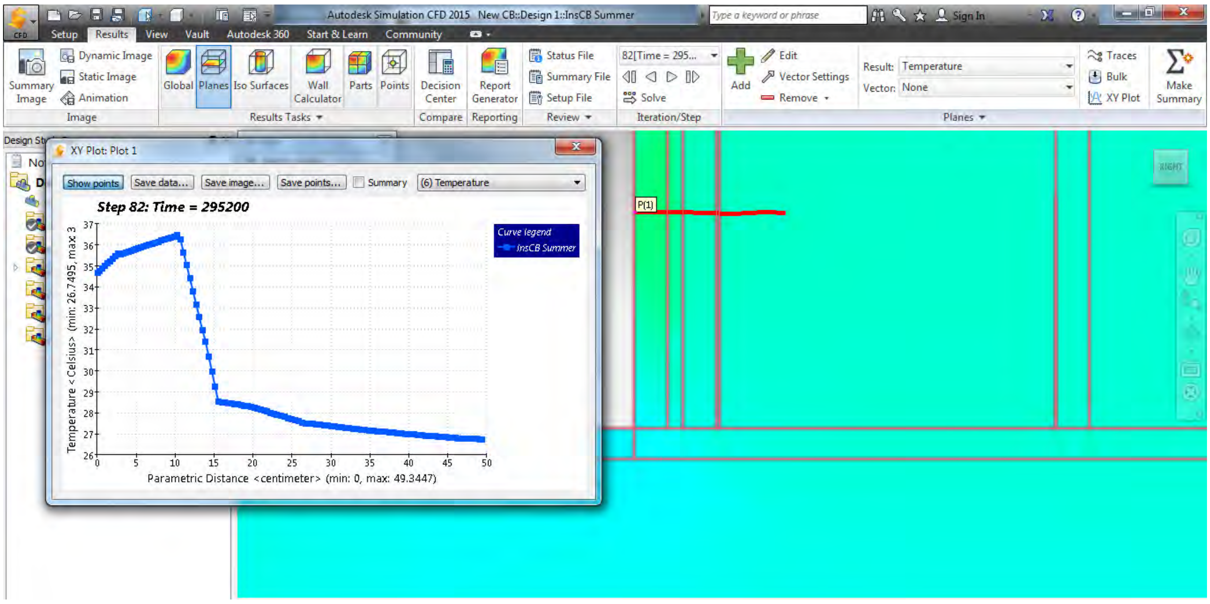

Figure H9. Temperature variation throughout western wall at: 1:30 AM. (Note; the red line shows the temperature changes location across the wall).

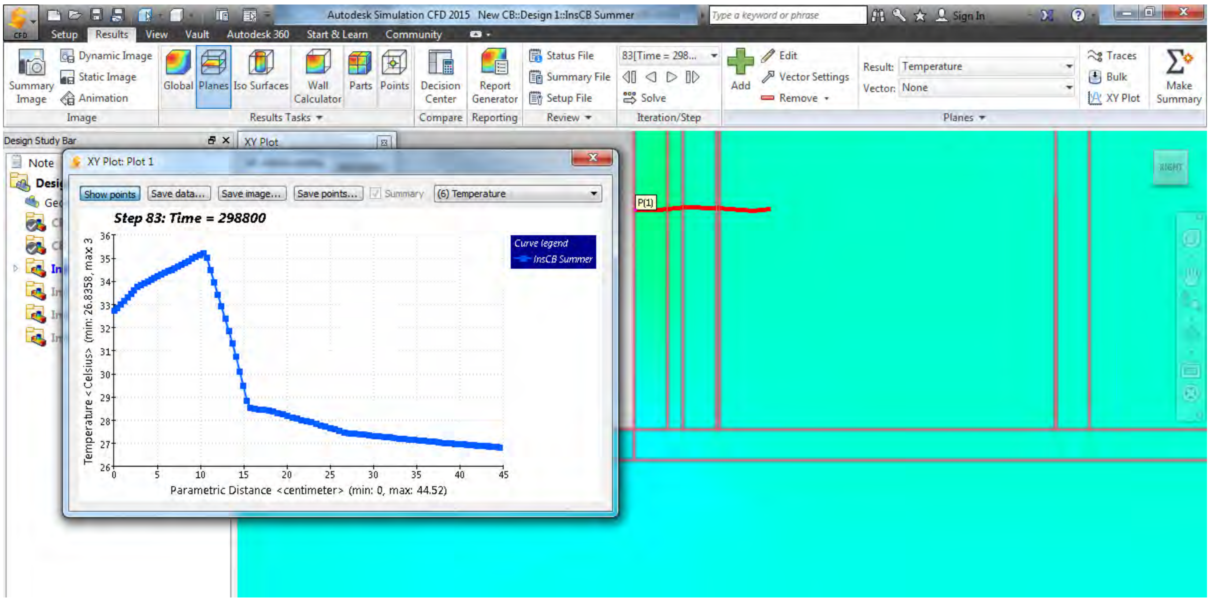

Figure H10. Temperature variation throughout western wall at: 2:30 AM. (Note; the red line shows the temperature changes location across the wall).

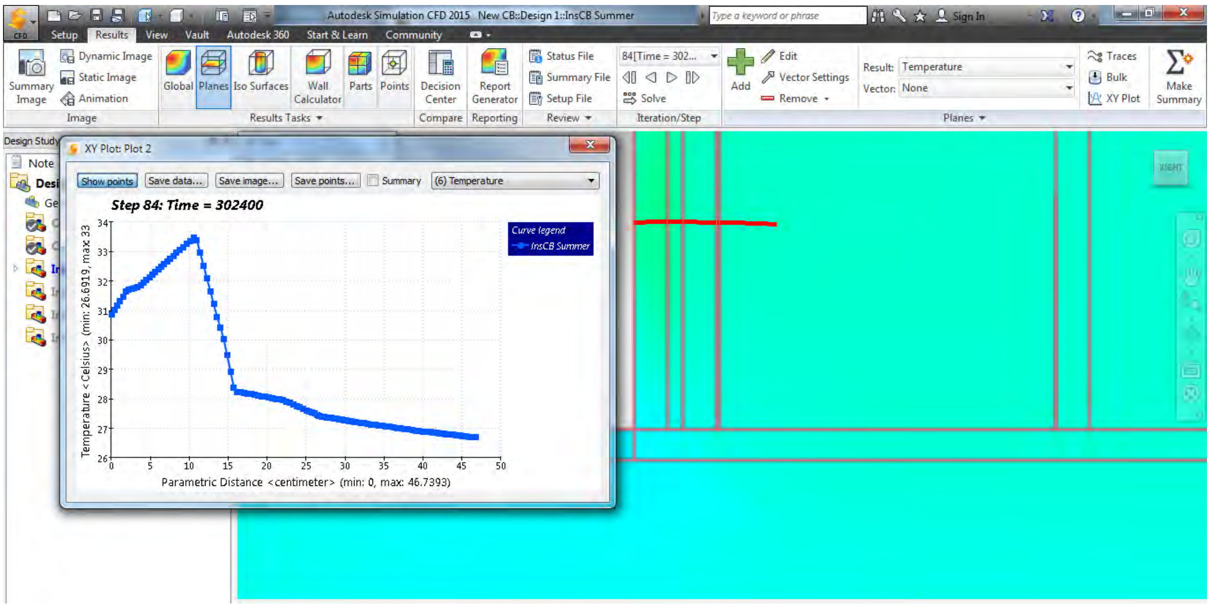

Figure H11. Temperature variation throughout western wall at: 3:30 AM. (Note; the red line shows the temperature changes location across the wall).

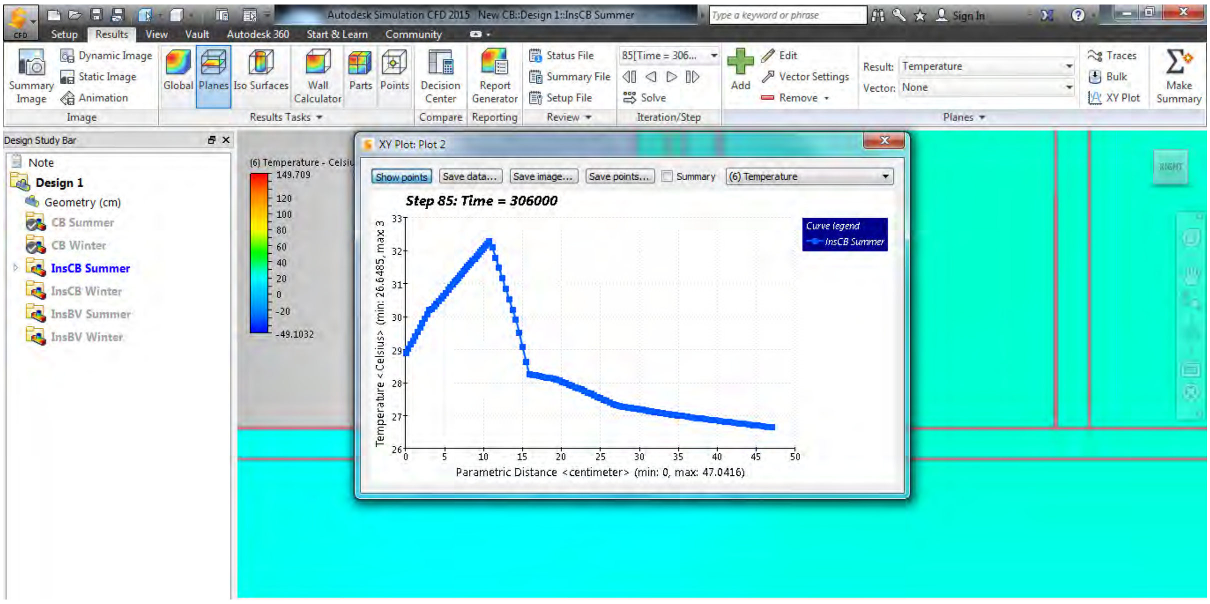

Figure H12. Temperature variation throughout western wall at: 4:30 AM. (Note; the red line shows the temperature changes location across the wall).

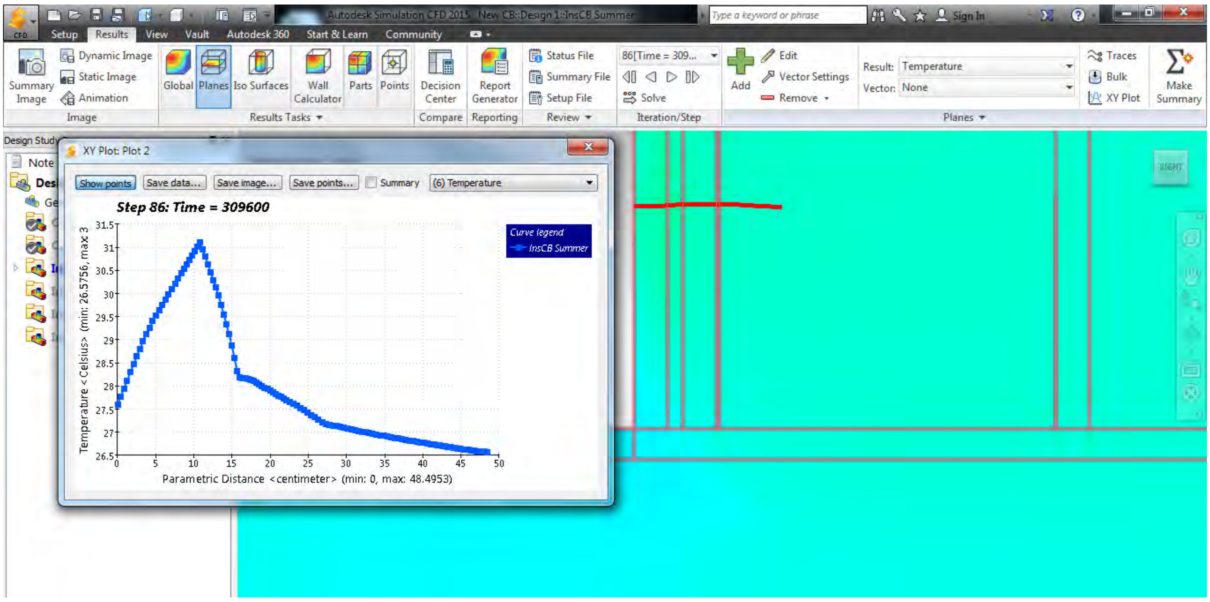

Figure H13. Temperature variation throughout western wall at: 5:30 AM. (Note; the red line shows the temperature changes location across the wall).

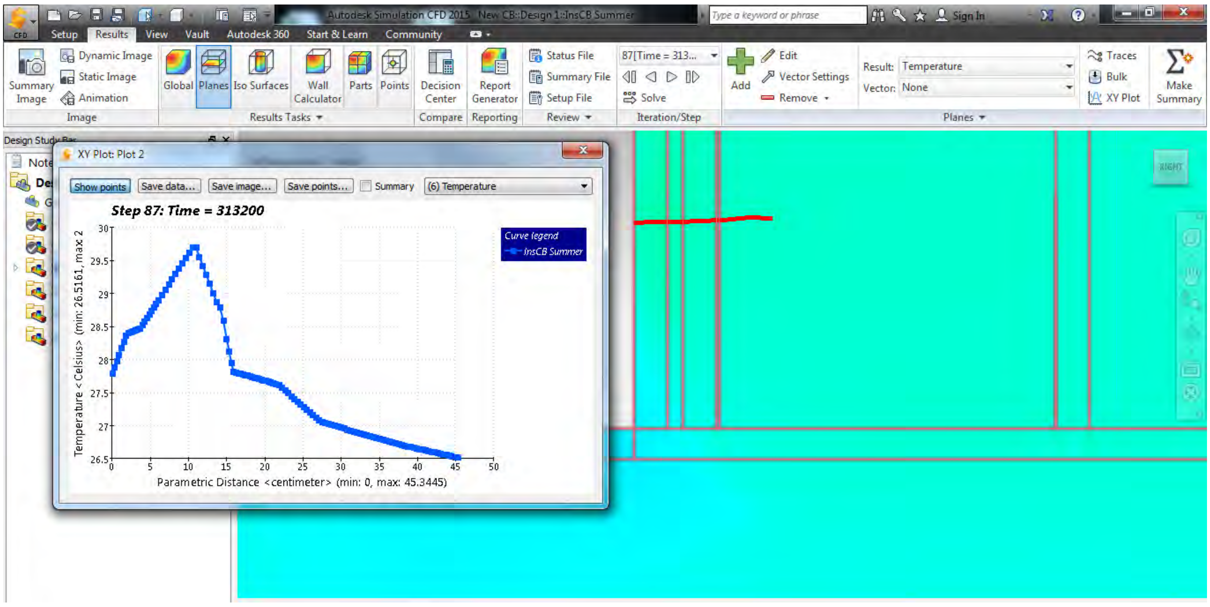

Figure H14. Temperature variation throughout western wall at: 6:30 AM. (Note; the red line shows the temperature changes location across the wall).

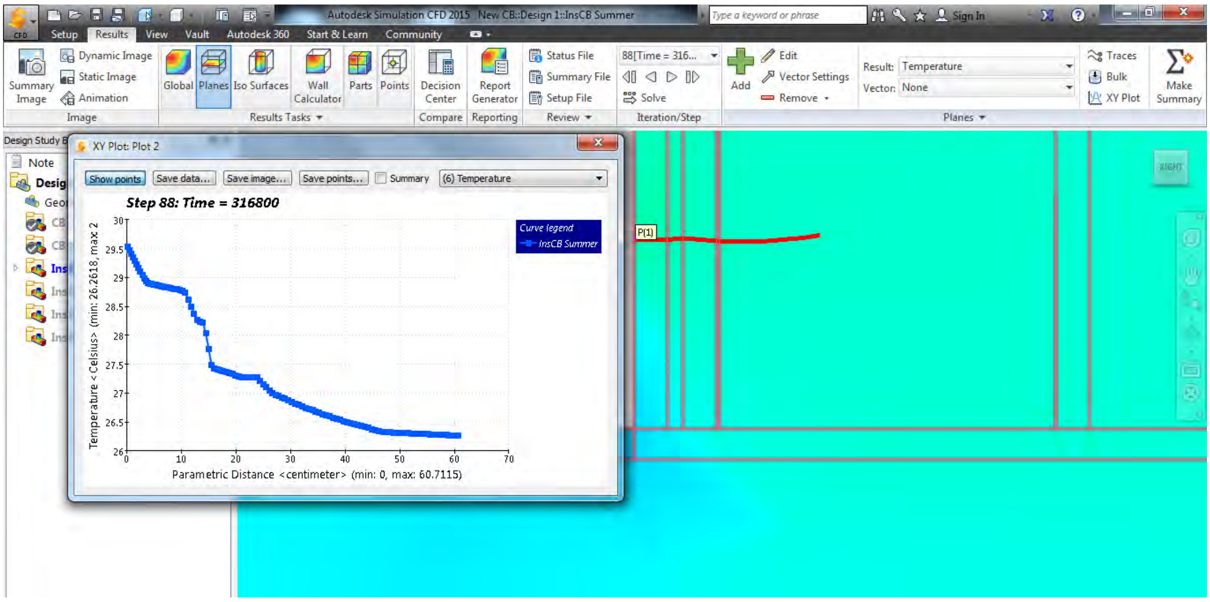

Figure H15. Temperature variation throughout western wall at: 7:30 AM. (Note; the red line shows the temperature changes location across the wall).

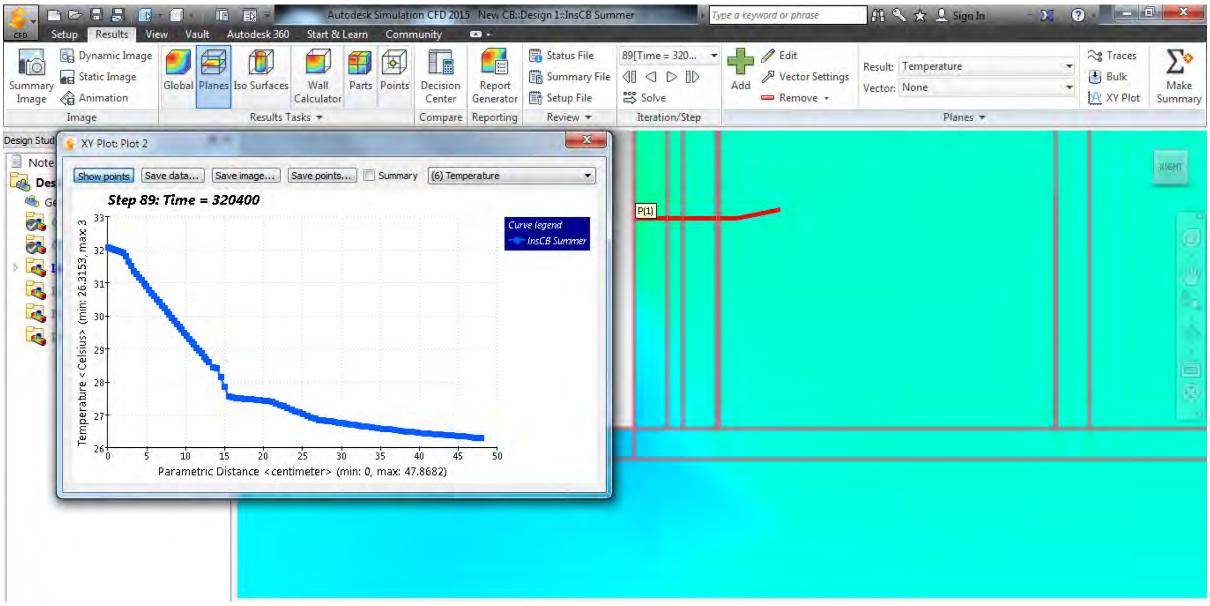

Figure H16. Temperature variation throughout western wall at: 8:30 AM. (Note; the red line shows the temperature changes location across the wall).

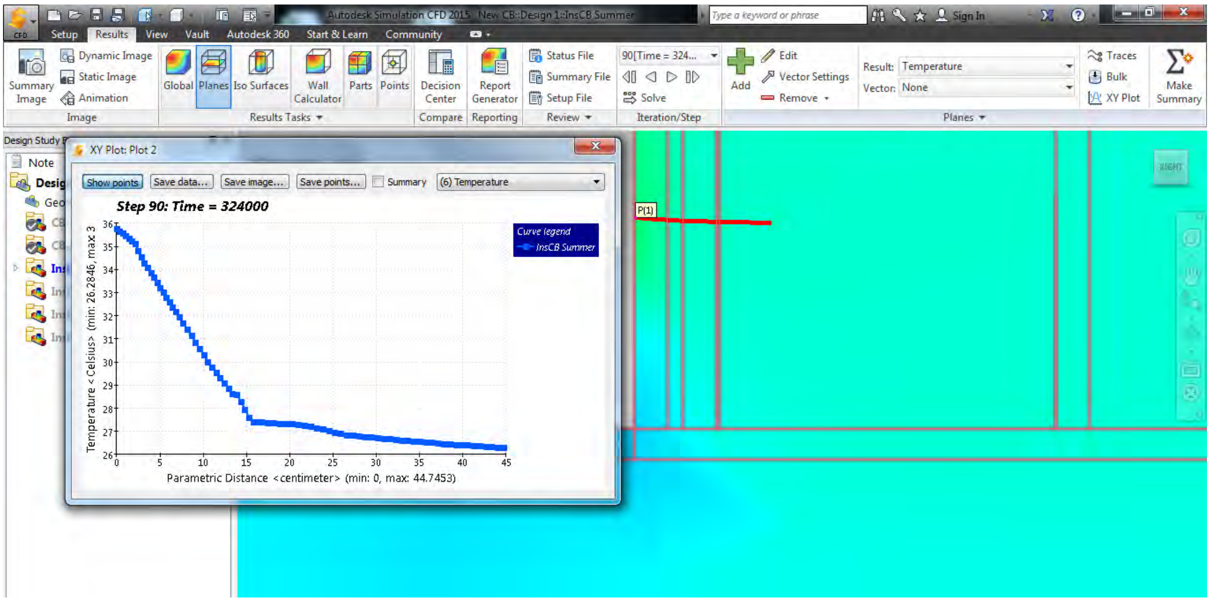

Figure H17. Temperature variation throughout western wall at: 9:30 AM. (Note; the red line shows the temperature changes location across the wall).

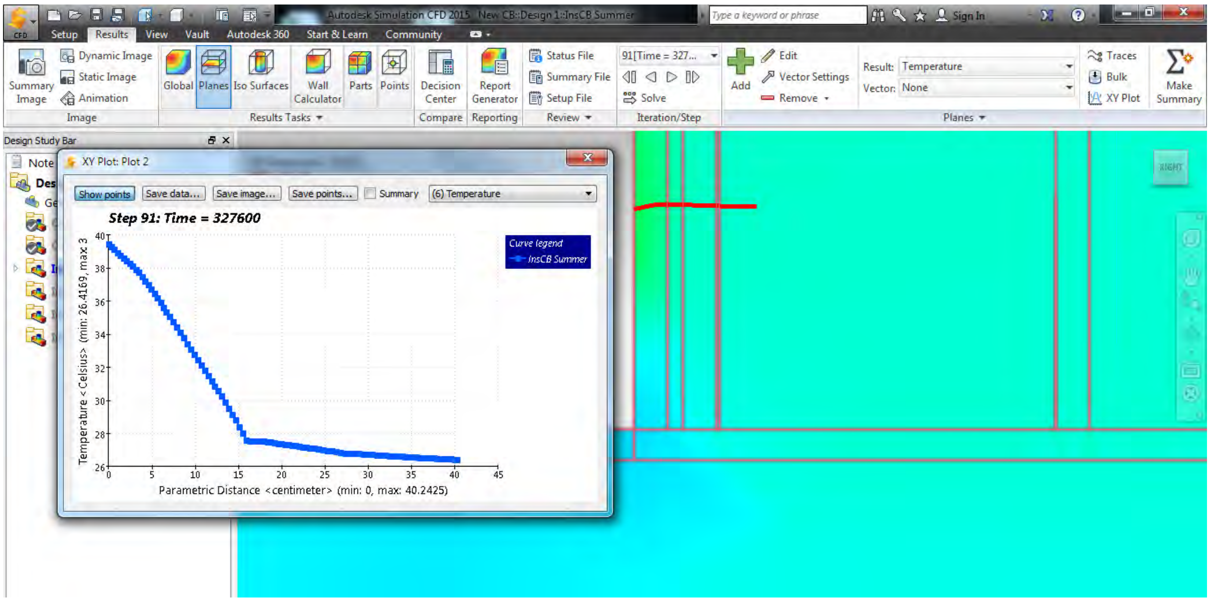

Figure H18. Temperature variation throughout western wall at: 10:30 AM. (Note; the red line shows the temperature changes location across the wall).

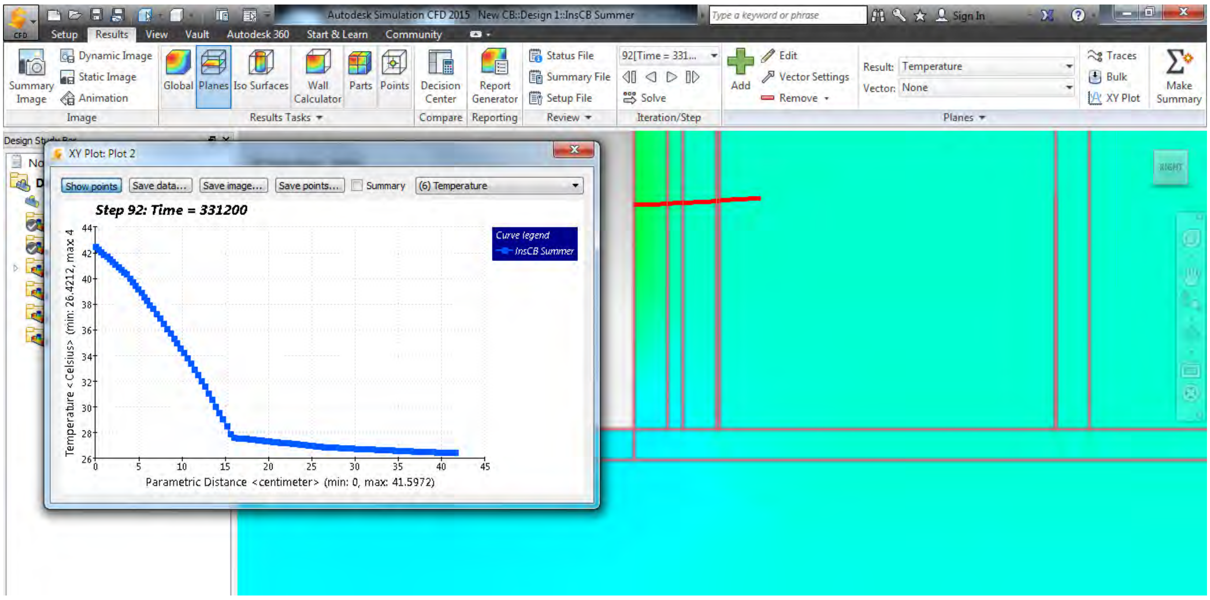

Figure H19. Temperature variation throughout western wall at: 11:30 AM. (Note; the red line shows the temperature changes location across the wall).

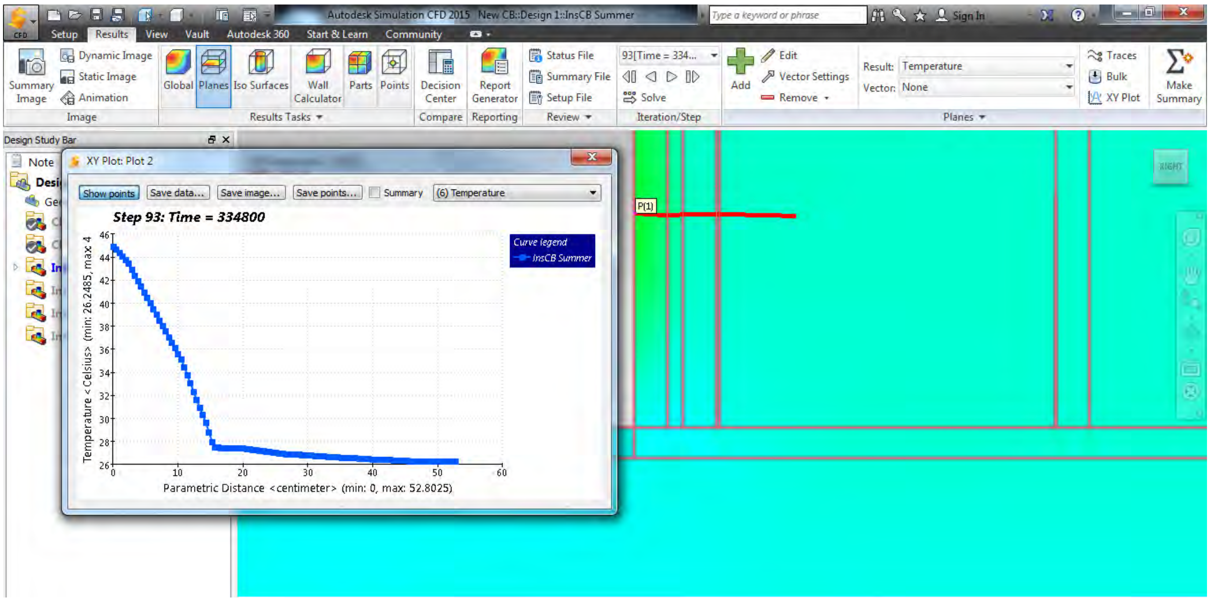

Figure H20. Temperature variation throughout western wall at: 12:30 PM. (Note; the red line shows the temperature changes location across the wall).

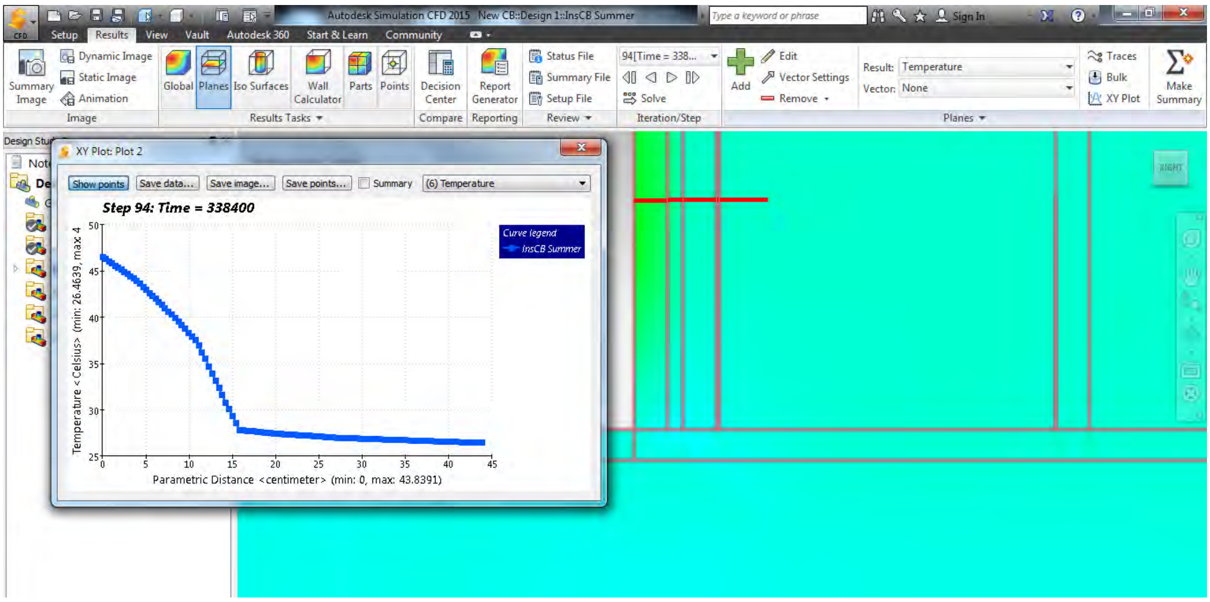

Figure H21. Temperature variation throughout western wall at: 1:30 PM. (Note; the red line shows the temperature changes location across the wall).

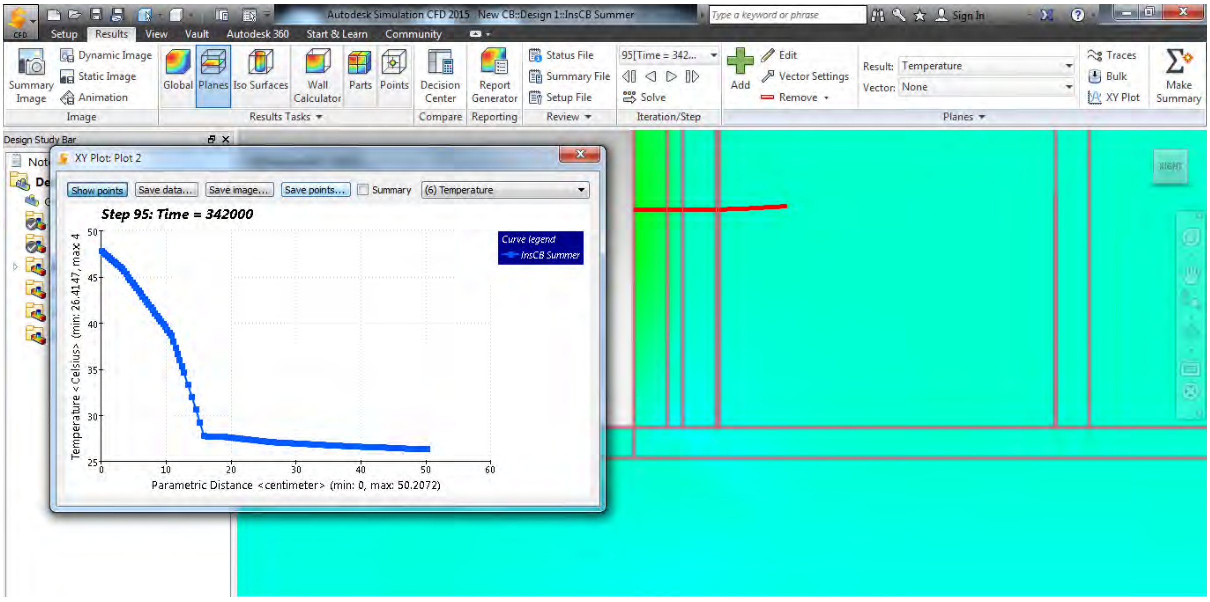

Figure H22. Temperature variation throughout western wall at: 2:30 PM. (Note; the red line shows the temperature changes location across the wall).

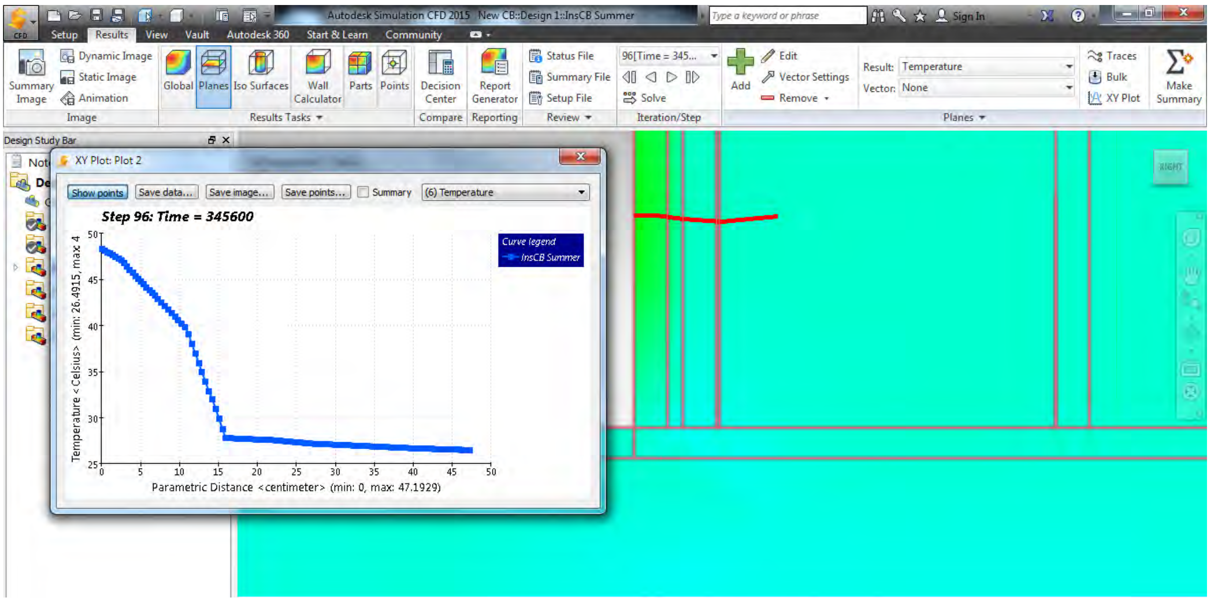

Figure H23. Temperature variation throughout western wall at: 3:30 PM. (Note; the red line shows the temperature changes location across the wall).

Appendix I. Final design materials and sizes taken from AccuRate final report

	AccuRate Sustainability V2.3.3.13 SP1 Nationwide House Energy Rating Scheme	
Project Name: Insulated Cavity Brick Module		
File Name: C:\literature review\PhD\FINAL A\Stage 3\AccuRate\InsCB.PRO		
Postcode: 2308	**Climate Zone:** 15	**Exposure:** Open
Client Name: Reseach		
Site Address:		
Design Option: Base Design		
Date: 13/12/2014	**Time:** 08:00:28	**Page:** 1

Construction details: External Walls		
Description: Cavity Brick (R1 polystyrene) + wet plaster		
External colour: Medium	**Internal colour:** Medium	**Area:** 57.6 m²
External absorptance (%): 50	**Internal absorptance (%):** 50	

Layer	Material	Thickness (mm)
1	Brickwork: generic extruded clay brick (typical density)	110
2	Air gap vertical 17-30 mm (20 nominal) unventilated non-reflective (0.9/0.9; E = 0.82)	20
3	Polystyrene expanded: R1.0	39
4	Brickwork: generic extruded clay brick (typical density)	110
5	Plaster (cement:sand 1:4)	15

Construction details: Windows		
Description: ALM-006-01 A Aluminium B DG Argon Fill Clear-Clear		
Manufacturer: DEFAULTS		
Version: 2.3.3.13.0.9	**Expiry Date:** 15/06/2019	
System U-value (NFRC): 4.50	**SHGC (NFRC):** 0.61	**Area:** 5.8 m²
Frame type: Custom	**Frame colour:** Medium	
Frame fraction (%): 28	**Frame absorptance (%):** 50	

Layer	Material	Thickness (mm)
1	Glass	4
2	Glazing air gap (generic)	12
3	Glass	4

Construction details: External Doors		
Description: Timber (solid)		
External colour: Medium	**Internal colour:** Medium	**Area:** 1.8 m²
External absorptance (%): 50	**Internal absorptance (%):** 50	

Layer	Material	Thickness (mm)
1	Timber (Mountain ash)	50

Construction details: Floor/Ceilings		
Description: Concrete Slab 100 mm: bare/bare		
Top colour: Paint: black	**Bottom colour:** Medium	**Area:** 36.0 m²
Top absorptance (%): 96	**Bottom absorptance (%):** 50	

Layer	Material	Thickness (mm)
1	Concrete: standard (2400 kg/m³)	100

	AccuRate Sustainability V2.3.3.13 SP1 Nationwide House Energy Rating Scheme	

Project Name: Insulated Cavity Brick Module		
File Name: C:\literature review\PhD\FINAL A\Stage 3\AccuRate\InsCB.PRO		
Postcode: 2308	**Climate Zone:** 15	**Exposure:** Open
Client Name: Reseach		
Site Address:		
Design Option: Base Design		
Date: 13/12/2014	**Time:** 08:00:28	**Page:** 2

Description: Plasterboard 13 mm + R2.5 bulk insulation		
Top colour: Medium	**Bottom colour:** Medium	**Area:** 47.6 m²
Top absorptance (%): 50	**Bottom absorptance (%):** 50	

Layer	Material	Thickness (mm)
1	Glass fibre batt: R3.5	154
2	Plasterboard	10

Construction details: Internal Walls

Description: Rammed earth 300 mm		
First colour: Paint: black	**Last colour:** Medium	**Area:** 14.4 m²
First absorptance (%): 96	**Last absorptance (%):** 50	

Layer	Material	Thickness (mm)
1	Rammed earth	300

Construction details: Roofs

Description: Tiles (concrete)		
External colour: Medium	**Internal colour:** Medium	**Area:** 47.6 m²
External absorptance (%): 50	**Internal absorptance (%):** 50	

Layer	Material	Thickness (mm)
1	Roof tiles (concrete)	20

	# AccuRate Sustainability V2.3.3.13 SP1 Nationwide House Energy Rating Scheme	

Project Name: Insulated Cavity Brick Module		
File Name: C:\literature review\PhD\FINAL A\Stage 3\AccuRate\InsCB.PRO		
Postcode: 2308	**Climate Zone:** 15	**Exposure:** Open
Client Name: Reseach		
Site Address:		
Design Option: Base Design		
Date: 13/12/2014	**Time:** 08:00:28	**Page:** 3

Habitable zones

Name	Type	Volume (m^3)	Floor height (m)	Ceiling height above floor (m)	Heated	Cooled
Zone : 1	Living/Kitchen	86.4	2.5	2.4	Y	Y

Habitable zones (continued)

Name	Chimneys		Wall/Ceiling vents	Exhaust fans		Vented downlights	Unflued gas heaters	Ceiling fans	Type
	U/S	S		U/S	S				
Zone : 1	0	0	0	0	0	0	0	0	-

Roofspace zones

Name	Volume (m^3)	Reflective	Sarking	Roof surface	Openness
Zone : 2	47.6	N	Sarked	Discontinuous	

AccuRate Sustainability V2.3.3.13 SP1

Nationwide House Energy Rating Scheme

Project Name: Insulated Cavity Brick Module		
File Name: C:\literature review\PhD\FINAL A\Stage 3\AccuRate\InsCB.PRO		
Postcode: 2308	**Climate Zone:** 15	**Exposure:** Open
Client Name: Reseach		
Site Address:		
Design Option: Base Design		
Date: 13/12/2014	**Time:** 08:00:28	**Page:** 4

Zone : 1: External walls main data

Wall	Construction	Azi (deg.)	L (m)	H (m)	Area (gross) (m²)	Area (net) (m²)	Fixed shade	Opening (m²)	Opening Type
1	Cavity Brick (R1 polystyrene) + wet plas	0	6.00	2.40	14.40	2.76	Scheme 1	5.82	Controlled
2	Cavity Brick (R1 polystyrene) + wet plas	180	6.00	2.40	14.40	10.80	Scheme 1	1.80	Controlled
3	Cavity Brick (R1 polystyrene) + wet plas	90	6.00	2.40	14.40	14.40	Scheme 1	0.00	Controlled
4	Cavity Brick (R1 polystyrene) + wet plas	270	6.00	2.40	14.40	14.40	Scheme 1	0.00	Controlled

Zone : 1: External walls horizontal shading data

		Eaves				Other fixed shading				
Wall	Name	Projection (m)	Horizontal Offset (m)	Vertical Offset (m)	Length (m)	Projection (m)	Horizontal Offset (m)	Vertical Offset (m)	Length (m)	Monthly blocking factors (%)
1	Scheme 1	0.45	0.00	0.00	6.90	0.00	0.00	0.00	0.00	100,100,100,100,100,100,100,100,100,100,100,100
2	Scheme 1	0.45	0.00	0.00	6.90	0.00	0.00	0.00	0.00	100,100,100,100,100,100,100,100,100,100,100,100
3	Scheme 1	0.45	0.00	0.00	6.90	0.00	0.00	0.00	0.00	100,100,100,100,100,100,100,100,100,100,100,100
4	Scheme 1	0.45	0.00	0.00	6.90	0.00	0.00	0.00	0.00	100,100,100,100,100,100,100,100,100,100,100,100

Zone : 1: Windows in walls

Wall	Window Name	Type	Construction	Azi. (deg.)	H (m)	W (m)	Area (m²)
1	North Window	Sliding	ALM-006-01 A Aluminium B DG Argon Fill Clear-Clear	0	2.05	2.84	5.82

Zone : 1: Windows in walls (continued)

Wall	Window Name	Indoor covering	Outdoor covering	Fixed shade	HH (m)	HO (m)	Opening (%)	Weather stripped	Gap size
1	North Window	Hollandblinds	None		2.10	0.00	0.00	N	S

Zone : 1: Doors in walls

Wall	Door Name	Construction	Azi (deg.)	H (m)	W (m)	Area (m²)	HO (m)	Openable (%)	Weather stripped	Gap size
2	Door	Timber(solid)	180	2.00	0.90	1.80	1.00	0	Y	

Zone : 1: Internal walls

Wall	Construction	L (m)	H (m)	Area (gross) (m²)	Area (net) (m²)	Adjacent Zone	Opening (m²)	Opening Type
1	Rammed earth 300 mm	6.00	2.40	14.40	14.4	Zone : 1	0.00	Controlled

Zone : 1: Floors

Floor	Construction	Area (gross) (m²)	Area (net) (m²)	Under the floor	Edge Ins.	Opening (m²)	Opening Type
1	Concrete Slab 100 mm: bare/bare	36.0	36.0	Ground		0.00	Controlled

Zone : 1: Ceilings

Ceiling	Construction	Area (gross) (m²)	Area (net) (m²)	Above the ceiling	Opening (m²)	Opening Type
1	Plasterboard 13 mm + R2.5 bulk insulation	47.6	47.6	Zone : 2	0.00	Controlled

	AccuRate Sustainability V2.3.3.13 SP1 Nationwide House Energy Rating Scheme	
Project Name: Insulated Cavity Brick Module		
File Name: C:\literature review\PhD\FINAL A\Stage 3\AccuRate\InsCB.PRO		
Postcode: 2308	**Climate Zone:** 15	**Exposure:** Open
Client Name: Reseach		
Site Address:		
Design Option: Base Design		
Date: 13/12/2014	**Time:** 08:00:28	**Page:** 5

Zone : 2: Floors

Floor	Construction	Area (gross) (m²)	Area (net) (m²)	Under the floor	Edge Ins.	Opening (m²)	Opening Type
1	Plasterboard 13 mm + R2.5 bulk insulation	47.6	47.6	Zone : 1		0.00	Controlled

Zone : 2: Roofs

Roof	Construction	Area (gross) (m²)	Area (net) (m²)	Azi (deg.)	Pitch (deg.)	Exposure
1	Tiles (concrete)	47.60	47.60	90	23	Normal

	AccuRate Sustainability V2.3.3.13 SP1 Nationwide House Energy Rating Scheme	

Project Name: Insulated Cavity Brick Module		
File Name: C:\literature review\PhD\FINAL A\Stage 3\AccuRate\InsCB.PRO		
Postcode: 2308	**Climate Zone:** 15	**Exposure:** Open
Client Name: Reseach		
Site Address:		
Design Option: Base Design		
Date: 13/12/2014	**Time:** 08:00:28	**Page:** 6

Shading Schemes

	Eaves				Other fixed shading				
Name	Projection (m)	Vert Offset (m)	Horiz Offset (m)	Length (m)	Projection (m)	Vert Offset (m)	Horiz Offset (m)	Length (m)	Monthly blocking factors (%)
Scheme 1	0.45	-0.25	0.45	6.90	0.00	0.00	0.00	0.00	100,100,100,100,100,100,100,100,100,100,100,100

Ventilation

Footprint: vertical dimension (m)	Footprint: horizontal dimension (m)	Azimuth of highlighted facade (degrees)	Insect screens
6.0	6.0	90	N